Within-host Dynamics of *Chlamydia trachomatis* Infection - Repeat Infections and the Immune Response

Morenikeji Deborah Akinlotan
BSc Hons (Mathematics), PGD (Mathematical Sciences), MSc (Mathematics)

under the supervision of

Prof. Dann Mallet, Dr Robyn Araujo,
and Dr Tim Moroney

School of Mathematical Sciences
Science and Engineering Faculty
Queensland University of Technology

2018

Submitted in fulfillment of the requirements of the degree of
Doctor of Philosophy

Keywords

Chlamydia trachomatis, within-host dynamics of *Chlamydia*, genital infection, *Chlamydia* vaccine, antibiotics, azithromycin, *Chlamydia* treatment failure, chronic *Chlamydia* infection, mathematical model of *Chlamydia*, ordinary differential equations, optimal control of *Chlamydia*, treatment of *Chlamydia* with tryptophan supplement, treatment of *Chlamydia* with proteasome-specific inhibitor.

Abstract

Chlamydia trachomatis is a Gram-negative obligate intracellular bacterial pathogen that infects the human genital tract and ocular epithelium. It is the most common bacterial sexually transmitted infection worldwide. The control of the incidence of genital *C. trachomatis* infection is a major public health challenge. At any point in time, over 100 million adults are infected with *Chlamydia* globally. *C. trachomatis* infection, often referred to as the 'silent epidemic', is asymptomatic in 85% of infected women, and 40% of infected men. Consequently, it is commonly undiagnosed and untreated. *Chlamydia trachomatis* infection in humans can also take several months before spontaneous clearance. Despite the fact that *Chlamydia* is curable with antibiotics, it remains one of the major preventable causes of disability and mortality.

Mathematical models are very useful in describing the interaction between *Chlamydia trachomatis* and the host immune system, as they provide insights into the dynamics of the infection process, related sequelae, and feasible intervention/control strategies. In this study, we use ordinary differential equation models to provide qualitative insights into the dynamics of *Chlamydia trachomatis* infection, the associated host immune response, and the *in vivo* control or treatment of the infection. Some crucial mathematical and biological questions are addressed by the thesis, especially those that pertain to the within-host dynamics of the development and progression of chlamydial infection, and of the control of the pathogen. The thesis examines optimal control/treatment strategies for genital chlamydial infection. The effective treatment of chronic *Chlamydia* infections induced by chlamydial persistence, and the subsequent host immune response on the dynamics of *C. trachomatis*, are explored.

Model results suggest that the use of combination treatments/drugs may facilitate improved clearance of genital chlamydial infection, while averting treatment failures and the development of chlamydial persistence *in vivo*. A model that investigates vaccination strategies that may proffer protective immunity against *Chlamydia* infections is also presented. Model results show that an imperfect *C. trachomatis* vaccine may proffer protective immunity against chlamydial infection and also facilitate immune-mediated clearance of intracellular *Chlamydia* forms. Qualitative results of the presented models provide frameworks for the design of new and improved treatment strategies for genital chlamydial infection.

Declaration

I hereby declare that this submission is my own work and to the best of my knowledge it contains no material previously published or written by another person, nor material which to a substantial extent has been accepted for the award of any other degree or diploma at QUT or any other educational institution, except where due acknowledgement is made in the thesis. Any contribution made to the research by colleagues, with whom I have worked at QUT or elsewhere, during my candidature, is fully acknowledged.

I also declare that the intellectual content of this thesis is the product of my own work, except to the extent that assistance from others in the project's design and conception or in style, presentation and linguistic expression is acknowledged.

Signature QUT Verified Signature Date June 14, 2018

Acknowledgments

All the glory belongs to you oh God! You made a way! When it looked as if we can't win; You wrapped us in your arms and stepped in! When my back was against the wall, and it looked as if it was over, Father! You made a way! Everything we needed, You supplied. You've got this figured out all along! I am standing here, only because you made a way! Thank you Jesus!

Special appreciation goes to my love, my special crony and admirer, my erudite and comely husband, Dr Adewale Dipo Ogunyemi. Honey, what would I do without you? You're such a great man - thou beloved of the Most High God! I am copiously blessed and greatly favoured to have you! Thank you very much for all your support, prayers, and immense sacrifices. You've got a heart of gold! Many oceans cannot and will not quench the fire of your love in me, even in Jesus' name! I wish I could paint this whole page with your name embossed in gold. You deserve much more than I can say! Thanks my love! May the Almighty God preserve you in Jesus' name! Special thanks to my 'PhD babies', Grace and Gloria Ogunyemi. I commenced the journey with the conception of Grace and I conceived Gloria towards its end. Your kicks while in my womb made the journey worthwhile, more meaningful and fulfilling! Thanks for your special love, and enduring patience, especially for the many times mum was away. May you fulfill your glorious destinies in Jesus' name! You shall be God's generals and the Kingdom of God you shall populate by the grace of the Almighty! Kisses, hugs, and blessings to my special parents, Mr and Mrs Akinlotan, and my loving siblings, Samuel, Grace, Gideon, and Joshua Akinlotan, for all your prayers, sacrifices, and love. Thank you very much mum, for always coming all the way from Nigeria, to look after your grand-children while I study and go on research trips. You are invaluable! You and dad shall eat the sweet fruits of your labours, in perfect all-round health, in Jesus' name! I love you very much! May we all finish strong and well, reigning with Christ as His bride at the end, in Jesus' name! Amen.

Many thanks to my humble principal supervisor, Professor Dann Mallet, for believing in me, and for all his academic and moral support throughout the years. I really appreciate you and your family for opening the doors of your home to me, giving me the first resting place I ever had in Australia. God bless you! Thank you! I also appreciate my co-supervisors, Dr Robyn Araujo and Dr Tim Moroney, for all their support. Robyn, I am really grateful for the wealth of knowledge and expertise you brought on the team. Your contributions are invaluable! I wish I had met you earlier! Thanks for always being there. I love you! I really appreciate Professors Graeme Pettet and Ian Turner for the fatherly support they also gave me. You took interest in me right from the beginning of my PhD studies, and you were so unrelenting, frequently advising and supporting me. I appreciate you deeply. Thank you! Special appreciation also goes to Dr. Michael Cholette

of QUT for his selflessness and assistance, especially when I ran into some optimisation numerical hurdles. I also appreciate Professor Abba Gumel for all his academic, moral, and even financial support, especially during my two months research visit to Arizona State University, USA. God bless you sir!

Many thanks to you my dear friends (home and abroad), church members, pastors, and colleagues for all your support and prayers. I wouldn't mention names for fear of leaving anyone out. I appreciate you all. However, necessity is laid upon me to make special mention of a few 'above and beyond' friends: my dear friend, PhD colleague, and brother, Johnny Thew, you are such a wonderful friend! Thanks for everything! God bless you! Mr. and Mrs. Oyelodi, Mr and Mrs Peters, Dr and Dr Mrs Akinboye, your families showed us the true meaning of brotherly kindness. Thanks for always being there. The Lord bless and keep you in Jesus' name! Special thanks goes to Andrea Russo, Michelle Spanton, and Amanda Kolovrat. You are all wonderful colleagues and mothers! Thanks for your love, encouragement, and support! God bless you all! Special thanks to Sandra Stevenson of the Fellowship Funds Incorporated (FFI) QLD, and her family, for housing me for three weeks when I had accommodation issues as a new arrival. You opened your doors even before meeting me in person. Thank you very much! God bless you!

With immense gratitude, I acknowledge that this doctoral study was generously supported with Higher Degree by Research tuition fee sponsorship by QUT, living allowances by the Faculty for the Future Fellowship of the Schlumberger Foundation, and by the Freda Bage Fellowship of the Fellowship Funds Incorporated, Queensland. Many thanks to QUT and the Schlumberger Foundation for conference travel grants.

Thank you dear Lord! To you alone be all the glory!

Contents

1 Introduction

Chlamydia trachomatis is a Gram-negative obligate intracellular bacterial pathogen that infects the human genital tract and ocular epithelium [10, 87, 127]. It has 18 serovars of which serovars A-C are responsible for trachoma (a leading cause of infectious blindness), and serovars D-K and lymphogranuloma venereum (LGV) are majorly responsible for bacterial sexually transmitted infections (STI) [10, 53]. *C. trachomatis* is the most common bacterial sexually transmitted infection worldwide [42,92,162]. It is also a major risk factor in HIV transmission [175]. *C. trachomatis* is the most commonly reported notifiable disease in developed countries, with over 1.4 million chlamydial infections reported in the United States in 2013 [22, 164].

The control of the incidence of genital *C. trachomatis* infection continues to present as a major public health challenge [164]. At any point in time, over 100 million adults are infected with *Chlamydia* globally [162]. *C. trachomatis* infection, often referred to as the 'silent epidemic', is asymptomatic in 85% of infected women, and 40% of infected men. It is even more asymptomatic in men than asymptomatic gonorrhoea infection. Consequently, it is commonly undiagnosed and untreated [42,162]. *Chlamydia trachomatis* infection in humans can also take several months before spontaneous clearance [18, 61]. The incidence of *C. trachomatis* is more prevalent in young adults (15 to 25 years), and much more prevalent in female adolescents (24.1%- 27%), [127]. Adolescent women are at a greater risk of recurrent chlamydial infections [38].

Despite the fact that *Chlamydia* is curable with antibiotics, it remains one of the major preventable causes of disability and mortality. During delivery, infected pregnant women can pass the infection to their infants, possibly resulting in neonatal pneumonia and opthalmia [22, 148]. Chlamydial genital infection has a more severe sequelae in women, as they develop serious health problems such as chronic pelvic pain, sterility, urethritis, and cervicitis. Untreated *C. trachomatis* plays a crucial causative role in severe sequelae such as pelvic inflammatory disease (PID), tubal factor infertility (TFI), life threatening ectopic pregnancy, and sepsis [42, 53, 61, 87, 164]. The infection can be associated with epididymitis and urethritis in men, and proctitis in men who have sex with men [126].

1.1 Motivation of the Thesis

A useful way of describing the interaction between *Chlamydia trachomatis* and the host immune system is via mathematical models, as they provide insights into the dynamics of the infection process, the succeeding effects and feasible intervention strategies [9,169]. The aims of this research are to provide qualitative insights into the dynamics of genital *Chlamydia trachomatis* infections, the associated host immune response, and the *in vivo* control or treatment of the infection. Some crucial mathematical and epidemiological questions are addressed by the thesis, especially those that pertain to the within-host dynamics of the development and progression of chlamydial infection, and of the control of the pathogen. These questions include:

1. Why are there treatment failures in the control of genital chlamydial infection? In particular, could existing treatment regimen be inhibiting intracellular *Chlamydia* growth later than expected, thereby resulting in some of them thriving for repeat infection? In the presence of antimicrobial treatments, what role does the different component of the chlamydial developmental cycle play in the pathogenesis of the disease? How can these treatment regimens be improved?
2. Are treatment failures consequences of sub-optimal treatment regimen? Under what treatment conditions can the effective and efficient clearance of *Chlamydia* be achieved *in vivo*? Do we need more therapeutic agents in the clearance of the infection? How and when should such treatments be initiated in infected individuals?
3. How do we treat chronic chlamydial infections effectively? In particular, how can we prevent, or even reverse, the development of severe sequelae of chlamydial infections in the human population?
4. How would an imperfect *Chlamydia* vaccine impact on the dynamics and prognosis of a genital chlamydial infection *in vivo*? How efficacious should a *Chlamydia* vaccine be if it must facilitate the prevention of the progression of a *Chlamydia* infection?

1.1.1 Research Objectives

The objectives of this research program are enumerated below:

1. Construction of new mathematical models of (genital) chlamydial infection in humans or animals that better account for the complexity of the immune response to infection, and importantly, reinfection events caused by chlamydial persistence, than existing models.
2. Enhancement of the above and existing models, such that they are able to describe the effects of existing treatments and of proposed vaccination strategies.
3. Formation of new hypotheses regarding repeated chlamydial infections based on model analysis.

4. Proposition of optimal treatment and vaccination strategies based on the above.

1.1.2 Methodology

In this research project, standard mathematical modelling approaches are used. Specifically:

- Relevant infectious diseases literature are surveyed to develop a knowledge in the area of *Chlamydia* biology/immunology/vaccinology.
- The above understanding is used to develop informed and relevant mathematical models of chlamydial infections and the immune response. These models use ordinary differential equations.
- Necessary computational methods are developed and tested, to investigate and solve the mathematical models developed as part of the research.
- Computational simulations and mathematical analysis are used to investigate the predictions and outcomes of the mathematical models.
- Discussion of the results of analysis and simulations revolve around the relevance and significance of findings to the formation of new hypotheses regarding the immune response to repeated chlamydial infections of humans and/or animals, the effective and efficient treatment of chlamydial infections, and in the development of an effective vaccine.

1.2 Overview of Thesis

In Chapter 2, we give a brief introduction into the biology of *Chlamydia* and its developmental cycle. Interactions between *Chlamydia* and its infected host system are also described. We also discuss existing treatment strategies for chlamydial infection. In conclusion, some existing mathematical models of *Chlamydia trachomatis* are reviewed.

Chapter 3 presents our first attempt at modelling intracellular chlamydial infections by investigating the interaction between *Chlamydia* body forms and the host cells. The model aims at gaining a better understanding of the impact of an antibiotic treatment on the within-host dynamics of chlamydial infections. In particular, the model investigates the chlamydial developmental cycle, in order to identify the stages at which *Chlamydia*'s intracellular growth can be best inhibited.

In Chapter 4, we present an ordinary differential equation model of the treatment of *Chlamydia* infection, which describes the interaction between *Chlamydia*, host cells, and the host immune response. The model uses methods of optimal control theory to explore optimal strategies associated with different kinds of treatment of chlamydial infections. Qualitative analysis of the model, including stability analysis of the *Chlamydia*-free equilibrium, is presented. The model is numerically simulated and results are analysed and interpreted.

Chapter 5 presents another ordinary differential equation model, this time focusing on the treatment of a chronic *Chlamydia* infection. In addition to accounting for the interaction between *Chlamydia*, host cells, and the host immune response, the model also incorporates host cells that are 'persistently infected'. The model also uses methods of optimal control theory to explore optimal treatment strategies for chlamydial infections. The chapter also presents some qualitative results of the model. Numerical simulations of the model are presented and results interpreted.

In Chapter 6, a deterministic model of an imperfect mucosal *Chlamydia* vaccine is presented. The model uses ordinary differential equations to describe the interactions between *Chlamydia* body forms, host cells, host immune cells, and secretions of the host immune cells. The model assesses the potential role of an effective anti-*Chlamydia* vaccine on the within-host dynamics of *Chlamydia trachomatis*. Equilibrium solutions of the model are presented, and the local and global stability analysis of the *Chlamydia*-free equilibrium are investigated. The chapter also conducts uncertainty and sensitivity analysis on the presented model. Numerical simulations of the model are presented and the concentrations of *Chlamydia* body forms and host cells, in the presence of the *Chlamydia* vaccine, are tracked.

Finally, Chapter 7 summarises the major contributions of the thesis and some future work is also discussed.

2 Literature Review

In this chapter, we provide a review of the current literature upon which the core chapters (Chapters 3-6) are based. We begin with a review of the biology of *Chlamydia trachomatis* and its pathogenesis. We then reviewed the current treatment guidelines for genital *Chlamydia* infections before discussing the issue of treatment failures. Furthermore, we discussed potential anti-*Chlamydia* treatments that are currently being developed before covering recent progresses on the development of potential anti-*Chlamydia* vaccines. Finally, we gave a brief summary of existing within-host mathematical models of *Chlamydia*.

2.1 Chlamydial Biology

Chlamydiae spp.[1] display a unique and complex biphasic developmental cycle involving eukaryotic cells. Within host, they appear in two disctinctive morphological forms: the extracellular, metabolically inert, infectious form, known as the elementary body (EB) and the intracellular, metabolically active, and replicative form, known as the reticulate body (RB). RBs are larger than EBs [10, 72, 178]. EBs are spore-like and are about 200 to 400 μm in diameter, while RBs are about 800 μm in diameter [66, 175]. Being an obligate intracellular pathogen, *C. trachomatis* infects its host by attaching to and invading susceptible host-epithelial cells using its EB form. The interactions of EBs occur in a two-stage process: the initial reversible attachment through electrostatic interactions of the EB particle with heparan sulfate proteoglycans (HSPGs) containing glycosaminoglycans, followed by their high-affinity irreversible binding to an unidentified secondary receptor, using chemically mutagenized cell lines [10, 178].

After the attachment of chlamydial EBs to the cell surface, within the first two hours post-infection (hPI), they are internalised into plasma membrane-bound vacuoles of the host cell called *inclusions* (see Figure 2.1). They then undergo morphological changes and differentiate into RBs. Typically between 12-18 hPI, RBs undergo repeated binary fission throughout this middle part of the chlamydial developmental cycle, thus replicating their DNA content approximately every 2-3 hours [72, 144, 178].

[1] spp. is an abbreviation for species and it is often used when the discussion applies to *Chlamydia* generally.

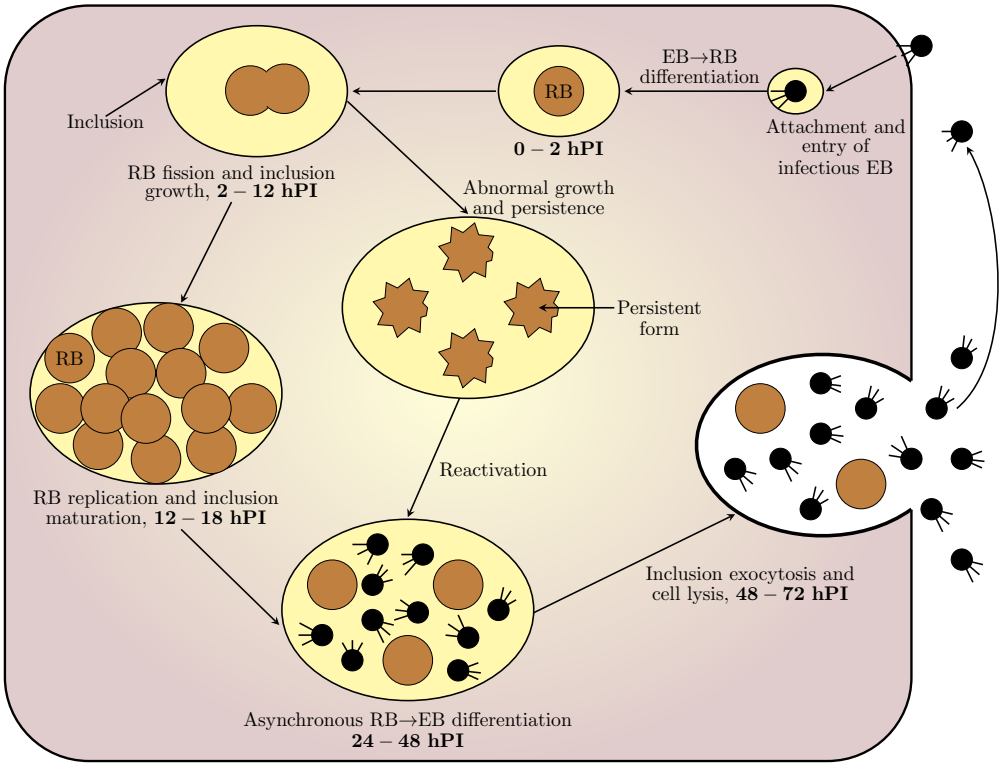

Figure 2.1: A schematic representation of the developmental cycle of *Chlamydia trachomatis*. After the internalisation of chlamydial elementary bodies (EBs) into the eukaryotic cell, they are internalised into plasma membrane-bound vacuoles of the host cell called inclusions within the first 2 hours postinfection (hPI). Between 2-6 hPI, the EBs commence differentiation into reticulate bodies (RBs). Until about 12-18 hPI, RBs undergo repeated binary fission. In the presence of growth inhibitors such as interferon-γ (IFN-γ) (which induces the production of enzymes that trigger starvation of the pathogen of tryptophan - an essential amino acid), nutrient deprivation, and antibiotic treatments, the development cycle of some of the RB form is altered, thus indefinitely taking on a non-replicating, persistent form. Between 18 and 24 hPI, the RBs peak numerically and commence asynchronous differentiation back to EBs. The lysis of the infected cell occurs at $\sim 48 - 72$ hPI, depending on the chlamydial species.

As RBs replicate, the inclusion expands, and after about 6-10 rounds of replication, some RBs de-differentiate back into EBs while other RBs continue to replicate (signifying an asynchronous de-differentiation stage). At the end of the cycle, *Chlamydia* is released from the infected cell in two mutually exclusive pathways: (1) the lytic (exocytosis) exit mechanisms, which occurs in an ordered sequence of membrane permeabilisations (inclusion, nucleus, and plasma membrane rupture), and (2) the non-lytic/extrusion/reverse endocytosis exit mechanism, which occurs when the inclusion slowly protrudes out of the cell within a cell membrane compartment, followed by an eventual detachment from the host infected cell [79, 175].

The lysis of *Chlamydia*-infected cells is a pervasive escape mechanism and it is a general phenomenon that has been commonly observed experimentally. In comparison, the chlamydial extrusion mechanism is an unusual escape pathway by intracellular bacteria [79]. Thus, in the remaining part of this thesis, we shall only consider the lytic and pervasive pathway of chlamydial release.

At the end of the chlamydial developmental cycle, when most of the RBs have returned to the EB form, the host cell lyses, after approximately 40-72 hours (depending on the *Chlamydia* species) of cell infection. This signifies the end of a complete intracellular *C. trachomatis* developmental cycle. The newly released EBs are then available to infect surrounding healthy epithelial cells [10, 53, 72].

In the subsections that follow, we discuss the different aspects of the immune system and how they respond to genital chlamydial infections. We also discuss intracellular chlamydial persistence and some mechanisms by which *Chlamydia* evade the activities of its host immune system. Finally, we discuss the pathogenesis of chlamydial infections and chronic chlamydial infections.

2.1.1 Immune response to chlamydial infections

Studies on human and animal models have shown that the immune response to *C. trachomatis* infection usually takes between four and seven days [9, 87]. The female reproductive tract has both innate and adaptive immune systems, which detect and respond to invading microbial pathogens [110, 112]. Host epithelial cells initiate inflammatory responses which dictate the pathogenesis of the infection. Inflammatory leukocytes are engaged at the infection site by the chemokine secretions of the infected epithelial cells and cellular inflammatory responses are elicited, due to the secretion of cytokines [61]. The inflammatory responses of these secretions is what promotes the recruitment of immune cells, thus buttressing the development of the innate and adaptative immune responses [18]. In most cases the response of the innate and adaptive immune cells to primary genital chlamydial infection is sufficient for the infection clearance [18].

The innate immune system, which is non-specific, is responsible for the first line of defense against pathogens [110,112]. When *Chlamydia* infects the epithelial cells of the endocervix of women, an intense inflammation occurs at the site of infection because the system is resisting *Chlamydia* by recruiting protective cells of the female reproductive tract to the infection site. These cells include neutrophils, dendritic cells, natural killer (NK) cells, and inflammatory cells (such as macrophages), which causes the early release of pro-inflammatory cytokines and chemokines [4, 105, 110, 112, 127].

The adaptive immune system, which is pathogen-specific, is triggered in response to a foreign antigen [61, 112]. Within-host, $CD4^+$ T cells modulate the immune response to an infection by differentiating into two distinct types: $CD4^+$ T helper type 1 (Th1) cells, which enhances the cell-mediated immune response to intracellular pathogen, and $CD4^+$ T helper type 2 (Th2) cells, which enhances the humoral immune response to extracellular pathogen [61]. Both immune responses to *Chlamydia* infection appear to be aimed at the sites of infection [105, 135].

Role of the humoral immune response

The humoral immune response to extracellular *Chlamydia* is primarily enhanced by Th2 cells via anti-inflammatory Th2 cytokines, especially interleukin (IL)-4 and IL-10 [61]. As noted by Schachter [135] and Loomis and Starnbach [105], the humoral arm of the immune response is believed to offer some protection against reinfection in an immune host. It does this by binding its mucosal and circulating antibodies to the pathogen, thus neutralising the antigen of some of the pathogens by blocking the ability of the infecting EBs to enter the mucosa. Antibodies also directly destroy the pathogen, thereby inactivating extracellular EBs [105, 112, 135]. Natural killer (NK) cells have also been commonly observed to lyse infected cells in a non-specific way [105,135]. Neutralising or bactericidal antibodies secreted by B cells, and targeted against the major outer membrane protein (MOMP) of *Chlamydia*, an important antigen in the clearance and control of *Chlamydia* infections, play important roles in the clearance and control of *Chlamydia* infection [4,105, 135]. However, neutralising bodies have not been confirmed to be able to offer protective immunity in human [135,176]. Their major known role is in the enhancement of T helper-1 (Th1) activation [4,112]. We note that the immune responses of Th2 cells are implicated in scarring resulting from chlamydial infections [112].

Role of the cell-mediated immune response

The cell-mediated immune response to intracellular *Chlamydia*, on the other hand, is primarily enhanced by Th1 cells via proinflammatory Th1 cytokines, especially interferon-γ (IFN-γ) (an antimicrobial, infiltrating cytokine which induces the production of enzymes that trigger starvation of *Chlamydia* of tryptophan - an essential amino acid) and interleukin (IL)-12, in humans [61]. The cell-mediated immune system removes established infection (that is, when the organisms have become intracellular) [105,135,168]. Although the mechanism behind the immuno-pathogenesis of *Chlamydia* infection is not fully understood [112], studies have, however, shown that the Th1-like $CD4^+$ T cell-mediated immune responses, as compared to the humoral immune response, plays the dominant role in protective immunity [4, 68, 105, 135, 176]. They are recognised to be of immense importance in the resolution (clearance) of the infection throughout the development cycle [61, 87]. While mature dendritic cells can activate *Chlamydia*-specific naive $CD8^+$ T cells, the optimal formation of *Chlamydia*-specific $CD8^+$ memory T cells requires the help of $CD4^+$ helper T cells [105]. The $CD8^+$ sequentially responds both by secreting IFN-γ [129, 137]) and by specifically lysing *Chlamydia*-infected cells. This lysing of *Chlamydia*-infected cells deprives them of their replicative *niche*, thereby disrupting their developmental cycles [96,105]. This is the key mechanism by which $CD8^+$ T cells control *Chlamydia* replication. Nevertheless, $CD8^+$ and $CD4^+$ T cells infiltrate during chronic or repeat infections driving a recurrent inflammatory response which eventually leads to the pathological effects of chlamydial infections [112].

In the clearance of a primary chlamydial infection, a wealth of data have shown that a central role is played by IFN-γ in producing Th1 responses, which develops over time during the infection [61, 106]. Besides lysing infected cells, IFN-γ also stimulates and activates other elements of the immune system. It is a potent activator of macrophages. IFN-γ-activated macrophages destroy elementary bodies phagocytosed at the site of infection [96]. IFN-γ has been seen to inhibit chlamydial growth in vitro [105]. IFN-γ can also destroy intracellular *Chlamydia* at the RB stage [96, 135]. Thus, the production of IFN-γ by *Chlamydia*-specific $CD4^+$ (primarily) and *Chlamydia*-specific $CD8^+$ T cells is of great importance to the resolution of, and protection of the host against *Chlamydia* infections [4, 96, 104, 105, 110, 135].

2.1.2 Persistent chlamydial infection

Irrespective of the fact that the host immune system initiates an inflammatory response during a primary infection, *C. trachomatis* still persists asymptomatically in many individuals [10]. Chlamydial persistence is a reversible state in which *Chlamydia* exists in a viable but non-cultivable form, resulting in a long-term association between *Chlamydia* and the infected host cell [75, 178]. These non-cultivable chlamydial forms, which are developed in the presence of some inducers, are morphologically large, non-infectious, non-replicating, and aberrant RBs, and are commonly referred to as the "persistent" form of *Chlamydia* [10, 18, 61, 178]. In the presence of growth inhibitors, such as IFN-γ, nutrient deprivation, iron deficiency, monocyte infection, phage infection, concomitant herpes simplex virus infection, and penicillin, the chlamydial developmental cycle of some of the intracellular *Chlamydia* (RB form) is altered (see Figure 2.1), thus assuming the persistent form indefinitely [10, 18, 178]. However, once these growth inhibitors are removed, the persistent bacteria differentiate back into infectious forms [18, 61].

Chlamydial persistence is also a key contributor to treatment failures [123]. Indeed, it has been reported that even after treatment, *Chlamydia* is able to exist in a persistent state which is undetectable by cell culture and immunoassay [43, 76, 117]. These persistent forms may allow subclinical progression of persistent *Chlamydia* infections [123].

In virtually all hosts of different *Chlamydiae* species, *Chlamydiae* also reside in the gastrointestinal (GI) tract chronically and asymptomatically [34, 128, 180]. It has been demonstrated that in humans, persistent chlamydial infections may actually be (mainly) caused by infection of the GI [128]. The innate and adaptive immune system is unable to clear *Chlamydia* from the GI reservoir, just like other microbiota in the gut. Thus, *Chlamydia* indefinitely remains in the gut, with continual shedding in feaces [128, 180]. Chlamydial infection of the GI tract is not a focus of this study, hence, it will not be elaborated upon.

2.1.3 Chlamydial evasion of the host defense system

Chlamydia has developed a number of mechanisms by which it protects infected cells from the host defense system. One mechanism involves the release of certain proteolytic enzymes. One such enzyme is the proteasome/protease-like activity factor (CPAF), which is able to cleave DNA and many other cellular proteins [78,141,174]. Another such enzyme is *Chla*Dub1, a protein encoded by *Chlamydia trachomatis*, which has deubiquitinating[2] activity, and can inhibit the transcription factor NF-κB - a key signalling protein involved in the regulation of the host inflammatory response [98].

CPAF plays a major role in *Chlamydia* pathogenesis, being a virulence factor. It plays a major role in inhibiting the presentation of chlamydial antigens by major histocompatibility complexes (MHC) to immune cells [10]. CPAF aids in the modification of cytoskeletal proteins that lead to cell lysis [175]. It is essential for *Chlamydia* replication [27]. Within the cytoplasm of infected cells, CPAF protein accumulates as the chlamydial developmental cycle progresses [78, 177]. The activity of CPAF peaks at about 36-48 hours post-infection, when most intracellular *Chlamydia* must have differentiated into infectious elementary bodies [78]. CPAF activity is indispensable in different stages of the chlamydial developmental cycle, such as the reticulate body stage which is the replicating stage [27]. CPAF is also thought to aid the cell-to-cell spread and ascension of C. trachomatis on its extracellular release from lysing infected cells [152].

Studies have also shown that genital serovars of *Chlamydia trachomatis* can escape IFN-γ-mediated clearance by using indole provided by the local microbial flora of the female genital tract to biosynthesise tryptophan [10, 18]. As discussed, *Chlamydia* exists in a persistent form within its host. One way *Chlamydia* maintains its persistence within host cells is by interferring with multiple proapoptotic pathways and potential necrotic cell death in order to guarantee survival within its host. *Chlamydia* has also evolved a mechanism whereby it limits the recognition of its pathogen-associated molecular patterns (PAMPs) (by the innate immune system) by ascertaining that the inclusions are stable during the intracellular stage of infections [10].

It has also been suggested that the extrusion mechanism of the release of *Chlamydia* bodies from an infected cell may also provide protective benefits for *Chlamydia*. *Chlamydia* bound by the extruded membrane may be shielded from pre-existing local immune responses. The ensuing lysis of the membrane, and release of free *Chlamydia*, may then happen when the membrane has moved to a 'safer' location [79]. On the other hand, the extrusion may be engulfed by macrophages, thereby promoting secondary infection and spread of *Chlamydia* within the host [79]. Thus, chlamydial exit mechanisms are suggested to be important determinants of chlamydial pathogenesis [175].

[2] A deubiquitinating enzyme is a protease that cleaves ubiquitin - a small regulatory protein found in most tissues of eukaryotic organisms - from proteins and other molecules.

2.1.4 Pathogenesis of genital chlamydial infection

It has been reported that severe pathological damages of *Chlamydia* infection are caused by tissue scarring and inflammation. The aspects of the immune response and cytokine levels that yield immunopathological disorders, such as pathological inflammation that does not mediate the removal of intracellular *Chlamydia*, however remains unclear, and is a crucial research priority [61]. Two main hypotheses of *Chlamydia* genital infection have been put forward: (1) the immunological hypothesis which supports the notion that tissue damages are central to pathogenesis, and they are induced by the host immune response. In humans, the presence of a high density of *Chlamydia*-specific antibody is highly correlated with severe sequelae such as tubal infertility; and (2), the cellular hypothesis which suggests that tissue damages are caused by persistently infected cells which stimulate the production of pro-inflammatory cytokines. These cytokines are deleterious and can cause tissue damage and chronic inflamamtory cellular responses [18, 131].

Another important issue that needs to be resolved in *Chlamydia trachomatis* infection studies is whether immunity to reinfection develops naturally, and if so, the duration of the immunity after a natural infection, and whether different time intervals of chlamydial treatment can affect the development of this immunity [127]. While a lot of useful insights into *Chlamydia* infection have been achieved with the use of animal models, limitations still exist in extrapolating data from these models to make inferences on humans. As *Chlamydia trachomatis* infection is to humans, so is *Chlamydia muridarum* (with its genes mostly identical to those of *Chlamydia trachomatis*) infection to mice, and *Chlamydia caviae* infection to guinea pig. However, *Chlamydia* infection in the latter two animal models are gut parasites [61, 127]. A fundamental difference between humans and animal models is the duration of infection; for example, *Chlamydia muridarum* infection in mice is mostly cleared in approximately 4 weeks while *Chlamydia trachomatis* infection in humans can take several months before spontaneous clearance [18, 61]. In addition, while *Chlamydia trachomatis* can evade the IFN-γ-mediated defence mechanism, *Chlamydia muridarum* cannot [18].

Some studies demonstrate that while *Chlamydia* innoculation in animal models generally leads to an initial rapid peak of *Chlamydia*, followed by an extended plateau level, and then a rapid clearance of *Chlamydia* in about 3-4 weeks, in humans, peak infection may not even occur for months. In addition, the probability of the resolution of infection increases over time, with about half of *Chlamydia* infections being spontaneously resolved approximately a year after initial testing of studied individuals, while the other half persists (see [61] and its references). Many studies actually report that chlamydial infection duration in humans is probably in the order of years [61]. This fundamental difference, coupled with the inavailability of precise data on the duration of the infection in humans, have been the major challenges of chlamydial studies. Another limiting difference between the infection in animal models and humans is that while animal models can be innoculated at controlled times (and mostly not via the natural route - sexual transmission), *Chlamydia* infection

in humans does not happen at just a single defined time. Rather, an individual may be repeatedly innoculated because sexual activity with an infected person can happen several times over a short period of time. The only animal model in which sexually transmitted infection has been achieved is the guinea pig, where the animals were observed to be immune to infection, which suggests that "sexual transmission elicits a protective immune response" [127].

2.1.5 Chronic or recurrent chlamydial infections: repeat/persistent infection

Chronic (or recurrent) chlamydial infections, which are consequences of either chlamydial persistence, or repeat infection (re-infection), are more precarious than acute infections [106]. Experimental studies indicate that the presence of the same chlamydial serovar (after a previously cleared infection) suggests chlamydial persistence, while a new serovar suggests reinfection [38]. Human epidemiological studies have also shown that with repeat chlamydial infection comes a higher risk of disease [35]. It has been observed that when chlamydial antigens give a chronic or recurrent stimulatory action, delayed hypersensitivity reactions or rare type 3 hypertensitivity reactions (Arthus reaction) are given off [106]. Animal models also show that there is a rapid and large infiltration of $CD4^+$ and $CD8^+$ T cells, as compared to neutrophils, during repeat oviduct infections [35]. This higher infiltration of cytotoxic cells, in comparison to what happens during a primary infection, leads to a robust inflammatory response [35]. Consequently, the recurrent inflammatory reactions, and other processes which occur during chronic chlamydial stimulatory actions, lead to fibrosis, tissue scarring, and cicatrisation within the organ affected [35, 106]. All these have been associated with severe sequelae such as pelvic inflammatory disease, ectopic pregnancy, infertility, and many other reproductive diseases [38, 106].

Although a single infection can elicit a long-term partial protective immune response or a short-term complete immunity, animal models have revealed no evidence of enhanced immunity as a consequence of multiple exposures [127]. Importantly, it has been reported that protective immunity does not remove the severe sequelae of the infection in the upper genital tract of its host [127]. Tissue damage at the level of the oviduct is the primary cause of the chronic morbidities of chlamydial infections. Since the goal of chlamydial control programs is to prevent complications in the reproductive tract, there is a need for the development of more effective (or alternative) treatment regimen for (chronic) chlamydial infections, especially before the oviduct becomes infected, or to shorten the duration of the infection of the oviduct [35, 38].

2.2 Antibiotic treatment of *Chlamydia trachomatis* genital infection

Chlamydia infection is treatable with antibiotics. Some antibiotics exert their antimicrobial activity on *Chlamydia* through the inhibition of its protein synthesis. The *Chlamydia* form that synthesises proteins is the reticulate body. Hence, for a successful and effective antimicrobial inhibition of *Chlamydia*, *Chlamydia* must be in the reticulate body stage of growth [129]. A class of antibiotics which is one of the most clinically important antibiotics are macrolides [58]. Macrolides inhibit protein synthesis, and consequently stall cell growth, by binding to the large ribosomal subunit which is inside the nascent peptide tunnel and in the vicinity of the peptidyl transferase centre [58, 90, 103, 122].

A study by Peuchant *et al.* [123], on the effects of antibiotics on the viability of *C. trachomatis*, has revealed that antibiotics such as azithromycin, doxycycline, moxifloxacin, and ofloxacin are only bacteriostatic, even at concentrations much higher than the minimum inhibitory concentration (MIC) [123]. The study, which used a quantitative real-time PCR assay to monitor the temporal accumulation of chlamydial chromosomal DNA, defined the antibiotic MIC as the concentration for which no chlamydial RNA was transcribed [123]. Several other studies have also confirmed that macrolides are typically bacteriostatic on *Chlamydia* [90, 123].

Azithromycin is an effective antimicrobial agent against sexually transmitted pathogens. It is the prototype of a subclass of macrolides (antibiotics) known as azalides [119]. It is a *broad spectrum antibiotic*, in that it is highly active against several Gram-positive and negative organisms [56,119]. Numerous *in vitro* studies have confirmed that azithromycin is highly active against several strains of *C. trachomatis*, as it successfully inhibits their growth [3,119,139]. It is effective in the treatment of uncomplicated genital *C. trachomatis* infections [99, 111]. In additon, azithromycin is expected to concentrate intracellularly in organelles with a low pH, such as lysosomes and phagosomes [119]. This implies that even pathogens that survive inside phagocytic cells, such as *Chlamydia*, can still be inhibited intracellularly by azithromycin.

The pharmacokinetic properties of antibiotics that inhibit *Chlamydia* can be highly variable. While azithromycin is transported to infection site via phagocytic cells (which are products of the host immune response to the infection), doxycycline, which has a high lipid solubility, is rapidly distributed into tissue and infection site [91]. In the treatment of upper reproductive tract infection, azithromycin reduces inflammation and may be more efficacious than doxycycline in this regard [126]. This is likely because azithromycin specifically accumulates at inflammation sites, due to its high cellular concentration, particularly in phagocytes [122]. Several studies have compared the effect of different antibiotics, which include a single 1-g oral dose of azithromycin and the 1-week long course of 200 mg/day of doxycycline, on *C. trachomatis*. The former has been observed to be as effective for the treatment of uncomplicated *C. trachomatis* infections as the

latter [3, 99, 111]. Ninety percent of cases of *C. trachomatis* infection have been seen to be inhibited by 0.5 μg/mL of azithromycin [119]. Some studies have however shown lower efficacy for azithromycin in comparison to doxycycline [92, 126].

Steingrimsson *et al.* [150], in a randomised third-party blinded two-phase study of 182 patients, compared three regimens of azithromycin and a standard regimen of doxycycline in the treatment of some sexually transmitted diseases (STDs), in order to test for their clinical efficacy and safety. The STD cases treated include *Neisseria gonorrhoeae*, *Ureaplasma urealyticum*, and *C. trachomatis*. The three oral doses of azithromycin administered were; a single-dose 1 g of azithromycin, a 500 mg twice a day dose for one day, and a 500 mg dose on the first day, followed by 250 mg on the second and third day. A standard regimen of doxycycline is 100 mg bd for seven days. Genital pathogens were isolated from 172 patients, of which 89 had *C. trachomatis* only, 19 had *N. gonorrhoeae* only, and nine had *U. urealyticum* only. The result of their study, which excludes those patients who had positive cultures during their follow-up visits (at one, two, and four weeks), and those that did not go for their follow-up visits, shows that azithromycin was highly effective in the treatment of their patients with *C. trachomatis*, of which 95% were cured. Azithromycin was also observed to be as effective or more effective than doxycycline. Their report concludes that azithromycin is close to being *"an ideal antibiotic for the treatment of sexually transmitted diseases than any of the antibiotics now commonly in use"*.

One of the major factors to be considered in the administration of multiple-dose regimens of antimicrobials to a patient, in the treatment of sexually transmitted diseases, is the patient's compliance to the drug regimen [150]. The fact that a single dose of azithromycin is effective in the treatment of many sexually transmitted infections makes it a great alternative to other effective antimicrobials [56, 150]. A good guide for predicting the efficacy of a drug is the drug's concentration at the tissue site of infection [119]. Azithromycin has been reported to achieve a high serum and (prolonged) tissue level sustenance [139]. It also has a high serum half-life, with its tissue concentrations being about 400 times that of its serum concentration [150]. Azithromycin's long half-life of about 2-4 days in most human tissue contributes to its being an efficient single-dose antibiotic in the treatment of chlamydial infections [56,150]. Its tissue levels are higher than the minimum inhibitory concentration (MIC) for many common pathogens.

Azithromycin's MIC for *C. trachomatis* is 0.25 μg/mL, but it requires 1.0 μg/mL for inclusion formation to be *absolutely* inhibited [43, 56, 150]. Azithromycin has also been reported to be well tolerated in most patients [150]. Its tissue concentration in the lung, tonsil, genital tissues, and many other tissues is > 3 mg/kg (or mg/L) [56,119]. Standard susceptibility testing for azithromycin reveals that organisms susceptible to its antimicrobial efficacy are those with MICs ≤ 2.0 mg/L, which is one that azithromycin can easily attain in tissues. Azithromycin has also been shown to be competent in treating infections in animal models and its efficacy with respect to its high tissue concentrations has also been established in animal models [56,150]. Thus, treatment guidelines for uncomplicated

urogenital *C. trachomatis* infection recommend the first line of treatment to be a single 1 g oral dose of azithromycin [91]. Another commonly recommended regimen is the twice daily 100 mg of doxycycline taken for 7 days, but this regimen is less preferred due to compliance issues [92, 126].

2.2.1 Chlamydial infection treatment failures

Despite *azithromycin*'s *in vitro* efficacy of about 85-95% [3, 111], there have been several debates as to whether *azithromycin* is actually the ideal antibiotic treatment for chlamydial infections [67]. This is because treatment failures are sometimes recorded even when azithromycin was appropriately administered and this is increasingly becoming a concern [15, 44, 91, 92], with some studies suggesting that higher organism load in individuals treated with azithromycin may be related to azithromycin treatment failure [15, 76, 92].

Moreover, although earlier studies have indicated that azithromycin has an efficacy of more than 95%, there is emerging evidence that significant proportions of repeat infections (>5%), that exclude reinfection, are consequences of treatment failures (see [76, 77, 92, 138], and their references). Treatment failures have often been attributed to reinfection but there is increasing evidence that relapses could be the results of chlamydial recurrence/persistence in treated patients [38, 43, 60, 76, 77, 117].

In women not at risk of reinfection, two studies have observed a treatment failure rate of approximately 8% [11, 60, 77]. These studies do not have the limitations of previous studies that report high (>95%) cure rates. Such limitations include short follow-up durations and the use of cultures or immunoassays rather than sensitive nucleic acid amplification testing (NAAT). In *in vitro* cell cultures, the lack of detection of chlamydial infection does not imply the absence of viable *Chlamydia* which can be revived after the removal of antibiotics [123]. Thus, previous high cure rates may have been overestimated [11, 67, 76, 77, 92]. On the contrary, evidence exist that persistent *Chlamydia* may not be detected by even NAAT if the sampled cells are from the mucosal surface only [38, 76].

These data suggest that regardless of the acceptance of a single-dose treatment with azithromycin, there is a need for improved treatment regimens to be sought [11, 67, 76, 77, 92]. Although treatment failure has been reported, chlamydial drug resistance have not been established [91, 126]. It is also worthy of note that more treatment failure has been observed with azithromycin administration than with doxycycline [59, 91].

Chlamydia infection of the GI tract may also largely contribute to chlamydial treatment failures. In animal models, it has been demonstrated that azithromycin is far less effective in the treatment of chlamydial GI infection than against genital chlamydial infections [128]. Thus, there is a possibility that women successfully treated of genital chlamydial infections remain infected in the GI tract, and can become genitally re-infected with *Chlamydia* by auto-innoculation from the GI tract [128, 180].

Treatment failure promotes ongoing transmission and is likely to put women at increased risk of developing chronic severe sequelae [76, 77]. Thus, in the clearance of chlamydial infections treated with bacteriostatic antibiotics, antibiotic activity alone does not suffice but also the ability of the host immune system to eradicate the remaining pathogen [123].

2.3 Potential anti-*Chlamydia* treatments

In this section, we discuss two potential anti-*Chlamydia* treatments that are currently being developed according to the literature.

2.3.1 The use of Tryptophan supplementation in the clearance of chlamydial persistence

As previously discussed in Subsection 2.1.1 and Subsection 2.3.1, IFN-γ inhibits bacterial growth by inducing indoleamine 2,3-dioxygenase (IDO), an enzyme regulated by the immune system, which depletes or metabolises L-tryptophan [131,136]. This IDO-mediated depletion of intracellular pools of tryptophan starves *Chlamydia trachomatis*, which is a tryptophan auxotroph [80], of this essential amino acid, thereby inducing bacteriostasis and leading to the development of persistent chlamydial forms [61, 131, 136]. A rapid re-differentiation of these persistent forms occurs when the pool of tryptophan returns to normal levels [131].

1-DL-Methyl-tryptophan (1-MT) is a biosynthetic analog of tryptophan (methylated tryptophan) [14, 20, 26, 31]. It is obtained from tryptophan (Trp) by the replacement of the hydrogen atom on the indole nitrogen of Trp by a methyl group [20]. *In vitro* experiments have shown that the addition of 1-MT is able to reverse or inhibit indoleamine 2,3-dioxygenase (IDO)-mediated tryptophan metabolism and its other antimicrobial or immunoregulatory functions, by directly permitting the growth of parasites or T cells [136].

While several *in vitro* models using different cell lines or cancer cells report that the L (but not D) isomer of 1-MT was able to abrogate the IDO-mediated arrest of T cell proliferation, and IDO activity in (IFN)-γ-treated HeLa cells, the D isomer of 1-MT was significantly more effective in the reversal of IDO-induced tumour growth *in vivo* [136]. An *in vitro* study by Schmidt *et al.* [136] reports that IDO-mediated antimicrobial effects (such as inhibition of bacterial growth) caused by tryptophan depletion can be abrogated by 1-L-MT. They also show that 1-L-MT can reinstate the immunoregulatory effects of IDO [136]. Another *in vitro* study by Ibana *et al.* [80] also reports that the use of levo-1-methyl-tryptophan (L-1MT), a specific IDO inhibitor (which can accumulate to equilibrium levels needed for adequate inhibition of IDO *in vivo*), in an *in vitro* model of IFN-γ-induced chlamydial persistence, delayed the depletion of tryptophan induced by the activity of IFN-γ until the late stage of the chlamydial developmental cycle. This delay caused a blockage of IFN-γ-induced chlamydial persistence. They also observed

that L-1MT reactivates established persistent *Chlamydia* forms, thereby becoming actively replicating RBs intracellularly. Ibana *et al.* [80] also reports that the addition of L-1MT to their IFN-γ-exposed infected HeLa cell culture does not support the productive replication of *Chlamydia* intracellularly, as the number of EBs produced by lysing infected cells was significantly reduced. The efficacy of antibiotics (doxycycline in particular) in the clearance of persistent *Chlamydia* was also improved. Singla [145] also suggested this, reporting that a better therapeutic treatment of chronic *Chlamydia* infection, if there is a sufficient supply of tryptophan, at about 48-72 hours post-infection, before, and with antibiotic treatment, persistence may be eradicated, thereby effectively treating the chronic infection. It was also suggested that this therapy may be useful even in acute infections as the treatment strategy would increase *Chlamydia*'s susceptibility to antibiotics, while also decreasing the production of persistent *Chlamydia* [145]. These results are promising and they point to the fact that a tryptophan and antibiotic combination treatment may facilitate an improved treatment of chronic *Chlamydia* infections.

2.3.2 The inhibition of CPAF activity in anti-*Chlamydia* drug development

The inhibition of CPAF activity can potentially play a role in the development of anti-*Chlamydia* drugs. [27, 78]. The inhibition of CPAF function is expected to restore the ability of *Chlamydia*-infected host cells to express their major histocompatibility complex antigen, which will in turn allow the presentation of chlamydial peptides to T cells [141]. Its inhibition can also prevent intracellular replication of *Chlamydia* in humans [27]. The proteolytic activity of CPAF cannot be blocked by protease inhibitors except the irreversible proteasome-specific inhibitor lactacystin [27, 30, 78, 141]. A modified tetrapeptide, z-WEHD-fmk (WEHD-fmk) also inhibits CPAF-dependent proteolysis [27]. These inhibitors provide opportunities for the development of anti-*Chlamydia* drugs [78]. In the reduction of chlamydial pathogenesis and burden, blocking CPAF may be an effective therapeutic strategy [27, 78].

2.4 The development of a *Chlamydia trachomatis* vaccine

Although no *Chlamydia* vaccine has been approved for use in humans, a number of candidate vaccines have been previously identified and tested in various delivery systems [4, 47, 48, 68, 82]. These candidate vaccines are largely based on the use of defined recombinant proteins (proteins whose codes are expressed by recombinant DNA) [104]. Tested vaccine candidates include inactivated, live whole organisms, subunit vaccines, various chlamydial antigens, recombinant proteins and peptide vaccines [4, 68, 86, 104]. The most promising subunit vaccine candidates are *C. trachomatis* outer membrane proteins such as MOMP, Outer membrane protein 2 (Omp2), and polymorphic membrane proteins (Pmps) amongst many others [46, 48, 63, 104]. More recent and promising vaccine candidates include, but are not limited to, live, attenuated (plasmid-free) strain of *C.*

trachomatis [84, 104] and *Vibrio cholerae* ghost (VCG; empty *V. cholerae* cell envelopes devoid of cytoplasmic contents and cholera toxin)-based chlamydial vaccines [45–48].

The types of potential anti-*Chlamydia* vaccines recommended by the World Health Organisation (WHO) are those with high efficacy and that confer long-term protection [163]. In other words, the ideal *Chlamydia* vaccine would be one that can reduce or eliminate infection significantly and confer sterilising immunity, while also reducing, or eliminating, the adverse pathology of the disease in the upper genital tract of females in particular [63, 81, 104]. Such a vaccine mimics, and should even be better than, the natural immune response to the infection, while not inducing the severe inflammatory reactions often associated with *Chlamydia* infection [110]. It has been suggested that for the development of such an efficacious chlamydial vaccine, more effective delivery systems need to be advanced, and effective immunomodulation should be used [48,68,82,86,110]. This is because effective delivery systems are expected to boost the induction of adequate levels of mucosal T-cells and antibody responses that mediate long-term protective immunity [48,68]. Studies have shown that *Chlamydia* vaccines delivered *via* mucosal routes are promising (as they (locally) induce high levels of *Chlamydia*-specific IFN-γ, and consequently, an enhanced protective immunity) [4, 48, 68, 82, 149]. However, while most *Chlamydia* vaccine trials have only evaluated protective immunity up to 4 weeks post vaccination [63], a recent experimental study by Stary *et al.* [149], which constitutes a major advancement in *C. trachomatis* immunobiology [17], have been able to identify some bio-profiles of a vaccine that can confer long-lived protective immunity [17, 48, 63, 149].

Stary *et al.* [149] report that mucosal vaccination of mice with ultraviolet light-inactivated *C. trachomatis* conjugated to charge-switching synthetic adjuvant nanoparticles (UV-Ct-cSAPs) brought about a robust *C. trachomatis*-specific antibody response that was equivalent to that elicited by *C. trachomatis* infection. This response was also twice as robust as vaccination with just ultraviolet light-inactivated *C. trachomatis* (UV-Ct). They stressed the fact that the vaccination route in eliciting long-lived protection is important, irrespective of the kind of vaccine given. The UV-Ct-cSAPs vaccine induces a wave of effector T cells (T_{EFF}) which seeded the uterine mucosa during the first week after vaccination. These T_{EFF} then established tissue-resident memory cells (T_{RM}) (in both resting and inflamed mucosal surfaces) thereafter, which persisted for at least six months even in the absence of local *Chlamydia* antigens. These cells were also referred to as first wave of mucosal-tropic memory cells. Non-mucosal vaccines do not induce this first wave.

There was also a second wave of vaccine-induced circulating memory T cells (T_{CM}) which preferentially resided in blood and lymphoid tissues, from where they survey the body for *Chlamydia* antigens. The concentration of these T_{CM} is more than that of T_{RM}. These T_{CM} were produced irrespective of the mucosal route. They however do not traffic to resting uterine mucosa. In the absence of pre-existing T_{RM}, they were slow to access the uterus when vaccinated mice were rechallenged with *C. trachomatis* via the uterus. However, in mucosal-vaccinated mice, upon *Chlamydia* rechallenge, uterine-T_{RM} instantly

responds to chlamydial infection and they initiate the speedy recruitment of *Chlamydia*-specific T_{CM} [149] to peripheral tissues, including uterine mucosa. For optimal clearance of *C. trachomatis*, T_{RM} must be established, otherwise, the clearance would be sub-optimal even in the presence of abundant circulating memory cells. The two waves of memory T cells are however crucial to optimal clearance of *C. trachomatis* infection. Interestingly, when humanised mice (mice that have been genetically reconstituted with a human immune system) who were vaccinated (*via* mucosal routes) with UV-Ct-cSAP were rechallenged with intrauterine *C. trachomatis* infection, a vigorous mucosal T_H1 response that cleared *C. trachomatis* infection was elicited. This suggests that such a vaccine may also elicit such protective immunity in humans [149].

2.5 Mathematical models of *Chlamydia trachomatis*

The ultimate goal of chlamydial control programs is to prevent reproductive tract complications. Because of this, it is imperative that an understanding of how chlamydial infection leads to sequelae be established [35]. Mathematical models are very useful in describing the within-host dynamics of *C. trachomatis* [9, 169], and they have become central tools used to comprehend infectious disease transmission and the epidemiological processes that underlies it. They also aid the design of effective control strategies [159]. Despite this fact, only a few (within-host) mathematical models of *Chlamydia* have been developed. In this section, we give a brief summary of such mathematical models to date, followed by a comprehensive review of selected models related to our study.

Wilson and colleagues have presented a number of models of the within-host dynamics and developmental cycle of *C. trachomatis*. Wilson *et al.* [170] developed a within-host model of the chlamydial developmental cycle (CDC) that fits a real-time polymerase chain reaction (PCR) technology data. Their model predicted an average RB generation time of 2.6 h for the CDC. In another in-host model, an expression for the valence (number of sites available for binding by antibodies) was developed [171]. Also incorporated into the model is the tracking of the aggregation of antibody fragment antigen-binding (Fab fragment) and host cell receptors over extracellular EBs. A mathematical model based on a contact-dependent type III secretion (TTS) system hypothesis has also been presented [167]. Their model showed that within an infected host cell, there is an optimal number of inclusions that are able to attain maturity and thus produce further progeny EB.

Several mathematical models have been used to describe the dynamics of *Chlamydia trachomatis* in humans. Many such recent models have their basic structure and derivation in Wilson's model [169]. Hoare *et al.* [72] developed a model of the CDC, under the assumption of an hypothesis (and which eventually confirmed the hypothesis) that tried to explain the mid-to-late stages of the CDC. The hypothesis states that an increase of the RB radius, and/or the number of inclusions per infected cell contributes to the development of persistent chlamydial infection. Mallet *et al.* [107] also proposed a one dimensional spatiotemporal mathematical model of chlamydial infection, which uses the

structure of the model proposed by Wilson [169], and it incorporates the host immune response and the movement of infectious *Chlamydia* in the host genital tract. Furthermore, another study by Bagher-Oskouei *et al.* [9], which is an extension of the model proposed in [107], proposed a two dimensional mathematical model that investigates the interaction between *Chlamydia trachomatis* and the host immune system. This model describes the ascension process of the pathogen up the female genital tract via diffusion and the migration of the host immune cells towards infected epithelial cells via chemo-tactic movements, with pro-inflammatory cytokine such as diffusable IFN-γ acting as the chemical (concentration) signals to which immune cells move (i.e. a region of higher concentration of IFN-γ molecules). The model allows for spatio-temporal variation in the biological species in question. Vickers and Osgood [159] also proposed an immuno-epidemiological model of *Chlamydia* transmission dynamics with an emphasis on how treatment impacts transmission. They used prototypical networks to group individuals in order to show how the population are evolving dynamically and the interdependencies present within, and between hosts. Other models have also been developed, looking at dynamics of cell populations and infectious *Chlamydia* forms [9, 19, 32, 107–109, 142, 160, 169], however these are not directly relevant in the present study.

In the subsections that follow, we present a comprehensive review of the literature on a few selected mathematical models of the within-host dynamics of *Chlamydia trachomatis* and the immune response. The reviewed models investigated the role of the immune system, both the humoral and cell-mediated immune responses, in the chlamydial development cycle. Wilson and colleagues used a mathematical model to understand the impact of the cell-mediated arm (adaptive immunity) of the immune system on the pathogenesis and clearance or control efficiency of chlamydial infections [168]. Wilson [169] also investigated chlamydial infection dynamics by presenting a mathematical model that describes the changes in the iterative processes between *Chlamydia* and the host cells. The study presented a mathematical framework upon which most mathematical models of *Chlamydia* to date are based. Sharomi and Gumel [142] also proposed two deterministic ordinary differential equations model of the transmission dynamics of *Chlamydia in vivo*. They incorporated the effects of the humoral immune response and the cell-mediated immune response. Vickers *et al.* [160] developed two ordinary differential equation models to investigate the dynamics of the host immune response under repeated chlamydial infection.

These models shall be discussed shortly.

2.5.1 Mathematical model for the Th1 cell-mediated immune response against *Chlamydia*

In order to comprehend the impact of the cell-mediated arm (adaptive immunity) of the immune system on the pathogenesis and clearance or control efficiency of chlamydial infections, Wilson *et al.* [168] did a theoretical investigation by developing a mathematical model. To the best of our knowledge, this is the first mathematical model of the

within-host dynamics of *Chlamydia* (and the immune response). The model investigates the effect of varying T helper-1 (Th1) cell-mediated response against infected cells over the chlamydial developmental cycle. Their within-host model incorporates the interconversion between RB and EB forms (the replicating and infectious forms of *Chlamydia* respectively) and tracks the population of *Chlamydia* inside one inclusion over a single developmental cycle. They also separately modelled the dynamics of cellular immunity and its efficiency was studied. Their model assumed that an immune response is triggered once RB replication commences, and the response is most effective when RB reaches its maximum intracellular population. It also assumed that the presence of *Chlamydia* peptides is in proportion to the number of RB forms and that lysing host cells contain EBs predominantly.

In their model, $C(t)$ represents the concentration of extracellular *Chlamydia* in the system under consideration, $A(t)$, the concentration of host cells on which *Chlamydia* have attached, and those already infected, $E(t)$, the concentration of infected cells in which EBs are converting to RBs, while $\Phi(t)$ and $B(t)$ are the concentrations of lysing host cells and cells in the persistent phase respectively. $R(t)$ and $I(t)$ are the total concentrations of host cells containing purely replicating RBs, and of host cells in which RBs are replicating (whilst RBs in other cells in this phase are differentiating to EBs) respectively. Since during one chlamydial development cycle, replicating or differentiating *Chlamydia* mature asynchronously and immune response varies at different *ages* of a phase, they introduced the concept of different stages of maturity into the model using a time parameter r (a continuous variable). r, $r_0 \leq r \leq r_3$ (stages), denotes the *maturity* of an infected cell, where; EB-to-RB differentiation occurs during the time/maturity from $r = r_0$ to $r = r_1$, an original RB triggers purely binary and successive waves of replication for $r_1 \leq r \leq r_2$, and RB-to-EB differentiation occurs from $r = r_2$ to $r = r_3$. The maturity of an infected cell is determined by the phase of the *Chlamydia* within its inclusion.

The population of RBs of maturity r within a single inclusion is denoted by $R_B(r)$, P is the burst size (number of EBs) of a lysed infected cell, and k_js are rate constants that specify the speed with which the development stage they represent (determined by their subscripts) progresses. The natural mortality rate of extracellular *Chlamydia* is denoted by λ and α is the proportion of *'burdened'* host cells that enter into the lysis stage from $\rho(r_2)$ $(0 \leq \alpha \leq 1)$. The effect of attachment blocking of EBs by antibodies is denoted by θ, with $(0 \leq \theta \leq 1)$, where $\theta = 1$ implies that that the host cell could not be infected (absolute blocking). The rate that models feedback from the persistent phase to the lytic cycle is denoted by β. The cytotoxic effect of the immune system against an infected cell of maturity r is denoted by $\mu(r)$, while η is the rate at which the immune system responds to one intracellular RB particle.

The dynamics of intracellular *Chlamydia* during one developmental cycle was described. In order to determine the within-inclusion RB and EB population during a *Chlamydia* developmental cycle, some essential assumptions were made. They assumed that by the time of lysis of infected cells, the differentiation of all RBs to EBs have commenced.

This does not exclude the likelihood of a significant number of RBs of being in the transformation process. Let the constant $\hat{k}$ be the RB binary fission rate and parameter $l(r)$, the conversion rate at which an RB commences differentiation to an EB. If the RB doubling time is an average of T hours, then $\hat{k} = (1/T)\ln 2$. The number of differentiating RB-to-EB bodies (at time/progression r, $r_2 \leq r \leq r_3$) that have progressed a maturity χ, $0 \leq \chi \leq r^*$, is denoted by $\tau(\chi, r)$. A fully mature EB is represented by $\tau(r* = r_1 - r_0 = r_3 - r_2)$. The relation $r_1 - r_0 = r_3 - r_2$ implies that EB-to-RB differentiation and RB-to-EB differentiation have the same time period. The total number of existing EBs at some time r through the developmental cycle is denoted by $E_B(r)$. Thus, the following system of equations determine the within-inclusion RB and EB population during a *Chlamydia* developmental cycle:

$$\frac{\mathrm{d}R_B}{\mathrm{d}r} = \begin{cases} \hat{k}R_B(r), & r_1 \leq r \leq r_2, \\ \hat{k}R_B(r) - l(r)R_B(r), & r_2 \leq r \leq r_3, \end{cases} \tag{2.1}$$

$$\frac{\partial \tau}{\partial r} = -\frac{\partial \tau}{\partial \chi}, \tag{2.2}$$

$$E_B(r) = \int_{r_2}^{r} \tau(\chi = r^*, \zeta)\mathrm{d}\zeta. \tag{2.3}$$

Equation (2.1) describes the change in RB population within an inclusion. Equation (2.2) is based on the assumption that RB-to-EB transformation progresses through the spectrum of chlamydial forms with time (that is an age-structured representation). It describes how the RB-to-EB transforming forms are maturing and it is simply states that the "species time rate of change is given by the rate at which the population gets older (matures)." Equation (2.3) describes the total existing EB population at some progression r through the developmental cycle. The initial condition of equation (2.1) is $R_B(r_1) = 1$, where $l(r) = a(r - r_2)/(r_3 - r)$ and a is the rate at which RBs stop replicating but commences differentiation into EBs. The boundary condition of equation (2.2) is $\mathrm{d}\tau(\chi = 0, r)/\mathrm{d}r = l(r)R_B(r) - k_\tau \tau(\chi = 0, r)$, which is supplied by no-longer-replicating RBs. The burst size (total EB population) upon host cell lysis, $E_{BT} = E_B(r_3)$.

An age-structured model, which could be solved in closed analytic form, was derived for equations that describe the species characterised by the variable r. If $\rho(r, t)$ and $i(r, t)$ are the concentrations of host cells containing purely replicating RBs, and of host cells in which RB forms are differentiating to EBs at time t respectively, but at a maturity stage between r and $r + \Delta r$, then,

$$R(t) = \int_{r_0}^{r_1} \rho(r,t)\mathrm{d}r \quad \text{and} \tag{2.4}$$

$$I(t) = \int_{r_1}^{r_2} i(r,t)\mathrm{d}r. \tag{2.5}$$

Based on the assumption that the immune system is slow to respond to the presence of RBs (in one development cycle), they modelled $\mu(r)$ using a constant population of immune cells. Thus,

$$\mu(r) = \eta R_B(r). \tag{2.6}$$

Nevertheless, they derived an equation that models a varying immune (cytotoxic T) cell population. If P_s represents a constant source of immune cells, δ_T is the natural death rate of the cells, and k_T is the rate at which peptides activate immune cells, then $T(t)$, the population of immune cells attacking infected cells (at time (t) is given by

$$\frac{\mathrm{d}T}{\mathrm{d}t} = P_s - \delta_T T(t) + k_T T(t)\left(\int_{r_1}^{r_2} R_B(r)\rho(r,t)\mathrm{d}r + \int_{r_2}^{r_3} R_B(r)i(r,t)\mathrm{d}r\right). \tag{2.7}$$

Thus, the system of equations that describes the impact of the Th1 immune response against *Chlamydia*-infected cells over the *Chlamydia* developmental cycle is given by:

$$\frac{\mathrm{d}C}{\mathrm{d}t} = Pk_1B(t) - k_2C(t) - \lambda C(t), \tag{2.8}$$

$$\frac{\mathrm{d}A}{\mathrm{d}t} = (1-\theta)k_2C(t) - k_3A(t), \tag{2.9}$$

$$\frac{\mathrm{d}E}{\mathrm{d}t} = k_3A(t) - k_4E(t), \tag{2.10}$$

$$\frac{\partial\rho}{\partial t} = -\frac{\partial(k_\rho(r)\rho(r,t))}{\partial r} - \mu(r)\rho(r,t), \quad r_1 \le r \le r_2, \tag{2.11}$$

$$\frac{\mathrm{d}\Phi}{\mathrm{d}t} = \alpha k_\rho(r_2)\rho(r_2,t) - \beta\Phi(t) - \delta\Phi(t), \tag{2.12}$$

$$\frac{\partial i}{\partial t} = -\frac{\partial(k_i(r)i(r,t))}{\partial r} - \mu(r)i(r,t), \quad r_2 \le r \le r_3, \tag{2.13}$$

$$\frac{\mathrm{d}B}{\mathrm{d}t} = k_6i(r_3,t) - k_1B(t), \tag{2.14}$$

with initial conditions $C(0) = C_0,\ A(0) = E(0) = R(0) = I(0) = B(0) = 0$. $C(0) = C_0$ means that there is an inoculum of EBs of density C_0 introduced into the system at time $t = 0$. The boundary conditions for ρ and i in equations (2.11) and (2.13) respectively are given by

$$\rho(0,t) = k_4 E(t) \qquad \text{and} \qquad \frac{\mathrm{d}i(r_2,t)}{\mathrm{d}t} = (1-\alpha)k_\rho(r_2)\rho(r_2,t) + \beta\Phi(t). \tag{2.15}$$

See [168] for full derivation of the equations. Using equations (2.1)-(2.3), Wilson *et al* were able to numerically track the number of RBs and EBs within a *Chlamydia*-infected cell's inclusion throughout one developmental cycle. System (2.8)-(2.14) was numerically solved and finite difference algorithms were employed. The critical behaviour of the numerical solution was shown to depend on the basic reproduction number, a threshold denoted by R_0, which they obtained to be

$$R_0 = \frac{Pk_5k_2(1-\theta)(\beta+\delta-\alpha\delta)}{(k_2+\lambda)(k_5+\eta)(\beta+\delta)} \exp\left(-\int_{r_0}^{r_2} \frac{\mu(\zeta)}{k(\zeta)}\mathrm{d}\zeta\right). \tag{2.16}$$

The usual R_0 interpretation was implemented, that is; $R_0 > 1$ implies that all the diseased species will increase boundlessly with time, indicating an *active disease* state; $R_0 = 1$ implies an equilibrium set up that ensures a continuing developmental cycle but a *controlled infection*; and $R_0 < 1$ implies that the infection can be asymptotically cleared as the population level diminishes. As opposed to equation (2.6) where η, the rate at which the immune system responds to one intracellular RB particle, is modelled as a constant, they investigated the secondary memory-induced Th1 response by modelling η as a function of time. This is in order to ensure that the strength of the maximum Th1 immune response increases in effectiveness with time. Let η_0 represent the naive lymphocyte strength prior to infection, η_{max}, the maximum strength increase from primary to secondary response, and $t_{1/2}$, the time it takes for an half-increase in the maximal increase in strength after primary contact with the antigen. Thus η, now the maximum immune response and which increases with time, is given by

$$\eta = \eta(t) = \frac{\eta_{max}t}{t_{1/2}+t} + \eta_0. \tag{2.17}$$

Using this secondary Th1 immune response, three possible outcomes for long-term pathogenesis of an infected individual or cell culture were arrived at. Solutions of the proposed model (system (2.8)-(2.14)) show that an increase in immune response will exponentially decrease the population of host cells within which *Chlamydia* are progressing through the replicating phase. This is an indicator of the importance and strength of the cell-mediated immunity in the clearance of secondary infections. The mathematical factors of the obtained R_0 in equation (2.16) were used to make useful inferences and to summarise the factors critical to disease progression. It was suggested that effectively decreasing the attachment of extracellular *Chlamydia* on host cells by antibodies, their clearance due to natural death and wash out will assist in the clearance or control of the pathogen. It was also suggested that in order to reduce secondary infection, persistent *Chlamydia* should be induced and ensured that they do not return to the lytic cycle. This will prevent fresh

bouts of infections. This can be done by proven ways such as nutrient deprivation, IFN-γ production, etc. In conclusion, it was also suggested that inclusions be maintained for longer periods, that is extend the length of the time of the lytic cycle, by slowing down the progression through the RB replicating phase. This will enhance the opportunity for immunological attacks on intracellular *Chlamydia* (which will lead to their clearance) and will thus not require a high efficiency from the Th1 immune response. Nevertheless, their model did not investigate the adverse effects of inducing persistent *Chlamydia* (which they admitted) and of lengthening the lytic cycle, which can lead to serious sequelae in the host's body [12, 61, 168].

2.5.2 Mathematical model for the interaction between *Chlamydia* and host cells

Wilson developed a simple mathematical model of the cellular (within-host) dynamics of *Chlamydia* by using parameters to describe the change in the interactive processes between *Chlamydia*, uninfected epithelial cells and *Chlamydia*-infected epithelial cells [169]. This is the model upon which many other mathematical models of the within-host dynamics of *Chlamydia* are based upon. The proposed model also investigates the role of the humoral and cell-mediated immunity in the *Chlamydia* development cycle. He proposed the system of ordinary differential equations

$$\begin{aligned} \frac{dC}{dt} &= Pk_2I(t) - \mu C(t) - k_1C(t)E(t), \\ \frac{dE}{dt} &= P_E - \delta_E E(t) - k_1C(t)E(t), \\ \frac{dI}{dt} &= k_1C(t)E(t) - \gamma I(t) - k_2I(t), \end{aligned} \tag{2.18}$$

where $C(t)$ is the concentration of free extracellular *Chlamydia*, $E(t)$, the number of uninfected mucosal epithelial cells, and $I(t)$, the number of *Chlamydia*-infected epithelial cells at time t. At a rate of k_2, P *Chlamydia* bodies are released from infected cells. The rate of clearance by macrophages is denoted by μ while the rate of epithelial cell infection (which may be reduced by antibodies) is denoted by k_1. The rate of production of epithelial cells is denoted by P_E while δ_E represents natural death rate of epithelial cells. The rate of clearance of infected cells, courtesy of cell-mediated immunity, is denoted by γ.

One of the main goals of epidemiology of infectious diseases is to eradicate the disease in question. For *Chlamydia* infection to be eradicated in the infected host, free extracellular *Chlamydia* and *Chlamydia*-infected epithelial cells have to be eliminated. Thus, to investigate the conditions under which this can be achieved, these quantities are set to zero.

Wilson [169] evaluated the disease free equilibrium of the model system (2.18), for which he obtained

$$\bar{C} = 0, \quad \bar{E} = P_E/\delta_E, \quad \bar{I} = 0, \tag{2.19}$$

and a non-trivial steady state (endemic equilibrium)

$$\begin{aligned} \bar{C} &= \frac{P_E[(P-1)k_2 - \gamma]}{\mu(\gamma + k_2)} - \frac{\delta_E}{k_1}, \\ \bar{E} &= \frac{\mu(\gamma + k_2)}{k_1[(P-1)k_2 - \gamma]}, \\ \bar{I} &= \frac{P_E}{\gamma + k_2} - \frac{\delta_E \mu}{k_1[(P-1)k_2 - \gamma]}. \end{aligned} \tag{2.20}$$

Utilising the threshold parameter called the basic reproduction number (or ratio) [41], he investigated some features that impact the pathogenesis of *Chlamydia* infection. The basic reproduction number (often denoted by $\mathcal{R}_0$) is the *"expected number of secondary cases produced, in a completely susceptible population, by a typical infected individual during his entire period of infectiousness"* [40]. In order to determine whether a disease can invade and persist in a (new host) population (or host body) when one infected individual (or cell) is introduced into the wholly susceptible population (or host body) [70, 157], the basic reproduction number (or ratio) plays a very indispensable role.

The threshold criterion states that "*the disease can invade the population (or host body) if* $\mathcal{R}_0 > 1$*, whereas, it cannot if* $\mathcal{R}_0 < 1$" [40]. This is because the threshold parameter has the property that if $\mathcal{R}_0 < 1$, the disease-free equilibrium (DFE) is locally asymptotically stable and the disease cannot invade the population (or host body), but if $\mathcal{R}_0 > 1$, then, the DFE is unstable and the disease can always invade the population (or host body) [70, 157]. In the computation of $\mathcal{R}_0$, the state variables appraised are those that pertain to the infected cells (or individuals), in which new infections are differentiated from all other change in state among infected cells (or individuals) [40, 41, 157].

Thus, evaluating the basic reproduction ratio $\mathcal{R}_0$ of the model system (2.18) when the profusion of infected epithelial cells are at pre-infection level, Wilson [169] obtained

$$\mathcal{R}_0 = \frac{P}{(1 + \gamma/k_2)(1 + \mu/(k_1 E_0))}, \tag{2.21}$$

where $E_0 = P_E/\delta_E$. As a consequence of the threshold criterion, Chlamydia infection will be cleared, and the DFE (2.19) will be locally asymptotically stable when $\mathcal{R}_0 < 1$. On the other hand, the infection will remain endemic in its host, and the DFE (2.19) will be unstable when $\mathcal{R}_0 > 1$.

Using the analysis of this $\mathcal{R}_0$, the report reveals that the three most important factors to be considered in the clearance of *Chlamydia trachomatis* infection are P, the number of *Chlamydia* released from the lysis of infected epithelial cells, μ, the rate of macrophage

engulfment of free extracellular *C. trachomatis* (a consequence of the humoral immunity response), and γ, the rate of clearance of infected cells, (a response of cytotoxic cells to intracellular *C. trachomatis*, courtesy of the cell-mediated immunity).

Hence, to facilitate an upswing in the clearance of infection of *C. trachomatis*, the following should be regarded:

1. Macrophage engulfment of antibodies-bound pathogen (mediated by B lymphocytes), before pathogen entry into healthy epithelial cells has occured (μ/k_1),
2. Cytotoxic T cell clearance of infected epithelial cells prior to lysis of the infected cell (γ/k_2), or
3. Reduction in the number of new *Chlamydia* forms (elementary bodies) released by the lysis of an infected cell (P).

The parameter estimates used in the report (as shown in the table below) also reflect the relative importance of these factors.

Parameters	**Description**	**Value**
P	Burst size per infected cell	200-500
k_1	Rate of cell infection	0.02 mm^3/day/cell
k_2	Rate of infected cells burst	0.33-0.6 $days^{-1}$
P_E	Rate of production of mucosal epithelial cells	40 cells/mm^3/day
δ_E	Rate of natural death of epithelial cells	2 $days^{-1}$
γ	Effectiveness of cell-mediated immunity	2-10 $days^{-1}$
μ	Effectiveness of humoral immunity	2-10 $days^{-1}$

Table 2.1: Parameter values and ranges used in numerical simulation [169].

2.5.3 Mathematical model for the transmission dynamics of *Chlamydia in vivo* and the immune response

Sharomi and Gumel [142] proposed two deterministic ordinary differential models to describe the transmission dynamics of *Chlamydia in vivo*. The first model was referred to as the 'basic model', while the second model was referred to as the 'extended model'. The models account for five different stages of the chlamydial developmental cycle (CDC), while also incorporating the effect of the host immune response in the extended model. The basic model included $E_b(t)$, the density of *Chlamydia* EB form, $R_b(t)$, the density of *Chlamydia* RB form, $H_e(t)$, the density of host epithelial cells, and $I_j(t)$, the density of *Chlamydia*-infected cells in Stage j, ($j = 1, 2, 3, 4, 5$) of the CDC, before infected cell lysis. The stages of the CDC within infected cells are described below.

- Stage 1: Attachment and inclusion of an EB to the surface of the host epithelial cell ($t : 2 - 4$ hours).
- Stage 2: Intracellular differentiation of EB forms to RB forms ($t : 8 - 12$ hours).
- Stage 3: Intracellular replication of RB forms ($t > 20$ hours).

- Stage 4: Intracellular de-differentiation of RB forms to EB forms ($t : 30-40$ hours).
- Stage 5: Lyses of infected epithelial cells to produce more EB forms ($t : 48-72$ hours).

Basic model

Healthy epithelial cells are produced by the host at a rate Π_h, and are infected by *Chlamydia* at a rate β, which is the effective contact rate. It is assumed that newly infected cells are in Stage 1. Infected cells in Stage j, (I_j) progress to Stage $j+1$ at a rate α_j $(j = 1, 2, 3, 4)$. The rate at which infected cells in Stage 5 disintegrate or lyse to release N_c *Chlamydia* bodies is γ, where $N_c \in [200, 500]$. It is assumed that a portion $N_1 \geq 1$ of N_c are *Chlamydia* EBs while the remaining portion $N_2 = N_c - N_1 \geq 1$ are non-infectious and remain in the R_b class. Healthy epithelial cells have a natural death rate of μ_h, while EB and RB forms have natural death rates of μ_e and μ_r, respectively. Based on the described dynamics, the following system of equations are proposed:

$$\begin{aligned}
\frac{\mathrm{dH}_e}{\mathrm{dt}} &= \Pi_h - \beta H_e E_b - \mu_h H_e, \\
\frac{\mathrm{d}I_1}{\mathrm{dt}} &= \beta H_e E_b - \alpha_1 I_1, \\
\frac{\mathrm{d}I_j}{\mathrm{dt}} &= \alpha_{j-1} I_{j-1} - \alpha_j I_j, \ j = 2, 3, 4, \\
\frac{\mathrm{d}I_5}{\mathrm{dt}} &= \alpha_4 I_4 - \gamma I_5, \\
\frac{\mathrm{d}E_b}{\mathrm{dt}} &= \gamma N_1 I_5 - \beta H_e E_b - \mu_e E_b, \\
\frac{\mathrm{d}R_b}{\mathrm{dt}} &= \gamma N_2 I_5 - \mu_r R_b,
\end{aligned} \tag{2.22}$$

The model system (2.22) was extensively analysed. Equilibrium solutions and stability analysis were presented. The threshold quantity $\mathcal{R}_0$, the basic reproduction number, for the system, was also estimated. The model is shown to have a globally asymptotically stable *Chlamydia*-free equilibrium (CFE) whenever $\mathcal{R}_0 < 1$. The *Chlamydia*-present equilibrium (CPE) exists whenever $\mathcal{R}_0 > 1$. Conditions under which the CPE is unique were also presented (see [142]).

Extended Model: Model with immune response

In their extended model, Sharomi and Gumel [142] incorporated the effect of the humoral and cell-mediated immune response in order to assess the impact of these immune responses on the *in vivo* dynamics of *Chlamydia trachomatis*. New compartments and parameters are introduced into the model system (2.22) to capture these responses. Let the density of healthy epithelial cells protected from chlamydial infection by the humoral immune response be $H_i(t)$. They modelled IFN-γ as immune cells and the density of these are denoted as $A_c(t)$. The model assumes that the rate at which IFN-γ cells are

produced is proportional to the number of newly infected epithelial cells in Stage 1 of the CDC, and this rate ie denoted by ω_2, $\omega_2 > 0$. IFN-γ cells are assumed to die at a rate μ_a. The humoral immune response protects healthy epithelial cells at a rate ϕ, with efficacy ε, $0 < \varepsilon < 1$, and the protection wanes at a rate ω_2. It is assumed that the natural death rate of protected and unprotected epithelial cells are the same, and is denoted by μ_h. It is assumed that IFN-γ cells are produced in the presence of a chlamydial infection, when the CDC is at the RB stage. The infected epithelial cells are disintegrated by the IFN-γ cells in Stage j ($j = 2, 3, 4, 5$), at a rate ρ_j ($j = 2, 3, 4, 5$). Based on the described dynamics, the following system of equations are proposed:

$$\begin{aligned}
\frac{\mathrm{dH}_e}{\mathrm{dt}} &= \Pi_h + \omega_1 H_i - \beta H_e E_b - k_1 H_e, \\
\frac{\mathrm{d}H_i}{\mathrm{dt}} &= \phi(1-\varepsilon) H_e - k_2 H_i, \\
\frac{\mathrm{d}A_c}{\mathrm{dt}} &= \omega_2 I_1 - \mu_a A_c, \\
\frac{\mathrm{d}I_1}{\mathrm{dt}} &= \beta H_e E_b - \alpha_1 I_1, \\
\frac{\mathrm{d}I_j}{\mathrm{dt}} &= \alpha_{j-1} I_{j-1} - \alpha_j I_j - \rho_j I_j A_c, \ j = 2, 3, 4, \\
\frac{\mathrm{d}I_5}{\mathrm{dt}} &= \alpha_4 I_4 - \gamma I_5 - \rho_5 I_5 A_c, \\
\frac{\mathrm{d}E_b}{\mathrm{dt}} &= \gamma N_1 I_5 - \beta H_e E_b - \mu_e E_b, \\
\frac{\mathrm{d}R_b}{\mathrm{dt}} &= \gamma N_2 I_5 - \mu_r R_b,
\end{aligned} \tag{2.23}$$

where $k_1 = \phi(1-\varepsilon) + \mu_h$ and $k_2 = \omega_1 + \mu_h$.

The model system (2.23) was also extensively analysed. Its equilibrium solutions and stability analysis were also presented. The model's associated $\mathcal{R}_{01}$, the basic reproduction number was estimated and the model is shown to have a globally asymptotically stable *Chlamydia*-free equilibrium (CFE) whenever $\mathcal{R}_{01} < 1$. It is also shown that the chlamydial infection persists whenever this threshold quantity $\mathcal{R}_{01} > 1$.

Numerical simulations of the model suggest that in the clearance of a *Chlamydia* infection, the cell-mediated immune response is more effective than the humoral immune response, as the humoral immune response only delivers a marginal effect in reducing *Chlamydia* burden. The study also suggests that in curtailing *Chlamydia* burden *in vivo*, a *Chlamydia* vaccine that boosts the cell-mediated immune response may be instrumental.

2.5.4 Mathematical model for the immunobiological outcomes during multiple chlamydial infections

Vickers *et al.* [160] presented two simple ordinary differential equations models to investigate the role of CD4+ T cell and the responses of anti-*Chlamydia* antibodies under

different exposures and re-exposure histories. Their first and second models were referred to as the 'basic' and 'extended' models respectively. The basic model included X, uninfected endothelial cells (EnCs), Y, infected EnCs, E, infectious EBs, and Z, T_H1 CD4+ cells. Uninfected EnCs were produced at a constant rate λ, and die at a rate δX. Infected cells are produced at rate βXE, recover at rate γZY, and die at a rate αY. Activated chlamydia-specific CD4+ T cells proliferate and differentiate at a rate cY, and die at a rate σZ. The rate of production of EBs from infected cells is εY and the decay rate of free EBs is qE.

The resulting equations are

$$\dot{X} = \lambda + \gamma ZY - \delta X - \beta XE, \tag{2.24}$$

$$\dot{Y} = \beta XE - \alpha Y - \gamma ZY, \tag{2.25}$$

$$\dot{Z} = cYZ - \sigma Z, \tag{2.26}$$

$$\dot{E} = \varepsilon Y - qE. \tag{2.27}$$

In order to incorporate antibody responses, they extended the basic model. They did not model immune memory explicitly. Rather, they were modelled by allowing the immune cells' (CD4+ cells or antibody) populations die off slower than other cells post-infection. Another state variable, U, the chlamydia-specific antibody, was introduced. Denoted by ξ is the antibody production rate, which was assumed to be proportional to the number of CD4+ cells. ϕ is the number of antibodies consumed in the formation of an EB-antibody complex , k is the efficacy of antibody-induced EB neutralisation, and η is the natural decay rate of the antibody population. The modifications to the basic model yielded an additional equation and a redefined Equation (2.27), which are

$$\dot{E} = \varepsilon Y - kUE - qE, \tag{2.28}$$

$$\dot{U} = \xi Z - \phi kUE - \eta U. \tag{2.29}$$

The models were numerically solved and results obtained. They examined the long-term in-host dynamics under four different re-exposure scenarios (see [160] for details). Their models were observed to reproduce experimentally-observed kinetics of primary and secondary chlamydial infections. Simulation results showed that a proportional antibody and CD4+ cell responses may have important roles in the resolution of primary infection, and in addition, an individual's immunity against reinfection. Their results also suggested that when reinfection occurs after being re-exposed in relatively rapid succession, the resulting infection is less severe and produces a decreased bacterial load. They also suggested that short term frequent chlamydial exposures allows partial immunity to decline up to near baseline levels. In addition, frequent re-exposure was suggested to have a possibility of yielding a stable and persistently raised immune memory.

2.5.5 Significance of Research

As the literature review has shown, quite a number of mathematical models have been developed to understand the dynamics of *Chlamydia trachomatis* within-host, which includes the influence of the humoral and cell-mediated responses [142, 168, 171] and the spatio-temporal progression [9,108,109] of *Chlamydia* body forms. However, none of these mathematical studies have considered the effects of repeated *Chlamydia* challenges induced by the intracellular persistence of *Chlamydia*, and the subsequent immune response on the within-host dynamics of *Chlamydia trachomatis*. In addition, no mathematical study has been developed to extensively investigate the impact of antibiotic treatment on the within-host (both intercellular and intracellular) dynamics of *Chlamydia*.

Furthermore, the developed models have not been able to address the concern of vaccination strategies that should be put in place in order to combat genital infections of *Chlamydia*. This project seeks to address this lack of understanding theoretically through the development of new mathematical models and the improvement of existing models of chlamydial infection.

3 Could late inhibition of chlamydial growth be contributing to treatment failures? An intracellular mathematical model of the chlamydial developmental cycle

---

It is obvious that several gaps exist in our understanding of the treatment of *Chlamydia trachomatis* infection, and of its efficacy. Thus, it is still an open area of study [67,76,91]. The pathogenesis, low virulence, and long-term persistence of *Chlamydia trachomatis* infections are not well understood [10, 132, 153]. Furthermore, as noted in Section 2.2, antimicrobial treatment failures exist. There is therefore a need for a further investigation of the role of the different components of the complex chlamydial developmental cycle (CDC) in chlamydial infections, in order to stimulate new therapeutic treatments of the disease [178].

In this chapter, we investigate the optimal timing of the inhibitory activity of antibiotic treatments in a typical chlamydial infection, and how this activity affects the net replication of *Chlamydia* over the chlamydial developmental cycle (CDC). We do this on a cellular level, by examining what happens within an infected epithelial cell. Our aim is to use mathematical modelling to gain a better understanding of the impact of antibiotic treatment on the within-host dynamics of *Chlamydia trachomatis* infection. We do this by investigating how different timing of the commencement of antibiotic inhibitory activity (in an active antibiotic delivery of an *in vitro* testing), within the CDC and on a single cell level, will impact on the prognosis of the disease.

Candidate vaccines and therapeutic drugs that can attack pathogens at different stages of their developmental cycle have been previously identified. Antiretroviral drugs used to treat HIV are good examples of antimicrobial drugs that target different stages of a pathogen's (here, HIV) life cycle, in order to abate the pathogen's growth [6]. In the bid to combat the malaria parasite *Plasmodium falciparum*, which has multiple life stages, several new candidate vaccines have been identified and are at different clinical stages [49, 62, 165, 166]. These vaccines/therapeutic drugs' developments are being made possible because potential biological targets, such as biomarkers, were recognised. An

example is the RTS,S, a malaria vaccine, which is currently undergoing advanced clinical trials. It targets the infectious phase (pre-erythrocytic stage) of the malaria parasite in order to prevent the infection of, or attack infected, host liver cells. The design of this vaccine was made possible because its developers identified a protein (antigen) on the surface of the parasite, at the pre-erythrocytic stage, which was engineered to stimulate immunogenic responses from the host [2, 118, 165]. Similarly, we investigate the intracellular/intercellular developmental stages of *Chlamydia* in order to identify the stage(s) at which its intracellular growth can best be inhibited, with the goal of more completely and efficiently clearing the infection. In the development of more effective anti-*Chlamydia* drugs, this study has the potential to influence the identification of biomarkers for such stage(s).

We develop a prototype mathematical model for this theoretical investigation. We use azithromycin as a prototype antibiotic treatment, because it is a recommended treatment for (genital) *Chlamydia* infection and because of its pharmacokinetic and pharmacodynamic properties (long tissue half-life, lysosomotrophic, bacteriostatic) on chlamydial infections, in order to determine the CDC stage(s) its effect will be 'most efficient'. In particular, we consider a dosage equivalent to a single 1-g oral dose. By 'most efficient', we mean the effective and efficient inhibition of chlamydial growth (replication and differentiation) and the inhibition of inclusion maturation (see Section 2.2). The CDC, as described by our model, commences with so many synchronised infected epithelial cells that are at the RB stage of growth. The infection process is normally initiated by the attachment of chlamydial EBs to the eukaryotic cell surface (mucosal epithelial cell). However, our chlamydial model's developmental cycle bypasses this stage, commencing instead at the point of EB-to-RB differentiation, since as discussed in Section 2.2, the inhibitory activity of azithromycin (and any other recommended anti-*Chlamydia* antibiotic in general) only becomes effective at the RB stage. The model, which mimics an *in vitro* chlamydial innoculation, considers the intracellular RB/EB developmental cycle and assumes that a single EB infects an epithelial cell at a time. Our model assumes that if chlamydial protein synthesis (which occurs at the RB stage as discussed in Section 2.2) is effectively inhibited, RB replication is also hindered, and formation of infectious progenies is drastically reduced or blocked consequently.

We present a list of parameters and their corresponding biologically plausible values in Table 3.1. Parameter estimation is discussed in Section 3.2. Our model is numerically implemented and preliminary numerical results from simulations of the mathematical model are presented in Section 3.3. Finally, we present a discussion on the implications of the findings of our mathematical model of intracellular chlamydial infection in Section 3.4.

3.1 Model Formulation

Here, we present a stripped-down ordinary differential equation (ODE) model to describe the dynamics of RB and EB populations within a single infected epithelial cell. The model

tracks the number of intracellular *Chlamydia* body forms within an inclusion, throughout the CDC (as defined for our model), similar to previous models developed by [168, 170], and [167] (see Section 2.5 and its subsections). Since the model was built at a cellular level, it conceptualises chlamydial infection kinetics in the female reproductive tract, when azithromycin is transported to the site of a vacuole which initially contains one RB form. In this vacuole, replication of the RB form occurs, which de-differentiates into EB forms at a latter stage of the developmental cycle (see Figure 3.2). These EB forms are eventually released into the surrounding genital mucosa on lysis of the infected host cell.

At time t post infection, we denote by R_B and E_B, the number of RB and EB forms of *Chlamydia* within an inclusion, respectively, and Z, the concentration of azithromycin transported to the site of the infected host cell. Z_{mic} is the minimum inhibitory concentration (MIC) of azithromycin for *C. trachomatis*. We let t_0 represent the time of the initial EB-RB differentiation, t_*, the time at which RB forms commence differentiating back into EB forms (de-differentiation), t_l, the time of lysis, t_z, $t_0 \leq t_z \leq t_l$, the time at which the inhibitory activity of azithromycin on chlamydial growth commences, and δ, the rate of RB-to-EB differentiation. A simple mathematical representation of the described phenomena is given by the following system of ordinary differential equations:

$$\frac{\mathrm{d}R_B}{\mathrm{d}t} = \begin{cases} \left(\dfrac{\ln(2)}{t_d}\right) R_B, & t_0 \leq t < t_* \\ \dfrac{1}{2}\left(1 - \tanh\left(\dfrac{Z - Z_{\text{mic}}}{\bar{Z}}\right)\right)\left(\dfrac{\ln(2)}{t_d}\right) R_B - \delta R_B, & t_* \leq t \leq t_l \end{cases} \tag{3.1}$$

$$\frac{\mathrm{d}E_B}{\mathrm{d}t} = \begin{cases} 0, & t_0 \leq t < t_* \\ \delta R_B, & t_* \leq t \leq t_l \end{cases} \tag{3.2}$$

$$\frac{\mathrm{d}Z}{\mathrm{d}t} = -KZ, \qquad t \geq 0, \tag{3.3}$$

with initial conditions $E_B(t_0) = 0$, $R_B(t_0) = 100$, and $Z(t_0) = Z_0 = 7.28 \times 10^{-8}$ mg/cell. $Z_{\text{mic}} = 2 \times 10^{-8}$ mg/cell (see Section 3.2 for discussion on these values). In order to appeal to the continuum assumption of the use of a deterministic framework, we use large sample sizes. Thus, we track the number of EB and RB forms of *Chlamydia* in a collection of healthy epithelial cells, each infected by one and only one EB. In particular, we track the changes within 100 infected epithelial cells, thus $R(t_0) = 100$, implies that there is only one RB form in each infected epithelial cell.

The model assumes that RB replication (through repeated binary fission) occurs exponentially at the start of the infection with doubling time of RB forms represented by t_d in the first term of equation (3.1) in the presented model system. Thus, the RB binary fission rate is $\ln(2)/t_d$. In order to account for the slowing down of the replication of RB forms by azithromycin, we consider a switch modelled by

$$T(Z) = \frac{1}{2}\left(1 - \tanh\left(\frac{Z - Z_{\text{mic}}}{\bar{Z}}\right)\right). \tag{3.4}$$

In the above expression, the magnitude of the scaling factor $1/\bar{Z}$ determines the sensitivity of the switch $T(Z)$ to Z. It also makes the argument of tanh dimensionless. The term $T(Z)$ implies that when the concentration $Z(t)$ of the administered drug exceeds its Z_{mic}, that is $0 < T(Z) < 1/2$, then RB replication is inhibited; when concentration $Z(t) = Z_{\text{mic}}$, that is $T(Z) = 1/2$, then RB replication is slightly inhibited; and when concentration $Z(t) < Z_{\text{mic}}$, that is $1/2 < T(Z) < 1$, then RB replication may only be slightly inhibited or even delayed. We illustrate the effect of the slowing down of RB replication by the switch $T(Z)$, by plotting its graph, as shown in Figure 3.1. Figure 3.1 also shows the sensitivity of the switch to the magnitude of the scaling factor $1/\bar{Z}$. It shows that the higher the scaling factor (or the lower the value of $\bar{Z}$), the faster the switch slows down RB replication.

Treatment failure of azithromycin occurs when it fails to effectively inhibit chlamydial growth. It rather inhibits inclusion formation by inducing the formation of temporarily metabolically inert (aberrant) persistent RBs [43, 128]. We assume that the maximum reduction achieved by azithromycin in the inhibition of RB replication is about half. The elimination rate constant of azithromycin is denoted by K. We assume that lysing host cells may contain some aberrant RB forms, but predominantly EB forms. We expect that several immunological processes, innate, and specific host immune responses will intervene in the clearance of *Chlamydia* body forms. However, these have not been captured in this model and we leave that for future work. In the subsection to follow, we vary t_z, and as such, Equations (3.1), (3.2), and (3.3), also vary slightly to cater for the presence or absence of azithromycin, Z. Parameter ranges, values, and sources are shown in Table 3.1.

Table 3.1: **Variables, parameters, chosen values, and reported ranges used in the model and simulations.**

Variables	**Description**	**Values**	**Ranges**
R_B	Number of RB forms of *Chlamydia*	$R_B(t_0) = 100$	
R_B	Number of EB forms of *Chlamydia*	$E_B(t_0) = 0$	
Z	Concentration of azithromycin	$Z(t_0) = Z_0$	
Parameter			
t_0	Time of initial EB-RB differentiation	0*	
t_d	Intracellular RB doubling time	2.6	1.45-2.6 hPI [167]
t_*	Inception time of RB-to-EB differentiation	15	12-28* hPI [9, 10]
t_l	Time of infected cell lysis	55	36-60* hPI [9, 10]
δ	Rate of RB-to-EB differentiation	0.333	0.333 h^{-1} [167]
K	Elimination rate constant of azithromycin	0.0072	0.0072-0.0144 mgh^{-1}
Z_{mic}	MIC of azithromycin for *C. trachomatis*	2×10^{-8}	2×10^{-8} mg/cell
$\bar{Z}$	Scaling factor in the expression for $T(Z)$	7.28×10^{-8}	7.28×10^{-8} mg/cell

Parameter estimation is briefly described later in this chapter. MIC = minimum inhibitory concentration. Asterisked values/ranges are further explained in Section (3.3). For the estimation of K, Z_0, and Z_{mic} values, see Section 3.2.

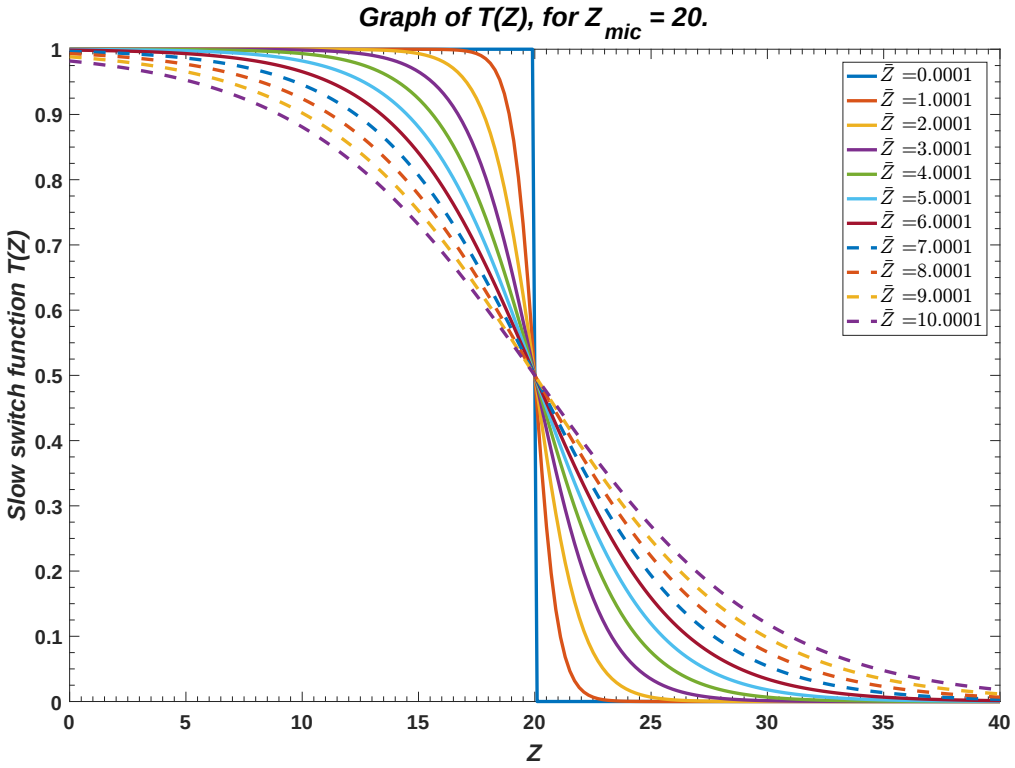

Figure 3.1: A graph that illustrates the potential effect of the switch function $T(Z)$ (Equation (3.4)) on the RB binary fission rate $\ln(2)/t_d$. $\bar{Z}$ and Z_{mic} are in mg/cell.

3.1.1 Time of Treatment Scenarios

Using the model equations (3.1)-(3.3), we investigate the effects of introducing azithromycin at different times in the cycle. We refer to these times as the times at which azithromycin's chlamydial inhibition commences. The five treatment time scenarios that we consider are $t_z = t_0$, $t_z \in (t_0, t_*)$, $t_z = t_*$, $t_z \in (t_*, t_l)$, and $t_z = t_l$, which we refer to as intervals I_1, I_2, I_3, I_4, and I_5 respectively, as shown in Figure 3.2.

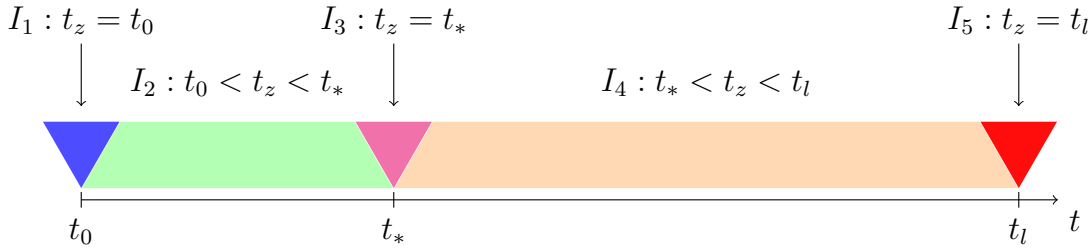

Figure 3.2: **Schematic showing intervals for t_z, the time at which azithromycin's chlamydial inhibition commences within the CDC.** t_0 indicates when the first EB form differentiates to an RB form, t_* is the point at which RBs commence differentiation back to EB form, and t_l is the time of infected host cell lysis.

3.1.2 Treatment coincides with initial EB-RB differentiation (I_1)

When the time at which azithromycin's chlamydial inhibition commences coincides with the initial differentiation of an EB to an RB, $t_z = t_0$. This means that the inhibitory effects of the antibiotic acts on the system at all times of interest (that is from $t_0 \to t_l$), until it is totally eliminated from the system or when it is no longer potent enough to combat the pathogen. The model is therefore comprised of two parts: the RB replication phase from t_0 to t_* and the RB-EB differentiation phase from t_* to t_l. For $t_z = t_0 \leq t < t_*$, we have

$$\begin{aligned} \frac{\mathrm{d}R_B}{\mathrm{d}t} &= \frac{1}{2}\left(1 - \tanh\left(\frac{Z - Z_{\text{mic}}}{\bar{Z}}\right)\right)\left(\frac{\ln(2)}{t_d}\right) R_B, \\ \frac{\mathrm{d}E_B}{\mathrm{d}t} &= 0, \\ \frac{\mathrm{d}Z}{\mathrm{d}t} &= -KZ, \end{aligned} \tag{3.5}$$

where initially, $R_B(t_0) = 100$, $E_B(t_0) = 0$, and $Z(t_0) = Z_0$.

Then for $t_* \leq t < t_l$, we have

$$\begin{aligned} \frac{\mathrm{d}R_B}{\mathrm{d}t} &= \frac{1}{2}\left(1 - \tanh\left(\frac{Z - Z_{\text{mic}}}{\bar{Z}}\right)\right)\left(\frac{\ln(2)}{t_d}\right) R_B - \delta R_B, \\ \frac{\mathrm{d}E_B}{\mathrm{d}t} &= \delta R_B, \\ \frac{\mathrm{d}Z}{\mathrm{d}t} &= -KZ, \end{aligned} \tag{3.6}$$

where we match solutions at t_*, so $R_B(t_*)$, $E_B(t_*)$, and $Z(t_*)$ are given by the solutions to equations (3.5) at t_*.

3.1.3 Treatment occurs during the RB replication phase (I_2)

Here, the time at which azithromycin's chlamydial inhibition commences is after RB replication has commenced. This implies that for this treatment scenario, $t_z \in (t_0, t_*)$. The model for this treatment scenario is in three parts: the RB replication phase from t_0 to t_z, the latter RB replication phase from t_z to t_*, and the RB-EB differentiation phase from t_* to t_l. For $t_0 \leq t < t_z$, we have

$$\begin{aligned} \frac{\mathrm{d}R_B}{\mathrm{d}t} &= \left(\frac{\ln(2)}{t_d}\right) R_B, \\ \frac{\mathrm{d}E_B}{\mathrm{d}t} &= 0, \\ \frac{\mathrm{d}Z}{\mathrm{d}t} &= 0, \end{aligned} \tag{3.7}$$

with initial conditions $R_B(t_0) = 100$, $E_B(t_0) = Z(t_0) = 0$.

The solutions of system (3.7) are

$$\begin{aligned} R_B(t) &= 100\exp\left(\frac{\ln(2)}{t_d}\right)t, \\ E_B(t) &= E_B(t_0), \quad \text{and} \\ Z(t) &= Z(t_0), \end{aligned} \tag{3.8}$$

respectively.

For $t_z \leq t < t_*$, we have

$$\begin{aligned} \frac{\mathrm{d}R_B}{\mathrm{d}t} &= \frac{1}{2}\left(1 - \tanh\left(\frac{Z - Z_{\text{mic}}}{\bar{Z}}\right)\right)\left(\frac{\ln(2)}{t_d}\right)R_B, \\ \frac{\mathrm{d}E_B}{\mathrm{d}t} &= 0, \\ \frac{\mathrm{d}Z}{\mathrm{d}t} &= -KZ, \end{aligned} \tag{3.9}$$

with initial conditions $R_B(t_z)$, $E_B(t_z)$, and $Z(t_z)$, which are given by solutions to equations (3.7), that is,

$$\begin{aligned} R_B(t_z) &= 100\exp\left(\frac{\ln(2)}{t_d}\right)t_z, \\ E_B(t_z) &= E_B(t_0) = 0, \quad \text{and} \\ Z(t_z) &= Z(t_0) = 0. \end{aligned} \tag{3.10}$$

For $t_* \leq t \leq t_l$, we again have equations (3.6), but with initial conditions $R_B(t_*)$, $E_B(t_*)$, and $Z(t_*)$, which are given by solutions to equations (3.9).

3.1.4 Treatment occurs at the start of RB-EB differentiation (I_3)

For this treatment scenario, the time at which azithromycin's chlamydial inhibition commences coincides with when RB-EB differentiation commences. This implies that for this treatment scenario, $t_z = t_*$. The model for this treatment scenario is in two parts: the RB replication phase from t_0 to t_* and the RB-EB differentiation phase from t_* to t_l.

For $t_0 \leq t < t_z = t_*$, the first part of this model has the same equations as equations (3.7), also with initial conditions $R_B(t_0) = 100$, $E_B(t_0) = 0$, and $Z(t_0) = 0$. While for $t_z \leq t \leq t_l$, we have equations (3.6), but with initial conditions $R_B(t_z)$, $E_B(t_z)$, and

$Z(t_z)$, which are given by solutions to the equations of the first part of the model for this treatment, that is,

$$\begin{aligned} R_B(t_z) &= 100\exp\left(\frac{\ln(2)}{t_d}\right)t_z, \\ E_B(t_z) &= E_B(t_0) = 0, \quad \text{and} \\ Z(t_z) &= Z(t_0) = 0. \end{aligned} \tag{3.11}$$

3.1.5 Treatment occurs during the RB-EB differentiation phase (I_4)

In this treatment scenario, the time at which azithromycin's chlamydial inhibition commences is between the time RB-EB differentiation commences and the time the infected cell lysis. This implies that for this treatment scenario, $t_z \in (t_*, t_l)$. The model for this treatment scenario is divided into three parts: the RB replication phase from t_0 to t_*, the first part of the RB-EB differentiation phase from t_* to t_z, and the second part of the RB-EB differentiation phase from t_z to t_l.

For $t_0 \leq t < t_*$, we have equations (3.7), with initial conditions $R_B(t_0) = 100$, $E_B(t_0) = 0$, and $Z(t_0) = 0$.

For $t_* \leq t < t_z$, we have

$$\begin{aligned} \frac{\mathrm{d}R_B}{\mathrm{d}t} &= \left(\frac{\ln(2)}{t_d}\right)R_B - \delta R_B, \\ \frac{\mathrm{d}E_B}{\mathrm{d}t} &= \delta R_B, \\ \frac{\mathrm{d}Z}{\mathrm{d}t} &= 0, \end{aligned} \tag{3.12}$$

with initial conditions $R_B(t_*)$, $E_B(t_*)$, and $Z(t_*)$, which are given by solutions to equations (3.7). Note that $\ln(2)/t_d - \delta < 0$. Substituting for $t = t_*$ in Equation (3.8), we have

$$\begin{aligned} R_B(t_*) &= 100\exp\left(\frac{\ln(2)}{t_d}\right)t_*, \\ E_B(t_*) &= E_B(t_0) = 0, \quad \text{and} \\ Z(t_*) &= Z(t_0) = 0. \end{aligned} \tag{3.13}$$

Thus, the solutions of system (3.12) are

$$\begin{aligned} R_B(t) &= R_B(t_*)\exp\left(\frac{\ln(2)}{t_d} - \delta\right)t, \\ E_B(t) &= E_B(t_*) + \delta R_B(t_*)/\left(\frac{\ln(2)}{t_d} - \delta\right)\left(\exp\left(\frac{\ln(2)}{t_d} - \delta\right)t - \exp\left(\frac{\ln(2)}{t_d} - \delta\right)t_*\right), \quad \text{and} \\ Z(t) &= Z(t_*), \ \text{respectively.} \end{aligned} \tag{3.14}$$

Finally, for $t_z \leq t \leq t_l$, we have equations (3.6), with initial conditions $R_B(t_z)$, $E_B(t_z)$, and $Z(t_z)$, which are given by solutions to equations (3.12), that is

$$\begin{aligned} R_B(t_z) &= R_B(t_*)\exp\left(\frac{\ln(2)}{t_d} - \delta\right)t_z, \\ E_B(t_z) &= E_B(t_*) + \delta R_B(t_*)/\left(\frac{\ln(2)}{t_d} - \delta\right)\left(\exp\left(\frac{\ln(2)}{t_d} - \delta\right)t_z - \exp\left(\frac{\ln(2)}{t_d} - \delta\right)t_*\right), \quad \text{and} \\ Z(t_z) &= Z(t_*). \end{aligned} \tag{3.15}$$

3.1.6 Treatment is delivered on cell lysis (I_5)

In this treatment scenario, the time at which azithromycin's chlamydial inhibition commences is at the time of the infected cell's lysis. Consequently, for this treatment scenario, $t_z = t_l$. The model for this treatment scenario is divided into three parts: the usual RB replication phase from t_0 to t_*, the RB-EB differentiation phase from t_* to t_l, and the point of cell lysis at time $t = t_l$.

For $t_0 \leq t < t_*$, the first part of this model also has the same equations as the system (3.7), with initial conditions $R_B(t_0) = 100$, $E_B(t_0) = 0$, and $Z(t_0) = 0$. For $t_* \leq t < t_l$, the second part of this model uses system (3.12), with initial conditions $R_B(t_*) = R_{B*3}$, $E_B(t_*) = E_{B*3}$, and $Z(t_*) = Z_{*3}$, which are given by solutions to the equations for the first part of this model. For the point $t_l = t_z$, the third part of this model uses equations (3.6), but with initial conditions $R_B(t_l) = R_{Bl}$, $E_B(t_l) = E_{Bl}$, and $Z(t_l) = Z_l$, which are given by the solutions to the equations that constitute the second part of this model.

3.2 Parameter Estimation

Several studies have isolated purified epithelial cells (EC) from the tissues of the fallopian tube, vaginal mucosa, endocervix, ectocervix and uterine endometrium of the human female reproductive tracts (HFRT). These cells have been successfully re-established in cultures on cell inserts (in cell chambers), and have been used to prepare purified epithelial sheets with high transepithelial resistance (TER) (an indicator of tight junction formation

in columnar epithelial cells, which maintains the integrity of the epithelial cell monolayers) [50, 51, 172, 173]. Using experimentally obtained data, and ensuring that the data are products of experimental methods that used the optimal way of seeding isolated purified ECs, we assume that 2ml of epithelial sheet weighs about 2.08g, and this contains about 8×10^5-to-1×10^6 viable uterine epithelial cells [50, 51, 161, 172]. We further assumed that about 7.28×10^{-8} mg of azithromycin is transported to the site of a single epithelial cell on administration of the standard single 1 g oral dose of azithromycin to a patient [56, 119, 121, 134, 140, 151, 156], that is, $Z_0 = 7.28 \times 10^{-8}$mg.

The MIC of azithromycin for the inhibition of inclusion formation in C. trachomatis infection is 1.0μ g/mL. Hence we take $Z_{\text{mic}} = 2 \times 10^{-8}$ mg/cell. Azithromycin has an half-life of about 2-4 days [56,150]. The decay constant k of any substance undergoing exponential decay is related to its half-life $t_{1/2}$ by the relation $k = \ln(2)/t_{1/2}$. Thus, the elimination rate constant K of azithromycin is drawn from the interval $[0.0072, 0.0144]$. The presented results are for $K = 0.0072$. We assume the mean time of RB-EB differentiation to be 3 h [167], thus, the rate of RB-EB differentiation, $\delta = 0.333$.

3.3 Results

We numerically implement the submodels presented in Subsections 3.1.2-3.1.6, along with the parameter values sampled from the ranges in Table 3.1 using *MATLAB*'s one-step solver ode45. Following the assumption that one EB form infects one vacuole at a time, after an EB form infects a healthy epithelial cell at time $t = 0$, the vacuole-bound EB form differentiates into an RB form after about 2-12 hours [9, 10, 178]. However, the chlamydial developmental cycle of our mathematical model starts at this time, and we thus take the time here to be $t_0 = 0$. Furthermore, the time (t_*) of asynchronous RB-to-EB differentiation has been reported in the literature to occur between 24-40 hours [9,10]. By virtue of our model's starting point, this time frame will be taken as between $t = 12$ and $t = 28$ hours. Furthermore, the actual time of lysis ranges between 48 and 72 hours, and so our model's time of lysis (t_l) ranges between $t = 36$ and $t = 60$ hours.

We first considered the case where there was no azithromycin administered, confirming that the burst size produced by our model simulation coincides with published reports (that about 200-500 new EBs are produced from the lysis of a chlamydial infected cell [167, 168]). Using our model, we numerically investigate the effect of altering the times at which azithromycin's chlamydial inhibition commences throughout the chlamydial developmental cycle. We considered five distinct scenarios of these times throughout the cycle as defined. These time scenarios are represented by the five time frames and a schematic of this is shown in Figure 3.3. Figure 3.4 shows the chlamydial developmental cycle in the absence of azithromycin. It can be seen that before the differentiation of RBs to their EB form ($0 \leq t < t_*$), RB forms were purely replicating, but EBs emerged after the differentiation commenced.

As previously mentioned in Section 3.1, we track the number of EB and RB forms of *Chlamydia* in a collection of healthy epithelial cells, each infected by one and only one EB. In particular, we track the changes within 100 infected epithelial cells, thus $R(t_0) = 100$, implies that there is only one RB form in each infected epithelial cell. Thus, the results of Figure 3.5-3.12 should be interpreted with regards to this. Figures 3.5-3.12 show the chlamydial developmental cycle in the presence of azithromycin.

In Figure 3.5, the number of EB forms contained within an infected cell is only approximately one ($E_B(t_f) \approx 1$). When one RB form within an infected cell gives rise to one and only EB form, an equilibrium condition is established. We define this state of equilibrium as a controlled infection. This is because, intuitively, the infected cell does not lyse (thereby continuing the infection process) as it is not expected to be burdened by the presence of one inclusion containing only one (metabolically inert and small) EB form which does not compete for its essential proteins. Such an infected epithelial cell will eventually die; at about the natural death rate of healthy epithelial cells, or cleared by the host immune response.

In the results presented in Figures 3.6 and 3.7, the time at which azithromycin's chlamydial inhibition commences is also at the RB stage of growth. As shown in Figures 3.6-3.7, for the different times at which azithromycin's chlamydial inhibition commences ($0 \leq t_z \leq 15$), it is observed that the burst sizes (number of infectious EB forms released on cell lysis) of lysing cells are strictly less than 7 and 55 EB progenies per lysing infected epithelial cell, respectively. However, when azithromycin's chlamydial inhibition commenced when most RB forms have replicated (that is when chlamydial protein synthesis has largely been concluded), while some RBs are asynchronously differentiating to EBs ($15 < t_z \leq 55$), it can be seen (as shown in Figures 3.8-3.12) that the effectiveness of the antibiotic in inhibiting chlamydial growth and inclusion formation was drastically reduced. This is made evident by the formation and survival of very significant numbers of EBs (greater than 190 EB progenies per lysing infected epithelial cell) that were released to the surrounding host cells on cell lysis, for further rounds of the infection process. As expected, when the time at which azithromycin's chlamydial inhibition commences coincides with the hour of host cell lysis, azithromycin has no effect on the inhibition of chlamydia replication, differentiation, or inclusion formation (see Figure 3.11). We note that the concentrations of the drug decay linearly in each treatment scenario since it is described by a linear separable variable differential equation as shown in Equation (3.3), whereas, the numbers of EBs and RBs decay exponentially, as shown, for example, by the solutions in Equations (3.8) and (3.14). We also note that in Figures 3.4-3.12, the number of RBs have essentially decayed to (approximately) zero[1].

[1]The number of cells are not technically zero in finite time, but for practical purposes, the number of cells are zero. Throughout this thesis, all references to zero concentration or number of cells at final time are simply approximations of numbers strictly less than unity.

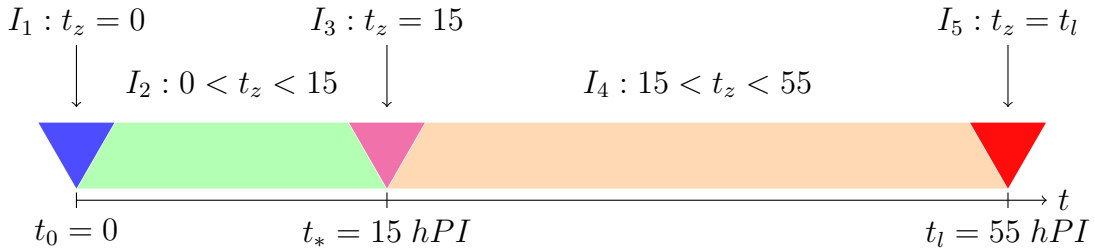

Figure 3.3: **A diagrammatic representation of the chlamydial developmental cycle, highlighting the times (t_z) at which the inhibitory effects of azithromycin on *Chlamydia* commences.** The time values on the schematic are typical values used in the simulation. hPI means hours postinfection. t_0 indicates when the first EB form differentiates to an RB form, t_* is the point at which RBs commence differentiation back to EB form, and t_l is the time of infected host cell lysis.

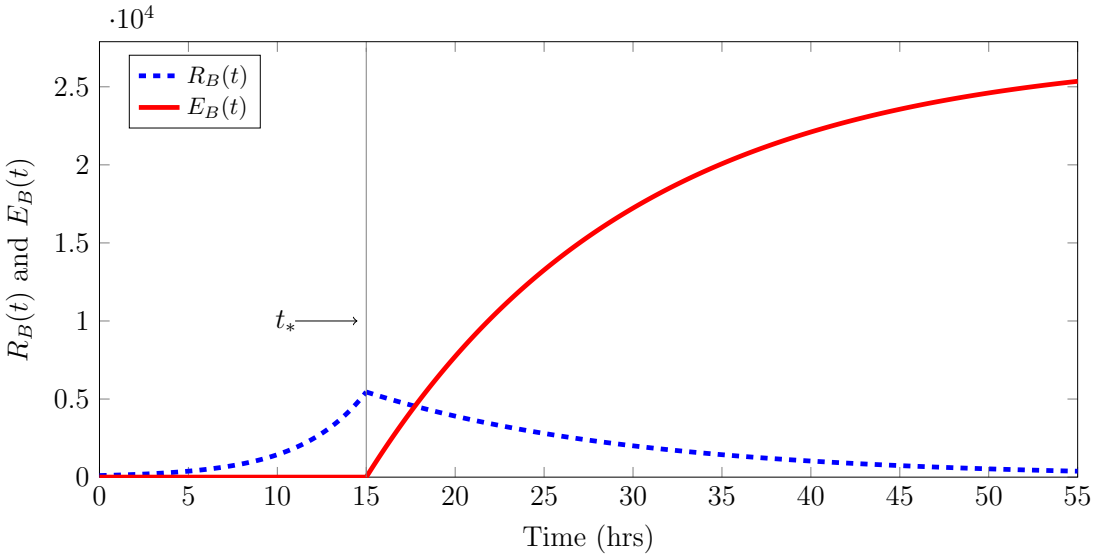

Figure 3.4: **RB and EB developmental cycle curves with no azithromycin administered.** t_* is the time at which RBs commence differentiation back to EB form.

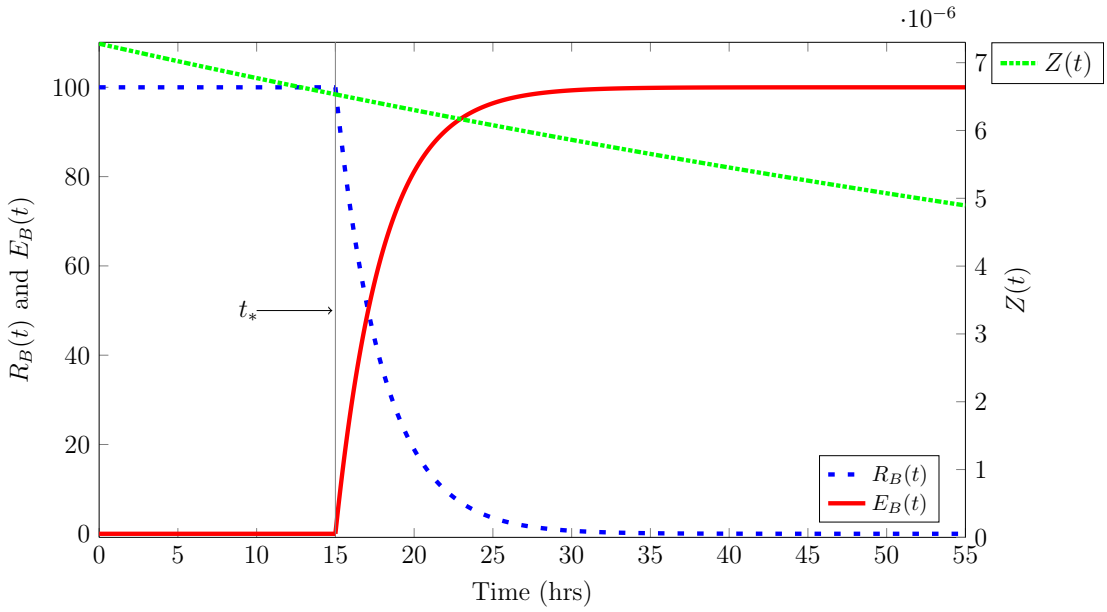

Figure 3.5: **RB and EB developmental cycle curves with azithromycin's chlamydial inhibition commencing at time $t_z = t_0 = 0$.** With respect to the model in Subsection 3.1.2, azithromycin's chlamydial inhibition commenced at the beginning of the chlamydial developmental cycle. t_* is the point at which RBs commence differentiation back to EB form.

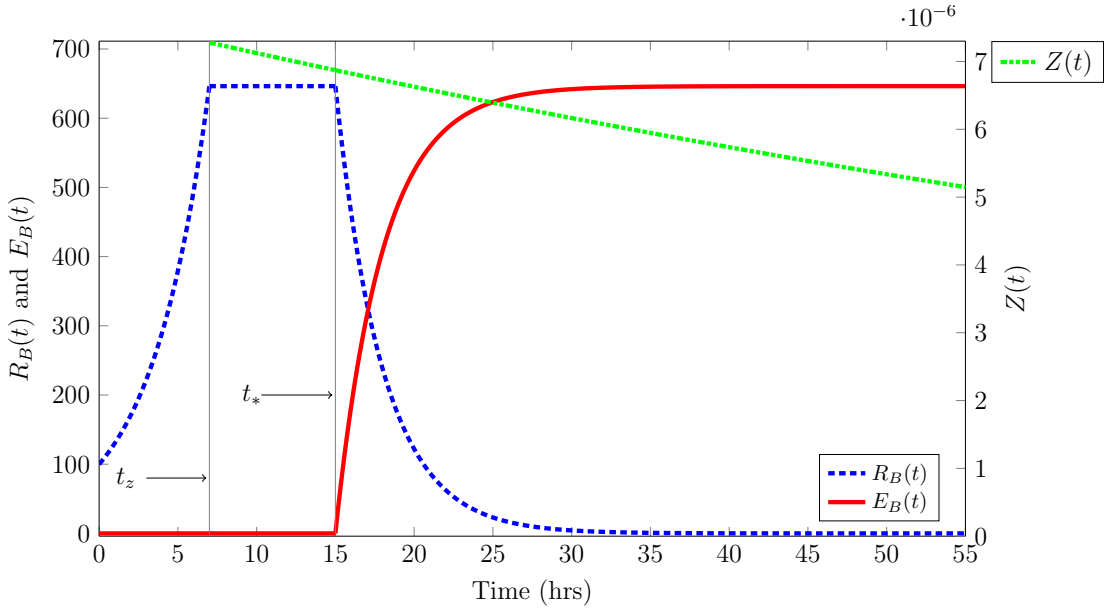

Figure 3.6: **RB and EB developmental cycle curves with azithromycin's chlamydial inhibition commencing at time $t_z = 7$ hPI**. This simulation was produced by numerical solutions of the submodel in Subsection 3.1.3. t_* is the point at which RBs commence differentiation back to EB form. hPI means hours postinfection.

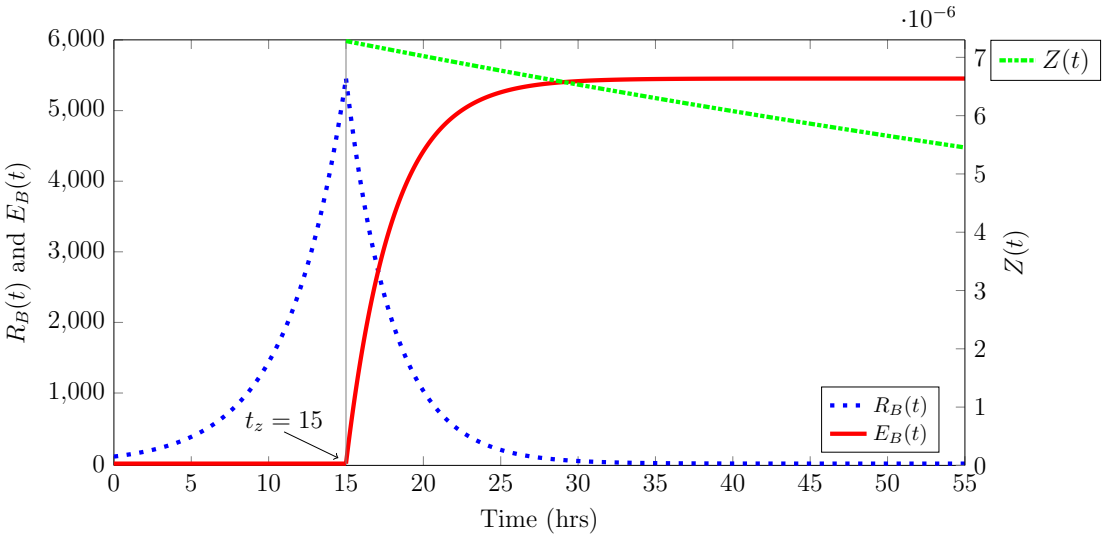

Figure 3.7: **RB and EB developmental cycle curves with azithromycin's chlamydial inhibition commencing at time $t_z = t_* = 15$ hPI.** This simulation was produced by numerical solutions of the submodel in Subsection 3.1.4. t_* is the point at which RBs commence differentiation back to EB form. hPI means hours postinfection.

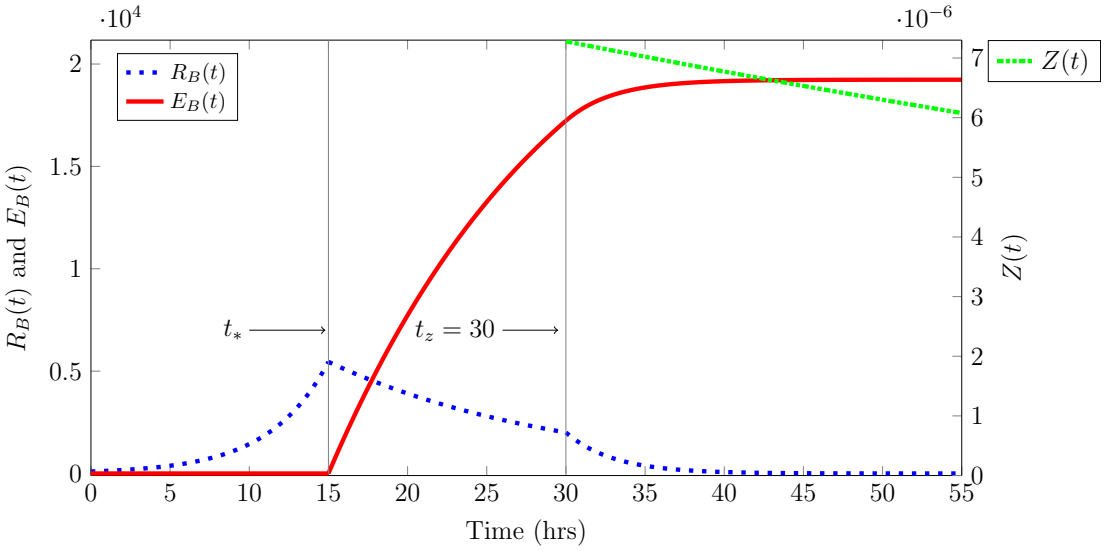

Figure 3.8: **RB and EB developmental cycle curves with azithromycin's chlamydial inhibition commencing at time $t_z = 30$ hPI.** This simulation was produced by numerical solutions of the submodel in Subsection 3.1.5. t_* is the point at which RBs commence differentiation back to EB form. hPI means hours postinfection.

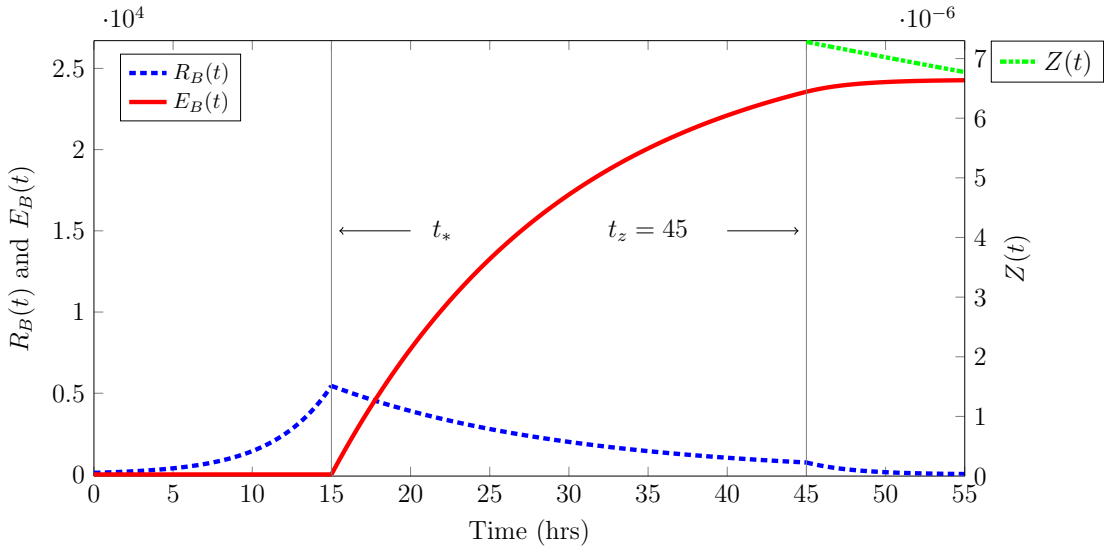

Figure 3.9: **RB and EB developmental cycle curves with azithromycin's chlamydial inhibition commencing at time $t_z = 45$ hPI.** This simulation was produced by numerical solutions of the submodel in Subsection 3.1.6. t_* is the point at which RBs commence differentiation back to EB form. hPI means hours postinfection.

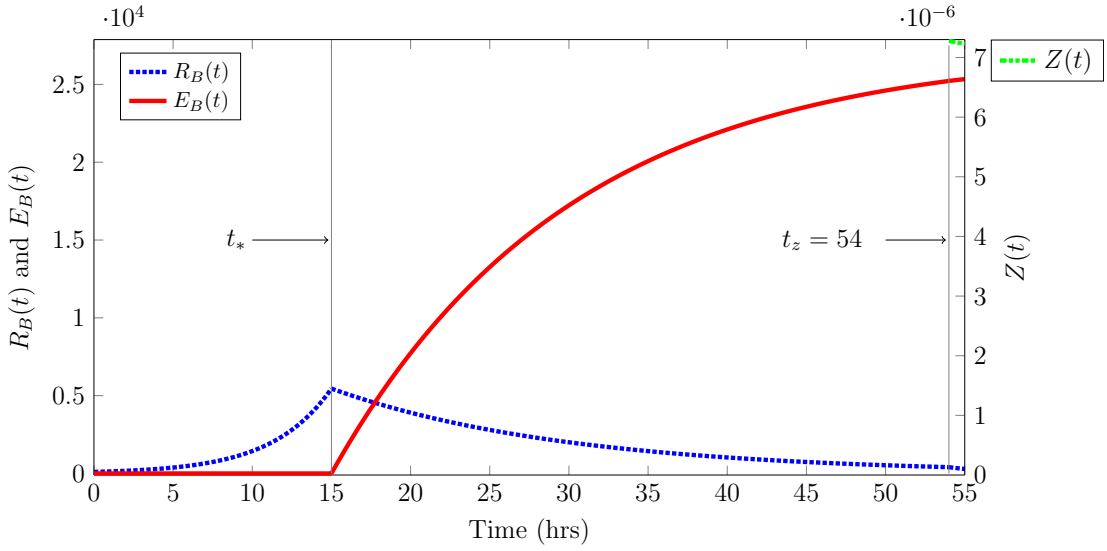

Figure 3.10: **RB and EB developmental cycle curves with azithromycin's chlamydial inhibition commencing at time $t_z = 54$ hPI.** This simulation was produced by numerical solutions of the submodel in Subsection 3.1.5. t_* is the point at which RBs commence differentiation back to EB form. hPI means hours postinfection.

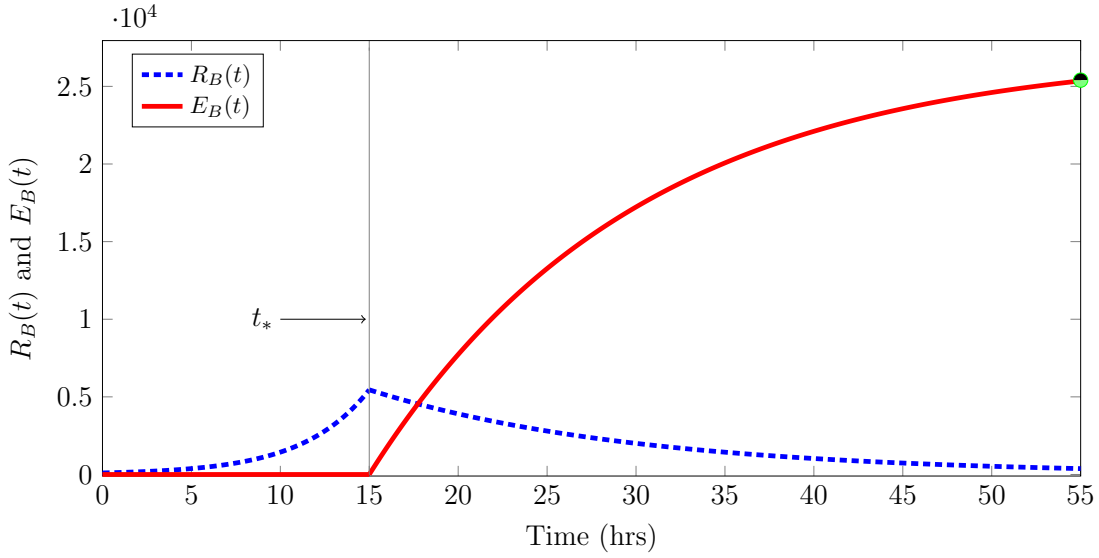

Figure 3.11: **RB and EB developmental cycle curves with azithromycin's chlamydial inhibition commencing at time $t_z = t_l = 55$ hPI.** This simulation was produced by numerical solutions of the submodel in Subsection 3.1.6. t_* is the point at which RBs commence differentiation back to EB form. hPI means hours postinfection.

3.4 Discussion

We constructed a model of the chlamydial developmental cycle (CDC) to investigate how different timing of active antibiotic delivery (and consequently the inhibitory activity of the treatment), within the CDC and on a single cell level, will impact on the prognosis of chlamydial infections. We used azithromycin as a prototype antibiotic treatment due to its pharmacokinetic and pharmacodynamic properties on chlamydial infections. In order to clear *Chlamydia*, our model, which describes an *in vitro* investigation, attempts to use the *in vivo* equivalence of a single 1-g oral dose treatment. The presented model was investigated under five different treatment scenarios: the time at which azithromycin's chlamydial inhibition commences (1) coincides with EB-RB differentiation; (2) occurs during RB replication; (3) coincides with RB-EB differentiation; (4) occurs during asynchronous RB-EB differentiation and RB replication; and (5) occurs at cell lysis.

Using numerical simulations, the model was able to generate the clearance of intracellular RBs, depending on the time at which azithromycin's chlamydial inhibition commences. A graphical illustration of the burst size of (number of infectious EBs released by) a lysing infected cell with respect to the time at which azithromycin's chlamydial inhibition commences within the CDC can be seen in Figure 3.12. Figure 3.12 shows that when azithromycin's chlamydial inhibition commenced, for example, at times $t_z = 0$, $t_z = 15$, and $t_z = 55$ (the time of cell lysis), the burst sizes were 1, 54, and 253 EB progenies per lysing infected epithelial cell, respectively. Thus, our model suggests that the later the time at which azithromycin's chlamydial inhibition commences within the CDC, the greater the burst size of lysing infected cells.

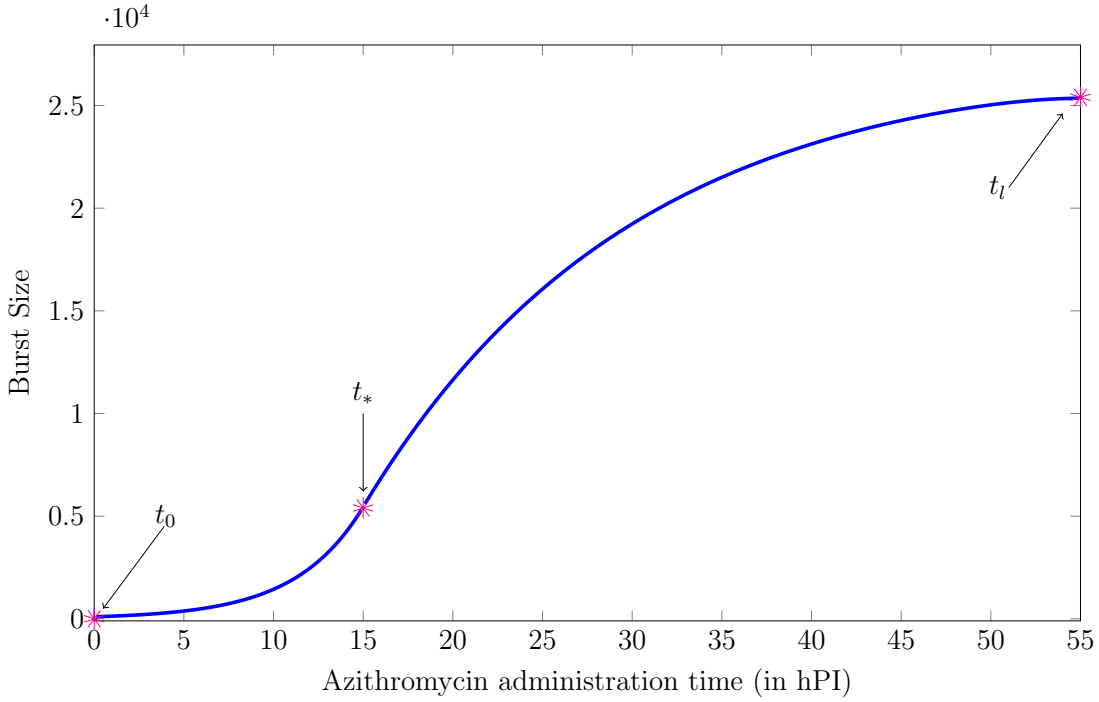

Figure 3.12: **A graphical representation of the times at which azithromycin's chlamydial inhibition commences (within the chlamydial developmental cycle (CDC)) against the burst size of lysing cells.** It can be seen that the later the time at which azithromycin's chlamydial inhibition commences within the CDC, the greater the burst size of lysing cells. t_0 indicates when the first EB form differentiates to an RB form, t_* is the point at which RBs commence differentiation back to EB form, and t_l is the time of infected host cell lysis. hPI means hours postinfection.

Chlamydia has a complex contact-dependent type III secretion (TTS) system for deploying its proteins which modulate host cell pathways. The chlamydial TTS is involved in the release of virulence proteins from intracellular *Chlamydia* into the host cell cytosol [27,52,167]. Since an EB infecting a host cell enters into a tightly closed membrane-bound vacuole, there is contact between it and the vacuole (inclusion). Even when the EB differentiates into an RB, the contact is intact [167]. However, it is hypothesised that a trigger for the later RB to EB differentiation is the detachment of the RB from the surface of the inclusion membrane, which is due to TTS inactivation [52,167]. Thus, the EBs produced in the late CDC accumulate mostly in the lumen of the inclusion [167].

As previously noted in Subsection 2.1.3, in a normal intracellular chlamydial development, the *Chlamydia* protease-like activity factor (CPAF), an important chlamydial virulence factor which may aid the expansion of chlamydial inclusion, accumulates in the mid-late CDC [27, 78]. CPAF activity is concentration-dependent [78]. We suppose that in the presence of only a few intracellular *Chlamydia* during the mid-late CDC, relatively fewer CPAF would be secreted. The lack of critical concentration of CPAF protein, needed for CPAF activity to be triggered, would cause the not-yet-secreted CPAF to remain dormant [78]. Thus, we suppose that the singular EB produced at the end of the cycle, when azithromycin's inhibitory activity commenced at the beginning of the cycle, does not cause the inclusion to grow or expand to a limit that cannot be contained within the

host cell [167]. Hence, there is no apoptosis of host infected cell because of a controlled CPAF activity, which is indeed a precursor for persistent infection condition [71, 78].

Model results suggest that for the effective antibiotic inhibition of *Chlamydia*, the efficient inhibitory activity of the drug should at least commence at the start of the cellular infection. A stronger and faster intracellular penetration of antibiotics may achieve this. We hypothesise that the discovery and development of more effective routes of antibiotic administration, through the targeted delivery of antibiotics, may bring about the effective treatment of a chlamydial infection. Targeted delivery of drugs is a treatment strategy that aims to selectively deliver antibiotics to the pathogen of interest at the infection site, where they can best exert their therapeutic effect [155]. Such a targeted drug delivery for chlamydial infection has been recently explored. In an *in vitro* system, Hai *et al.* [64] treated *C. trachomatis* by using transferrin as a carrier for targeted delivery of amoxicillin into the vacuole of *Chlamydia trachomatis*. The strategy proved to be significantly more effective in the suppression of *Chlamydia* more than the amoxicillin alone. At low concentrations, the transferrin-amoxicillin combination was observed to be bactericidal on *Chlamydia* as compared to the use of amoxicillin alone. The targeted drug was also observed to be targeted at the chlamydial inclusion as compared to free amoxicillin [64]. Such a result as this is promising and it suggests that targeted drug delivery, which may facilitate a faster and higher delivery of antibiotics to the intracellular pathogen before its developmental cycle progresses, may be a solution to the effective treatment of chlamydial infections.

Despite the known complexity of the CDC, we have kept the model simple. The use of such simple models can often lead to important insights of a general nature into the factors or processes that shape epidemiological patterns [57]. As such, the proposed hypotheses and insights presented in this study should be considered in context and used to simulate further theoretical and experimental research [107]. However, this model can be built upon for the development of more complicated models that capture more of the processes that are fundamental to chlamydial infection. Possible extension of the presented model include (1) the use of a suitable Heaviside function in the switching function; (2) the investigation of the impact of treatment/drugs that boost or strengthen the immune system's response to chlamydial infections; (3) the investigation of the impact of an enhanced cell-mediated immune response; and (4) the execution of uncertainty and sensitivity analyses because there can be significant uncertainty in the determination of (biological) parameter values (which may be patient-specific) related to a disease such as *Chlamydia*.

4 Optimal control of the treatment of *Chlamydia trachomatis* infection within-host

Whereas in the preceding chapter we considered the timing of antibiotic delivery, relative to the chlamydial developmental cycle (CDC), and its effect on chlamydial replicative potential (burst size), we now pursue a more comprehensive mathematical picture of the optimal timing of antibiotic delivery. In particular, we investigate the intracellular interactions between *Chlamydia* and host epithelial cells, in order to determine optimal treatment strategies needed for the clearance of an *in vivo* chlamydial infection.

The quest for improvements to therapeutic regimens for *C. trachomatis* infection remains an area of open research [67, 77]. As discussed in Section 2.2, some antibiotics, such as azithromycin and doxycycline (which are recommended antibiotics for treatment of *Chlamydia* infection), are bacteriostatic on intracellular *Chlamydia*. Data from *in vitro* testing also suggest that prolonged exposure of *C. trachomatis* to an antimicrobial is required for optimum efficacy [76, 77]. As previously discussed in Section 2.1.3, the proteasome/protease-like activity factor (CPAF), an enzyme released by *Chlamydia* for the evasion of the host defense system, is a major virulence factor in chlamydial infections. The inhibition of CPAF, which is a potential anti-*Chlamydia* therapeutic strategy (as discussed in Section 2.3.2), is expected to inhibit intracellular *Chlamydia* growth [27] and also restore the presentation of chlamydial peptides to T cells [141]. Consequently, these are expected to facilitate clearance of the infection by the host immune cells. Wilson [169] also suggested that there will be an increased ability to clear *Chlamydia* infection if the cytotoxic immune response clears infected epithelial cells prior to lysis of the cells.

Hence, based on the literature, we propose that alongside antibiotic activity, the presence of a proteasome-specific inhibitor, such as lactacystin, may enhance the capacity of the cell-mediated immune response in the clearance of *Chlamydia* infection. We also hypothesise that treatment failures are perhaps the consequences of sub-optimal treatment regimens. Thus, we explore optimal strategies for such treatments using optimal control techniques.

Optimal control theory is a source of very useful and flexible tools for research activities in optimal therapies in medicine, optimal strategies in economics, and in many other

fields of applied sciences [7, 125]. It is a powerful mathematical tool that can be used to make decisions involving complex biological situations. Its use has thus been on the rise in epidemiological and biological models [100]. The impacts of optimal control on the spread of infectious diseases have been studied in many epidemiological models (see [33, 54, 143, 154] and references within). In particular, several within-host models of infectious diseases have used optimal control to predict optimal therapeutic intervention strategies [33, 54, 83, 85, 89]. However, to the best of our knowledge, no within-host mathematical model has been developed to study optimal intervention strategies for *Chlamydia* infections.

In this chapter, we present a deterministic mathematical model of *C. trachomatis* infection, within-host, with a particular focus on determining the optimal scheme(s) for the treatment of (genital) chlamydial infections, that is, when and how treatment should be initiated. Our work aims to determine hypothetical optimal treatment strategies that not only minimise the production of free extracellular *Chlamydia*, but possibly enhance the cell-mediated immune response (that is, cytotoxic immune response) in the clearance of chlamydial infection. The presented model also aims to maximise the concentration of healthy epithelial cells. In Section 4.1, we develop a model for the optimal control of *Chlamydia* infection and present a mathematical analysis of the model. In particular, using an existence result, we guarantee the existence of an optimal control pair with finite objective functional in Section 4.2. In Section 4.3, we use Pontryagin's Maximum Principle to characterise the optimal control pair. We present numerical results of simulation of the model system in Section 4.4. Our conclusions are discussed in Section 4.5.

4.1 Model Formulation

We develop a mathematical model of the cellular (within-host) dynamics of *Chlamydia*, to investigate the impact of treatment on the within-host dynamics of chlamydial infection. The model has its basic structure and derivation in Wilson's model [169]. Ordinary differential equations were used to model the cellular dynamics of the interactive processes between extracellular *Chlamydia*, uninfected epithelial cells and *Chlamydia*-infected epithelial cells. The model also describes the role of the humoral and cell-mediated immunity in the *Chlamydia* developmental cycle.

We denote by $C(t)$, the concentration of free extracellular *Chlamydia* (elementary body form of *Chlamydia*, in particular), by $E(t)$, the concentration of uninfected mucosal epithelial cells, and by $I(t)$, the concentration of *Chlamydia*-infected epithelial cells at time t. Thus, the model presented by Wilson [169], which we shall refer to as the "basic *Chlamydia* model" is described by the following system of ordinary differential equations:

$$\frac{\mathrm{d}C}{\mathrm{d}t} = Pk_2I - \mu C - k_1CE, \tag{4.1}$$
$$\frac{\mathrm{d}E}{\mathrm{d}t} = P_E - \delta_E E - k_1CE, \tag{4.2}$$
$$\frac{\mathrm{d}I}{\mathrm{d}t} = k_1CE - k_2I - \gamma I, \tag{4.3}$$

with initial conditions $C(t_0) = C_0$, $E(t_0) = E_0$, and $I(t_0) = I_0$, where t_0 is the initial time. The model assumes that at a rate of k_2, P *Chlamydia* bacteria are released from infected cells. The rate of clearance by macrophages is μ, the rate of epithelial cell infection (which may be reduced by antibodies) is denoted by k_1, the rate of production of epithelial cells is denoted by P_E, the natural death rate of epithelial cells is denoted by δ_E, and the rate of clearance of infected cells, due to of cell-mediated immunity is denoted by γ. See Table 4.1 for a concise presentation of the variables and parameters described.

We apply techniques of optimal control theory to the model system (4.1)-(4.3), and explore optimal control strategies associated with different kinds of treatment of chlamydial infections.

Thus, the following system of equations is proposed:

$$\frac{\mathrm{d}C}{\mathrm{d}t} = (1-u_1)Pk_2I - \mu C - k_1CE, \tag{4.4}$$
$$\frac{\mathrm{d}E}{\mathrm{d}t} = P_E - \delta_E E - k_1CE, \tag{4.5}$$
$$\frac{\mathrm{d}I}{\mathrm{d}t} = k_1CE - k_2I - (\gamma + u_2)I, \tag{4.6}$$

with initial conditions $C(t_0) = C_0$, $E(t_0) = E_0$, and $I(t_0) = I_0$, where t_0 is the initial time.

The functions u_1 and u_2 represent two different treatment strategies. The functions u_1 and u_2, respectively, represent, the bio-available and deliverable amount of drugs that reduce, or possibly eliminate, the production of viable *Chlamydia* (bacteriostatic or bactericidal agents, respectively), and of drugs that act as proteasome-specific inhibitor, which may enhance the cell-mediated immune response in the clearance of chlamydial infection prior to the lysis of infected epithelial cells. The functions u_1 and u_2 are bounded Lebesgue integrable functions satisfying $0 \leq u_1(t) \leq 1$ and $0 \leq u_2(t) \leq m \leq 1$, where m is the maximum attainable amount/proportion of treatment $u_2(t)$ (and 1 is the maximum attainable amount/proportion of treatment $u_1(t)$) at the site of infection. The use of a *Chlamydia* proteasome-specific inhibiting treatment/drug is hypothetical, that is, it not a clinically tested treatment. Consequently, there is a lot of gap in our knowledge of its potential *in vivo* spatio-temporal dynamics, such as its serum and tissue concentrations, and its half-life. Thus, we assume that the maximum amount of the treatment that

concentrates at the site of infection, that is m, is lesser than or equal to its maximum tolerable amount, that is 1.

The coefficient $(1 - u_1(t))$ in Equation (4.4) is a linearly decreasing factor in the control u_1 for the production of more infectious progeny (extracellular *Chlamydia*) by bursting infected cells as a result of the administration of bacteriostatic treatments. The factor aims to reduce the concentration of extracellular *Chlamydia* that are being released by infected cell lysis for the continuity of the infection process.

The control functions are defined on fixed time intervals since the treatment of chlamydial infections (or antibiotics generally) are not expected to be administered for an infinite period of time. Thus the controls are defined for $t_{\text{initial}} \leq t \leq t_{\text{final}}$, that is $t_0 \leq t \leq t_f$, where for current recommended treatment guidelines, $t_f - t_0 \leq 7$ days [3, 99, 111] (Also see Section 2.2).

The concentrations of C, E, and I cells are per millimetre cube of human (genital) tissue, for example, the female reproductive tract. Thus the units of C, E, and I are cells/mm^3. For the dimensions in Equations (4.4)-(4.6) to be correct and biologically sensible, the model parameters should have the following units: P, no unit (it is just a number- of cells); k_1, mm^3/day/cell; k_2, day^{-1}; P_E, cells/mm^3/day; δ_E, day^{-1}; γ, day^{-1}; μ, day^{-1}; u_1 and u_2, no units (they are concentrations of drugs/treatments that have been scaled by the largest tolerable drug dosage, in concentration, of each treatment. Thus, they are proportions/amounts of drugs); and m, no unit (it is a proportion/amount of treatment).

Our goal is to minimise the concentration of *Chlamydia*, infected cells, and systemic costs of treatment/drug to the body, and to maximise the concentration of healthy epithelial cells present at the end of a therapeutic intervention strategy. Hence, we seek an optimal control pair (u_1^*, u_2^*), such that

$$J(u_1^*, u_2^*) = \min_{u_1, u_2 \in \Gamma} J(u_1, u_2), \tag{4.7}$$

where Γ, the set of admissible controls is defined as

$$\Gamma = \{(u_1, u_2) | u_1 \text{ and } u_2 \text{ are Lebesgue measurable}, 0 \leq u_1 \leq 1, 0 \leq u_2 \leq m \leq 1, t \in [0, t_f]\}. \tag{4.8}$$

The objective functional to be minimized is

$$J(u_1, u_2) = \int_{t_0}^{t_f} \left[C(t) + A_1 I(t) + \frac{A_2}{2} u_1^2 + \frac{A_3}{2} u_2^2 \right] \mathrm{d}t + A_4 C(t_f) - A_5 E(t_f), \tag{4.9}$$

where t_f is the final time of the therapeutic intervention strategy, and the positive constant weights A_1, A_2, A_3, A_4, and A_5, measure the relative costs of implementing the respective

treatment strategies over the period $[0, t_f]$. Their values will depend on the relative importance of each of the control measures in the treatment of the disease.

Costs are chosen to be quadratic functions because they need to be twice differentiable. Thus, the relationship between drug quantities and the concentration of interacting species takes the specified form.

We assume that the controls are quadratic in the cost functions because they need to be twice differentiable. Thus, the relationship between the effects of the treatments and the interacting species (*Chlamydia* and host cells) takes the a nonlinear form. This is in line with several other literatures [5, 83, 85, 143, 154].

The terms $C(t)$ and $A_1 I(t)$ represent the costs of the clearance of viable *Chlamydia*, and that of the infection of healthy epithelial cells, respectively. The terms $\frac{A_2}{2}u_1^2$ and $\frac{A_3}{2}u_2^2$ describe the costs associated with administering the respective intervention strategies. The terms $A_4 C(t_f)$ and $A_5 E(t_f)$ are terminal costs associated with the minimisation of the concentration of *Chlamydia*, and the maximisation of the concentration of healthy epithelial cells, respectively, by the end of the treatment.

Variables	**Description**	**Values**
C	Free extracellular *Chlamydia*	$C_0 = 50$ cells/mm^3
E	Healthy mucosal epithelial cells	$E_0 = 200$ cells/mm^3
I	*Chlamydia*-infected epithelial cells	$I_0 = 0$ cells/mm^3
Parameters		
P	Burst size per infected cell	200-500 [169]
k_1	Rate of cell infection	0.02 mm^3/day/cell [169]
k_2	Rate of infected cells burst	0.33-0.6 day^{-1} [169]
P_E	Rate of production of mucosal epithelial cells	40 cells/mm^3/day [169]
δ_E	Rate of natural death of epithelial cells	[0.25-0.26] day^{-1} [8, 21]
γ	Effectiveness of cell-mediated immunity	2-10 day^{-1} [169]
μ	Effectiveness of humoral immunity	2-10 day^{-1} [169]
m	Maximum attainable amount of control $u_2(t)$	[0.1-0.9] [estimated]

Table 4.1: Variables, parameters, and values used in numerical simulations.

4.1.1 Basic Properties

In this section, we present some basic qualitative results for the basic *Chlamydia* model (4.1)-(4.3), in order to ascertain that the problem is mathematically and biologically well posed.

Positivity of solutions

First, a plausible biological model requires non-negative populations. Since the model system (4.1)-(4.3) describes the dynamics of cell populations, it is essential that all its state variables remain non-negative for all time. This implies that the solutions of the system will remain positive for all $t > 0$ when given positive initial conditions. We establish this important condition via the following lemma:

Lemma 4.1.1. *Given non-negative initial values of the state variables in Equations* (4.1)-(4.3)*, non-negative solutions are generated for all time* $t > 0$.

Proof. Let $(C(0), E(0), I(0))$ be a positive initial condition and denote by $[0, t_{\max}]$, the maximum interval of existence of the corresponding solution. In order to prove that the solution is positive in $[0, +\infty]$, it suffices to show that it is positive in $[0, t_{\max}]$.

Let $t_s = \sup\{0 < t < t_{\max} : C(t) > 0, E(t) > 0, I(t) > 0 \text{ on } [0, t]\}$.

$t_s > 0$ since $C(0)$, $E(0)$, and $I(0)$ are non-negative. Suppose $t_s < t_{\max}$.

From Equation (4.1),

$$\frac{\mathrm{d}C}{\mathrm{d}t} + (\mu + k_1 E)C = Pk_2 I.$$

Thus,

$$\frac{\mathrm{d}}{\mathrm{d}t}\left[C(t)\exp\left\{\mu t + k_1\int_0^t E(\tau)\mathrm{d}\tau\right\}\right] = Pk_2 I(t)\left(\exp\left\{\mu t + k_1\int_0^t E(\tau)\mathrm{d}\tau\right\}\right),$$

so that

$$\begin{aligned} C(t_s)\exp\left\{\mu t_s + k_1\int_0^{t_s} E(\tau)\mathrm{d}\tau\right\} - C(0) \\ = \int_0^{t_s}\left[Pk_2 I(\hat{\tau})\exp\left\{\mu\hat{\tau} + k_1\int_0^{\hat{\tau}} E(\tau)\mathrm{d}\tau\right\}\right]\mathrm{d}\hat{\tau}. \end{aligned}$$

Hence,

$$\begin{aligned} C(t_s) &= C(0)\exp\left\{-\left(\mu t_s + k_1\int_0^{t_s} E(\tau)\mathrm{d}\tau\right)\right\} \\ &+ \exp\left\{-\left(\mu t_s + k_1\int_0^{t_s} E(\tau)\mathrm{d}\tau\right)\right\}\int_0^{t_s}\left[Pk_2 I(\hat{\tau})\exp\left\{\mu\hat{\tau} + k_1\int_0^{\hat{\tau}} E(\tau)\mathrm{d}\tau\right\}\right]\mathrm{d}\hat{\tau} \\ &> 0. \end{aligned}$$

It can be shown by a similar argument that $E(t_s) > 0$ and $I(t_s) > 0$.

This contradicts the fact that t_s is the supremum because at least one of the state variables should be equal to zero at t_s. Therefore $t_s = t_{\max}$. Thus, $C(t) \geq 0$, $E(t) \geq 0$ and $I(t) \geq 0$, for all time $t > 0$. This completes the proof. □

Invariant region

We consider the long term behaviour of the system (4.1)-(4.3) in an apposite biologically feasible region $\mathcal{D}$.

Since all the parameters and state variables of model system (4.1)-(4.3) are non-negative for all $t \geq 0$, from Equation (4.1), it follows that

$$\begin{aligned}\frac{\mathrm{d}C}{\mathrm{d}t} &= Pk_2I - \mu C - k_1CE - u_1Pk_2I \\ &\leq Pk_2I - \mu C.\end{aligned}$$

This implies that

$$\frac{\mathrm{d}C}{\mathrm{d}t} + \mu C \leq Pk_2I.$$

Thus,

$$C(t) \leq C(0)e^{-\mu t} + e^{-\mu t}Pk_2 \int_0^t I(\tau)e^{\mu\tau}\mathrm{d}\tau.$$

Since the interval $[0, t]$ is compact, and since the integrand, $I(\tau)e^{\mu\tau}$, is continuous on that interval, the corresponding integral is finite. Therefore

$$C(t) \leq e^{-\mu t}(C(0) + Pk_2m_1) = \bar{m_1},$$

where $m_1 = \int_0^t I(\tau)\, e^{\mu\tau}\mathrm{d}\tau$.

From Equation (4.2),

$$\frac{\mathrm{d}E}{\mathrm{d}t} \leq P_E - \delta_E E.$$

This implies that

$$\frac{\mathrm{d}E}{\mathrm{d}t} + \delta_E E \leq P_E.$$

Thus,

$$\begin{aligned}E(t) &\leq E(0)e^{-\delta_E t} + \frac{P_E}{\delta_E}(1 - e^{-\delta_E t}), \\ &= E(0)e^{-\delta_E t} + E^*(1 - e^{-\delta_E t}), \\ &= E^* - (E^* - E(0))e^{-\delta_E t}.\end{aligned}$$

$E(t)$ either approaches E^* asymptotically or there exists some finite time after which $E(t) \leq E^*$.

From Equation (4.3),

$$\frac{\mathrm{d}I}{\mathrm{d}t} \leq k_1CE - k_2I,$$

that is

$$\frac{\mathrm{d}I}{\mathrm{d}t} + k_2I \leq k_1CE.$$

Using a standard comparison theorem by Lakshmikantham *et al.* [95], it can be shown that

$$I(t) \leq I(0)e^{-k_2 t} + e^{-k_2 t} k_1 \int_0^t C(\tau)E(\tau)e^{k_2 \tau} \mathrm{d}\tau.$$

Again, the integral is finite since a continuous function, $C(\tau)E(\tau)e^{k_2\tau}$, is integrated over a compact interval. Therefore

$$I(t) \leq I(0)e^{-k_2 t} + e^{-k_2 t} k_1 m_2 = \bar{m_2},$$

where $m_2 = \int_0^t C(\tau)E(\tau)e^{k_2\tau}\mathrm{d}\tau$.

Hence, the region $\mathcal{D} = \left\{(C(t), E(t), I(t)) \in \mathbb{R}^3_+ : C(t) \leq \bar{m_1}, E(t) \leq E^*, I(t) \leq \bar{m_2}\right\}$ is positively invariant and attracting for the model system (4.1)-(4.3), that is, every feasible solution of the model with initial conditions in $\mathcal{D}$, will remain in $\mathcal{D}$, for all $t \geq 0$. We establish this result via the following lemma:

Lemma 4.1.2. *The biologically feasible region $\mathcal{D}$ is positively invariant and attracting with respect to the model system* (4.1)-(4.3) *with initial conditions in $\mathbb{R}^3_+$.*

It is clear that the right hand sides of the model equations (4.1)-(4.3) are smooth. Hence, initial value problems have unique solutions on the region $\mathcal{D}$. Also, since paths are confined in $\mathcal{D}$, solutions exist for all time $t \geq 0$. It follows that solutions to system (4.1)-(4.3) exist in $\mathcal{D}$ and are unique. Having thus confirmed that the model system is mathematically and biologically well posed, we proceed to study the dynamics of the flow induced by the model system (4.1)-(4.3) in $\mathcal{D}$.

4.1.2 Existence and stability of equilibria

Basic reproduction number

The most important and widely used quantity in infectious disease epidemiology is the basic reproduction number, denoted by $\mathcal{R}_0$ [69]. It is a quantity that measures the expected number of new or secondary cases produced by one typical individual in a completely susceptible population, during its entire infectiousness period [40, 70, 157]. From the definition of $\mathcal{R}_0$, one can deduce that if $\mathcal{R}_0 < 1$, each infected individual averagely produces less than one secondary case, and the infection will be cleared from the population. However, if $\mathcal{R}_0 > 1$, each infected individual would averagely produce more than one secondary case, and the infection will invade the population [69]. This is referred to as the *threshold criterion*, which summarily states that "*the disease can invade if* $\mathcal{R}_0 > 1$, *whereas it cannot if* $\mathcal{R}_0 < 1$" [40]. The $\mathcal{R}_0$ threshold also has the property that if $\mathcal{R}_0 < 1$, the disease-free equilibrium (DFE) of the system is locally asymptotically stable, but if $\mathcal{R}_0 > 1$, the DFE is unstable [70,157]. Thus, $\mathcal{R}_0$ is considered the threshold

quantity that plays the vital role of determining when an infection will invade and persist in a new host population [69, 70].

In the computation of $\mathcal{R}_0$ for models with more than one class of infectives, the general method used in the literature is the next generation method (NGM) [69]. The NGM is a standard procedure used to evaluate the $\mathcal{R}_0$ expression in models that include multiple classes of infected species/individuals [69,101,157]. The method is a generalisation of the Jacobian method of estimating $\mathcal{R}_0$ whereby the nonlinear system of differential equations is linearised around the DFE equilibrium [40].

In this method, for the computation of $\mathcal{R}_0$, the only states regarded are those that apply to infected individuals/species [41, 157]. Equations matching this criterion in the ODE system, which are referred to as the *infected subsystem* [41], are those that describe the production of new infections and other changes in state among infected species/individuals [41, 157]. The first step is the linearisation of the infected subsystem, which must have been distinguished into new infections, and the transfer of species/individuals in and out of the infected compartments.

Consider the following general autonomous system:

$$\dot{x} = f(x), \quad x \in \mathbb{R}^n. \tag{4.10}$$

Let there be m infected compartments out of all n compartments. Sort the compartments so that the first m compartments correspond to infected individuals/species. Define $\mathbf{X}_s = \{x \geq 0 | x_i = 0, i = 1, \ldots, m\}$ as the set of all disease free states. Let $\mathcal{F}_i(x)$ be the rate of appearance of only new infections in compartment i, $\mathcal{V}_i^+(x)$, the rate of transfer of species/individuals into compartment i by all other means, and $\mathcal{V}_i^-(x)$, the rate of transfer of species/individuals out of the ith compartment. Then,

$$\dot{x}_i = f_i(x) = \mathcal{F}_i(x) - \mathcal{V}_i(x), \tag{4.11}$$

where $\mathcal{V}_i(x) = \mathcal{V}_i^-(x) - \mathcal{V}_i^+(x)$. Each of the functions satisfies the assumptions in Section 2 of [157] (see Appendix for the assumptions). Then, the next generation operator $\boldsymbol{F}\boldsymbol{V}^{-1}$ can be formed from matrices of partial derivatives $\boldsymbol{F}$ and $\boldsymbol{V}$ as described below.

$$\boldsymbol{F} = \left[\frac{\partial \mathcal{F}_i(x_0)}{\partial x_j}\right] \quad \text{and} \quad \boldsymbol{V} = \left[\frac{\partial \mathcal{V}_i(x_0)}{\partial x_j}\right], \tag{4.12}$$

where $1 \leq i, j \leq m$, and x_0 is the disease-free equilibrium of the ODE system (4.10). Thus, $\mathcal{R}_0$ is evaluated as the spectral radius (dominant eigenvalue) of matrix $\boldsymbol{F}\boldsymbol{V}^{-1}$, that is $\rho(\boldsymbol{F}\boldsymbol{V}^{-1})$ [41,69,157]. The entries of the linear operators $\boldsymbol{F}$, $\boldsymbol{V}$, and $\boldsymbol{V^{-1}}$ have biological meanings. For example, in the matrix $\boldsymbol{-V^{-1}}$, the $(\boldsymbol{-V^{-1}})_{ij}$ entry is the expected time

that a specie presently at stage j will spend in stage i during its entire future 'life' (in an epidemiological sense) [41]. Hence the (i, j) entry of the operator $\boldsymbol{FV}^{-1}$ gives the rate at which the infected individual/specie originally introduced into compartment j produces new infections in compartment i [69, 157].

Remark: In many mathematical models of diseases, especially models with more than one disease state (such as those with an intermediate host, e.g. mosquito-borne disease), the $\mathcal{R}_0$ value generated from the NGM, like from most other method of estimating the $\mathcal{R}_0$, is not actually the number of (new) infectives produced by one infected specie/individual in a wholly susceptible population. The $\mathcal{R}_0$ obtained from this method also does not always produce the mean number of secondary infections. Nevertheless, the $\mathcal{R}_0$ threshold estimated from the method is a measure of disease spread, mostly satisfying the *threshold criterion*. [101].

Due to this shortcoming of the NGM, in the context of the basic *Chlamydia* model (4.1)-(4.3), the basic reproduction number $\mathcal{R}_0$ shall simply be referred to as a disease outbreak threshold with the (true) property that the chlamydial infection will invade the host (reproductive) system if $\mathcal{R}_0$ is greater than unity, but will be cleared if $\mathcal{R}_0$ is less than (or can be brought below) unity.

Local stability of the *Chlamydia*-free equilibrium

The *Chlamydia*-free equilibrium (CFE) can be obtained by the setting the right-hand sides of the basic *Chlamydia* model (4.1)-(4.3) to zero and then choosing solutions where $C = I = 0$. This CFE is given by $\mathbb{F}_0$,

$$\mathbb{F}_0 = (C^*, E^*, I^*) = (0, \hat{E}, 0), \tag{4.13}$$

where $\hat{E} = \dfrac{P_E}{\delta_E}$.

The linear stability of this equilibrium $\mathbb{F}_0$ can be established using the next generation method described in Subsection 4.1.2, on the model system (4.1)-(4.3).

The class of infectives in the model system (4.1)-(4.3) are *Chlamydia* (C) and *Chlamydia*-infected host cells (I), since these two classes facilitate the chlamydial infection process. Thus, the *infected subsystem* of the model system (4.1)-(4.3) is given by Equations (4.1) and (4.3), that is, $(\dot{C}, \dot{I})$. Hence we sort the model system (4.1)-(4.3) so that the first two compartments correspond to the class of infectives, that is $(\dot{C}, \dot{I}, \dot{E})$.

Preserving notations, the rate of appearance of new infections in the three compartments, is denoted by $\mathcal{F}$,

$$\mathcal{F} = \begin{pmatrix} 0 \\ k_1 CE \\ 0 \end{pmatrix}, \tag{4.14}$$

while the rate of transfer of each of the interacting species in and out of the three compartments is denoted by $\mathcal{V}$,

$$\mathcal{V} = -\begin{pmatrix} Pk_2 I - \mu C - k_1 CE \\ -(k_2 + \gamma) I \\ P_E - \delta_E E - k_1 CE \end{pmatrix}. \tag{4.15}$$

Hence, the matrices of partial derivatives $\boldsymbol{F}$ and $\boldsymbol{V}$, for the *infected subsystem*, are respectively given by

$$\boldsymbol{F} = \begin{pmatrix} \frac{\partial \mathcal{F}_1(\mathbb{F}_0)}{\partial C} & \frac{\partial \mathcal{F}_1(\mathbb{F}_0)}{\partial I} \\ \frac{\partial \mathcal{F}_2(\mathbb{F}_0)}{\partial C} & \frac{\partial \mathcal{F}_2(\mathbb{F}_0)}{\partial I} \end{pmatrix} = \begin{pmatrix} 0 & 0 \\ k_1 \hat{E} & 0 \end{pmatrix}, \tag{4.16}$$

and

$$\boldsymbol{V} = \begin{pmatrix} \frac{\partial \mathcal{V}_1(\mathbb{F}_0)}{\partial C} & \frac{\partial \mathcal{V}_1(\mathbb{F}_0)}{\partial I} \\ \frac{\partial \mathcal{V}_2(\mathbb{F}_0)}{\partial C} & \frac{\partial \mathcal{V}_2(\mathbb{F}_0)}{\partial I} \end{pmatrix} = \begin{pmatrix} \mu + k_1 \hat{E} & -Pk_2 \\ 0 & k_2 + \gamma \end{pmatrix}. \tag{4.17}$$

The operator $\boldsymbol{V}^{-1}$ is given by

$$\boldsymbol{V}^{-1} = \frac{1}{(\mu + k_1 \hat{E})(k_2 + \gamma)} \begin{pmatrix} k_2 + \gamma & Pk_2 \\ 0 & \mu + k_1 \hat{E} \end{pmatrix}. \tag{4.18}$$

Hence, the spectral radius of $\boldsymbol{F}\boldsymbol{V}^{-1}$, which is the basic reproduction number $\mathcal{R}_{01}$ of the basic *Chlamydia* model (4.1)-(4.3), is given by

$$\mathcal{R}_{01} = \frac{Pk_1 k_2 \hat{E}}{(\mu + k_1 \hat{E})(k_2 + \gamma)}. \tag{4.19}$$

By inspecting the basic reproduction number $\mathcal{R}_{01}$, one can track the contribution of the infected and infectious classes (infected epithelial cells and elementary bodies, respectively) to the infection process. It can be seen from the expression in (4.19), that the basic reproduction number $\mathcal{R}_{01}$ is the product of the infection rate of healthy epithelial

cells by *Chlamydia*, $k_1\hat{E}$, the number of infectious progenies released by a lysing infected cell, P, the duration of infectiousness of an EB, $\dfrac{1}{\mu + k_1\hat{E}}$, and the proportion of infected cells that survive up to the stage of lysis, $\dfrac{k_2}{k_2+\gamma}$.

We establish the following result by implementing *Theorem 2* of van den Driessche and Watmough [157].

Lemma 4.1.3. *The Chlamydia-free equilibrium (CFE)* $\mathbb{F}_0$*, of the basic Chlamydia model* (4.1)-(4.3)*, is locally stable whenever* $\mathcal{R}_{01} < 1$ *and unstable if* $\mathcal{R}_{01} > 1$*.*

Lemma 4.1.3 implies that when $\mathcal{R}_{01} < 1$, the *in vivo* clearance of *Chlamydia* body forms can be achieved if the initial sizes of the subpopulations of the model (C, E, I) are in the basin of attraction of the CFE $\mathbb{F}_0$.

In order to ensure that the therapeutic effects of an effective *Chlamydia* infection treatment regimen in an *in vivo* or *in vitro* setting system does not depend on either the initial size of *Chlamydia* bodies or innoculum, respectively, or the initial sizes of other subpopulations of the model (E and I), we show that the CFE is globally asymptotically stable (GAS) when $\mathcal{R}_{01} < 1$.

Global stability of the *Chlamydia*-free equilibrium

Theorem 4.1.4. *The Chlamydia-free equilibrium (CFE)* $\mathbb{F}_0$*, of the basic Chlamydia model* (4.1)-(4.3)*, is globally asymptotically stable in* $\mathcal{D}$*, whenever* $\mathcal{R}_{01} < 1$ *and unstable otherwise. The CFE* $\mathbb{F}_0$ *is the only equilibrium when* $\mathcal{R}_{01} \leq 1$*.*

Proof. Consider the candidate Lyapunov function

$$\mathbb{Y} = Pk_2I + (\gamma + k_2)C, \tag{4.20}$$

with Lyapunov derivative (where a dot represents differentiation with respect to t) given by

$$\begin{aligned}
\dot{\mathbb{Y}} &= Pk_2\dot{I} + (\gamma + k_2)\dot{C} \\
&= Pk_2(k_1CE - k_2I - \gamma I) + (\gamma + k_2)(Pk_2I - \mu C - k_1CE) \\
&= Pk_1k_2CE - (k_2(\mu + k_1E) + \gamma(\mu + k_1E))C \\
&= (k_2 + \gamma)(\mu + k_1E)\left(\frac{Pk_1k_2E}{(k_2+\gamma)(\mu + k_1E)} - 1\right)C \\
&\leq (k_2 + \gamma)(\mu + k_1E^*)\left(\frac{Pk_1k_2E^*}{(k_2+\gamma)(\mu + k_1E^*)} - 1\right)C \quad (\text{since } E(t) \leq E^* \text{ in } \mathcal{D}) \\
&= (k_2 + \gamma)(\mu + k_1E^*)(\mathcal{R}_{01} - 1)C \leq 0, \quad \text{when } \mathcal{R}_{01} \leq 1.
\end{aligned}$$

Since all the model parameters and variables are non-negative, it follows that $\dot{\mathbb{Y}} \leq 0$ for $\mathcal{R}_{01} \leq 1$, with equality if $\mathcal{R}_{01} = 1$ or $C = 0$. Moreover, for $\mathcal{R}_{01} < 1$, $\dot{\mathbb{Y}} = 0$ if and only if $C = 0$. Hence, $\mathbb{Y}$ is a Lyapunov function on $\mathcal{D}$. Furthermore, $\mathcal{D}$ is a compact and absorbing subset of $\mathbb{R}^3_+$, and the largest compact invariant set in $\{(C, E, I) \in \mathcal{D} : \dot{\mathbb{Y}} = 0\}$, when $\mathcal{R}_{01} \leq 1$, is the singleton $\mathbb{F}_0$. Therefore, $\mathbb{F}_0$ is the only steady state when $\mathcal{R}_{01} \leq 1$. Thus, by LaSalle's invariance principle [65, 94] (See Section A.1 for the principle), $I \to 0$ and $C \to 0$ as $t \to \infty$. Substituting $I = C = 0$ into the model equations (4.1)-(4.3) shows that $E \to E^*$ as $t \to \infty$. Hence, every solution of the basic *Chlamydia* model system (4.1)-(4.3), with initial conditions in $\mathcal{D}$, approaches the CFE $\mathbb{F}_0$ as $t \to \infty$ (that is, the CFE $\mathbb{F}_0$ is GAS in $\mathcal{D}$) whenever $\mathcal{R}_{01} < 1$ and unstable otherwise. □

Existence of the *Chlamydia*-present equilibrium

We show that the basic *Chlamydia* model system (4.1)-(4.3) has a unique *Chlamydia*-present equilibrium (CPE), that is the equilibrium for which *Chlamydia* persists within-host, if and only if $\mathcal{R}_{01} > 1$. In order to obtain the CPE, we set the right hand sides of the model equations (4.1)-(4.3) to zero, and solve for all its non-zero state variables. We also express the state variables in terms of the force of infection

$$\Lambda^{**} = k_1 C^{**}, \tag{4.21}$$

of model system (4.1)-(4.3). Thus, the right hand sides of the model system (4.1)-(4.3) at steady states gives

$$C^{**} = \frac{\Lambda^{**} P_E (P k_2 - k_2 - \gamma)}{\mu(\delta_E + \Lambda^{**})(k_2 + \gamma)}, \tag{4.22}$$

$$E^{**} = \frac{P_E}{\delta_E + \Lambda^{**}}, \tag{4.23}$$

$$I^{**} = \frac{\Lambda^{**} P_E}{(\delta_E + \Lambda^{**})(k_2 + \gamma)}. \tag{4.24}$$

Thus, the CPE of the basic *Chlamydia* model (4.1)-(4.3) is given by

$$\mathbb{F}_1 = (C^{**}, E^{**}, I^{**}). \tag{4.25}$$

Substituting (4.22)-(4.24) into the expression for Λ^{**} in (4.21), and simplifying, we obtain a quadratic expression that the non-zero CPE $\mathbb{F}_1$ of model system (4.1)-(4.3) satisfies, that is

$$\Lambda^{**}(\mu(k_2+\gamma)\Lambda^{**}+\delta_E\mu(k_2+\gamma)-k_1P_E(Pk_2-k_2-\gamma))=0. \tag{4.26}$$

The solutions of Equation (4.26) are either

$$\Lambda^{**}=0 \tag{4.27}$$

or

$$\Lambda^{**}=\frac{(k_2+\gamma)(\mu+k_1E^*)(\mathcal{R}_{01}-1)}{\mu/\delta_E(k_2+\gamma)}. \tag{4.28}$$

The trivial solution (4.27) implies the disease-free steady state which corresponds to the CFE described by (4.13). This is not our equilibrium of interest at this point. Thus, the unique and non-trivial solution (4.28) is valid.

From (4.28), it follows that if $\mathcal{R}_{01}<1$, then $\Lambda^{**}<1$, which is biologically meaningless. In addition, if $\mathcal{R}_{01}=1$, then $\Lambda^{**}=0$, which again corresponds to the CFE described by (4.13). Thus, the model system (4.1)-(4.3) has no positive CPE in these two cases. It can be clearly seen that the unique solution (4.28) of (4.26) is positive if and only if $\mathcal{R}_{01}>1$, since all the model parameters are positive.

Hence, the three components C^{**}, E^{**}, and I^{**} of the CPE $\mathbb{F}_1$, can be explicitly determined by substituting (4.28) into (4.22)-(4.24), to obtain

$$C^{**}=\frac{P_E(k_2(P-1)-\gamma)}{\mu(k_2+\gamma)}-\frac{\delta_E}{k_1}, \tag{4.29}$$

$$E^{**}=\frac{\mu(k_2+\gamma)}{k_1(k_2(P-1)-\gamma)}, \tag{4.30}$$

$$I^{**}=\frac{P_E}{k_2+\gamma}-\frac{\mu\delta_E}{k_1(k_2(P-1)-\gamma)}, \tag{4.31}$$

which is exactly the same CPE expressions presented by Wilson [169]. These results are summarised below.

Theorem 4.1.5. *The basic Chlamydia model* (4.1)-(4.3) *has a unique CPE given by* $\mathbb{F}_1$*, whenever* $\mathcal{R}_{01}>1$ *and no CPE otherwise.*

Local stability of the *Chlamydia*-present equilibrium (CPE)

Theorem 4.1.6. *The unique CPE* $\mathbb{F}_1$ *is locally asymptotically stable in* $\mathcal{D}$ *when* $\mathcal{R}_{01}>1$.

Proof. The Jacobian matrix of system (4.4)-(4.6) at $\mathbb{F}_1$ is given by

$$J(\mathbb{F}_1) = \begin{pmatrix} -(\mu + k_1 E^{**}) & -k_1 C^{**} & Pk_2 \\ -E^{**} k_1 & -(\delta_E + k_1 C^{**}) & 0 \\ Ek_1 & C^{**} k_1 & -(\gamma + k_2) \end{pmatrix}. \tag{4.32}$$

The characteristic equation is

$$\lambda^3 + a_1\lambda^2 + a_2\lambda + a_3 = 0, \tag{4.33}$$

where

$$\begin{aligned} a_1 &= k_1 C^{**} + k_1 E^{**} + \delta_E + \gamma + k_2 + \mu, \\ a_2 &= k_1 k_2 (C^{**} + E^{**} - PE^{**}) + \gamma k_1 (C^{**} + E^{**}) + k_1(\mu C^{**} + \delta_E E^{**}) + \delta_E(\gamma + k_2 + \mu) \\ &\quad + \mu(\gamma + k_2) \\ a_3 &= \delta_E \mu(\gamma + k_2) + (Pk_2 - k_2 - \gamma) k_1 E^{**}(k_1 C^{**} - \delta_E). \end{aligned} \tag{4.34}$$

It is easy to see that $a_1 > 0$. Using the mathematical relations in Equations(4.4)-(4.6) and (4.29), it can be seen that $(Pk_2 - k_2 - \gamma) = \mu(k_2 + \gamma)/k_1 E^{**} > 0$ and $k_1 C^{**} > \delta_E$. Thus $a_3 > 0$. By direct calculation, we have that $a_1 a_2 > a_3$ for $\mathcal{R}_{01} > 1$. Then, by the Routh-Hurwitz criterion, it follows that the *Chlamydia*-present equilibrium $\mathbb{F}_1$ is locally asymptotically stable.

□

As Theorems 4.1.4 and 4.1.5 imply, it suffices to explore therapeutic strategies that can drive the disease outbreak threshold $\mathcal{R}_{01}$ below unity. In order to demonstrate how the two proposed treatment strategies (controls u_1 and u_2) affect the expression for the basic reproduction number, we derive the expression for the basic reproduction number in the presence of the two controls. Using the NGM, as described above, on the model system (4.4)-(4.6), we obtain

$$\mathcal{R}_{0U} = \frac{Pk_1 k_2 \hat{E}(1 - u_1)}{(\mu + k_1 \hat{E})(k_2 + \gamma + u_2)}. \tag{4.35}$$

In Equation (4.35), it can be clearly seen that for $u_1 \equiv 1, \mathcal{R}_{0U} = 0$.

We differentiate $\mathcal{R}_{0U}$ with respect to control u_1. This gives

$$\frac{\partial \mathcal{R}_{0U}}{\partial u_1} = -\frac{Pk_1k_2\hat{E}}{(\mu + k_1\hat{E})(k_2 + \gamma + u_2)}. \tag{4.36}$$

Equation (4.36) shows that $\mathcal{R}_{0U}$ is a decreasing function of control u_1, which implies that high quantities of bacteriostatic treatment u_1 may reduce the value of the disease outbreak threshold $\mathcal{R}_{0U}$, thereby driving it below unity.

We differentiate $\mathcal{R}_{0U}$ with respect to control u_2. This gives

$$\frac{\partial \mathcal{R}_{0U}}{\partial u_2} = -\frac{Pk_1k_2\hat{E}(1-u_1)(\mu + k_1\hat{E})}{((\mu + k_1\hat{E})(k_2 + \gamma + u_2))^2}. \tag{4.37}$$

Equation (4.37) shows that $\mathcal{R}_{0U}$ is a decreasing function of control u_2, which implies that high quantities of proteasome-specific inhibiting treatment u_2 may reduce the value of the disease outbreak threshold $\mathcal{R}_{0U}$, thereby driving it below unity.

Equations (4.36) and (4.37) suggest that the two controls u_1 and u_2, respectively, would be instrumental to the clearance of a *Chlamydia* infection. From Equations (4.19) and (4.35), it can also be seen that the infection would be cleared if the burst size P, of infected epithelial cells, can be driven down to zero. Thus we proceed to study the dynamics of the optimal control problem (4.4)-(4.6), and use the optimal controls to eradicate the chlamydial infection.

4.2 Existence of an optimal control pair

In this section, we show that the existence of an optimal control pair with finite objective functional is guaranteed for our optimal control model (4.4)-(4.6). We begin with a re-statement of an established Theorem (Theorem 4.2.1 below) from Fleming and Rishel [55] (refer to the conditions in III.2.4, Theorem III.4.1, and its corresponding Corollary III.4.1) which gives sufficient conditions for the existence of an optimal control pair, for a given model, and a given objective functional. We then show (Theorem 4.2.2) that our system (4.4)-(4.6) and objective functional (4.9) meet the conditions of Theorem 4.2.1, thus establishing the existence of an optimal control pair for our model.

Theorem 4.2.1 (from Fleming and Rishel [55])**.** *Consider an optimal control problem with system equations*

$$\dot{x} = f(t, x(t), u_1(t), u_2(t)), \quad t_0 \leq t \leq t_f, \tag{4.38}$$

where the vector $x \in \mathbb{R}^n$ denotes the state system, $(u_1^*, u_2^*) \in \Gamma$ as defined in (4.8), and $x(t_0) = x_0$ are the initial conditions. Let the objective functional of the system be

$$J(u_1, u_2) = \int_{t_0}^{t_f} G(t, x(t), u_1(t), u_2(t))dt + \phi(x(t_f)), \tag{4.39}$$

where $\phi(x(t_f))$, called the payoff term, is a goal with respect to the final state $x(t_f)$.

Suppose that

1. *The set of all solutions to state equations* (4.38) *with corresponding control functions in* Γ *is non-empty.*
2. *The admissible control set* Γ *is closed and convex.*
3. *The right hand side of the state system, f, is continuous, and moreover, there exist positive constants C_1, C_2 such that*
   (a) *f is bounded above by a sum of the bounded control and the state, i.e., $|f(t, x, u_1, u_2)| \leq C_1(1 + |x| + |u_1| + |u_2|)$;*
   (b) *$|f(t, \hat{x}, u_1, u_1) - f(t, x, u_1, u_2)| \leq C_2|\hat{x} - x|(1 + |u_1| + |u_2|)$;*
   (c) *f can be written as a linear function of the control variables with coefficients depending on time and the state variables, i.e. $f(t, x, u) = \eta(t, x) + \rho(t, x)u_1 + \theta(t, x)u_2$;*
4. *The integrand of the objective functional is convex on* Γ*;*
5. *There exist constants $c_1 > 0$, c_2, and $\beta > 1$ such that the integrand G, of the objective functional, satisfies*

$$G(t, C, I, u_1, u_2) \geq c_1(|(u_1, u_2)|^{\beta}) - c_2, \tag{4.40}$$

$\forall\ t \in \mathbb{R}, x, \hat{x} \in \mathbb{R}^n$, and $(u_1^*, u_2^*) \in \Gamma$. Then, there exist optimal controls u_1^* and u_2^* minimising $J(u_1, u_2)$, with $J(u_1^*, u_2^*)$ finite.

Remark: If f is $\mathcal{C}^1$, then conditions 3(a) and 3(b) are implied by suitable bounds on partial derivatives of f and on $f(t, 0, 0, 0)$.

Analysis of Super-solutions

In order to prove that the system (4.4)-(4.6) is bounded, we use the established approach of [36,37]. We use the fact that the super-solutions $\bar{C}$, $\bar{E}$, and $\bar{I}$ of C, E, and I, respectively, in (4.4)-(4.6) are bounded on a finite time interval. The sub-solutions are zero. Let $C_{\max}$, $E_{\max}$, and $I_{\max}$ be upper bound solutions associated with C, E, and I, respectively, and with $C(t) \geq 0$, $E \geq 0$, and $I \geq 0$.

Consider the system

$$\frac{\mathrm{d}\bar{C}}{\mathrm{d}t} = Pk_2\bar{I}, \tag{4.41}$$

$$\frac{\mathrm{d}\bar{E}}{\mathrm{d}t} = P_{\bar{E}}, \tag{4.42}$$

$$\frac{\mathrm{d}\bar{I}}{\mathrm{d}t} = k_1\bar{C}\bar{E}, \tag{4.43}$$

with initial conditions $\bar{C}(0) = \bar{C}_0$, $\bar{E}(0) = \bar{E}_0$, and $\bar{I}(0) = \bar{I}_0$, and solutions $\bar{C}$, $\bar{E}$, and $\bar{I}$.

From Equation (4.41),

$$\bar{C}(t) = Pk_2 \int_0^t \bar{I}\mathrm{d}\tau + \bar{C}_0. \tag{4.44}$$

The integral in (4.44) is finite since the continuous function $I(\tau)$ is integrated over the compact interval $[0, t]$.

From Equation (4.42),

$$\bar{E}(t) = P_{\bar{E}}t + \bar{E}_0. \tag{4.45}$$

From Equation (4.43),

$$\bar{I}(t) = k_1 \int_0^t \bar{C}(\tau)\bar{E}(\tau)\mathrm{d}\tau + \bar{I}_0. \tag{4.46}$$

Again, the integral in (4.46) is finite since the continuous function $\bar{C}(\tau)\bar{E}(\tau)$ is integrated over the compact interval $[0, t]$.

Hence, the solutions $\bar{C}$, $\bar{E}$, and $\bar{I}$ of system (4.41)-(4.43) are bounded over the finite time interval $[0, t]$. By using the bounds $C_{\max} = \bar{C}(t_f)$, $E_{\max} = \bar{E}(t_f)$, and $I_{\max} = \bar{I}(t_f)$, we have formed a set of upper bound solutions for system (4.4)-(4.6).

Theorem 4.2.2. *For the optimal control problem with state equations* (4.4)-(4.6)*, there exists an optimal control pair* $(u_1^*, u_2^*) \in \Gamma$ *which minimises the objective functional* $J(u_1, u_2)$ *in equation* (4.9)*.*

Proof. To prove this theorem, we show that our optimal control model meets the five conditions given in Theorem 4.2.1, being sufficient conditions for the existence of an optimal control pair for our model.

1. To verify condition 1, we refer to Theorem 3.1 by Picard-Lindelöf [29,39]. Based on the theorem, if the solutions of the state equations (4.4)-(4.6) are a *priori* bounded

and if the state equations are continuous and Lipschitz-continuous in the state variables, then there is a unique solution corresponding to every admissible control pair in Γ. Since for all $(C, E, I) \in \mathcal{D}$, the model states are bounded below and above (see Section 4.1.1), then, the solutions to the state equations are bounded.
We have earlier shown that solutions of the state equations (4.4)-(4.6) are bounded. The right sides of the state equations (4.4)-(4.6) are also continuously differentiable functions of the dependent variables C, E, and I. These demonstrate the fact that the system is locally Lipschitz-continuous with respect to the state variable [28]. Thus, condition 1 is fulfilled.

2. By the definition of the admissible control set Γ (Equation (4.8)), it is closed and bounded. Let $\|\cdot\|$ be some norm in $\mathbb{R}^2$, for example, the Euclidean norm

$$\|\vec{U}\|_2 = \|(u_1, u_2)\|_2 = \sqrt{u_1^2 + u_2^2}. \tag{4.47}$$

Then, the set $\{\vec{U} | \vec{U} \in \Gamma, \text{ and } \|\vec{U}\| \leq \sqrt{2}\}$ is a convex set [93, Page 210]. To see this, suppose $\vec{U}, \vec{V} \in \mathbb{R}^2$, with $\|\vec{U}\| \leq \sqrt{2}$, $\|\vec{V}\| \leq \sqrt{2}$, and $0 \leq \theta \leq 1$. Let $\vec{W} = \theta\vec{U} + (1-\theta)\vec{V}$. Then

$$\begin{aligned} \|\vec{W}\| &= \|\theta\vec{U} + (1-\theta)\vec{V}\| \\ &\leq \|\theta\vec{U}\| + \|(1-\theta)\vec{V}\| \quad \text{(triangle inequality)} \\ &= \theta\|\vec{U}\| + (1-\theta)\|\vec{V}\| \quad \text{(positive homogeneity property of the norm)} \\ &\leq \sqrt{2}. \end{aligned} \tag{4.48}$$

Hence, condition 2 is fulfilled.

3. Let $\vec{\Theta}(t, \vec{X})$ be a vector-valued function which represents the right hand side (RHS) of system (4.4)-(4.6), except for the terms of $\vec{U} = (u_1, u_2)'$, and define

$$\vec{f}(t, \vec{X}, \vec{U}) = \vec{\Theta}(t, \vec{X}) + \begin{pmatrix} -u_1 P k_2 I \\ 0 \\ -u_2 I \end{pmatrix}, \text{ with } \vec{X} = \begin{pmatrix} C \\ E \\ I \end{pmatrix}. \tag{4.49}$$

Using the boundedness of the solutions, it can be seen that

$$\begin{aligned} \left|\vec{f}(t, \vec{X}, \vec{U})\right| &\leq \left| \begin{pmatrix} 0 & 0 & Pk_2 \\ 0 & 0 & 0 \\ k_1 E_{\max} & 0 & 0 \end{pmatrix} \begin{pmatrix} C \\ E \\ I \end{pmatrix} \right| + \left| \begin{pmatrix} 0 \\ P_{\bar{E}} \\ 0 \end{pmatrix} \right| \\ &\leq C_1 \left(\left|\vec{X}\right| + \left|\vec{U}\right| \right), \end{aligned} \tag{4.50}$$

where C_1 depends on the coefficients of the system.
The right side of the model system (4.4)-(4.6) is Lipschitz-continuous. Thus, it is obviously continuous and bounded. Furthermore, from Equation (4.49), it can be

seen that

$$\vec{f}(t,\vec{X},\vec{U}) = \vec{\Theta}(t,\vec{X}) + \vec{\Pi}(t,\vec{X})u_1 + \vec{\Xi}(t,\vec{X})u_2,$$

where $\vec{\Pi}(t,\vec{X})$ and $\vec{\Xi}(t,\vec{X})$ represent coefficient vectors depending on time and the state variables. Thus, the state system is bilinear in u_1 and u_2. Hence condition 3 is satisfied.

4. The integrand $G(t,C,I,U_1,U_2)$ is convex if and only if its Hessian matrix (or the quadratic form associated with it) is positive semidefinite [93, Page 211]. The Hessian matrix of G is given by

$$\begin{aligned} H(G) = \frac{\partial^2 \mathrm{G}}{\partial \mathrm{x}_i \partial \mathrm{x}_j} &= \begin{pmatrix} G_{CC} & G_{CI} & G_{Cu_1} & G_{Cu_2} \\ G_{IC} & G_{II} & G_{Iu_1} & G_{Iu_2} \\ G_{u_1C} & G_{u_1I} & G_{u_1u_1} & G_{u_1u_2} \\ G_{u_2C} & G_{u_2I} & G_{u_2u_1} & G_{u_2u_2} \end{pmatrix} \\ &= \begin{pmatrix} 0 & 0 & 0 & 0 \\ 0 & 0 & 0 & 0 \\ 0 & 0 & A_2 & 0 \\ 0 & 0 & 0 & A_3 \end{pmatrix} \end{aligned} \tag{4.51}$$

The eigenvalues of the diagonal matrix $H(G)$ are the entries on its main diagonal, that is $0, 0, A_2$, and A_3. The weight parameters A_2, and A_3 are positive. Thus, the Hessian matrix $H(G)$ is positive semidefinite [13, Theorem 2.17, Page 20], which implies that the integrand G of the objective functional is convex on the admissible set Γ. Thus condition 4 is satisfied.

5. Let $\alpha = \min(A_2, A_3)$, and $\kappa = \frac{1}{2}\alpha$. Then,

$$\begin{aligned} G &= \frac{A_2}{2}u_1^2 + \frac{A_3}{2}u_2^2 + C + A_1 I \\ &\equiv \frac{1}{2}\left\{\alpha(u_1^2 + u_2^2) + \nu_1 u_1^2 + \nu_2 u_2^2\right\} + (C + A_1 I) \\ &\geq \kappa(u_1^2 + u_2^2) + (C + A_1 I) \\ &\geq \kappa(u_1^2 + u_2^2) - c_2 \\ &= \kappa(|u_1|^2 + |u_2|^2) - c_2, \end{aligned}$$

for any $c_2 > 0$, where $0 \leq \nu_1 \leq A_2$ and $0 \leq \nu_2 \leq A_3$. Note that $\alpha, \kappa \geq 0$. Hence the integrand satisfies the inequality (4.40), with $\beta = 2$.

This completes the proof. □

4.3 Characterisation of the optimal control pair

In this section, we derive the conditions of optimality for the control problem (4.4)-(4.9). Pontryagin's Maximum Principle [125] provides the necessary conditions an optimal control and corresponding state must satisfy. The principle converts the optimal control problem (4.4)-(4.9) into one of minimising a Hamiltonian H, with respect to the control $(u_1(t), u_2(t))$ [100, pg 14].

Theorem 4.3.1. *Given optimal controls u_1^*, u_2^* and solutions C^*, E^*, and I^* of the corresponding state system* (4.4)-(4.6)*, there exist adjoint variables λ_C, λ_E, and λ_I satisfying:*

$$\dot{\lambda_C} = -1 + \mu\lambda_C + k_1 E^*(\lambda_C + \lambda_E - \lambda_I), \tag{4.52}$$

$$\dot{\lambda_E} = \delta_E\lambda_E + k_1 C^*(\lambda_C + \lambda_E - \lambda_I), \tag{4.53}$$

$$\begin{aligned}\dot{\lambda_I} = -\Bigg[A_1 + \left(1 - \min\left\{\max\left(0, \frac{\lambda_C P k_2 I^*}{A_2}\right), 1\right\}\right) P k_2 \lambda_C \\ -\lambda_I\left(\gamma + k_2 + \min\left\{\max\left(0, \frac{\lambda_I I^*}{A_3}\right), m\right\}\right)\Bigg],\end{aligned} \tag{4.54}$$

with transversality conditions

$$\lambda_C(t_f) = A_4,\ \lambda_E(t_f) = -A_5, \quad \textit{and } \lambda_I(t_f) = 0. \tag{4.55}$$

Furthermore, the control functions can be shown to satisfy the following, called the control characterisations:

$$u_1^*(t) = \min\left\{\max\left(0, \frac{\lambda_C P k_2 I^*}{A_2}\right), 1\right\},$$

$$u_2^*(t) = \min\left\{\max\left(0, \frac{\lambda_I I^*}{A_3}\right), m\right\}.$$

Proof. Define the Hamiltonian $H(C, E, I, u_1, u_2, \lambda_C, \lambda_E, \lambda_I)$ as

$$\begin{aligned}H = C(t) + A_1 I + \frac{A_2}{2}u_1^2 + \frac{A_3}{2}u_2^2 \\ + \lambda_C((1-u_1)Pk_2 I(t) - \mu C(t) - k_1 C(t)E(t)) \\ + \lambda_E(P_E - \delta_E E(t) - k_1 C(t)E(t)) \\ + \lambda_I(k_1 C(t)E(t) - \gamma I(t) - k_2 I(t) - u_2 k_3 I(t)).\end{aligned} \tag{4.56}$$

Using Pontryagin's Maximum Principle [125],

$$\lambda_C^{'} = -\frac{\partial H}{\partial C},\ \lambda_E^{'} = -\frac{\partial H}{\partial E},\ \text{and}\ \lambda_I^{'} = -\frac{\partial H}{\partial I}. \tag{4.57}$$

Using the Hamiltonian in (4.56) and the relations in (4.57), the adjoint system can be written as

$$\lambda_C^{'} = -1 + \mu\lambda_C + k_1 E^*(\lambda_C + \lambda_E - \lambda_I), \tag{4.58}$$
$$\lambda_E^{'} = \delta_E\lambda_E + k_1 C^*(\lambda_C + \lambda_E - \lambda_I), \tag{4.59}$$
$$\lambda_I^{'} = -\left(A_1 + (1-u_1^*)Pk_2\lambda_C - \lambda_I(\gamma + k_2 + u_2)\right), \tag{4.60}$$

with transversality conditions (terminal conditions) expressed in the form provided in (4.55).

The Hamiltonian H is minimised with respect to the controls at the optimal control pair, thus we differentiate H with respect to u_1 and u_2 on the sets $\{t \,|\, 0 \le u_1 \le 1\}$ and $\{t \,|\, 0 \le u_2 \le m\}$ respectively. Thus, the optimality equations are

$$\frac{\partial H}{\partial u_1} = A_2 u_1^* - \lambda_C Pk_2 I^* = 0 \quad \text{at } u_1^*, \tag{4.61}$$
$$\frac{\partial H}{\partial u_2} = A_3 u_2^* - \lambda_I I^* = 0 \quad \text{at } u_2^*. \tag{4.62}$$

Solving for u_1^* and u_2^* on the interior sets, we obtain

$$u_1^* = \frac{\lambda_C Pk_2 I^*}{A_2}, \tag{4.63}$$
$$u_2^* = \frac{\lambda_I I^*}{A_3}. \tag{4.64}$$

By standard control arguments involving the bounds on the controls (see Sections 8.1 and 12.1 of [100]), we conclude that

$$u_1^* = \begin{cases} 0 & \text{if} \quad \dfrac{\lambda_C Pk_2 I^*}{A_2} \le 0 \\ \dfrac{\lambda_C Pk_2 I^*}{A_2} & \text{if} \quad 0 < \dfrac{\lambda_C Pk_2 I^*}{A_2} < 1 \\ 1 & \text{if} \quad 0\dfrac{\lambda_C Pk_2 I^*}{A_2} \ge 1 \end{cases}, \tag{4.65}$$

which in compact notation can be characterised as

$$u_1^*(t) = \min\left\{\max\left(0, \frac{\lambda_C P k_2 I^*}{A_2}\right), 1\right\}. \tag{4.66}$$

Similarly, we conclude that

$$u_2^* = \begin{cases} 0 & \text{if} \quad 0\dfrac{\lambda_I I^*}{A_3} \leq 0, \\ \dfrac{\lambda_I I^*}{A_3} & \text{if} \quad 0 < \dfrac{\lambda_I I^*}{A_3} < 1 \\ m & \text{if} \quad 0\dfrac{\lambda_I I^*}{A_3} \geq 1 \end{cases} \tag{4.67}$$

which in compact notation can also be characterised as

$$u_2^*(t) = \min\left\{\max\left(0, \frac{\lambda_I I^*}{A_3}\right), m\right\}. \tag{4.68}$$

This completes the proof. □

Utilising the control characterisations (4.66) and (4.68), the optimality system that characterises the optimal control pair (u_1^*, u_2^*) is

$$\begin{aligned}
\dot{C} &= \left(1 - \min\left\{\max\left(0, \frac{\lambda_C P k_2 I^*}{A_2}\right), 1\right\}\right) P k_2 I - \mu C - k_1 C E \\
\dot{E} &= P_E - \delta_E E(t) - k_1 C(t) E(t) \\
\dot{I} &= k_1 C(t) E(t) - \gamma I(t) - k_2 I(t) - \min\left\{\max\left(0, \frac{\lambda_I I^*}{A_3}\right)\right\} k_3 I(t) \\
\dot{\lambda_C} &= -1 + \mu\lambda_C + k_1 E^*(\lambda_C + \lambda_E - \lambda_I) \\
\dot{\lambda_E} &= \delta_E \lambda_E + k_1 C^*(\lambda_C + \lambda_E - \lambda_I) \\
\dot{\lambda_I} &= -\left[A_1 + \left(1 - \min\left\{\max\left(0, \frac{\lambda_C P k_2 I^*}{A_2}\right), 1\right\}\right) P k_2 \lambda_C \right. \\
&\qquad \left. -\lambda_I\left(\gamma + k_2 + \min\left\{\max\left(0, \frac{\lambda_I I^*}{A_3}\right), m\right\}\right)\right],
\end{aligned} \tag{4.69}$$

subject to the initial conditions $C(t_0) = C_0$, $E(t_0) = E_0$, and $I(t_0) = I_0$, and terminal conditions $\lambda_C(t_f) = A_4$, $\lambda_E(t_f) = -A_5$, $\lambda_I(t_f) = 0$.

Due to the a *priori* boundedness of the state and adjoint solutions, the right sides of the state and adjoint equations become Lipschitz in those solutions. The uniqueness of the solutions of the optimality system is guaranteed by this Lipschitz property, for a

sufficiently small final time t_f. This small time length restriction is due to the opposite time orientation of the state equations (4.4)-(4.6), and the adjoint equations (4.52)-(4.54); the state system has initial time conditions and the adjoint equations have final time conditions. Uniqueness of solutions of the optimality system implies the uniqueness of the optimal controls [100]. See Fisher et. al [54] for a uniqueness proof using Lipschitz properties.

4.4 Numerical Results

4.4.1 Disease dynamics with no control

In this section, we present numerical results of the dynamics of the interacting species (that is, *Chlamydia*, healthy epithelial cells, and infected epithelial cells). Setting the controls u_1 and u_2 to zero, the model system (4.4)-(4.6) is reduced to the system of ODEs in (4.1)-(4.3). Since the concentrations of C, E, and I cells are per millimetre cube of human (female reproductive tract) tissue, we suppose that at the onset of an acute *Chlamydia* infection, a millimetre cube tissue contains 200 healthy epithelial cells, 50 *Chlamydia* bacteria, and no infected epithelial cell, as shown on Table 4.1. Figures 4.1a-4.1c show that in the presence of only the humoral and cell-mediated immunity, the infection may not be abated. We observe that each of the interacting species approached their endemic steady states. The final values for each interacting species are $C(t_f) = 406, E(t_f) = 5$, and $I(t_f) = 7$, which coincide with the numerical values of the analytical *Chlamydia*-present steady states (4.29), (4.30), and (4.31), respectively. The parameter values and initial conditions used in all the simulations are given in Table 4.1.

4.4.2 Optimal Control

In this section, we numerically study optimal treatment strategies of the model system (4.4)-(4.6) and present numerical solutions of the optimality system (4.69). Numerical techniques for optimal control problems can be classified as either direct or indirect (See [115] and [23, Pg. 161]). The initial solutions of the two-point boundary value problem (4.69) were obtained by using an indirect method in which the differential-algebraic system generated by Pontryagin's Maximum Principle is numerically solved, a numerical technique generally referred to as the Forward-Backward Sweep Method (FBSM) [100, 115]. First, using a fourth order Runge-Kutta scheme, the state equations are solved forward in time, with initial conditions (see Table 4.1) and initial guesses for the controls. By virtue of the transversality conditions (4.55) being at the final time, the adjoint equations are solved by a backward (in time) fourth order Runge-Kutta scheme, using the current iteration solution of the state equations. The controls are then updated by using a convex combination ($u = 0.5(u_{prev} + u_{char})$) of the previous controls (u_{prev}) and the value from the characterisations (4.66) and (4.68) (u_{char}). This process is repeated and the iteration stops when convergence is achieved [100].

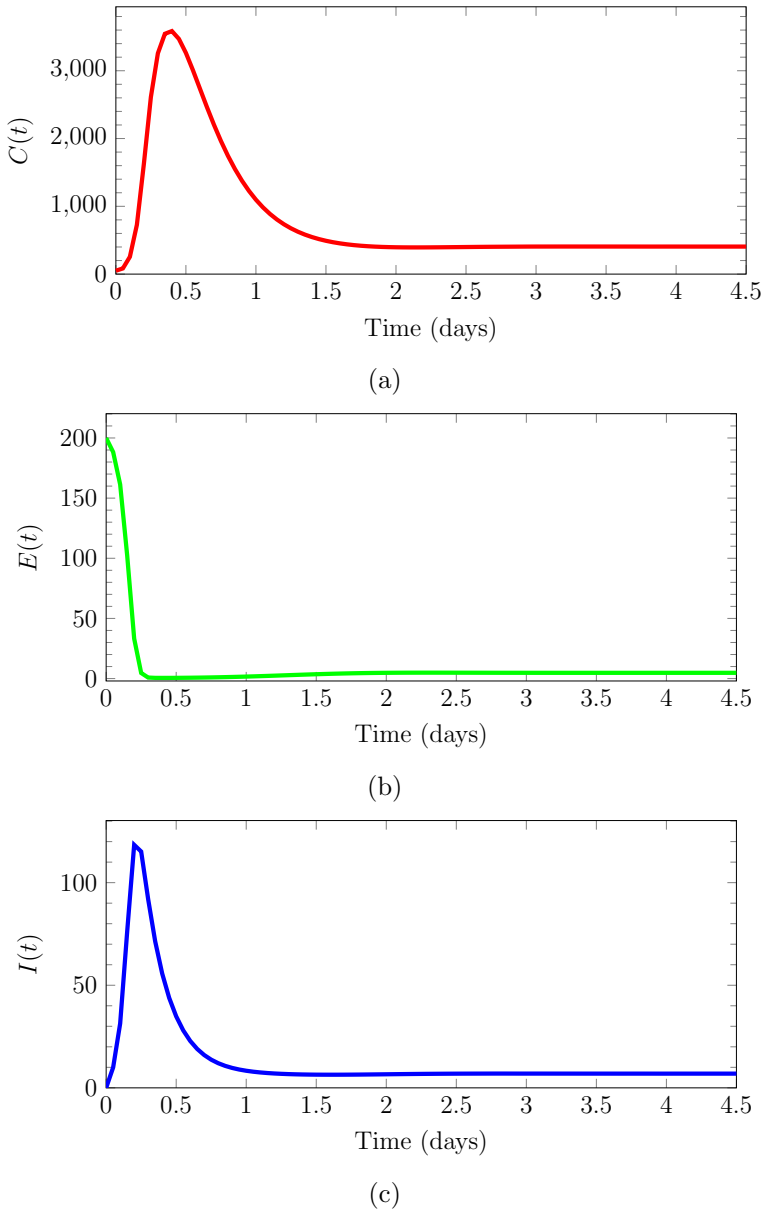

Figure 4.1: Numerical simulation of the *Chlamydia* model (4.4)-(4.6) showing the time course plot of (a) $C(t)$, the concentration of *Chlamydia*, (b) $E(t)$, the concentration of healthy epithelial cells, and (c) $I(t)$, the concentration of *Chlamydia*-infected epithelial cells, with no controls applied. Here, $\mathcal{R}_0 > 1$, indicating active disease. Parameter values used are in Table 4.1.

The described iterative method of obtaining the optimal treatment strategy was used to obtain solutions of the system when either controls was used. However, when both controls were used, the simulations took several hours to run, which made variation of parameters a time-consuming task. Thus, in addition to the method, the optimal control problem (4.4)-(4.9) was solved using MATLAB's in-built non-linear optimisation tool *fmincon* [114]. fmincon is a constrained optimization toolbox that is based on a direct (sequential) method in which the differential equations (4.4)-(4.6) and the integral (4.9) are discretised, and the problem is converted into a nonlinear programming problem [23, 115]. We first reformulate the optimal control problem into the Mayer form (see [24]) and then set it up for fmincon [114]. In order to investigate the occurrence of any discrepancy in the solutions obtained when either the FBSM or MATLAB's fmincon was used, fmincon was

used to regenerate some of the previous results obtained from the FBSM. We note that there were no discrepancies.

We investigate and compare numerical results of three different optimal therapy scenarios: (i) when u_1, the drug that eliminates or reduces the production of viable *Chlamydia*, is optimised while treatment u_2 is set to zero (ii) when u_2, the drug that acts as a proteasome-specific inhibitor is optimised while treatment u_1 is set to zero, and (iii) when both treatments u_1 and u_2 are optimised. We only track the amount of bio-available treatment/drug the system is supplied with, with respect to time. In this study, we do not investigate the complete degradation of the drug/treatment to be administered, but rather the bio-availability and delivery of the treatment into the system. We also investigate the effect of how variation in weight factors affect drug dosages.

The model was simulated for different combinations of values of the weight parameters A_1, A_2, A_3, A_4, and A_5, which are the balancing cost factors due to scales (that is, they adjust the balance between the benefit of clearing of *Chlamydia*, reduction of infected cells and maximisation of healthy epithelial cells that do not get infected, and the systemic cost of the treatments) and the importance of the six parts of the objective functional. In all the presented figures, we use the same set of weight factors, $A_1 = 5$, $A_2 = 50$, $A_3 = 50$, $A_4 = 1$, and $A_5 = 5$, and initial state variables $C(0) = 50$, $E(0) = 200$, and $I(0) = 0$, to illustrate the effects of different optimal therapies on a chlamydial infection. The weight parameters were chosen to have the presented magnitudes (some on the order of one and some a ten) because of the assumption that within a millimetre cube of human tissue, the magnitude of the concentration of *Chlamydia* (hundreds) is much larger than the magnitude of the concentrations of infected and healthy epithelial cells (tens), and the magnitude of the concentrations of the two treatments (floating point numbers less than one) in the objective functional in (4.9). Thus, this difference in magnitudes is balanced by the orders of the weight parameters. For brevity, we have only presented results for one parameter combination. This is particularly because when we varied the respective weight parameters within the same order, there was no significant effect (with regards to clinical outcomes) of the variation on the qualitative results of the optimal controls. However, in Section B.1 of the Appendix, we have investigated and discussed in details, the effects of different weight parameter combinations on the qualitative results of the optimal control problem (this include the time series of interacting species, the optimal controls, and the corresponding values of the objective functional). The duration of treatments, in number of days, are varied for the three treatment scenarios considered, by varying the final time. We also found that there was not much variation in the optimal solution of the model system (with regards to clinical outcomes). These results are also not shown for brevity but they are discussed in Section B.2 of the Appendix. We only show results for four and a half days of treatment.

Control with bacteriostatic agents ($u_2 \equiv 0$)

We consider monotherapy with u_1 alone. Numerical simulations are performed using the FBSM and MATLAB's fmincon as described in Section 4.4.2, for $A_3 \equiv 0$ when $u_2 \equiv 0$. Then, the optimal control problem is defined by

$$J(u_1) = \int_{t_0}^{t_f} G(t, x(t), u_1(t))\mathrm{d}t + \phi(x(t_f)), \tag{4.70}$$

subject to

$$\begin{cases} \dot{x} = f(t, x(t), u_1(t)), \quad t_0 \leq t \leq t_f, \\ x(t_0) = x_0, \end{cases} \tag{4.71}$$

where $x = (C, E, I)$, f is the right side of the model (state) system (4.4)-(4.6), $\phi(x(t_f)) = A_4C(t_f) - A_5E(t_f)$, and $G(t, x, u_1) = C(t) + A_1I(t) + \frac{A_2}{2}u_1^2$. Figures 4.2, 4.3, and 4.4 show clear and significant differences between the concentration of free extracellular *Chlamydia*, healthy epithelial cells, and *Chlamydia*-infected epithelial cells, respectively, between the cases with control u_1 (solid lines) and the cases without control (dashed lines). Figure 4.2 reveals a sharp decrease in the concentration of free extracellular *Chlamydia*, after which the pathogen is no longer produced. Figure 4.3 reveals a slight decrease in the concentration of healthy epithelial cells but a gradual increase thereafter, after which it attains its maximum capacity. Figure 4.4 shows that on implementation of the control strategy, there will be an increase in the concentration of *Chlamydia*-infected epithelial cells, but a rapid decline thereafter. The optimal control function $u_1(t)$ in Figure 4.5 is continuous and decreases with respect to increasing time. It reveals that for the treatment to be optimal, it should be given at its highest tolerable concentration for the first two days and then allowed to wane from the system. We observe in Figures 4.2-4.4 that accurate application of a bacteriostatic treatment will be optimal in truncating the progression of a *Chlamydia* infection. The value of the objective functional (4.9) for this investigation is 136.0853.

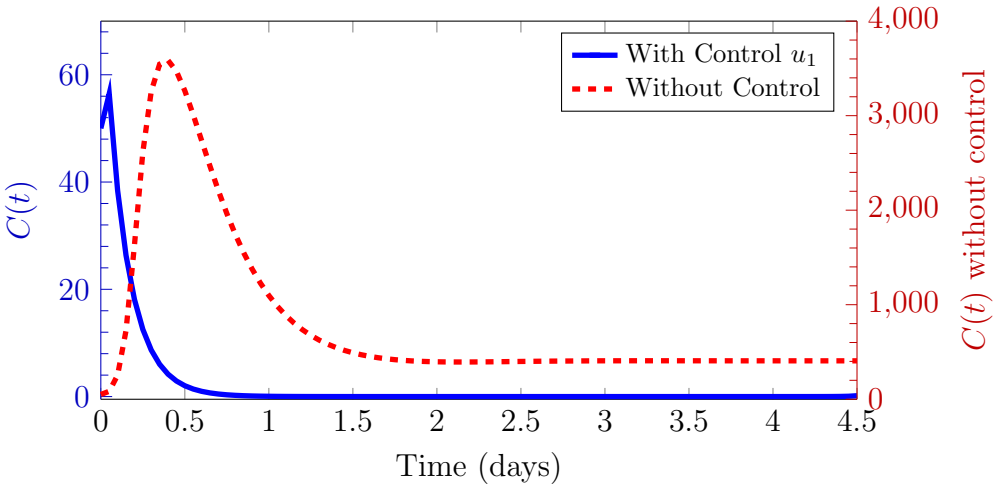

Figure 4.2: Time series of *Chlamydia* model (4.4)-(4.6) showing the effect of using control u_1 (optimal bacteriostatic treatment) only on $C(t)$, the concentration of free extracellular *Chlamydia*.

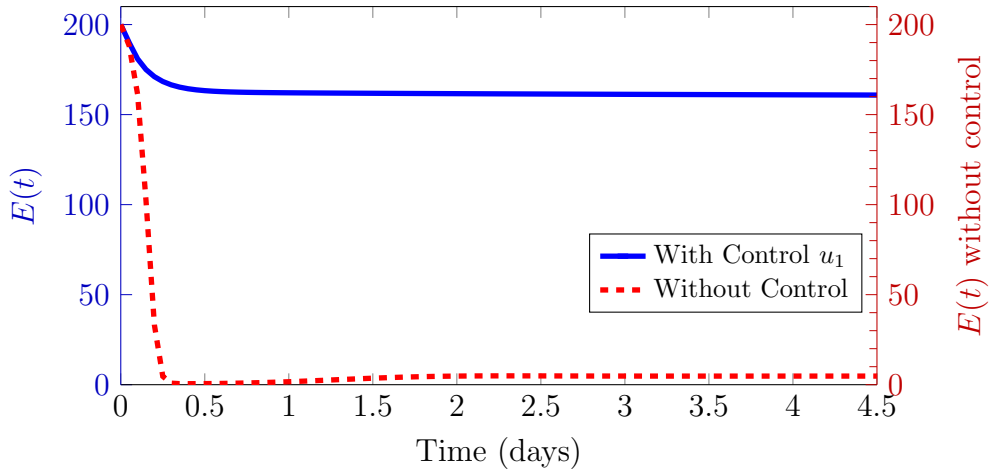

Figure 4.3: Time series of *Chlamydia* model (4.4)-(4.6) showing the effect of using control u_1 (optimal bacteriostatic treatment) only on $E(t)$, the concentration of healthy epithelial cells.

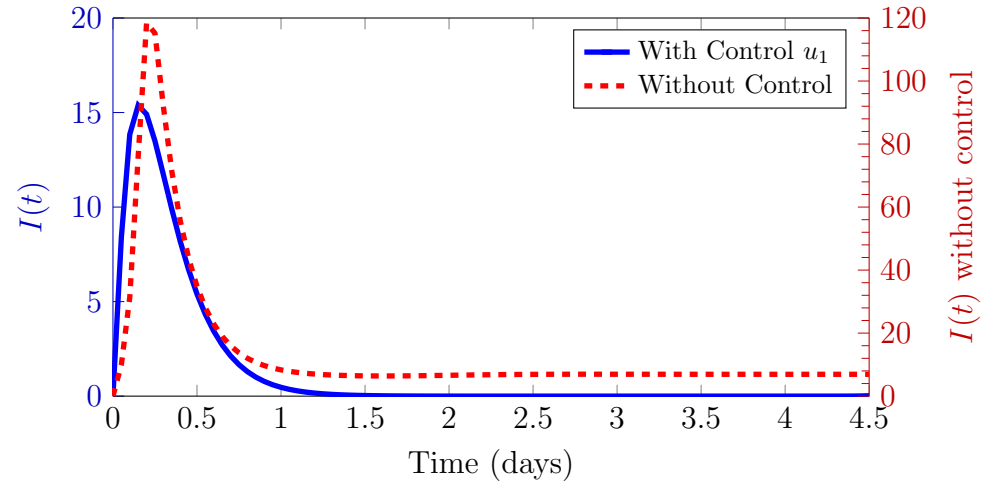

Figure 4.4: Time series of *Chlamydia* model (4.4)-(4.6) showing the effect of using control u_1 (optimal bacteriostatic treatment) only on $I(t)$, the concentration of *Chlamydia*-infected epithelial cells.

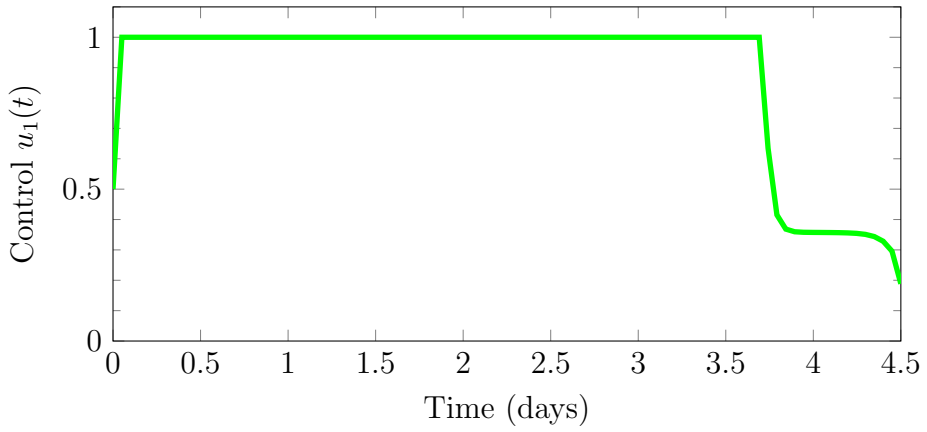

Figure 4.5: Optimal evolution for control u_1.

Control with proteasome-specific inhibiting agents ($u_1 \equiv 0$)

We again consider monotherapy, this time with the drug that acts as a proteasome-specific inhibitor, represented by u_2, with $u_1 \equiv 0$. Numerical simulations are performed using the FBSM and MATLAB's fmincon as described in Section 4.4.2, for $A_2 \equiv 0$ when $u_1 \equiv 0$. Then, the optimal control problem is defined by relations similar to (4.70) and (4.71), but with u_2 ($0 \leq u_2 < m = 0.5$) instead of u_1, and $G(t, x, u_1) = C(t) + A_1 I(t) + \frac{A_3}{2} u_2^2$.

Figure 4.7 shows some decrease in the concentration of free extracellular *Chlamydia* when control u_2 was used ($C(t_f) = 371$), as compared to when no control was used ($C(t_f) = 406$). However, Figures 4.8 and 4.9 show no significant difference between the concentration of healthy epithelial cells and *Chlamydia*-infected epithelial cells, respectively, when either control u_2 was used or when no control was used ($E(t_f) = 5$ in both cases, but $I(t_f) = 7$ with no control, and $I(t_f) = 6$ with control u_2). The optimal control function $u_2(t)$ in Figure 4.5 is continuous but does not decrease with respect to increasing time. It reveals that for the treatment to be optimal, it should be given at its highest tolerable concentration until the end of the intervention. These results however show that treatment of chlamydial infection with proteasome-specific inhibitors alone does not suffice in clearing the *Chlamydia* infection. The value of the objective functional (4.9) for this investigation is 3662.4.

Since the optimal control suggests that in the presence of u_2 only, the *Chlamydia* infection will not be abated, this suggests that $\mathcal{R}_{0U} > 1$ under this scenario. We investigate the value of $0 < m \leq 1$, the maximum amount of treatment u_2, which may force the basic reproduction number $\mathcal{R}_{0U}$ to be below unity in the presence of u_2 only.

From Equation (4.35) Setting $u_1 \equiv 0$, $u_2 \equiv m$, and using other parameter values in Table 4.1 we obtain the mathematical relationship between $\mathcal{R}_{0U}$ and m. The relation is

$$\mathcal{R}_{0U}(m) = \frac{768}{40.32 + 7.2m}. \tag{4.72}$$

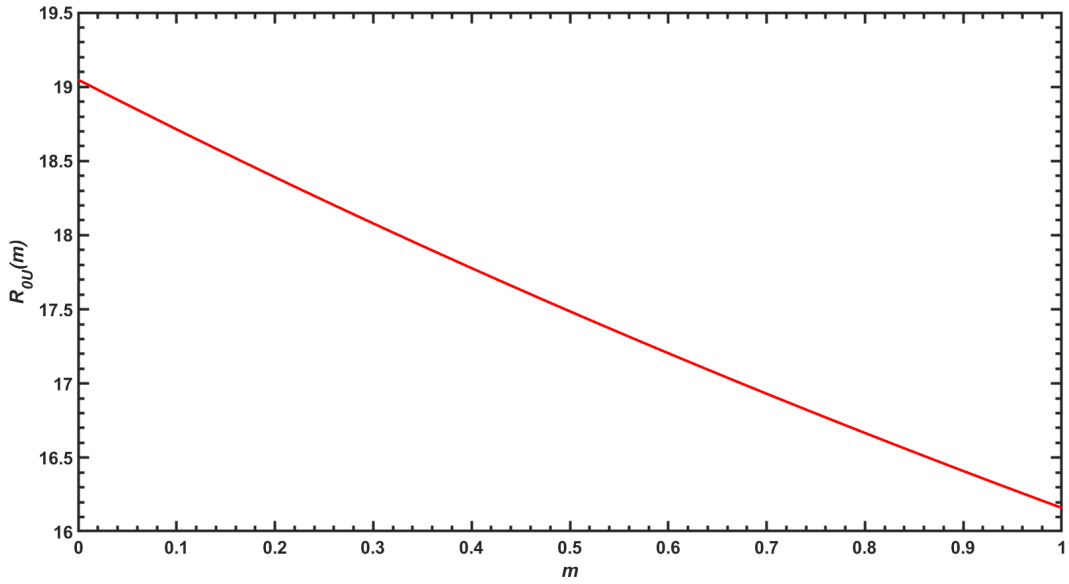

Figure 4.6: A graph of m, the highest tolerable amount of treatment u_2 (optimal proteasome-specific inhibitor), against the basic reproduction number $\mathcal{R}_{0U}(m)$ in Equation (4.72).

As shown on Figure 4.6, even at the maximum concentration of treatment u_2, $\mathcal{R}_{0U} > 1$. This again confirms the results of the optimal control that treatment u_2 alone does not suffice for the clearance of the infection.

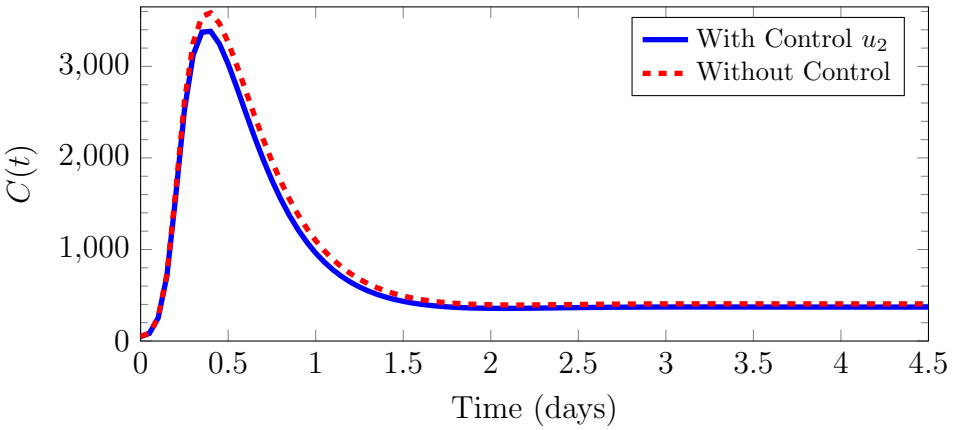

Figure 4.7: Time series of *Chlamydia* model (4.4)-(4.6) showing the effect of using control u_2 (optimal proteasome-specific inhibitor) only on $C(t)$, the concentration of free extracellular *Chlamydia*.

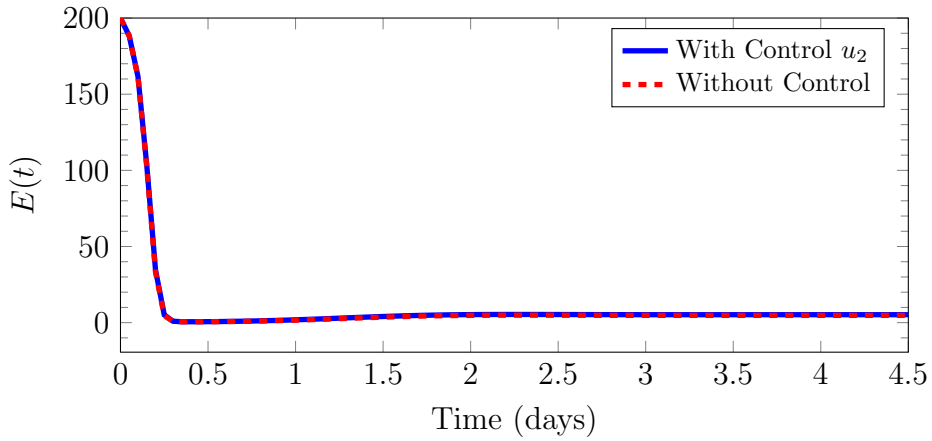

Figure 4.8: Time series of *Chlamydia* model (4.4)-(4.6) showing the effect of using control u_2 (optimal proteasome-specific inhibitor) only on $E(t)$, the concentration of healthy epithelial cells.

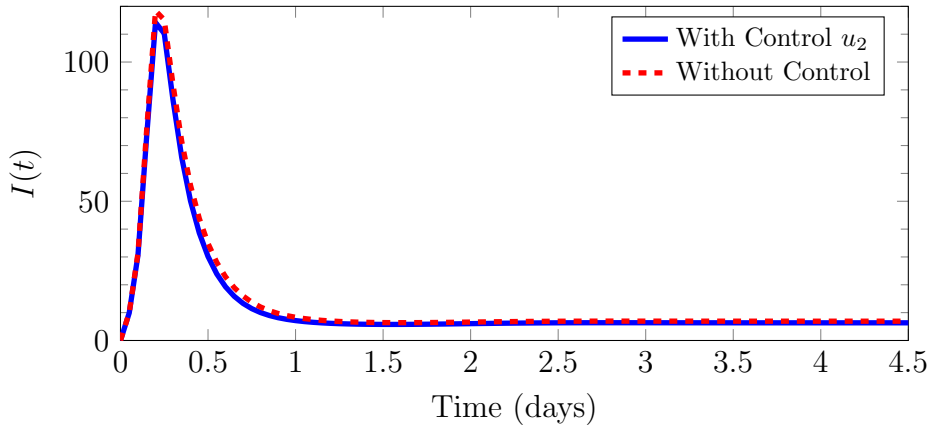

Figure 4.9: Time series of *Chlamydia* model (4.4)-(4.6) showing the effect of using control u_2 (optimal proteasome-specific inhibitor) only on $I(t)$, the concentration of *Chlamydia*-infected epithelial cells.

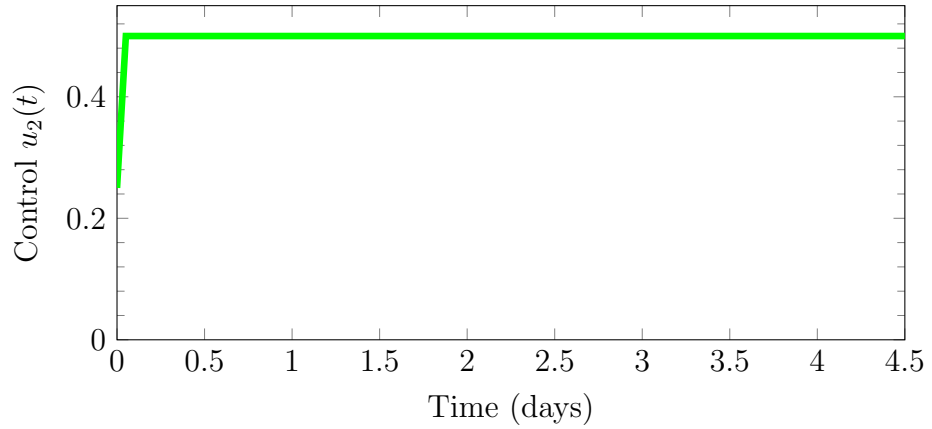

Figure 4.10: Optimal evolution for control u_2.

4.4.3 A Comparative Effect of Using Either Controls on the Clearance of a *Chlamydia* Infection

Figures 4.11-4.13 show (side-by-side graphical) comparative effects of using either control u_1 or u_2 on the evolution of the *Chlamydia* infection. The figures clearly show that the use of bacteriostatic agents alone is more effective in the clearance of a *Chlamydia* infection than the use of only proteasome-specific inhibiting agents.

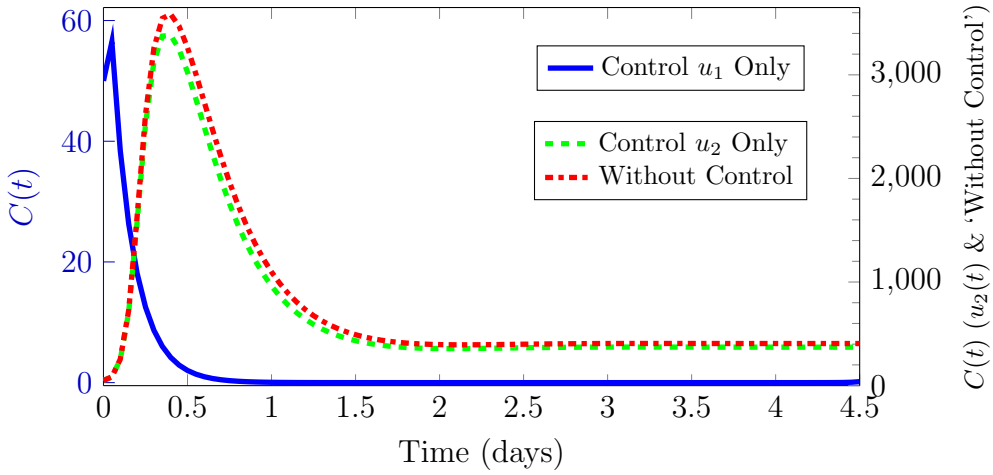

Figure 4.11: Time course of *Chlamydia* model (4.4)-(4.6) showing the comparative effects of using either control u_1 (optimal bacteriostatic treatment) or u_2 (optimal proteasome-specific inhibitor) on $C(t)$, the concentration of free extracellular *Chlamydia*.

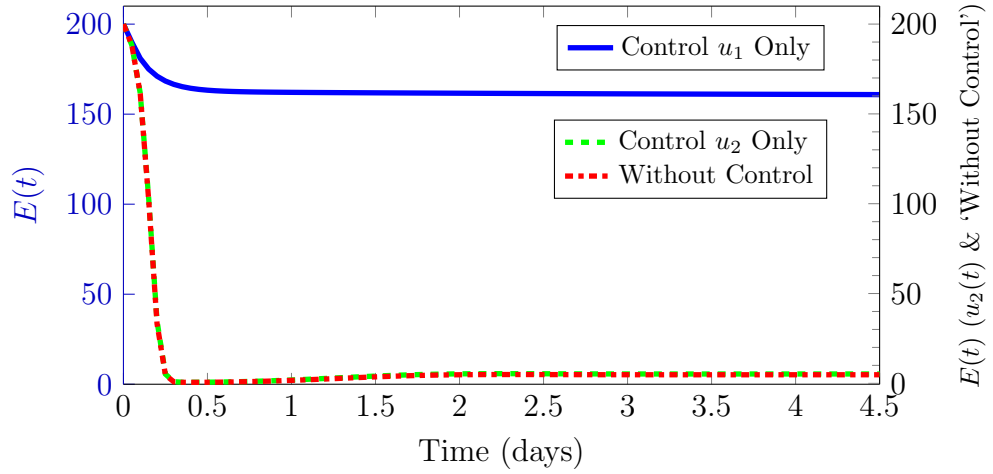

Figure 4.12: Time course of *Chlamydia* model (4.4)-(4.6) showing the comparative effects of using either control u_1 (optimal bacteriostatic treatment) or u_2 (optimal proteasome-specific inhibitor) on $E(t)$, the concentration of healthy elementary bodies.

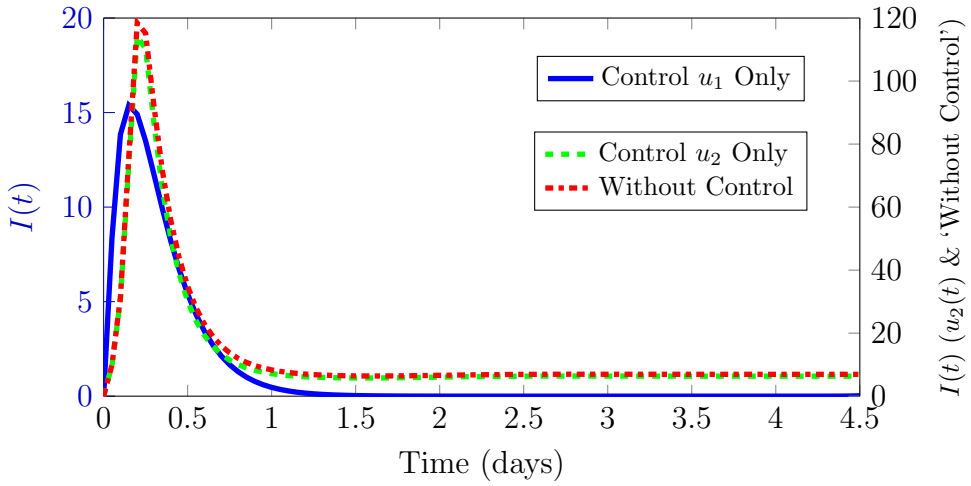

Figure 4.13: Time course of *Chlamydia* model (4.4)-(4.6) showing the comparative effects of using either control u_1 (optimal bacteriostatic treatment) or u_2 (optimal proteasome-specific inhibitor) on $I(t)$, the concentration of *Chlamydia*-infected epithelial cells.

Optimal combination treatment

With this treatment strategy, the bacteriostatic control u_1 and proteasome-specific inhibiting control u_2 are both used to optimise the objective functional J as in (4.9). In Figure 4.14, it can be observed that there was a rapid decrease in the concentration of free extracellular *Chlamydia* they were all cleared. Figure 4.15 shows that with the combination regimen, the concentration of healthy epithelial cells hardly decreased but rather attained their maximum (steady state) by the end of day one post-intervention, and remained steady throughout the course of the intervention. Figure 4.16 also suggests that only few naive healthy epithelial cell were infected throughout the course of the intervention, and not one *Chlamydia*-infected epithelial cell remained by the end of the treatment.

The optimal control functions $u_1(t)$ and $u_2(t)$ in Figure 4.17 are continuous and decrease with respect to increasing time. Figure 4.17 suggests that for the combination therapy to be optimal, u_1, the bacteriostatic treatment, should be administered at its highest tolerable concentration for the first three and a half days and then allowed to wane from the (host) system. It also suggests that u_2, the proteasome-specific inhibitor, should be administered at its highest tolerable concentration for one day and then allowed to wane from the system rapidly. These results reveal that the two therapies, when administered efficiently, may be optimal in the total clearance and truncation of the progression of a *Chlamydia* infection. The value of the objective functional (4.9) for this investigation is 126.8092.

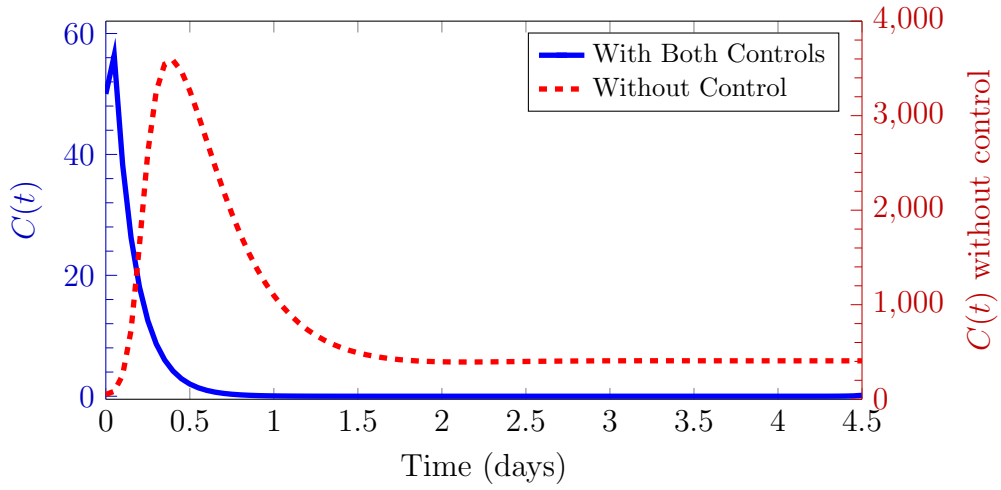

Figure 4.14: Time course of *Chlamydia* model (4.4)-(4.6) showing the effect of using controls u_1 (optimal bacteriostatic treatment) and u_2 (optimal proteasome-specific inhibitor) on $C(t)$, the concentration of free extracellular *Chlamydia*.

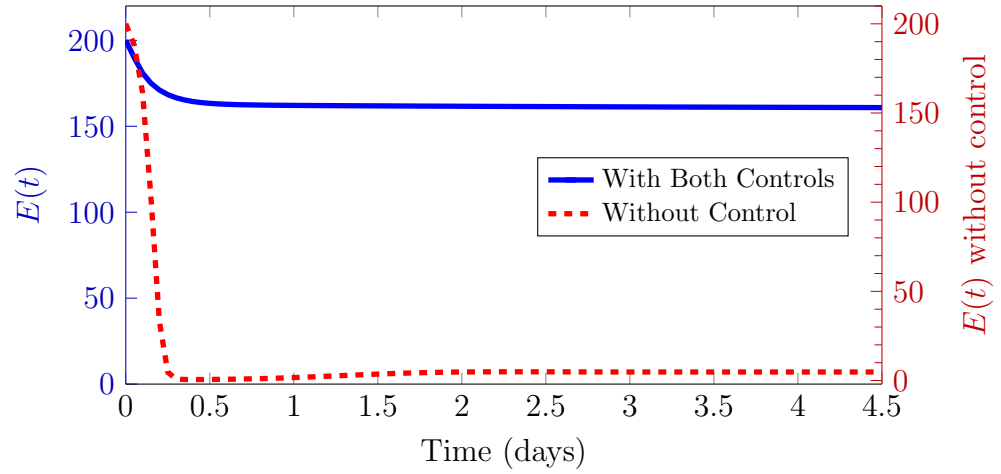

Figure 4.15: Time course of *Chlamydia* model (4.4)-(4.6) showing the effect of using controls u_1 (optimal bacteriostatic treatment) and u_2 (optimal proteasome-specific inhibitor) on $E(t)$, the concentration of healthy epithelial cells.

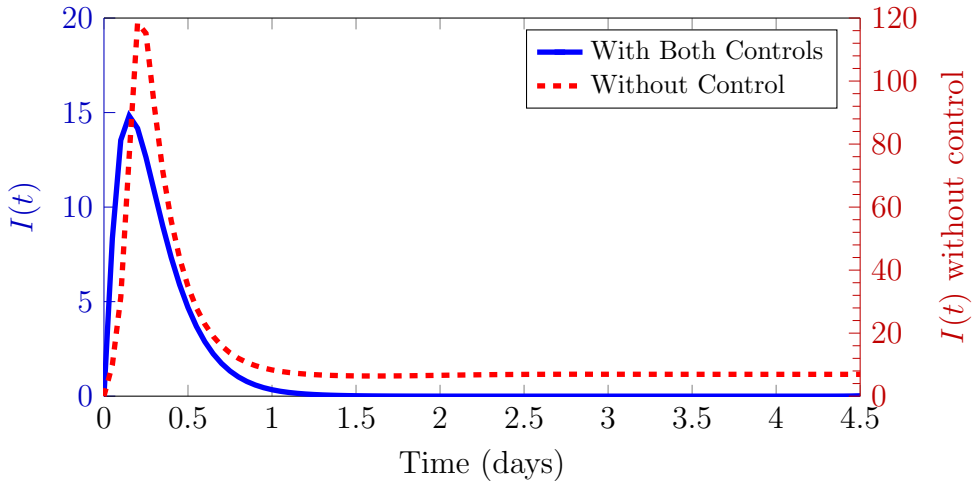

Figure 4.16: Time course of *Chlamydia* model (4.4)-(4.6) showing the effect of using controls u_1 (optimal bacteriostatic treatment) and u_2 (optimal proteasome-specific inhibitor) on $I(t)$, the concentration of *Chlamydia*-infected epithelial cells.

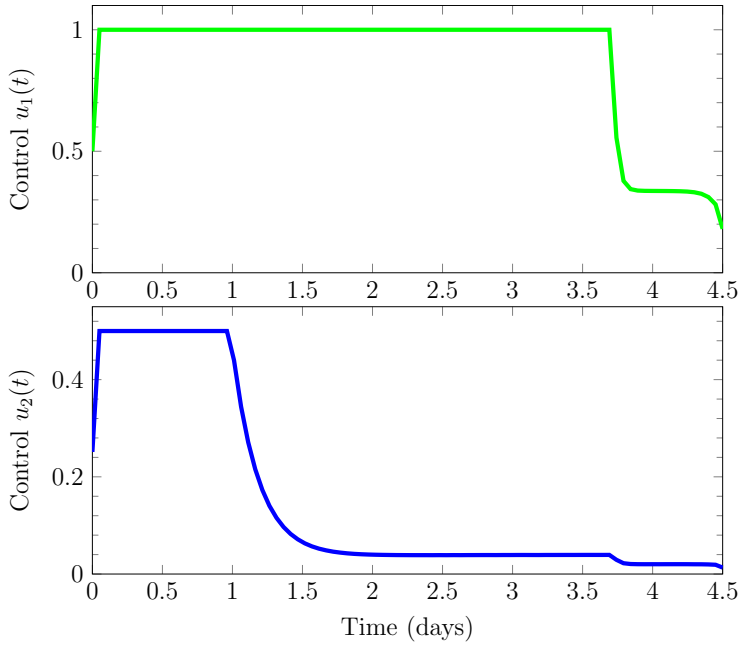

Figure 4.17: Optimal evolution for controls u_1 (optimal bacteriostatic treatment) and u_2 (optimal proteasome-specific inhibitor), respectively.

Delayed Treatment

In real life scenarios, therapeutic treatments do not often commence at the onset of an infection. Thus, we investigate the application of therapeutic interventions at 30 days PI. For the first 30 days, numerical results are obtained by simulating the disease dynamics (without control) which was set up as in Section 4.4.1, by setting the controls u_1 and u_2 to zero, with the model system (4.4)-(4.6) being reduced to the system of ODEs in [169]. For the days of therapeutic interventions which commenced at 30 days PI and lasted for 4.5 days, numerical results are obtained by simulating the optimal control problem

(4.4)-(4.9). The initial conditions for this second part of the simulation are the end points (*Chlamydia*-present equilibrium) of the previous (treatment-free) simulation. For this treatment strategy, both bacteriostatic control u_1, and proteasome-specific inhibiting control u_2, are used to optimise the objective functional J as in (4.9).

Figures 4.18-4.20 reveal that even when the optimal treatments are delayed, the *Chlamydia* infection can be stopped from progressing and eventually cleared if the treatments are administered efficiently. Figure 4.21 shows that the optimal control functions $u_1(t)$ and $u_2(t)$ are continuous and decrease with respect to time. It suggests that for the delayed combination therapy to be optimal, u_1, the bacteriostatic treatment, should be administered at its highest tolerable concentration for the first four days post-intervention and then allowed to wane from the system. It also suggests that u_2, the proteasome-specific inhibiting treatment, should be administered at the highest tolerable concentration for the first one and a half days post-intervention and then allowed to wane from the system quite rapidly. These results reveal that the two therapies, when administered efficiently, even if not administered shortly after infection, may be optimal in the total clearance and truncation of the progression of the *Chlamydia* infection.

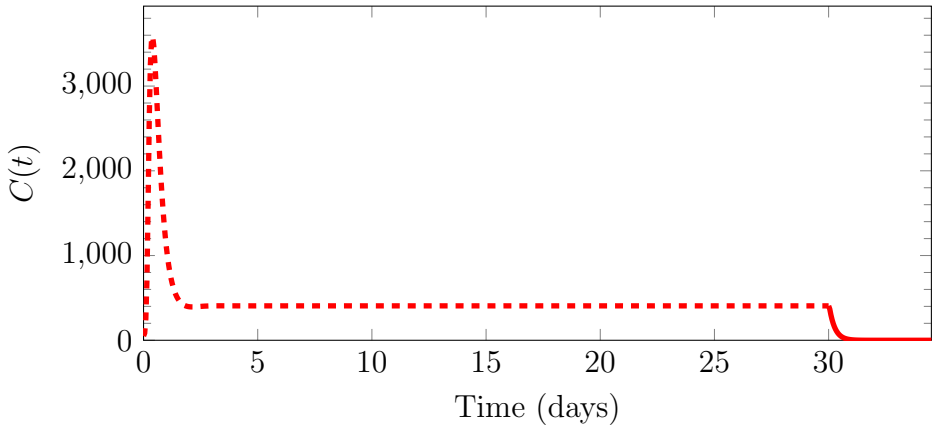

Figure 4.18: Numerical simulation of the *Chlamydia* model (4.4)-(4.6) showing the effect of delaying the use of both the optimal bacteriostatic treatment u_1 and the optimal proteasome-specific inhibitor u_2, on the time course plot of $C(t)$, the concentration of *Chlamydia*. No control was applied for the first 30 days post-infection. The treatments were applied on day 30 post-infection, and were administered for a period of 4.5 days.

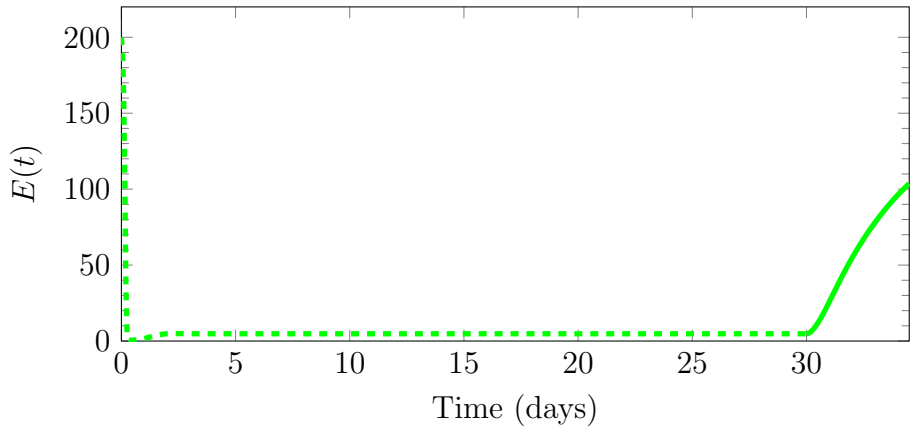

Figure 4.19: Numerical simulation of the *Chlamydia* model (4.4)-(4.6) showing the effect of delaying the use of both the optimal bacteriostatic treatment u_1 and the optimal proteasome-specific inhibitor u_2, on the time course plot of $E(t)$, the concentration of healthy elementary bodies. No control was applied for the first 30 days post-infection. The treatments were applied on day 30 post-infection, and were administered for a period of 4.5 days.

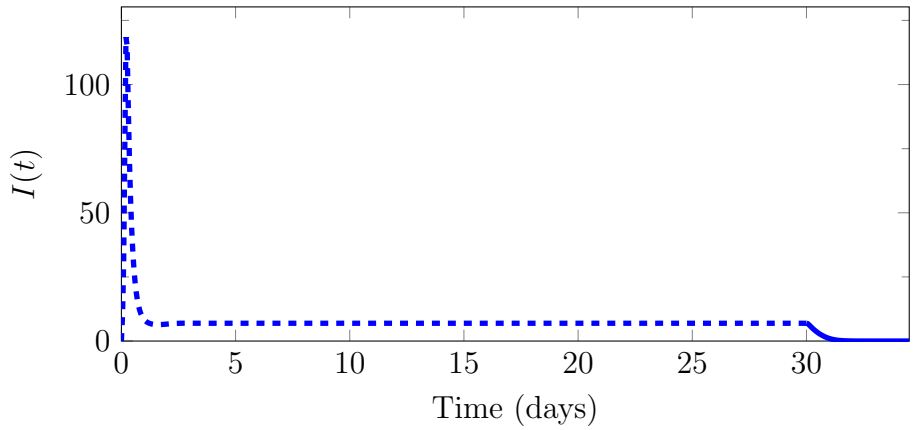

Figure 4.20: Numerical simulation of the *Chlamydia* model (4.4)-(4.6) showing the effect of delaying the use of both the optimal bacteriostatic treatment u_1 and the optimal proteasome-specific inhibitor u_2, on the time course plot of $I(t)$, the concentration of *Chlamydia*-infected epithelial cells. No control was applied for the first 30 days post-infection. The treatments were applied on day 30 post-infection, and were administered for a period of 4.5 days.

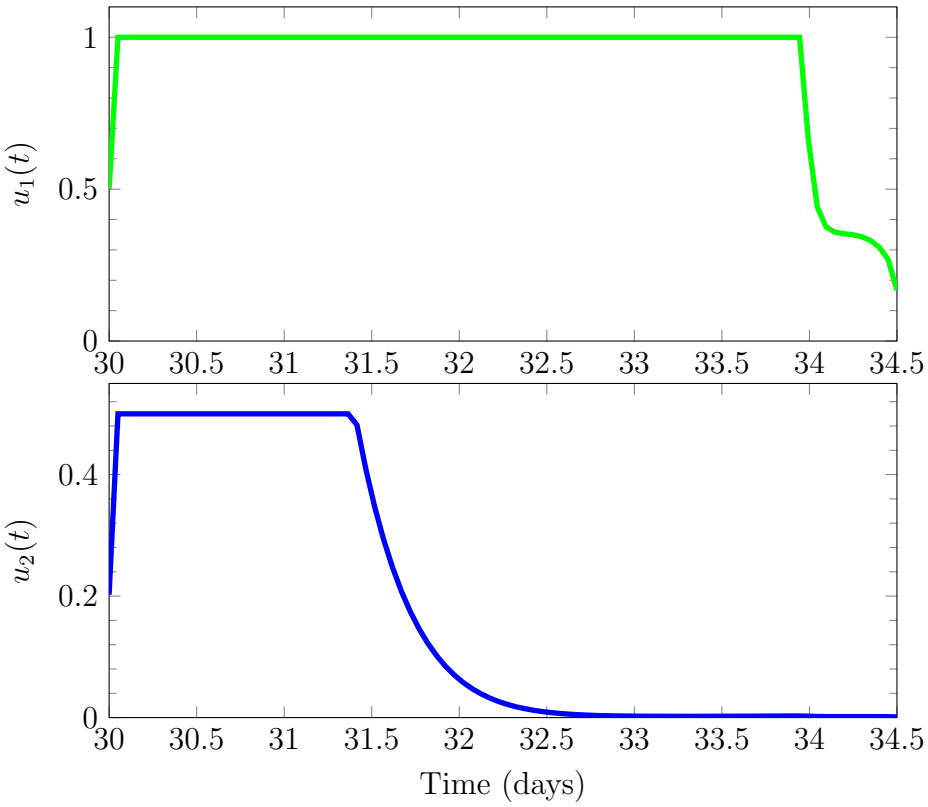

Figure 4.21: Optimal evolution for both controls: Both controls u_1 and u_2 were used to treat the infection 30 days post-infection and were administered for a period of 4.5 days.

4.5 Conclusion

In this chapter, by extending a model of within-host *Chlamydia* infection, we have investigated the dynamics of interacting species with and without two different therapeutic control strategies. We propose that alongside antibiotic activity, the presence of a proteasome-specific inhibitor such as lactacystin may enhance the capacity of the cell-mediated immune response in the clearance of *Chlamydia* infection. We hypothesise that treatment failures are perhaps the consequences of sub-optimal treatment regimens. Qualitative analysis of the model, including stability analysis of the *Chlamydia*-free equilibrium, is presented. We use methods of optimal control to derive and analyse the conditions for optimal control/treatment of the disease with agents that are bacteriostatic on *Chlamydia* and with agents that are proteasome-specific inhibiting. Existence and uniqueness of the optimal controls were proved. We also characterised the controls using Pontryagin's Maximum Principle and the resulting optimality system was numerically solved.

Using numerical simulations, we explored the different impacts of these two optimal control strategies. We note that when both controls/treatments u_1 and u_2 are used, the objective functional value was 126.8092. When control/treatment u_1 alone was used, the objective functional value was 136.0853. Whereas, when control/treatment u_2 alone was used, the objective functional value was 3662.4. These are very relevant observations. The

results imply that although the use of either both treatments (u_1 and u_2) or treatment u_1 alone clears the chlamydial infection, the systemic cost of the treatments (toxicity) to the host is minimal when both treatments are used, as opposed to when only treatment u_1 is used. These numerical results also show that when treatment u_2 alone is used to treat a chlamydial infection, the systemic cost (toxicity) of the treatment u_2 to the host is very high, despite the fact that the treatment does not result in the clearance of the chlamydial infection.

Numerical results indicate that an optimal and effective clearance and truncation of the progression of a *Chlamydia* infection may be achieved by the administration of a combined chemotherapy of agents that are bacteriostatic on *Chlamydia* and of agents that are proteasome-specific inhibiting. The results show that the optimal combination therapy is a dynamic one, in that the treatment is adjusted over the course of the treatment intervention whereby one begins with a (maximal) strong dosing scheme, followed by a lessening of treatment over time, either by the reduction of drug dosage or strength. The control problem however indicates that bacteriostatic agents that will increase the chances of the survival of health epithelial cells are especially essential for timely reduction of free extracellular *Chlamydia* and the overall clearance of a *Chlamydia* infection. We suggest that therapeutic interventions that adhere to these control strategies may be very effective in combating *Chlamydia* infections.

As previously discussed in Section 2.2, a major factor to be considered in the administration of multiple-dose regimens of antimicrobials is patients' compliance to the drug regimen [150]. The optimal treatment strategies suggested by our model require that strong doses of the two drugs - bacteriostatic agents and proteasome-inhibitors - be administered and maintained within a therapeutic band for days. This could mean that patients have to take multiple-doses of the treatment regimen. This is unrealistic because of the issue of patience compliance. However drug delivery systems that can make such treatment regimens a reality can be designed.

Effective drug delivery systems, that can ensure a controlled release/delivery of drugs, while also maintaining the drugs' concentration within a therapeutic band, over a particular period of time, have previously been engineered. One such application is the use of polymer therapeutics, a system that can use polymer chain as the inert carrier to which a drug is covalently linked. Such conjugation can be used to elicit *in vivo* spatiotemporal release of drugs designed to attain desired therapeutically effective concentration, with other benefits including reduction in immunogenicity, protection of the drug from proteolytic enzymes, potential for targeted delivery, and increased plasma half-life which would imply that less frequent doses of the drug are required [97, 102]. Diseases for which polymer conjugates have been successfully designed include hepatitis B and C, and ischemia [102, 158].

Such new and bio-compatible drug delivery system that can enhance the permeability and spatiotemporal release of chlamydial antibiotics (such as azithromycin, which already

has a long half-life) at concentrations higher than the minimum inhibitory concentration (MIC) of *Chlamydia*, may facilitate its bioavailability at very high concentrations for several days. The use of a transdermal patch to constantly deliver desired concentrations of the drug over time may also be able to provide the therapeutically effective drug concentration that suits our model's suggested optimal treatment strategy.

We however note that there are several limitations to this study: (1) model parameters that describe biological processes may not have been accurate. For example, the effects of the immune response may have been over-emphasised, thereby resulting in an improved clearance of a chlamydial infection as compared to what happens *in vivo*. In the case of an infectious disease such as genital *Chlamydia*, it is not unreasonable to anticipate that the values of some (biological) parameters are patient specific. Consequently, there can be significant uncertainty in the determination of (biological) parameter values. Thus, the presented model could be usefully extended by the carrying out of uncertainty and sensitivity analyses; (2) Results of the optimisation of the treatments are subject to change when weight parameters are varied. For example, while we observed that when systemic cost of using the bacteriostatic treatment (A_2) was increased, more of both treatments were required over time. Despite this, the infection was not effectively cleared. However, when the systemic cost of using the proteasome-specific inhibiting treatment (A_3) was increased, the treatments needed to be applied for only about 0.5 day more, but this does not necessarily improve the prognosis of the infection (results shown in the Appendix).

We observed that the initiation of treatments at 30 days post-infection does not significantly change the effect of the treatment as compared to when the treatments were administered on infection. The only difference observed was that the starting strong dosing scheme would be given for a longer time (about 0.5 days more) and also followed by a lessening of treatment, either by the reduction of drug dosage or strength. We also observed that the effects of the therapies on the disease dynamics does not depend on the treatment duration, that is, increasing the length of the treatment interval does not necessarily yield better outcomes. Numerical results for this are presented in the Appendix. Our approach provides a framework for the design of new protocols for chlamydial infection treatment strategies.

5 An Optimal control model of the treatment of chronic *Chlamydia trachomatis* infection using antibiotic and tryptophan supplementation

In the preceding chapter, an optimal control model of the treatment of chlamydial infection has been investigated. The model gave some insights into an optimal chlamydial treatment strategy. However, the model does not address the concern of the development of *Chlamydia* persistence in chronic infections. In order to account for the prevention, and even reversal, of the development of *Chlamydia* persistence which causes severe sequelae in chronic chlamydial infections, there is the need for us to investigate other treatment strategies that can facilitate such objectives. As suggested in the literature (see Subsection 2.3.1), the combination of a tryptophan and antibiotic treatment may facilitate an improved treatment of chronic *Chlamydia* infections characterised by chlamydial persistence. Hence, we consider a mathematical model of the treatment of chronic *Chlamydia* infections, using optimal control tools.

In this chapter, we present a deterministic mathematical model of *C. trachomatis* infection, within-host, with a particular focus on determining the optimal scheme(s) (that is, when and how treatment should be initiated) for the treatment of chronic chlamydial infections using antibiotics and tryptophan supplementation. Our work aims to determine optimal treatment strategies that not only minimise the production of free extracellular *Chlamydia*, but also minimise the production of persistent intracellular *Chlamydia* by blocking the formation of persistent *Chlamydia*, and reversing already established persistence into actively replicating *Chlamydia* forms, for clearance by the immune system and antibiotics. In Section 5.1, we develop a model for the optimal control of *Chlamydia* infection. We also present basic properties of the developed model in Section 5.1. Using an existence result, we guarantee the existence of an optimal control pair with finite objective functional in Section 5.2. In Section 5.3, we use Pontryagin's Maximum Principle to characterise the optimal control pair. We present numerical results of simulation of the model system in Section 5.4. Our conclusions are discussed in Section 5.5.

5.1 Model Formulation

We develop a mathematical model of the cellular dynamics of *Chlamydia* and the infected host system in order to investigate the impact of treatment on the within-host dynamics of a chronic chlamydial infection. Ordinary differential equations were used to model the cellular dynamics of the interactive processes between extracellular *Chlamydia*, uninfected epithelial cells, *Chlamydia*-infected epithelial cells, and *Chlamydia*-infected epithelial cells within which *Chlamydia* is in the persistent state. The model describes the role of the humoral and cell-mediated immunity in the course of a *Chlamydia* infection, while also capturing the effects of different treatment strategies in the clearance of a *Chlamydia* infection. We apply techniques of optimal control theory to the resulting system of ordinary differential equations and explore optimal control strategies associated with different kinds of treatment of chlamydial infections.

We denote by $C(t)$, the concentration of free extracellular *Chlamydia*, $E(t)$, the concentration of uninfected mucosal epithelial cells, $I(t)$, the concentration of *Chlamydia*-infected epithelial cells, and $I_P(t)$, the concentration of *Chlamydia*-infected epithelial cells that are in the persistent state. We shall refer to I_P simply as persistently infected cells. The functions u_1 and u_2 represent two different treatments. The function u_1 represents the bio-available and deliverable amount of tryptophan, in the form of 1-MT, which blocks the intracellular formation of persistent *Chlamydia*, while also facilitating the 'recovery' of persistently infected cells by reversing IFN-γ-induced persistence in intracellular *Chlamydia* (thereby increasing the susceptibility of *Chlamydia* to antibiotic treatment). The function u_2 represents the bio-available and deliverable amount of bacteriostatic agents (which reduces the concentration of infected cells by blocking the intracellular growth of *Chlamydia*, thereby inducing chlamydial persistence). The functions u_1 and u_2 are bounded Lebesgue integrable functions satisfying $0 \leq u_1(t) \leq m_1 \leq 1$ and $0 \leq u_2(t) \leq m_2 \leq 1$, where m_1 and m_2 are the maximum attainable amount/proportion of $u_1(t)$ and $u_2(t)$, respectively. Note that treatments u_1 and u_2 are drug concentrations that have been scaled by the maximum tolerable concentration of the respective treatments. Thus they are now proportions with no units. We define the control functions on fixed time intervals since the treatment of chlamydial infections (or antibiotics generally) are not expected to be administered for an infinite period of time. Thus the controls are defined for $t_{start} = t_0 \leq t \leq t_{final}$, where for current recommended treatment guidelines, $t_{final} - t_{start} \leq 7$ days.

The following system of equations is proposed:

$$\frac{\mathrm{d}C}{\mathrm{d}t} = Pk_2I - \mu C - k_1CE, \tag{5.1}$$
$$\frac{\mathrm{d}E}{\mathrm{d}t} = P_E - \delta_E E - k_1CE, \tag{5.2}$$
$$\frac{\mathrm{d}I}{\mathrm{d}t} = k_1CE + \rho u_1 I_P - \gamma I - k_2 I - \alpha u_2 I - cu_1u_2 I, \tag{5.3}$$
$$\frac{\mathrm{d}I_P}{\mathrm{d}t} = \gamma(1 - cu_1)I + Q\alpha u_2 I - \rho u_1 I_P - \delta_P I_P, \tag{5.4}$$

with initial conditions $C(t_0) = C_0$, $E(t_0) = E_0$, $I(t_0) = I_0$, and $I_P(t_0) = I_{P0}$, where t_0 is the initial time. At a rate of k_2, P *Chlamydia* are released from infected cells. The rate of epithelial cell infection (which may be reduced by antibodies) is denoted by k_1, the rate of production of epithelial cells is denoted by P_E, the natural death rates of healthy epithelial cells and persistently infected (epithelial) cells are denoted by δ_E and δ_P, respectively. We assume that infected cells either burst/lyse (after the maturation of their intracellular chlamydial developmental cycle) or become persistently infected (either by the inhibitory activity of IFN-γ or the bacteriostatic activity therapeutic treatments/drugs). Thus we do not account for their natural deaths. The rate of clearance of infected cells, due to cell-mediated immunity (predominantly by the secretion of IFN-γ) is denoted by γ.

We model two different processes into the parameter μ. When $u_1 \equiv 0$, $\mu = \mu_m$, the rate of clearance of extracellular *Chlamydia* by macrophages. When $u_1 > 0$, $\mu = \mu_m + \mu_\tau$, where μ_τ is the rate at which 1-MT facilitates the reduction in the amount of EBs produced on lysis of infected epithelial cells. The rate at which 1-MT blocks the formation of IFN-γ-induced persistence in intracellular *Chlamydia* is c, while the rate at which it reverses already formed persistence in intracellular *Chlamydia* is ρ. The rate at which antibiotics inhibit chlamydial growth, thereby reducing the pool of infected cells, is α. Persistence is induced in a fraction Q $(0 < Q < 1)$ of the infected cells within which chlamydial growth has been inhibited by antibiotics.

In the absence of controls u_1 and u_1, the model system (5.1)-(5.4) reduces to the following system of equations, which we shall refer to as the 'basic *Chlamydia* persistence model':

$$\frac{\mathrm{d}C}{\mathrm{d}t} = Pk_2I - \mu C - k_1CE, \tag{5.5}$$
$$\frac{\mathrm{d}E}{\mathrm{d}t} = P_E - \delta_E E - k_1CE, \tag{5.6}$$
$$\frac{\mathrm{d}I}{\mathrm{d}t} = k_1CE - \gamma I - k_2 I, \tag{5.7}$$
$$\frac{\mathrm{d}I_P}{\mathrm{d}t} = \gamma I - \delta_P I_P, \tag{5.8}$$

also with initial conditions $C(t_0) = C_0$, $E(t_0) = E_0$, $I(t_0) = I_0$, and $I_P(t_0) = I_{P0}$, where t_0 is the initial time.

As discussed, after treatment with 1-MT, those chlamydial forms that must have recovered from persistence become more susceptible to the antimicrobial potency of antibiotics. Thus, we model the increased susceptibility of *Chlamydia* to antibiotics, in the presence of tryptophan, by the term cu_1u_2I. We have assumed that the rate at which this increased susceptibility occurs is the same as the rate at which 1-MT blocks the formation of IFN-γ-induced persistence in intracellular *Chlamydia*.

The goal of treatment is to minimise the concentrations of extracellular *Chlamydia*, infected cells, and persistently infected cells, and the systemic costs of the treatments/drugs to the body over the course of the treatment, while also minimising the concentrations of extracellular *Chlamydia* and persistently infected cells present at the end of the therapeutic intervention strategy. Hence, we seek an optimal control pair (u_1^*, u_2^*), such that

$$J(u_1^*, u_2^*) = \min_{u_1, u_2 \in \hat{\Gamma}} J(u_1, u_2), \tag{5.9}$$

where $\hat{\Gamma}$, the set of admissible controls, is defined as

$$\hat{\Gamma} = \{(u_1, u_2) | u_1 \text{ and } u_2 \text{ are Lebesgue measurable}, 0 \leq u_1 \leq m_1, 0 \leq u_2 \leq m_2,\ m_1, m_2 \leq 1, t \in [0, t_f]\}. \tag{5.10}$$

The objective functional to be minimized is

$$J(u_1, u_2) = \int_{t_0}^{t_f} \left(C(t) + A_1 I(t) + A_2 I_P(t) + \frac{A_3}{2} u_1^2 + \frac{A_4}{2} u_2^2 \right) \mathrm{d}t + A_5 C(t_f) + A_6 I_P(t_f), \tag{5.11}$$

where t_f is the final time of the therapeutic intervention strategy, and the positive constant weights A_1, A_2, A_3, A_4, A_5, and A_6, measure the relative costs of implementing the respective treatment strategies over the period $[0, t_f]$. Their values will depend on the relative importance of each of the control measures in the treatment of the disease. We assume that the weight factor A_4 associated with control u_2 is greater than or equal to the weight factor A_3, which is associated with control u_1. This is because as u_2 is an antibiotic treatment/drug, which may be toxic to the human body if administered in high doses whereas, u_1, which is tryptophan, a harmless nutritional supplement, is not expected to be toxic to the human body [145]. We suppose that the cost function is a nonlinear function of u_1 and u_2 because of the fact it needs to be twice differentiable. Thus, the relationship between the effects of the drugs on *Chlamydia* and host cells takes the specified non-linear form. Thus, we assume that the controls are quadratic, which is in line with several other literatures [5, 83, 85, 143, 154].

The terms $C(t)$, $A_1I(t)$, and $A_2I_P(t)$ represent the costs of the clearance of viable *Chlamydia*, infected healthy epithelial cells, and persistently infected epithelial cells, respectively. The terms $\frac{A_3}{2}u_1^2$ and $\frac{A_3}{2}u_2^2$ describe the costs associated with administering the respective intervention strategies. The terms $A_5C(t_f)$ and $A_6I_P(t_f)$ are terminal costs associated with the minimisation of the concentrations of *Chlamydia* and persistently infected cells, respectively, by the end of the treatment.

Variables	**Description**	**Values**	**Ranges**
C	Free extracellular *Chlamydia*	$C_0 = 500$ cells/mm^3	
E	Healthy mucosal epithelial cells	$E_0 = 5000$ cells/mm^3	
I	*Chlamydia*-infected epithelial cells	$I_0 = 100$ cells/mm^3	
I_P	Persistently infected epithelial cells	$I_{P0} = 1000$ cells/mm^3	
Parameters			
P	Burst size per infected cell	200 [169]	200-500
k_1	Rate of cell infection	0.02 cell/mm^3/day [169]	
k_2	Rate of infected cells burst	0.33 day^{-1} [169]	[0.33-0.6]
P_E	Rate of production of mucosal epithelial cells	44 cells/mm^3/day [32, 169]	[30-60]
δ_E	Rate of natural death of epithelial cells	0.25 day^{-1} [8, 21]	[0.25-0.26]
δ_P	Rate of natural death of I_P	0.35 day^{-1}	
γ	Effectiveness of cell-mediated immunity	2 day^{-1} [169]	2-10
μ_m	Effectiveness of humoral immunity	2 day^{-1} [169]	[2-10]
μ_τ	Reduction of EB production as induced by 1-MT	1.5 day^{-1}	[0.1-2]
ρ	Rate at which Tryp. reverses persistence	1.7 day^{-1}	
c	Rate at which Tryp. blocks the induction of persistence	1.43 day^{-1}	
α	Rate at which antibiotics clear infection	6.5 day^{-1}	
Q	Fraction of antibiotics-induced I_P	0.8	(0,1)
m_1	Maximum dosage of control $u_1(t)$	0.7	
m_2	Maximum dosage of control $u_2(t)$	0.9	

Table 5.1: Variables, parameters, values, and ranges used in numerical simulations. Tryp. is tryptophan.

5.1.1 Basic Properties

In this section, we present some basic qualitative results for the model system (5.1)-(5.4), in order to ascertain that the problem is mathematically and biologically well posed.

Positivity of solutions

The model system (5.1)-(5.4) describes the dynamics of cell populations. Hence, it is essential that all its state variables remain non-negative for all time. This implies that the solutions of the system will remain positive for all $t > 0$ when given positive initial conditions. We establish this important condition via the following lemma:

Lemma 5.1.1. *Given non-negative initial values of the state variables in Equations* (5.1)-(5.4)*, non-negative solutions are generated for all time* $t > 0$.

Proof. Let $(C(0), E(0), I(0), I_P(0))$ be a positive initial condition and denote by $[0, t_{\max}]$, the maximum interval of existence of the corresponding solution. In order to prove that the solution is positive in $[0, +\infty]$, it suffices to show that it is positive in $[0, t_{\max}]$.

Let $t_s = \sup\{0 < t < t_{\max} : C(t) > 0, E(t) > 0, I(t) > 0, I_P(t) > 0 \text{ on } [0, t]\}$.

$t_s > 0$ since $C(0)$, $E(0)$, $I(0)$, and $I_P(0)$ are non-negative. Suppose $t_s < t_{\max}$.

From Equation (5.1),

$$\frac{\mathrm{d}C}{\mathrm{d}t} + (\mu + k_1 E)C = Pk_2 I.$$

Thus,

$$\frac{\mathrm{d}}{\mathrm{d}t}\left(C(t)\exp\left\{\mu t + k_1\int_0^t E(\tau)\mathrm{d}\tau\right\}\right) = Pk_2 I(t)\left(\exp\left\{\mu t + k_1\int_0^t E(\tau)\mathrm{d}\tau\right\}\right),$$

so that

$$\begin{aligned} &C(t_s)\exp\left\{\mu t_s + k_1\int_0^{t_s} E(\tau)\mathrm{d}\tau\right\} - C(0) \\ &\quad = \int_0^{t_s}\left(Pk_2 I(\hat{\tau})\exp\left\{\mu\hat{\tau} + k_1\int_0^{\hat{\tau}} E(\tau)\mathrm{d}\tau\right\}\right)\mathrm{d}\hat{\tau}. \end{aligned}$$

Hence,

$$\begin{aligned} C(t_s) &= C(0)\exp\left\{-\left(\mu t_s + k_1\int_0^{t_s} E(\tau)\mathrm{d}\tau\right)\right\} \\ &+ \exp\left\{-\left(\mu t_s + k_1\int_0^{t_s} E(\tau)\mathrm{d}\tau\right)\right\}\int_0^{t_s}\left(Pk_2 I(\hat{\tau})\exp\left\{\mu\hat{\tau} + k_1\int_0^{\hat{\tau}} E(\tau)\mathrm{d}\tau\right\}\right)\mathrm{d}\hat{\tau} \\ &> 0. \end{aligned}$$

It can be shown by a similar argument that $E(t_s) > 0$, $I(t_s) > 0$, and $I_P(t_s) > 0$.

This contradicts the fact that t_s is the supremum because at least one of the state variables should be equal to zero at t_s. Therefore $t_s = t_{\max}$. Thus, $C(t) \geq 0$, $E(t) \geq 0$, $I(t) \geq 0$, and $I_P(t) \geq 0$, for all time $t > 0$. This completes the proof. □

Invariant region

We consider the long term behaviour of the system (5.1)-(5.4) in an apposite biologically feasible region $\hat{\mathcal{D}}$.

Since all the parameters and state variables of model system (5.1)-(5.4) are non-negative for all $t \geq 0$, from the Equation (5.1), it follows that

$$\begin{aligned} \frac{\mathrm{d}C}{\mathrm{d}t} &= Pk_2 I - \mu C - k_1 CE \\ &\leq Pk_2 I - \mu C. \end{aligned}$$

This implies that

$$\frac{\mathrm{d}C}{\mathrm{d}t} + \mu C \leq Pk_2 I.$$

Thus,

$$C(t) \leq C(0)e^{-\mu t} + e^{-\mu t} Pk_2 \int_0^t I(\tau)e^{\mu\tau}\mathrm{d}\tau.$$

Since the interval $[0, t]$ is compact, and since the integrand, $I(\tau)e^{\mu\tau}$, is continuous on that interval, the corresponding integral is finite. Therefore

$$C(t) \leq e^{-\mu t}(C(0) + Pk_2 n_1) = \bar{n_1},$$

where $n_1 = \int_0^t I(\tau)\, e^{\mu\tau}\mathrm{d}\tau$.

From Equation (5.2),

$$\frac{\mathrm{d}E}{\mathrm{d}t} \leq P_E - \delta_E E.$$

This implies that

$$\frac{\mathrm{d}E}{\mathrm{d}t} + \delta_E E \leq P_E.$$

Thus,

$$\begin{aligned} E(t) &\leq E(0)e^{-\delta_E t} + \frac{P_E}{\delta_E}(1 - e^{-\delta_E t}), \\ &= E(0)e^{-\delta_E t} + E^*(1 - e^{-\delta_E t}), \\ &= E^* - (E^* - E(0))e^{-\delta_E t}. \end{aligned}$$

$E(t)$ either approaches E^* asymptotically or there exists some finite time after which $E(t) \leq E^*$.

From Equation (5.3),

$$\frac{\mathrm{d}I}{\mathrm{d}t} \leq k_1 CE + \rho u_1 I_P - k_2 I,$$

that is

$$\frac{\mathrm{d}I}{\mathrm{d}t} + k_2 I \leq k_1 CE + \rho u_1 I_P.$$

Thus,

$$I(t) \leq I(0)e^{-k_2 t} + e^{-k_2 t} \int_0^t (k_1 C(\tau)E(\tau) + \rho u_1(\tau) I_P(\tau))e^{k_2\tau}\mathrm{d}\tau.$$

Again, the integral is finite since continuous functions, $C(\tau)E(\tau)e^{k_2\tau}$ and $\rho u_1(\tau)I_P(\tau)e^{k_2\tau}$ are integrated over a compact interval. Therefore

$$I(t) \leq I(0)e^{-k_2 t} + e^{-k_2 t} n_2 = \bar{n_2},$$

where

$$n_2 = \int_0^t (k_1 C(\tau)E(\tau) + \rho u_1(\tau) I_P(\tau)) e^{k_2 \tau} \mathrm{d}\tau.$$

From Equation (5.4),

$$\frac{\mathrm{d}I_P}{\mathrm{d}t} \leq \gamma I + Q\alpha u_2 I - \delta_P I_P,$$

that is

$$\frac{\mathrm{d}I_P}{\mathrm{d}t} + \delta_P I_P \leq \gamma I + Q\alpha u_2 I.$$

Thus,

$$I_P(t) \leq I_P(0)e^{-\delta_P t} + e^{-\delta_P t} \int_0^t (\gamma I(\tau) + Q\alpha u_2(\tau) I(\tau)) e^{\delta_P \tau} \mathrm{d}\tau.$$

Again, the integral is finite since continuous functions, $\gamma I(\tau)e^{\delta_P \tau}$ and $Q\alpha u_2(\tau)I(\tau)e^{\delta_P \tau}$ are integrated over a compact interval. Therefore

$$I_P(t) \leq I_P(0)e^{-\delta_P t} + e^{-\delta_P t} n_3 = \bar{n_3},$$

where

$$n_3 = \int_0^t (\gamma I(\tau) + Q\alpha u_2(\tau) I(\tau)) e^{\delta_P \tau} \mathrm{d}\tau.$$

Hence, the region

$$\hat{\mathcal{D}} = \left\{ (C(t), E(t), I(t), I_P(t)) \in \mathbb{R}_+^4 : C(t) \leq \bar{n_1}, E(t) \leq E^*, I(t) \leq \bar{n_2}, I_P(t) \leq \bar{n_3} \right\}$$

is positively invariant and attracting for the model system (5.1)-(5.4), that is, every feasible solution of the model with initial conditions in $\hat{\mathcal{D}}$, will remain in $\hat{\mathcal{D}}$, for all $t \geq 0$. We establish this result via the following lemma:

Lemma 5.1.2. *The biologically feasible region $\hat{\mathcal{D}}$ is positively invariant and attracting with respect to the model system* (5.1)-(5.4) *with initial conditions in $\mathbb{R}_+^4$.*

It is clear that the right hand sides of the model equations (5.1)-(5.4) are smooth. Hence, initial value problems have unique solutions on the region $\hat{\mathcal{D}}$. Also, since paths are confined in $\hat{\mathcal{D}}$, solutions exist for all time $t \geq 0$. It follows that solutions to system (5.1)-(5.4) exist in $\hat{\mathcal{D}}$ and are unique. Having thus confirmed that the model system is mathematically and biologically well posed, we proceed to study the dynamics of the flow induced by the model system (5.1)-(5.4) in $\hat{\mathcal{D}}$.

5.1.2 Existence and stability of equilibria

In this section, we determine the equilibria of the basic *Chlamydia* persistence model (5.5)-(5.8) and analyse their stability.

Local stability of the *Chlamydia*-free equilibrium

The *Chlamydia*-free equilibrium (CFE) can be obtained by the setting the right-hand sides of the basic *Chlamydia* persistence model (5.5)-(5.8) to zero and then choosing solutions where $C = I = I_P = 0$. This CFE is given by $\mathbb{F}_{02}$,

$$\mathbb{F}_{02} = (C^*, E^*, I^*, I_P^*) = (0, \hat{E}, 0, 0), \tag{5.12}$$

where $\hat{E} = \dfrac{P_E}{\delta_E}$.

The linear stability of this equilibrium $\mathbb{F}_{02}$ can be established using the next generation method described in Subsection 4.1.2, on the model system (5.5)-(5.8).

The class of infectives in the model system (5.5)-(5.8) are *Chlamydia* (C), *Chlamydia*-infected host cells (I), and persistently infected host cells (I_P), since these three classes facilitate the chronic chlamydial infection process. Thus, the *infected subsystem* of the model system (5.5)-(5.8) is given by Equations (5.5), (5.7) and (5.8), that is, $(\dot{C}, \dot{I}, \dot{I_P})$. Hence we sort the model system (5.5)-(5.8) so that the first three compartments correspond to the class of infectives, that is $(\dot{C}, \dot{I}, \dot{I_P}, \dot{E})$.

The rate of appearance of new infections in the three compartments, is denoted by $\mathcal{F}_1$,

$$\mathcal{F}_1 = \begin{pmatrix} 0 \\ k_1 CE \\ 0 \\ 0 \end{pmatrix}, \tag{5.13}$$

while the rate of transfer of each of the interacting species in and out of the three compartments is denoted by $\mathcal{V}_1$,

$$\mathcal{V}_1 = -\begin{pmatrix} Pk_2 I - \mu C - k_1 CE \\ -(k_2 + \gamma) I \\ P_E - \delta_E E - k_1 CE \end{pmatrix}. \tag{5.14}$$

Hence, the matrices of partial derivatives $\boldsymbol{F_1}$ and $\boldsymbol{V_1}$, for the *infected subsystem*, are respectively given by

$$\boldsymbol{F_1} = \begin{pmatrix} \frac{\partial \mathcal{F}_1(\mathbb{G}_0)}{\partial C} & \frac{\partial \mathcal{F}_1(\mathbb{G}_0)}{\partial I} & \frac{\partial \mathcal{F}_1(\mathbb{G}_0)}{\partial I_P} \\ \frac{\partial \mathcal{F}_2(\mathbb{G}_0)}{\partial C} & \frac{\partial \mathcal{F}_2(\mathbb{G}_0)}{\partial I} & \frac{\partial \mathcal{F}_2(\mathbb{G}_0)}{\partial I_P} \\ \frac{\partial \mathcal{F}_3(\mathbb{G}_0)}{\partial C} & \frac{\partial \mathcal{F}_3(\mathbb{G}_0)}{\partial I} & \frac{\partial \mathcal{F}_3(\mathbb{G}_0)}{\partial I_P} \end{pmatrix} = \begin{pmatrix} 0 & 0 & 0 \\ k_1\hat{E} & 0 & 0 \\ 0 & 0 & 0 \end{pmatrix}, \tag{5.15}$$

and

$$\boldsymbol{V_1} = \begin{pmatrix} \frac{\partial \mathcal{V}_1(\mathbb{G}_0)}{\partial C} & \frac{\partial \mathcal{V}_1(\mathbb{G}_0)}{\partial I} & \frac{\partial \mathcal{V}_1(\mathbb{G}_0)}{\partial I_P} \\ \frac{\partial \mathcal{V}_2(\mathbb{G}_0)}{\partial C} & \frac{\partial \mathcal{V}_2(\mathbb{G}_0)}{\partial I} & \frac{\partial \mathcal{V}_2(\mathbb{G}_0)}{\partial I_P} \\ \frac{\partial \mathcal{V}_3(\mathbb{G}_0)}{\partial C} & \frac{\partial \mathcal{V}_3(\mathbb{G}_0)}{\partial I} & \frac{\partial \mathcal{V}_3(\mathbb{G}_0)}{\partial I_P} \end{pmatrix} = \begin{pmatrix} \mu + k_1\hat{E} & -Pk_2 & 0 \\ 0 & k_2+\gamma & 0 \\ 0 & -\gamma & \delta_P \end{pmatrix}. \tag{5.16}$$

The operator $\boldsymbol{V_1}^{-1}$ is given by

$$\boldsymbol{V_1}^{-1} = \frac{1}{(\mu + k_1\hat{E})(k_2+\gamma)} \begin{pmatrix} k_2+\gamma & Pk_2 & 0 \\ 0 & \mu + k_1\hat{E} & 0 \\ 0 & \frac{\gamma(\mu + k_1\hat{E})}{\delta_P} & \frac{(\mu + k_1\hat{E})(k_2+\gamma)}{\delta_P} \end{pmatrix}. \tag{5.17}$$

$$\boldsymbol{F_1 V_1}^{-1} = \frac{1}{(\mu + k_1\hat{E})(k_2+\gamma)} \begin{pmatrix} 0 & 0 & 0 \\ k_1\hat{E}(k_2+\gamma) & Pk_1k_2\hat{E} & 0 \\ 0 & 0 & 0 \end{pmatrix}. \tag{5.18}$$

Hence, the spectral radius of $\boldsymbol{F_1 V_1}^{-1}$, which is the basic reproduction number $\mathcal{R}_{02}$ of the basic *Chlamydia* persistence model (5.5)-(5.8), is given by

$$\mathcal{R}_{02} = \frac{Pk_1k_2\hat{E}}{(\mu + k_1\hat{E})(k_2+\gamma)}. \tag{5.19}$$

By inspecting the basic reproduction number $\mathcal{R}_{02}$, one can track the contribution of the infected and infectious classes (infected epithelial cells and elementary bodies, respectively) to the infection process. From the expression in (5.19), it can be seen that the basic reproduction number $\mathcal{R}_{02}$ is the product of the infection rate of healthy epithelial cells by *Chlamydia*, $k_1\hat{E}$, the number of infectious progenies released by a lysing infected

cell, P, the duration of infectiousness of an EB, $\dfrac{1}{\mu + k_1\hat{E}}$, and the proportion of infected cells that survive up to the stage of lysis, $\dfrac{k_2}{k_2+\gamma}$.

We establish the following result by implementing *Theorem 2* of van den Driessche and Watmough [157].

Lemma 5.1.3. *The Chlamydia-free equilibrium (CFE)* $\mathbb{F}_{02}$*, of the basic Chlamydia persistence model* (5.5)-(5.8)*, is locally stable whenever* $\mathcal{R}_{02} < 1$ *and unstable if* $\mathcal{R}_{02} > 1$*.*

Lemma 5.1.3 implies that when $\mathcal{R}_{02} < 1$, the *in vivo* clearance of *Chlamydia* body forms can be achieved if the initial sizes of the subpopulations of the model (C, E, I, I_P) are in the basin of attraction of the CFE $\mathbb{F}_{02}$.

In order to ensure that the therapeutic effects of an effective *Chlamydia* infection treatment regimen in an *in vivo* or *in vitro* setting system does not depend on either the initial size of *Chlamydia* body forms or innoculum, respectively, or the initial sizes of other subpopulations of the model (E, I, and I_P), we show that the CFE is globally asymptotically stable (GAS) when $\mathcal{R}_{02} < 1$.

Global stability of the *Chlamydia*-free equilibrium

Theorem 5.1.4. *The Chlamydia-free equilibrium (CFE)* $\mathbb{F}_{02}$*, of the basic Chlamydia persistence model* (5.5)-(5.8)*, is globally asymptotically stable in* $\hat{\mathcal{D}}$*, whenever* $\mathcal{R}_{02} < 1$ *and unstable otherwise. The CFE* $\mathbb{F}_{02}$ *is the only equilibrium when* $\mathcal{R}_{02} \leq 1$*.*

Proof. Consider the candidate Lyapunov function

$$\mathbb{Y} = Pk_1k_2I + k_1(\gamma + k_2)C, \tag{5.20}$$

with Lyapunov derivative (where a dot represents differentiation with respect to t) given by

$$\begin{aligned}
\dot{\mathbb{Y}} &= Pk_1k_2\dot{I} + k_1(\gamma + k_2)\dot{C} \\
&= Pk_1k_2(k_1CE - k_2I - \gamma I) + k_1(\gamma + k_2)(Pk_2I - \mu C - k_1CE) \\
&= Pk_1^2k_2CE - (k_2(\mu + k_1E) + \gamma(\mu + k_1E))k_1C \\
&= k_1(k_2 + \gamma)(\mu + k_1E)\left(\frac{Pk_1k_2E}{(k_2+\gamma)(\mu + k_1E)} - 1\right)C \\
&\leq k_1(k_2 + \gamma)(\mu + k_1E^*)\left(\frac{Pk_1k_2E^*}{(k_2+\gamma)(\mu + k_1E^*)} - 1\right)C \quad (\text{since } E(t) \leq E^* \text{ in } \mathcal{D}) \\
&= k_1(k_2 + \gamma)(\mu + k_1E^*)(\mathcal{R}_{02} - 1)C \leq 0, \quad \text{when } \mathcal{R}_{02} \leq 1.
\end{aligned}$$

Since all the model parameters and variables are non-negative, it follows that $\dot{\mathbb{Y}} \leq 0$ for $\mathcal{R}_{02} \leq 1$, with equality if $\mathcal{R}_{02} = 1$ or $C = 0$. Moreover, for $\mathcal{R}_{02} < 1$, $\dot{\mathbb{Y}} = 0$ if and only if $C = 0$. Hence, $\mathbb{Y}$ is a Lyapunov function on $\hat{\mathcal{D}}$. Furthermore, $\hat{\mathcal{D}}$ is a compact and absorbing subset of $\mathbb{R}^4_+$, and the largest compact invariant set in $\{(C, E, I, I_P) \in \hat{\mathcal{D}} : \dot{\mathbb{Y}} = 0\}$, when $\mathcal{R}_{02} \leq 1$, is the singleton $\mathbb{F}_{02}$. Therefore, $\mathbb{F}_{02}$ is the only steady state when $\mathcal{R}_{02} \leq 1$. Thus, by LaSalle's invariance principle [65,94] (See Section A.1 for the principle), $C \to 0$, $I \to 0$, and $I_P \to 0$ as $t \to \infty$. Substituting $C = I = I_P = 0$ into the model equations (5.5)-(5.8) shows that $E \to E^*$ as $t \to \infty$. Hence, every solution of the basic *Chlamydia* model system (5.5)-(5.8), with initial conditions in $\hat{\mathcal{D}}$, approaches the CFE $\mathbb{F}_{02}$ as $t \to \infty$ (that is, the CFE $\mathbb{F}_{02}$ is GAS in $\hat{\mathcal{D}}$) whenever $\mathcal{R}_{02} < 1$ and unstable otherwise.

□

Existence of the *Chlamydia*-present equilibrium

We show that the basic *Chlamydia* persistence model system (5.5)-(5.8) has a unique *Chlamydia*-present equilibrium (CPE), that is the equilibrium for which *Chlamydia* persists within-host, if and only if $\mathcal{R}_{02} > 1$. In order to obtain the CPE, we set the right hand sides of the model equations (5.5)-(5.8) to zero, and solve for all its non-zero state variables. We also express the state variables in terms of the force of infection

$$\Lambda^{**} = k_1 C^{**}, \tag{5.21}$$

of model system (5.5)-(5.8). Thus, the right hand sides of the model system (5.5)-(5.8) at steady states gives

$$C^{**} = \frac{\Lambda^{**} P_E (P k_2 - k_2 - \gamma)}{\mu(\delta_E + \Lambda^{**})(k_2 + \gamma)}, \tag{5.22}$$

$$E^{**} = \frac{P_E}{\delta_E + \Lambda^{**}}, \tag{5.23}$$

$$I^{**} = \frac{\Lambda^{**} P_E}{(\delta_E + \Lambda^{**})(k_2 + \gamma)}, \tag{5.24}$$

$$I_P^{**} = \frac{\gamma I^{**}}{\delta_P}. \tag{5.25}$$

Thus, the CPE of the basic *Chlamydia* persistence model (5.5)-(5.8) is given by

$$\mathbb{F}_{12} = (C^{**}, E^{**}, I^{**}, I_P^{**}). \tag{5.26}$$

Substituting (5.22)-(5.25) into the expression for Λ^{**} in (5.21), and simplifying, we obtain a quadratic expression that the non-zero CPE $\mathbb{F}_{12}$ of model system (5.5)-(5.8) satisfies, that is

$$\Lambda^{**}(\mu(k_2+\gamma)\Lambda^{**} + \delta_E\mu(k_2+\gamma) - k_1P_E(Pk_2 - k_2 - \gamma)) = 0. \tag{5.27}$$

The solutions of Equation (5.27) are either

$$\Lambda^{**} = 0 \tag{5.28}$$

or

$$\Lambda^{**} = \frac{(k_2+\gamma)(\mu + k_1E^*)(\mathcal{R}_{02}-1)}{\mu/\delta_E(k_2+\gamma)}. \tag{5.29}$$

The trivial solution (5.28) implies the disease-free steady state which corresponds to the CFE described by (5.12). This is not our equilibrium of interest at this point. Thus, the unique and non-trivial solution (5.29) is valid.

From (5.29), it follows that if $\mathcal{R}_{02} < 1$, then $\Lambda^{**} < 1$, which is biologically meaningless. In addition, if $\mathcal{R}_{02} = 1$, then $\Lambda^{**} = 0$, which again corresponds to the CFE described by (5.12). Thus, the model system (5.5)-(5.8) has no positive CPE in these two cases. It can be clearly seen that the unique solution (5.29) of (5.27) is positive if and only if $\mathcal{R}_{02} > 1$, since all the model parameters are positive.

Hence, the four components C^{**}, E^{**}, I^{**}, and I_P^{**} of the CPE $\mathbb{F}_{12}$, can be explicitly determined by substituting (5.29) into (5.22)-(5.25), to obtain

$$C^{**} = \frac{P_E(k_2(P-1)-\gamma)}{\mu(k_2+\gamma)} - \frac{\delta_E}{k_1}, \tag{5.30}$$

$$E^{**} = \frac{\mu(k_2+\gamma)}{k_1(k_2(P-1)-\gamma)}, \tag{5.31}$$

$$I^{**} = \frac{P_E}{k_2+\gamma} - \frac{\mu\delta_E}{k_1(k_2(P-1)-\gamma)}, \tag{5.32}$$

$$I_P^{**} = \frac{\gamma}{\delta_P}\left(\frac{P_E}{k_2+\gamma} - \frac{\mu\delta_E}{k_1(k_2(P-1)-\gamma)}\right). \tag{5.33}$$

These results are summarised below.

Theorem 5.1.5. *The basic Chlamydia persistence model* (5.5)-(5.8) *has a unique CPE given by* $\mathbb{F}_{12}$*, whenever* $\mathcal{R}_{02} > 1$ *and no CPE otherwise.*

As Theorems 5.1.4 and 5.1.5 imply, it suffices to explore therapeutic strategies that can drive the disease outbreak threshold $\mathcal{R}_{02}$ below unity.

5.2 Existence of an optimal control pair

In this section, we show that the existence of an optimal control pair with finite objective functional is guaranteed for our model system (5.1)-(5.4). Using an established theorem in Fleming and Rishel [55], as re-stated in Theorem 4.2.1, we show that our system (5.1)-(5.4) and objective functional (5.11) meet the conditions of Theorem 4.2.1, thus establishing the existence of an optimal control pair for our model.

Theorem 5.2.1. *For the optimal control problem with state equations* (5.1)-(5.4)*, there exists an optimal control pair* $(u_1^*, u_2^*) \in \hat{\Gamma}$ *which minimises the objective functional* $J(u_1, u_2)$ *in equation* (5.11)*.*

Proof. To prove this theorem, we show that our optimal control model meets the five conditions given in Theorem 4.2.1, being sufficient conditions for the existence of an optimal control pair for our model.

1. To verify condition 1, we refer to Theorem 3.1 by Picard-Lindelöf [29,39]. Based on the theorem, if the solutions of the state equations (5.1)-(5.4) are a *priori* bounded and if the state equations are continuous and Lipschitz-continuous in the state variables, then there is a unique solution corresponding to every admissible control pair in $\hat{\Gamma}$. Since for all $(C, E, I, I_P) \in \hat{\mathcal{D}}$, the model states are bounded below and above (see Section 5.1.1), then, the solutions to the state equations are bounded. The boundedness of the partial derivatives with respect to the state variables in the state system can be shown directly. The right sides of the state equations (5.1)-(5.4) are also continuously differentiable functions of the dependent variables C, E, I, and I_P. These demonstrate the fact that the system is locally Lipschitz-continuous with respect to the state variable [28]. Thus, condition 1 is fulfilled.
2. The control set is closed and convex by definition. Hence, condition 2 is fulfilled.
3. The right side of the model system (5.1)-(5.4) is Lipschitz-continuous. Thus, it is obviously continuous and bounded. The state equations (5.1)-(5.4) are also bilinear in u_1 and u_2, hence condition 3 is satisfied.
4. The integrand $\hat{G} = C(t) + A_1 I(t) + A_2 I_P(t) + \dfrac{A_3}{2}u_1^2 + \dfrac{A_4}{2}u_2^2$, of the objective functional, has a positive semidefinite Hessian, hence it is convex on the admissible set $\hat{\Gamma}$. Thus condition 4 is satisfied.
5. Let $\eta = \min(A_2, A_3)$, and $\theta = \dfrac{1}{2}\eta$. Then,

$$\begin{aligned} G &= \frac{A_3}{2}u_1^2 + \frac{A_4}{2}u_2^2 + C + A_1 I + A_2 I_P \\ &\equiv \frac{1}{2}\left\{\eta(u_1^2 + u_2^2) + \sigma_1 u_1^2 + \sigma_2 u_2^2\right\} + (C + A_1 I + A_2 I_P) \\ &\geq \theta(u_1^2 + u_2^2) + (C + A_1 I + A_2 I_P) \\ &\geq \theta(u_1^2 + u_2^2) - c_2 \\ &= \theta(|u_1|^2 + |u_2|^2) - c_2, \end{aligned}$$

for any $c_2 > 0$, where $0 \leq \sigma_1 \leq A_3$ and $0 \leq \sigma_2 \leq A_4$. Note that $\eta, \theta \geq 0$. Hence the integrand satisfies the inequality (4.40), with $\beta = 2$.

This completes the proof. □

5.3 Characterisation of the optimal control pair

In this section, we derive the conditions of optimality for the control problem (5.1)-(5.11). We use Pontryagin's Maximum Principle [125], which provides the necessary conditions that an optimal control and corresponding state must satisfy, to convert the optimisation problem (5.1)-(5.11) into one of minimising a Hamiltonian $\hat{H}$, with respect to the control $(u_1(t), u_2(t))$ [100, pg 14].

Theorem 5.3.1. *Given optimal controls u_1^*, u_2^*, and solutions C^*, E^*, I^*, and I_P^* of the corresponding state system* (5.1)-(5.4)*, that minimise the objective functional* (5.11) *over $\hat{\Gamma}$, there exist adjoint variables λ_C, λ_E, λ_I, and λ_{I_P} satisfying:*

$$\dot{\lambda_C} = -1 + (\mu + k_1 E^*)\lambda_C + k_1 E^* \lambda_E - k_1 E^* \lambda_I, \tag{5.34}$$

$$\dot{\lambda_E} = k_1 C^* \lambda_C + (\delta_E + k_1 C^*)\lambda_E - k_1 C^* \lambda_I, \tag{5.35}$$

$$\dot{\lambda_I} = -A_1 - Pk_2\lambda_C + (\gamma + k_2 + \alpha u_2^*(t) + cu_1^*(t)u_2^*(t))\lambda_I - (\gamma(1 - cu_1^*(t)) + Q\alpha u_2^*(t))\lambda_{I_P} \tag{5.36}$$

$$\dot{\lambda_{I_P}} = -A_2 - \rho u_1^*(t)\lambda_I + \rho u_1^*(t)\lambda_{I_P} + \delta_P \lambda_{I_P}, \tag{5.37}$$

with transversality conditions

$$\lambda_C(t_f) = A_5,\ \lambda_{I_P}(t_f) = A_6, \quad \textit{and } \lambda_E(t_f) = \lambda_I(t_f) = 0. \tag{5.38}$$

Furthermore, the control functions can be shown to satisfy the following, called the control characterisations:

$$u_1^*(t) = \min\left\{\max\left(0, \frac{V^*}{A_3A_4 - M^2}\right), m_1\right\},$$

$$u_2^*(t) = \min\left\{\max\left(0, \frac{1}{A_4}\left(\frac{MV^*}{A_3A_4 - M^2} + T_4 - T_5\right)\right), m_2\right\},$$

where $V^* = -A_4T_1 + MT_4 - MT_5 + A_4T_2 + A_4T_3$, $M = cI^*\lambda_I$, $T_1 = \rho I_P^*\lambda_I$, $T_2 = c\gamma I^*\lambda_{I_P}$, $T_3 = \rho I_P^*\lambda_{I_P}$, $T_4 = \alpha I^*\lambda_I$, $T_5 = Q\alpha I^*\lambda_{I_P}$, *and* $A_3A_4 \neq M^2$.

Proof. We define the Hamiltonian $\hat{H}(C, E, I, I_P, u_1, u_2, \lambda_C, \lambda_E, \lambda_I, \lambda_{I_P})$ as

$$\begin{aligned}\hat{H} &= C(t) + A_1I(t) + A_2I_P(t) + \frac{A_3}{2}u_1^2 + \frac{A_4}{2}u_2^2 \\ &+ \lambda_C(Pk_2I(t) - \mu C(t) - k_1C(t)E(t)) \\ &+ \lambda_E(P_E - \delta_E E(t) - k_1C(t)E(t)) \\ &+ \lambda_I(k_1C(t)E(t) + \rho u_1(t)I_P(t) - \gamma I(t) - k_2I(t) - \alpha u_2(t)I(t) - cu_1(t)u_2(t)I(t)) \\ &+ \lambda_{I_P}(\gamma(1 - cu_1(t))I(t) + Q\alpha u_2(t)I(t) - \rho u_1(t)I_P(t) - \delta_P I_P(t)). \end{aligned} \tag{5.39}$$

Using Pontryagin's Maximum Principle [125],

$$\lambda_C^{'} = -\frac{\partial H}{\partial C},\ \lambda_E^{'} = -\frac{\partial H}{\partial E}, \lambda_I^{'} = -\frac{\partial H}{\partial I},\ \text{and}\ \lambda_{I_P}^{'} = -\frac{\partial H}{\partial I_P}. \tag{5.40}$$

Thus adjoint system (5.34)-(5.37), with transversality conditions (terminal conditions) expressed in the form provided in (5.38), was obtained from the Hamiltonian (5.39) and the relations in (5.40).

The Hamiltonian $\hat{H}$ is minimised with respect to the controls at the optimal control pair $u^* = (u_1^*, u_1^*)$. Thus we differentiate $\hat{H}$ with respect to u_1 and u_2 on the interior sets $\{t \,|\, 0 \leq u_1 \leq m_1\}$ and $\{t \,|\, 0 \leq u_2 \leq m_2\}$ respectively. Thus, the optimality equations are

$$\frac{\partial \hat{H}}{\partial u_1} = A_3u_1^* + \rho I_P^*\lambda_I - cu_2^*I^*\lambda_I - c\gamma I^*\lambda_{I_P} - \rho I_P^*\lambda_{I_P} = 0 \quad \text{at } u_1^*, \tag{5.41}$$

$$\frac{\partial \hat{H}}{\partial u_2} = A_4u_2^* - \alpha I^*\lambda_I - cu_1^*I^*\lambda_I + Q\alpha I^*\lambda_{I_P} = 0 \quad \text{at } u_2^*. \tag{5.42}$$

Solving for u_1^* and u_2^* on the interior sets, we obtain

$$u_1^* = \frac{V^*}{A_3A_4 - M^2}, \tag{5.43}$$

$$u_2^* = \frac{1}{A_4}\left(\frac{MV^*}{A_3A_4 - M^2} + T_4 - T_5\right), \tag{5.44}$$

where $V^* = -A_4T_1 + MT_4 - MT_5 + A_4T_2 + A_4T_3$, $M = cI^*\lambda_I$, $T_1 = \rho I_P^*\lambda_I$, $T_2 = c\gamma I^*\lambda_{I_P}$, $T_3 = \rho I_P^*\lambda_{I_P}$, $T_4 = \alpha I^*\lambda_I$, $T_5 = Q\alpha I^*\lambda_{I_P}$, and $A_3A_4 \neq M^2$.

By standard control arguments involving the bounds on the controls (see Sections 8.1 and 12.1 of [100]), we conclude that

$$u_1^* = \begin{cases} 0 & \text{if} \quad \dfrac{V^*}{A_3A_4 - M^2} \leq 0 \\ \dfrac{V^*}{A_3A_4 - M^2} & \text{if} \quad 0 < \dfrac{V^*}{A_3A_4 - M^2} < m_1 \\ m_1 & \text{if} \quad \dfrac{V^*}{A_3A_4 - M^2} \geq m_1 \end{cases}, \tag{5.45}$$

which in compact notation can be characterised as

$$u_1^*(t) = \min\left\{\max\left(0, \frac{V^*}{A_3A_4 - M^2}\right), m_1\right\}. \tag{5.46}$$

Similarly, we conclude that

$$u_2^* = \begin{cases} 0 & \text{if} \quad \dfrac{1}{A_4}\left(\dfrac{MV^*}{A_3A_4 - M^2} + T_4 - T_5\right) \leq 0, \\ \dfrac{1}{A_4}\left(\dfrac{MV^*}{A_3A_4 - M^2} + T_4 - T_5\right) & \text{if} \quad 0 < \dfrac{1}{A_4}\left(\dfrac{MV^*}{A_3A_4 - M^2} + T_4 - T_5\right) < m_2 \\ m_2 & \text{if} \quad \dfrac{1}{A_4}\left(\dfrac{MV^*}{A_3A_4 - M^2} + T_4 - T_5\right) \geq m_2 \end{cases} \tag{5.47}$$

which in compact notation can also be characterised as

$$u_2^*(t) = \min\left\{\max\left(0, \frac{1}{A_4}\left(\frac{MV^*}{A_3A_4 - M^2} + T_4 - T_5\right)\right), m_2\right\}. \tag{5.48}$$

This completes the proof. □

Remark 5.3.2. *The optimality system that characterises the optimal control pair* (u_1^*, u_2^*) *consists of the state system* (5.1)-(5.4) *with its associated initial conditions, the adjoint system* (5.34)-(5.37) *with its transversality conditions* (5.38)*, and the control characterisations* (5.45) *and* (5.47)*.*

Due to the a priori boundedness of the state and adjoint solutions, the right sides of the state and adjoint equations become Lipschitz in those solutions. The uniqueness of the solutions of the optimality system is guaranteed by this Lipschitz property, for a sufficiently small final time t_f*. This small time length restriction is due to the opposite time orientation of the state equations* (5.1)-(5.4)*, and the adjoint equations* (5.34)-(5.37)*; the state system has initial time conditions and the adjoint equations have final time conditions. Uniqueness of solutions of the optimality system implies the uniqueness of the optimal controls [100]. See Fisher et. al [54] for a uniqueness proof using Lipschitz properties.*

5.4 Numerical Results

In this section, we present numerical results of the model system (5.1)-(5.4) under different scenarios.

5.4.1 Disease dynamics with no treatment (control)

In this section, we present numerical results for the dynamics of the extracellular *Chlamydia*, healthy epithelial cells, infected epithelial cells, and persistently infected epithelial cells. We set the controls u_1 and u_2 to zero and solve the resulting system of ODEs. Figures 5.1a-5.1d show that in the absence of any therapeutic intervention, the infection may not be abated, even when the antimicrobial responses of the humoral and cell-mediated immunity are present. It is observed that each of the interacting species approached their endemic states. The parameter values and initial conditions used in all the simulations are given in Table 5.1.

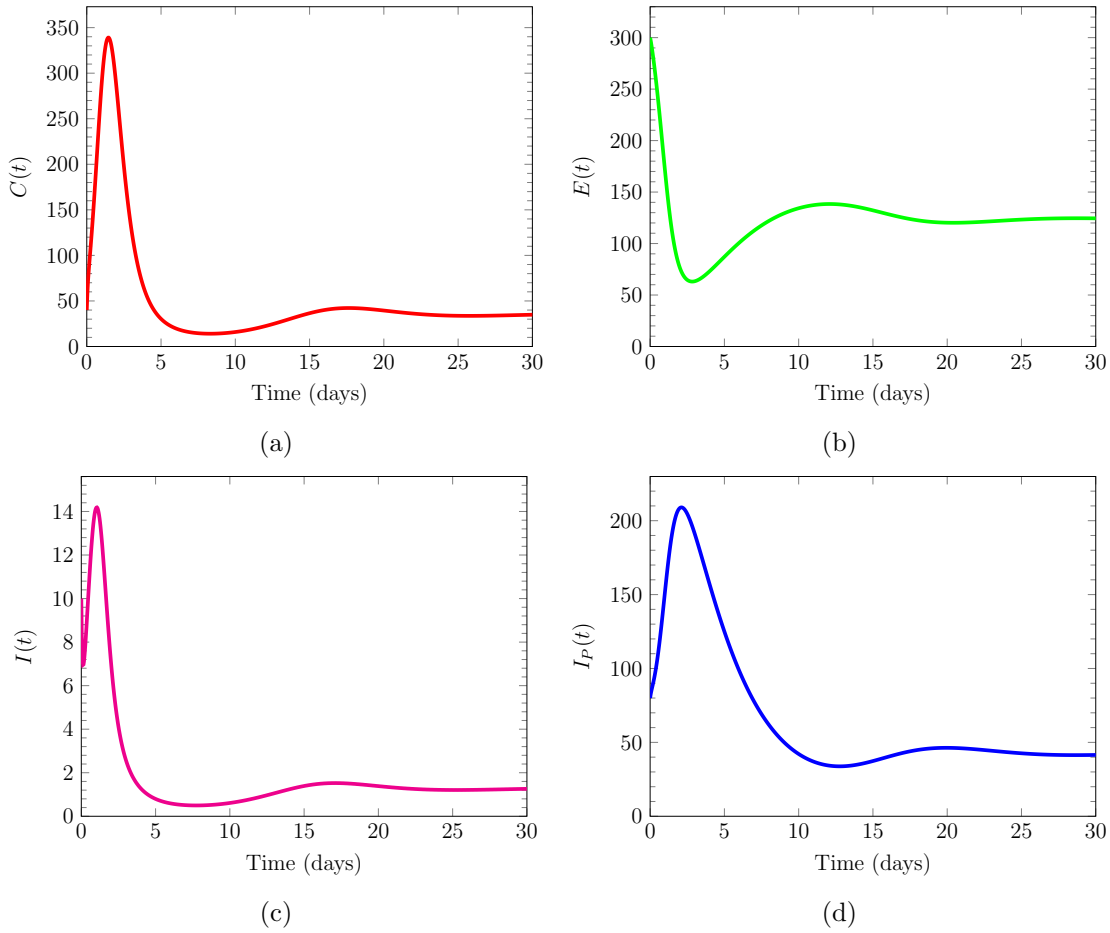

Figure 5.1: Numerical simulation of the tryptophan supplementation *Chlamydia* treatment model (5.1)-(5.4) showing the time course plot of (a) $C(t)$, concentration of *Chlamydia*, (b) $E(t)$, concentration of healthy epithelial cells, (c) $I(t)$, concentration of infected epithelial cells, and (d) $I_P(t)$, concentration of persistently infected epithelial cells, respectively, with no controls applied. Note that the final time values of each state variable, which are also their calculated steady states, rounded up to the next integer, are $C(t_f) = 36$, $E(t_f) = 124$, $I(t_f) = 2$, $I_P(t_f) = 43$, respectively.

5.4.2 Optimal Control

In this section, we numerically study and present the numerical solutions of the optimality system described in Remark 5.3.2, over $T_f = 5$ days. Our goal is to find the optimal treatment strategies, that is the most effective and efficient temporal drug usage at each time point, that ensures the clearance of a chronic *Chlamydia* infection, while minimizing the drugs levels and their systemic costs. We solve the optimal control problem (5.1)-(5.11) using MATLAB's in-built non-linear optimisation tool *fmincon* [114] as described in Section 4.4.2.

In order to obtain an optimal therapy during a chronic chlamydial infection, we assume that at the time of commencement of the treatment, the infected host has reached chronic steady state values $\overline{C} = 36$ cells/mm^3, $\overline{E} = 124$ cells/mm^3, $\overline{I} = 2$ cells/mm^3, and $\overline{I_P} = 43$ cells/mm^3, respectively. These steady state values were obtained by setting the right hand size of the model system (5.1)-(5.4) to zero in the absence of any treatment, that is

$u_1 \equiv u_2 \equiv 0$, and solving the resulting system of nonlinear equations using MATLAB's in-built solver *fsolve*.

We investigate and compare numerical results of three different optimal therapy scenarios: (i) when u_1, tryptophan supplement, is optimised while treatment u_2 is set to zero, (ii) when u_2, the drug that is bacteriostatic on *Chlamydia*, is optimised while treatment u_1 is set to zero, and (iii) when both treatments u_1 and u_2 are optimised. We only track the amount of bio-available treatment/drug the system is supplied with, with respect to time. In this study, we do not investigate the complete degradation of the drug/treatment to be administered, but rather the bio-availability and delivery of the treatment into the system.

We simulated the model for different combination of values of the weight parameters A_1, A_2, A_3, A_4, A_5, and A_6, which are the balancing cost factors due to scales (that is, they adjust the balance between the clearance of the infection and the systemic cost of the treatments) and the importance of the seven parts of the objective functional. In all the presented figures, we use the same set of weight factors, $A_1 = 70$, $A_2 = 20$, $A_3 = 90$, $A_4 = 20$, $A_5 = 1$, and $A_6 = 5$ to illustrate the effects of various optimal therapies on a chlamydial infection. The order of the parameters are mostly on the order of ten and A_4 on the order of a hundred. This is because the magnitude of the concentration of *Chlamydia* is much larger than the magnitude of the concentration of infected and persistently infected cells, and the magnitude of the concentrations of the treatments, in the objective functional in (5.11). Hence, we balance this difference in magnitudes by the orders of the weight parameters. As in the preceding chapter, we have only presented results for one parameter combination for brevity. This is because there was no significant effect (with regards to clinical outcomes) of the variation on the qualitative results of the optimal controls when the respective weight parameters were varied within the same order. However, in Section B.3 of the Appendix, we have investigated and discussed in details, the effects of different weight parameters combinations on the qualitative results of the optimal control problem (this include the time series of interacting species, the optimal controls, and the corresponding values of the objective functional). We also investigate the three different treatment scenarios discussed for different treatment duration (in number of days) by varying the final time of treatment. We observe that the optimal solution of the model system (with respect to clinical outcomes) is not sensitive with respect to the final time. This implies that similar optimal solutions are obtained even when the duration of treatment is increased. These results are also not shown for brevity. We only show results for five days of treatment. We have however discussed these results in details in Section B.4.

Control with tryptophan supplementation only ($u_2 \equiv 0$)

We consider monotherapy with u_1, the tryptophan supplement, alone. Numerical simulations are performed using MATLAB's fmincon as described in Section 4.4.2, for $A_4 \equiv 0$ when $u_2 \equiv 0$. Then, the optimal control problem is defined by

$$J(u_1) = \int_{t_0}^{t_f} G(t, x(t), u_1(t))\mathrm{d}t + \phi(x(t_f)), \tag{5.49}$$

subject to

$$\begin{cases} \dot{x} = f(t, x(t), u_1(t)), \quad t_0 \leq t \leq t_f, \\ x(t_0) = x_0, \end{cases} \tag{5.50}$$

where $x = (C, E, I, I_P)$, f is the right side of the model (state) system (5.1)-(5.4), $\phi(x(t_f)) = A_5 C(t_f) + A_6 I_P(t_f)$, and $G(t, x, u_1) = C(t) + A_1 I(t) + A_2 I_P(t) + \frac{A_3}{2} u_1^2$.

For this therapy, as explained in Section 5.1, μ_τ, the rate at which the tryptophan supplement (1-MT) facilitates the reduction in the amount of EBs produced on lysis of infected epithelial cells, is 1.5. As shown in Figure 5.2, the optimal control problem predicts that the chronic chlamydial infection is cleared by the fifth day after the therapy commenced. It can also be seen that in the presence of the tryptophan supplement, healthy epithelial cells recovered from their diminished state and proliferated normally. The optimal control function $u_1(t)$ in Figure 5.2e is continuous and decreases with respect to increasing time. Our simulations show that for the chronic infection to be cleared, the optimal control will be the maximum dosage of the tryptophan supplement for about four days, as shown in Figure 5.2e. We note that the value of the objective functional (5.11) for this simulation is 1440.5.

Control with bacteriostatic agents only ($u_1 \equiv 0$)

We again consider monotherapy, this time with the bacteriostatic agent represented by u_2 and with $u_1 \equiv 0$. Numerical simulations are performed using MATLAB's fmincon as described in Section 4.4.2, for $A_2 \equiv 0$ when $u_1 \equiv 0$. Then, the optimal control problem is defined by relations similar to (5.49) and (5.50), but with u_2 instead of u_1, and $G(t, x, u_1) = C(t) + A_1 I(t) + A_2 I_P(t) + \frac{A_4}{2} u_2^2$.

For this therapy, as explained in Section 5.1, $\mu_\tau = 0$. Thus, $\mu = \mu_m = 2$ (see Table 5.1). As shown in Figure 5.3, the optimal control problem predicts that the chronic chlamydial infection may not be cleared when only bacteriostatic agents are used for the treatment of a chronic chlamydial infection. It can be seen that at the end of the therapy, the persistently infected cells were not cleared. There were also a few EBs present at the end of the therapy. The optimal control function $u_2(t)$ for these results, as shown in Figure 5.3e is continuous and decreases with respect to time. Our simulations show that the optimal control model does not result in the clearance of the chronic infection even when $u_2 = 0.9$ (the maximum dosage) for about four days, as shown in Figure 5.3e. We note that the value of the objective functional (5.11) for this simulation is 3037.2.

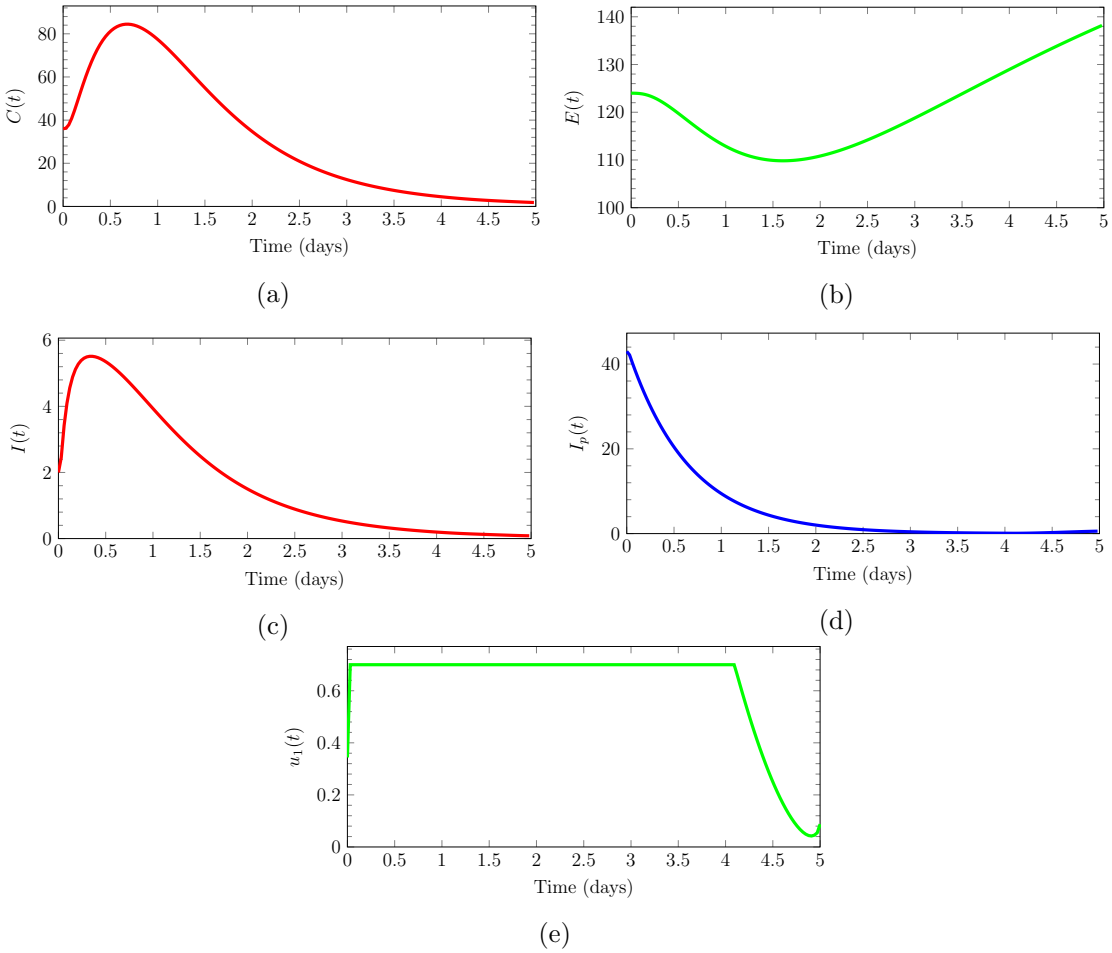

Figure 5.2: Time course of the tryptophan supplementation *Chlamydia* treatment model (5.1)-(5.4) showing the effect of using control u_1 (tryptophan Supplementation treatment) only on (a) $C(t)$, concentration of *Chlamydia*, (b) $E(t)$, concentration of healthy epithelial cells, and (c) $I(t)$, concentration of infected epithelial cells, and (d) $I_P(t)$, concentration of persistently infected epithelial cells, respectively. (e) Optimal evolution for control u_1. Note that the initial conditions for this treatment model are the steady state solutions of the no treatment model, that is $C(t_0) = 36$, $E(t_0) = 124$, $I(t_0) = 2$, $I_P(t_0) = 43$, respectively, while the final time values of the state variables are $0, 139, 0$, and 0, respectively.

Optimal combination treatment

With this treatment strategy, the tryptophan supplementation control u_2 and bacteriostatic control u_1 are both used to optimise the objective functional J as in (5.11).

For this therapy, as explained in Section 5.1, μ_τ, the rate at which the tryptophan supplement (1-MT) facilitates the reduction in the amount of EBs produced on lysis of infected epithelial cells, is also 1.5. The numerical results of the state variables for this combination therapy is very similar to that of the tryptophan-only supplement. As shown in Figure 5.4, the optimal control problem predicts that the chronic chlamydial infection is cleared by the fifth day after the therapy commenced. It can also be seen that in the presence of the two controls, healthy epithelial cells recovered from their diminished state and proliferated normally. The optimal control functions $u_1(t)$ and $u_2(t)$, as shown in Figures 5.4e and 5.4f, respectively, are continuous and decrease with respect to time. Our simulations show that for the chronic infection to be cleared, the optimal control $u_1(t)$

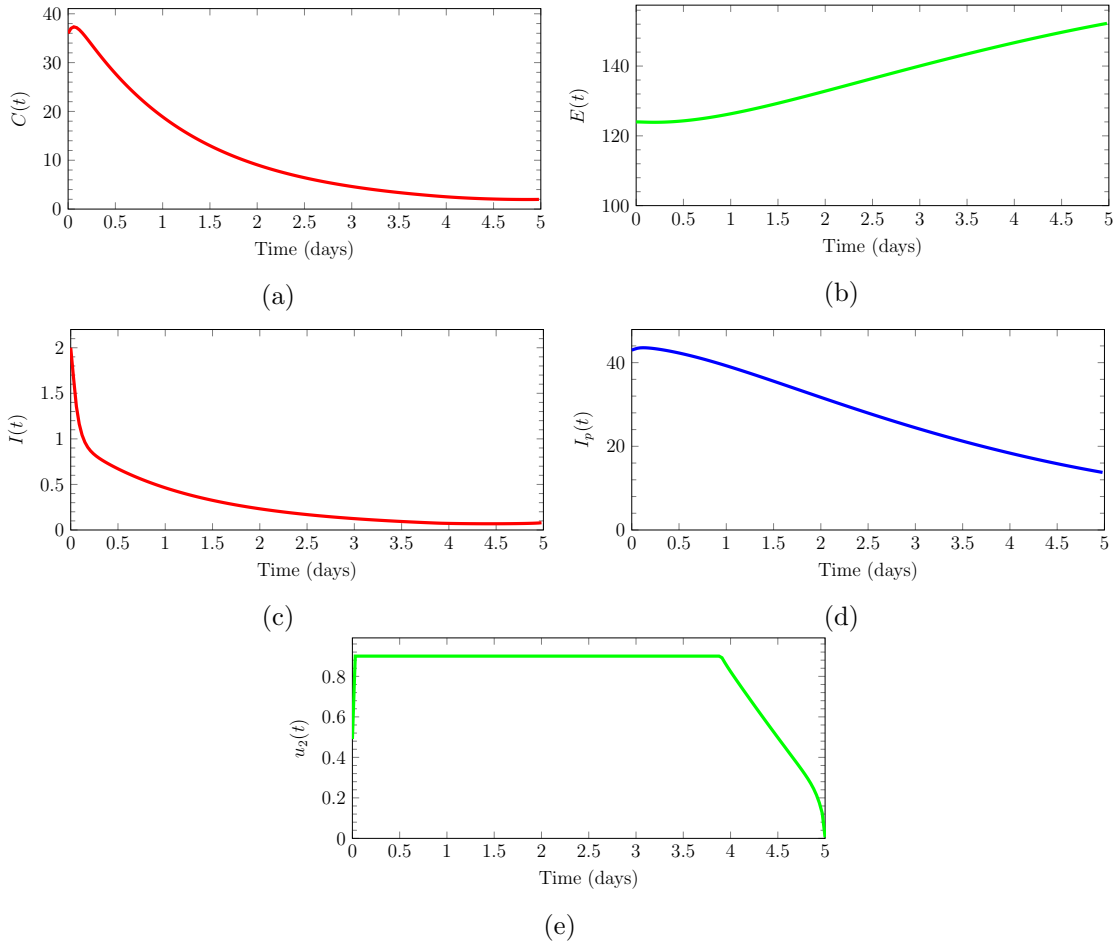

Figure 5.3: Time course of the tryptophan supplementation *Chlamydia* treatment model (5.1)-(5.4) showing the effect of using control u_2 (bacteriostatic agents) only on (a) $C(t)$, concentration of *Chlamydia*, (b) $E(t)$, concentration of healthy epithelial cells, and (c) $I(t)$, concentration of infected epithelial cells, and (d) $I_P(t)$, concentration of persistently infected epithelial cells, respectively. (e) Optimal evolution for control u_2. Note that the initial conditions for this treatment model are the steady state solutions of the no treatment model, that is $C(t_0) = 36$, $E(t_0) = 124$, $I(t_0) = 2$, $I_P(t_0) = 43$, respectively, while the final time values of the state variables are $2, 153, 0$, and 14, respectively.

will be the maximum dosage of the tryptophan supplement for about 4 days, while the optimal control $u_2(t)$ will be half the maximum dosage of the bacteriostatic agent at the initiation of the therapy, followed by a higher dosage after about 2.5 days.

5.5 Conclusion

In this chapter, we have used an optimal control theory paradigm to model the treatment of chronic chlamydial infection. Our approach couples a model of within-host interaction of *Chlamydia* and the immune system with an additional class for persistently infected epithelial cells. We have investigated the dynamics of the interacting species with and without two different therapeutic control strategies. We use methods of optimal control to derive and analyse the conditions for optimal treatment of the disease with a tryptophan supplement and bacteriostatic agents/drugs. Existence and uniqueness of the optimal

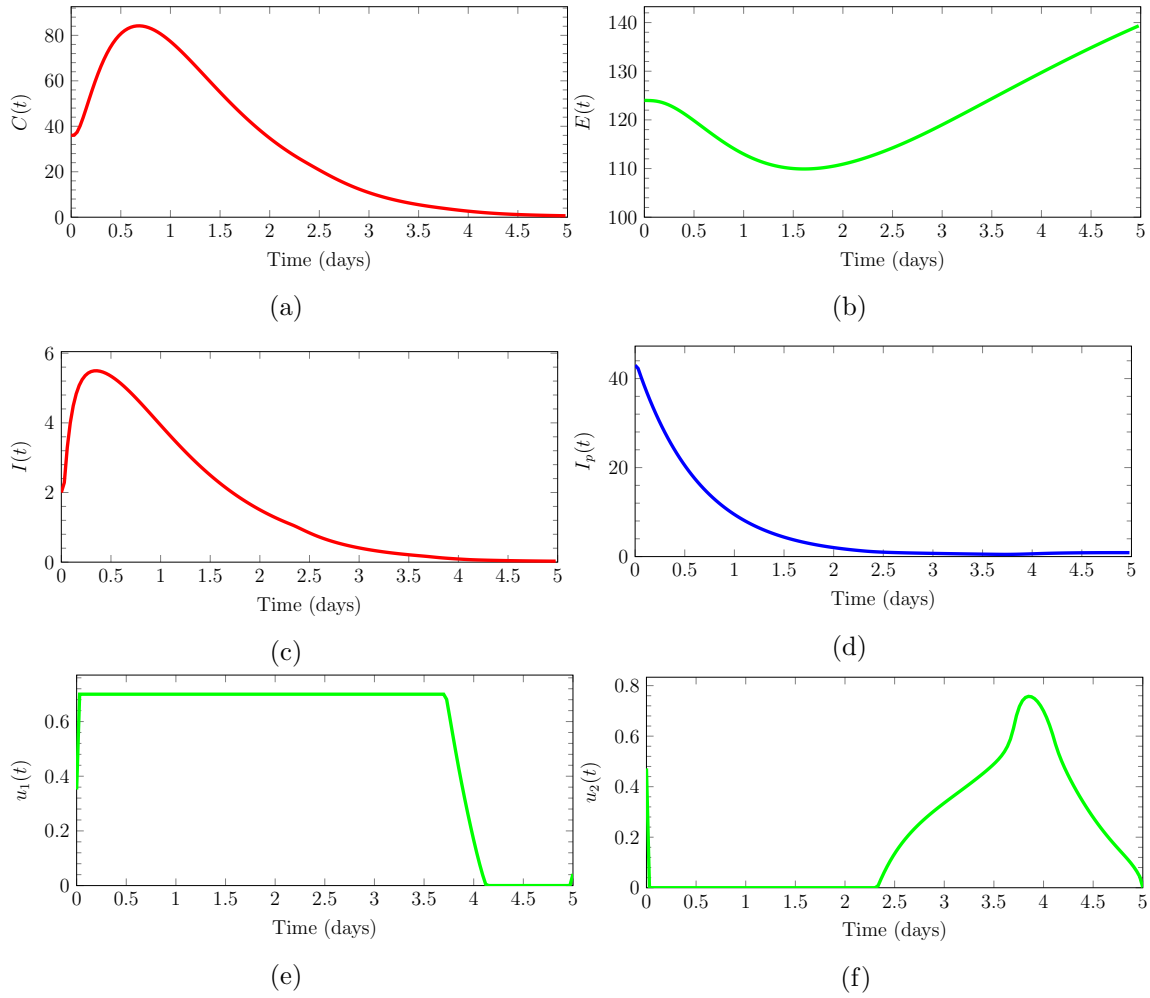

Figure 5.4: Time course of the tryptophan supplementation *Chlamydia* treatment model (5.1)-(5.4) showing the effect of using both controls u_1 (tryptophan Supplementation treatment) and u_2 (bacteriostatic agents) on (a) $C(t)$, concentration of *Chlamydia*, (b) $E(t)$, concentration of healthy epithelial cells, and (c) $I(t)$, concentration of infected epithelial cells, and (d) $I_P(t)$, concentration of persistently infected epithelial cells, respectively. (e) Optimal evolution for control u_1. (f) Optimal evolution for control u_2. Note that the initial conditions for this treatment model are the steady state solutions of the no treatment model, that is $C(t_0) = 36$, $E(t_0) = 124$, $I(t_0) = 2$, $I_P(t_0) = 43$, respectively, while the final time values of the state variables are $0, 144, 0$, and 0, respectively.

controls were proved. We also characterised the controls using Pontryagin's Maximum Principle (see Section A.3) and the resulting optimality system was numerically solved.

Our optimal control problem accounts for: (i) the blockage of IFN-γ-induced persistence by tryptophan supplementation; (ii) the reversal of established chlamydial persistence, either induced by IFN-γ or antibiotics, using tryptophan supplementation; (iii) the effects of the humoral and cell-mediated immune responses; (iv) the antimicrobial effects of an antibiotic therapy; (v) reduction of the production of EBs; and (vi) short duration of treatment with minimal dosage administration. We numerically explored the different impacts of the two optimal control strategies. Interestingly, monotherapy with tryptophan supplement alone suffices for the clearance of the chronic infection. We also investigated the three different treatment scenarios discussed for different treatment duration by varying the final time of treatment. We observed that the optimal solution of the model

system is not sensitive with respect to the final time. This implies that similar optimal solutions were obtained even when we increased the duration of treatment. These results are not shown.

The optimal control problem indicates the necessity of the high immunomodulatory effects of the tryptophan supplement 1-MT. The numerical results of the model suggest that single therapy with a tryptophan supplement, in the presence of a strong immune system, may be the optimal course of action in the clearance of a chronic *Chlamydia* infection, as it aids the clearance of the pathogen itself, limitation of side effects of drugs, and the survival of healthy epithelial cells.

We note that when both controls/treatments u_1 and u_2 were used, the objective functional value was 1433.6. When control/treatment u_1 alone was used, the objective functional value was 1440.5. Whereas, when control/treatment u_2 alone was used, the objective functional value was 3037.2. These are very relevant observations. The results imply that although the use of either both treatments (u_1 and u_2) or treatment u_1 alone clears the chronic chlamydial infection, the systemic cost of the treatments (toxicity) to the host is minimal when both treatments are used, as opposed to when only treatment u_1 is used. These numerical results also show that when treatment u_2 alone is used to treat a chronic chlamydial infection, the systemic cost (toxicity) of the treatment u_2 to the host is very high, despite the fact that the treatment does not result in the clearance of the chronic chlamydial infection.

The numerical results suggest that the optimal therapy is a dynamic one, in that the treatment is adjusted over the duration of the treatment, whereby one administers the maximum dosage for some days and then gradually lessen the treatment either in strength or concentration. We suggest that therapeutic interventions that adhere to these control strategies may be effective in treating chronic *Chlamydia* infections. We however note that even if the immune system is not at its best, the optimal course of action in the clearance of the infection may be a combination therapy with a bacteriostatic agent and tryptophan supplement, as the bacteriostatic agent may clear the actively replicating *Chlamydia* while tryptophan aids with the clearance of persistence.

Importantly, we acknowledge the likely adverse impact of tryptophan on the host immune system. When a tryptophan supplement is taken, indoleamine 2,3-dioxygenase (IDO) 1 is expressed. This leads to tryptophan depletion and the generation of bioactive catabolites known as kynurenines. This process can induce the suppression of the innate and adaptive immunity by some cells of the immune system, thereby promoting tolerogenic responses. The kynurenine pathway of tryptophan catabolism modifies immunological and neurological responses to inflammation. It promotes neurological comorbidities such as pain, depression, and fatigue [116]. These are undesirable health consequences. As such, the use of tryptophan supplements in the treatment of chronic chlamydial infection should be used with caution and subjected to thorough clinical tests.

The optimal treatment strategies suggested by our model require that strong doses of the two drugs - bacteriostatic agents and tryptophan supplements - be administered and maintained within a therapeutic band for days. This could mean that patients have to take multiple-doses of the treatment regimen. This may not be achievable because of the issue of patients' compliance to the drug regimen [150]. However, as suggested in Section 6.3, designs of drug delivery systems, that can ensure a controlled release/delivery of drugs over a particular period of time, while also maintaining the drugs' concentration within a therapeutic band, can make such treatment regimens a reality.

Some limitations in this study include the following: (1) model parameters that describe biological processes may have been over-estimated. In particular, the effects of the cell-mediated immune response may have been over-emphasised, thereby resulting in an improved clearance of a chlamydial infection as compared to what happens *in vivo*; (2) Optimal control solutions are subject to change when weight parameters are varied. For example, while we observed that when systemic cost of using the tryptophan supplement, A_2, was significantly increased, the maximum dosage of the supplement was required throughout the duration of the treatment. Despite this, the chronic infection was not effectively cleared as a few infectious progenies and infected epithelial cells were produced at the end of the therapy. Healthy epithelial cells also did not recover efficiently (results not shown).

The presented model has been kept fairly generic and further studies are required in order for a more accurate model of the interaction between *Chlamydia*, host epithelial cells, and the immune response, to be incorporated. There can be significant uncertainty in the determination of (biological) parameter values. Furthermore, in the case of a disease such as chronic genital *Chlamydia*, it is not unreasonable to anticipate that the values of some (biological) parameters are patient specific. Thus, the presented model could be usefully extended by the carrying out of uncertainty and sensitivity analyses. In addition, direct pharmacology for monotherapy and combination therapy of treatments need to be investigated further. The presented model and subsequent analysis provides a framework for the design of new and improved treatment strategies for chronic chlamydial infection.

6 Mathematical Modelling of the Role of a Mucosal Vaccine on the Within-host Dynamics of *Chlamydia trachomatis*

In the preceeding chapters, the chlamydial developmental cycle, and the antibiotic treatment of chlamydial infections have been modelled. However, none of these models took into account the fact that antimicrobial treatments reduce natural immunity to chlamydial infection and this facilitates the transmission of infection in the population [18, 104, 110, 130, 159]. After a naturally-occurring *Chlamydia* infection, protective immunity is developed by an infected individual [105, 135]. However, this immunity is not perfect, since it only offers partial protection against reinfection [82, 104, 105, 110], and it also often leads to severe immunopathology [104].

In addition, *Chlamydia* antibiotic treatment failures also exist as discussed in Subsection 2.2.1. More treatment failures have been recorded in practice than originally thought, with failure rates ranging from 8% to 23% [74, 76, 77, 92, 104, 138, 179]. For these reasons, and because of the morbidity and high health costs associated with chlamydial infection, the development of a prophylactic *Chlamydia* vaccine has become crucial, and is considered to be the only feasible solution to the effective population level control of chlamydial infections (and its associated complications) [17, 18, 48, 81, 104, 110, 176].

Although some within-host models for assessing the impact of a vaccine have been developed and used in the literature (such as the in-host malaria model developed by Niger and Gumel [120]), no such model has been designed for a potential *C. trachomatis* vaccine. This study extends prior *Chlamydia* within-host modelling studies by theoretically assessing the potential role of an effective anti-*Chlamydia* vaccine on the within-host dynamics of *C. trachomatis*. In this chapter, we present a mathematical model of the within-host dynamics of *C. trachomatis* infection in the presence of a mucosal vaccine. The purpose of the study in this chapter is to investigate the impact of a potentially effective mucosal *Chlamydia* vaccine on the within-host dynamics and prognosis of genital chlamydial infection. The model uses a prototype vaccine that induces similar protective immunity like that described by the study of Stary *et al.* [149], which has been discussed in Section 2.4.

6.1 Model Formulation

The model to be developed is that of the dynamics of *C. trachomatis* within the body of an infected host subject to a mucosal anti-*Chlamydia* vaccine. The model, which builds on the model presented by Sharomi and Gumel [142], is designed as follows. Let $H_e(t)$ represent the concentration of healthy epithelial cells, $H_h(t)$, the concentration of healthy epithelial cells protected by the humoral immune response against EB attachment, and $I(t)$, the concentration of infected epithelial cells. Furthermore, let $T_r(t)$ and $T_c(t)$ represent the concentrations of *Chlamydia*-specific mucosal resident memory T cells (T_{RM}) and *Chlamydia*-specific circulating memory T cells (T_{CM}), respectively. Let $F(t)$ be the concentration of IFN-γ molecules secreted by T cells, $E_b(t)$ be the concentration of chlamydial elementary bodies, and $R_b(t)$ be the concentration of reticulate bodies. See Table 6.1 for a concise description of the state variables used in this chapter.

The model for the in-host dynamics of *C. trachomatis*, subject to a mucosal anti-*Chlamydia* vaccine, is given by the following deterministic, non-linear system of differential equations:

$$\frac{\mathrm{dH}_e}{\mathrm{dt}} = \Pi_h + \omega H_h - \gamma(1-\varepsilon_v)H_e E_b - \phi\varepsilon_h H_e - \mu_h H_e, \tag{6.1}$$

$$\frac{\mathrm{d}H_h}{\mathrm{dt}} = \phi\varepsilon_h H_e - \omega H_h - \mu_h H_h, \tag{6.2}$$

$$\frac{\mathrm{d}I}{\mathrm{dt}} = \gamma(1-\varepsilon_v)H_e E_b - \kappa I - \rho I F, \tag{6.3}$$

$$\frac{\mathrm{d}T_r}{\mathrm{dt}} = \varepsilon_r \Lambda_v + \tau_1 F T_r - \mu_t T_r, \tag{6.4}$$

$$\frac{\mathrm{d}T_c}{\mathrm{dt}} = \varepsilon_c \Omega_v + \tau_2 F T_c - \mu_c T_c, \tag{6.5}$$

$$\frac{\mathrm{d}F}{\mathrm{dt}} = \psi_1 T_r E_b + \psi_2 T_c E_b - \rho I F, \tag{6.6}$$

$$\frac{\mathrm{d}E_b}{\mathrm{dt}} = N_E \kappa I - \gamma(1-\varepsilon_v)H_e E_b - \varepsilon_a \alpha E_b - \mu_e E_b, \tag{6.7}$$

$$\frac{\mathrm{d}R_b}{\mathrm{dt}} = N_{R1}\kappa I + N_{R2}\rho I F - \mu_r R_b. \tag{6.8}$$

Healthy epithelial cells are replenished by non-differentiated stem cell precursors [147], at a rate Π_h, and are naturally protected against EB attachment by the humoral immune response at a rate ϕ [142, 168], with efficacy $0 < \varepsilon_h \leq 1$ (where $\varepsilon_h = 0$ means a totally ineffective humoral immune response, and $\varepsilon_h = 1$ represents a perfect humoral immune response). This immunity is assumed to wane at a rate ω. EBs infect unprotected healthy epithelial cells at a rate γ. The presence of a *Chlamydia* vaccine is expected to boost the body's defense mechanism (*via* antibody blocking) against *Chlamydia* infection. Thus, it is assumed that the number of newly-infected epithelial cells depends largely on the efficacy of the vaccine (with a 100% vaccine efficacy implying that new epithelial cell infections are prevented). The efficacy of the vaccine is represented by $0 < \varepsilon_v \leq 1$ (where $\varepsilon_v = 0$ means a totally ineffective vaccine, and $\varepsilon_v = 1$ represents a perfectly

efficacious vaccine). The natural mortality rate of epithelial cells is μ_h. We assume that the *Chlamydia* vaccine works by reducing the probability of host infection by an (infectious) EB form of *Chlamydia*.

C. trachomatis infection triggers the rapid release of cytokines (IFN-γ in particular) by the tissue-T_{RM} and T_{CM} [105, 110, 112, 113, 149]. Thus, it is plausible to assume that the rate of production of IFN-γ is proportional to the number of EB forms and the concentration of T_{RM} and T_{CM}. The production rates of IFN-γ by T_{RM} and T_{CM} are ψ_1 and ψ_2, respectively. In an uninfected host, the genital tract mucosa contains relatively few lymphocytes. Thus, the recruitment of circulating lymphocytes is a very important component of the immune response [110]. The concentration of *Chlamydia*-specific T_{CM} has been observed to be significantly higher than that of *Chlamydia*-specific (tissue) T_{RM} [149]. Thus, it is assumed that the rate of production of T_{CM} (Ω_v) is greater than the rate of production of T_{RM} (Λ_v). That is, $\Omega_v > \Lambda_v$. Furthermore, it is assumed that there are are vaccine-induced increases in the production of *Chlamydia*-specific T_{RM} and T_{CM}, which are accounted for by the modification parameters $\varepsilon_r > 1$ and $\varepsilon_c > 1$, respectively. The tissue-T_{RM} confers substantial protection against *Chlamydia* infection even when the influx of T_{CM} is impeded [149]. Thus, it is assumed that $\varepsilon_r > \varepsilon_c$. Cytokines, such as IFN-γ, account for the enhancement of cellular proliferation [112,147]. Thus, there is an IFN-γ-induced proliferation of T cells - T_{RM} (T_r) and T_{CM} (T_c), represented by the rates τ_1 and τ_2, respectively. The natural mortality rates of T_{RM} and T_{CM} are μ_t and μ_c, respectively. We assume that they are equal, thus, $\mu_t = \mu_c$.

Infected epithelial cells lyse (after maturation of their intracellular inclusions) at a rate κ, and are lysed/destroyed prematurely (that is, before the CDC is completed) by IFN-γ at a rate ρ. While antibodies are involved in the signalling of macrophages for the engulfment of bound pathogen [169], IFN-γ activation of macrophages empowers them more to destroy phagocytosed EBs [96, 110]. Thus, it is assumed that there is a vaccine-induced increase in the rate at which antibodies destroy phagocytosed EBs. This is accounted for by the modification parameter $1 \leq \varepsilon_a \leq 2$. The rate at which macrophages engulf free extracellular EB forms is α. The natural mortality rates of EBs and RBs are μ_e and μ_r, respectively. Since within-cell chlamydial replication is inhibited at the RB stage in the presence of IFN-γ [96,135], it is assumed that there will be an IFN-γ-induced increase in the number of RBs that will be released on infected epithelial cell lysis [96]. It is expected that the presence of IFN-γ will lead to a marked decrease in the amount of EB forms that will be released from IFN-γ-induced cell lysis [96]. Furthermore, it is assumed that infected cells in the advanced stage of the CDC mainly contain EBs [168]. Hence, the number of EBs released when infected cells lyse (N_E) is greater than both the number of RBs released when "mature" infected cells lyse (N_{R1}) and the number of RBs released when infected cells lyse due to the inhibitory action of IFN-γ on the CDC (N_{R2}). That is, $N_E > N_{R1}$ and $N_E > N_{R2}$. However, if the inhibitory effect of IFN-γ on the CDC is very potent (which is one of the goals of a potentially effective anti-*Chlamydia* vaccine), it can be expected that $N_{R2} > N_E$ and $N_{R2} > N_{R1}$.

State Variables	**Description:** Concentration (cells/mm^3) of
$H_e(t)$	Healthy epithelial cells
$H_h(t)$	Epithelial cells protected by humoral immune response
$I(t)$	Infected epithelial cells
$T_r(t)$	Resident memory T-cells (T_{RM})
$T_c(t)$	Circulating memory T-cells
$F(t)$	IFN-γ molecules produced by the cell-mediated immune response
$E_b(t)$	Chlamydial elementary bodies
$R_b(t)$	Chlamydial reticulate bodies

Table 6.1: Description of state variables of the model system (6.1)-(6.8).

The new within-host model system (6.1)-(6.8) is an extension of the within-host *Chlamydia* models by Sharomi and Gumel [142] discussed in Section 2.5.3. In particular, in addition to the incorporation of the effects of a potentially efficacious mucosal *Chlamydia* vaccine, the model system (6.1)-(6.8) extends the model in [142] by, *inter alia*,

(i) adding a new compartment for the dynamics of *Chlamydia*-specific resident memory T cells (T_r);
(ii) adding a new compartment for the dynamics of *Chlamydia*-specific circulating memory T cells (T_c);
(iii) allowing for the proliferation of resident memory T cells (at a rate τ_1), and circulating memory T cells (at a rate τ_2);
(iv) allowing for a vaccine-induced (additional) protective immunity against infection of healthy epithelial cells by *Chlamydia* via antibody blocking (binding of mucosal and circulating antibodies to EBs, thereby neutralising the antigen of some EBs and blocking their ability to enter the mucosa [105,112,135]), modelled by the term $\gamma(1-\varepsilon_v)H_eE_b$;
(v) adding a compartment for the inhibitory action of IFN-γ (F).

We note that the notations used in this model are similar to those used in shaetgum10. For easy correlation between the previously developed model(s), in Table 6.2, we present the state variables and parameters that are common to the models built in Chapters 5 and 6.

Variables	**Chapter 5**	**Chapter 6**
Free extracellular *Chlamydia*	C	E_b
Healthy mucosal epithelial cells	E	H_e
Infected epithelial cells	I	I
Parameters		
Rate of production of healthy epithelial cells	P_E	Π_h
Rate of infection of epithelial cells by EB forms	k_1	γ
Number of Chlamydia (EB) released on cell lysis	P	N_E
Macrophage engulfment rate of extracellular EB forms	μ	α
Rate of lysis of infected cells	k_2	κ
Rate at which IFN-γ clear infected cells	γ	ρ
Natural mortality rate of healthy epithelial cells	δ_E	μ_h

Table 6.2: State variables and parameters that are common to the models built in Chapters 5 and 6

A schematic representation of the above dynamics is presented in Figure 6.1. The description of the state variables and parameters of the model are shown in Tables 6.1 and 6.3 respectively. In the section to follow, we give the basic properties of model system (6.1)-(6.8).

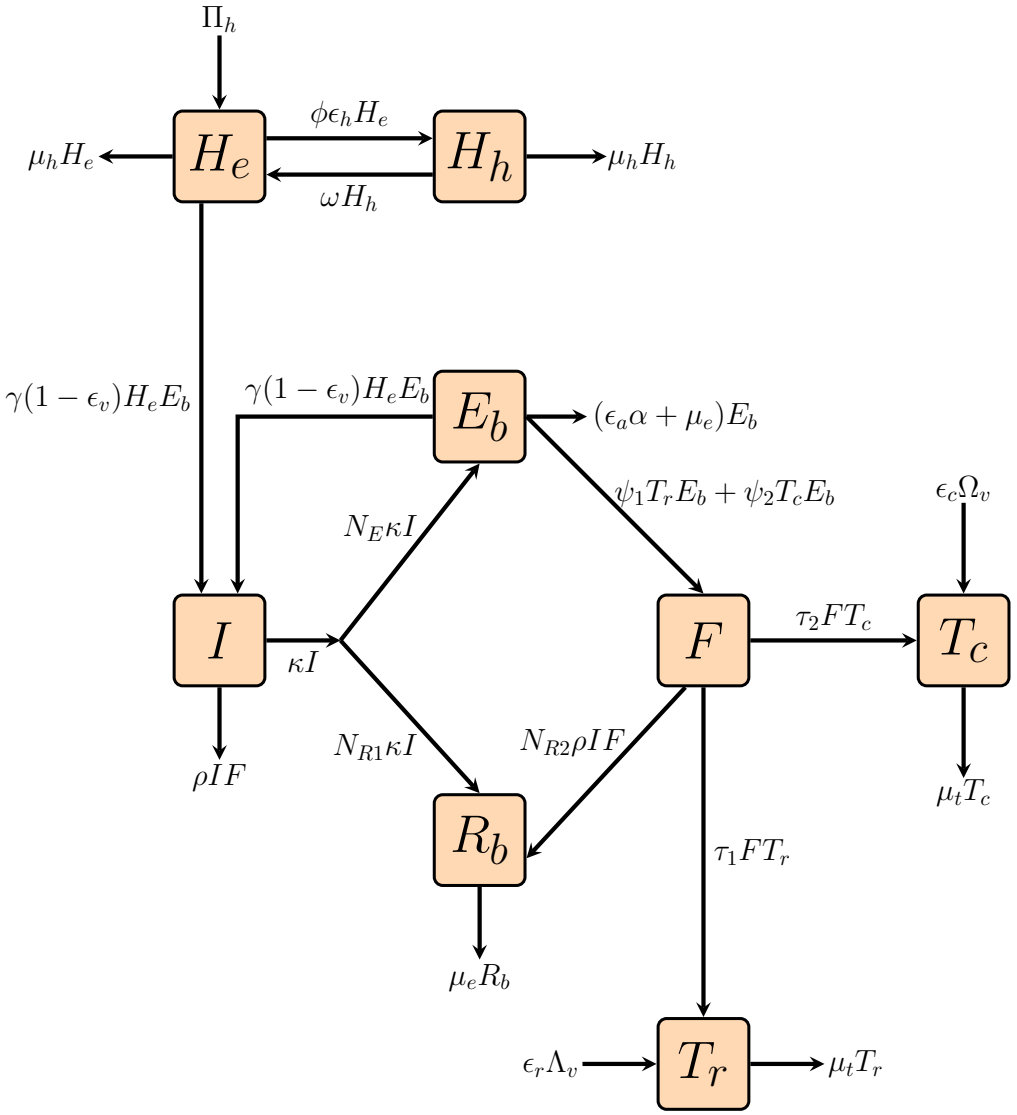

Figure 6.1: A schematic representation of model system (6.1)-(6.8).

Parameters	Description
Π_h	Rate of replenishment of healthy epithelial cells
γ	Effective contact rate between healthy epithelial cells and EB forms
ϕ	Rate of protection of healthy epithelial cells by the humoral immune response
ω	Waning rate of the protection of healthy epithelial cells by humoral immune response
Λ_v	Production rate of resident memory T cells
Ω_v	Production rate of circulating memory T cells
κ	Rate at which infected cells lyse/burst
ρ	Rate at which IFN-γ lyse/destroy infected cells
α	Rate of macrophage engulfment of free extracellular EB forms
ε_v	Efficacy of vaccine
ε_h	Efficacy of the humoral response in protecting healthy epithelial cells
ε_r	Modification parameter accounting for vaccine-induced increase in the production of *Chlamydia*-specific T_{RM}
ε_c	Modification parameter accounting for vaccine-induced increase in the production of *Chlamydia*-specific T_{CM}
ε_a	Modification parameter accounting for vaccine-induced increase in the EB-engulfment rate of antibodies
τ_1	IFN-γ-induced proliferation rate of resident memory T cells
τ_2	IFN-γ-induced proliferation rate of circulating memory T cells
ψ_1	Vaccine-induced increase in production rate of IFN-γ by resident memory T cells
ψ_2	Vaccine-induced increase in production rate of IFN-γ by circulating memory T cells
μ_h	Natural mortality rate of host epithelial cells
μ_t	Natural mortality rate of resident memory T-cells
μ_c	Natural mortality rate of circulating memory T-cells
μ_e	Natural mortality rate of EB forms
μ_r	Natural mortality rate of RB forms
N_E	Number of EBs released on lysis of infected cells
N_{R1}	Number of RBs released on lysis of infected cells
N_{R2}	Number of RBs released on lysis of infected cells due to IFN-γ's inhibitory action on the CDC

Table 6.3: Description of the parameters of the model system (6.1)-(6.8). T_{RM} (or T_{CM}) means resident (or circulating) memory cells.

6.1.1 Basic Properties

Positivity of solutions.

It is crucial to prove that all the state variables of the model system (6.1)-(6.8) subjected to positive initial conditions remain non-negative for all time $t > 0$. This is to certify that the model system is epidemiologically meaningful.

Lemma 6.1.1. *Given that the initial values of the state variables of the model system* (6.1)-(6.8) *are non-negative, the model does not predict negative values for the state variables at any future time.*

Proof. Let $H_e(0) > 0$, $H_h(0) \geq 0$, $I(0) \geq 0$, $T_r(0) \geq 0$, $T_c(0) \geq 0$, $F(0) \geq 0$, $E_b(0) \geq 0$, and $R_b(0) \geq 0$ be non-negative initial conditions. Denote by $[0, t_{\max}]$, the maximum interval of existence of the corresponding solution. In order to prove that the solution is positive in $[0, +\infty]$, it suffices to show that it is positive in $[0, t_{\max}]$.

Also let $\hat{t} = \sup\{0 < t < t_{\max} : H_e(t) > 0, H_h(t) > 0, I(t) > 0, T_r(t) > 0, T_c(t) > 0, F(t) > 0, E_b(t) > 0, R_b(t) > 0\} \in [0, t]$.

$\hat{t} > 0$ since $H_e(0)$, $H_h(0)$, $I(0)$, $T_r(0)$, $T_c(0)$, $F(0)$, $E_b(0)$, and $R_b(0)$ are non-negative. Suppose $\hat{t} < t_{\max}$.

From Equation (6.1), we have

$$\begin{aligned}
&\frac{\mathrm{d}}{\mathrm{d}t}\left(H_e(t)\exp\left\{(\phi\varepsilon_h+\mu_h)t+\int_0^t(\gamma(1-\varepsilon_v)E_b(\theta)-\tau_1F(\theta))\mathrm{d}\theta\right\}\right)\\
&=(\Pi_h+\omega H_h)\exp\left\{(\phi\varepsilon_h+\mu_h)t+\int_0^t(\gamma(1-\varepsilon_v)E_b(\theta)-\tau_1F(\theta))\mathrm{d}\theta\right\}.
\end{aligned}$$

This implies that

$$\begin{aligned}
&H_e(\hat{t})\exp\left\{(\phi\varepsilon_h+\mu_h)\hat{t}+\int_0^{\hat{t}}(\gamma(1-\varepsilon_v)E_b(\theta)-\tau_1F(\theta))\mathrm{d}\theta\right\}-H_e(0)\\
&=\int_0^{\hat{t}}(\Pi_h+\omega H_h)\exp\left\{(\phi\varepsilon_h+\mu_h)\eta+\int_0^{\eta}(\gamma(1-\varepsilon_v)E_b(\theta)-\tau_1F(\theta))\mathrm{d}\theta\right\}\mathrm{d}\eta.
\end{aligned}$$

Thus,

$$\begin{aligned}
H_e(\hat{t}) &= H_e(0)\exp\left\{-\left((\phi\varepsilon_h+\mu_h)\hat{t}+\int_0^{\hat{t}}(\gamma(1-\varepsilon_v)E_b(\theta)-\tau_1F(\theta))\mathrm{d}\theta\right)\right\}\\
&\quad+\exp\left\{-\left((\phi\varepsilon_h+\mu_h)\hat{t}+\int_0^{\hat{t}}(\gamma(1-\varepsilon_v)E_b(\theta)-\tau_1F(\theta))\mathrm{d}\theta\right)\right\}\\
&\quad\times\int_0^{\hat{t}}(\Pi_h+\omega H_h)\exp\left\{(\phi\varepsilon_h+\mu_h)\eta+\int_0^{\eta}(\gamma(1-\varepsilon_v)E_b(\theta)-\tau_1F(\theta))\mathrm{d}\theta\right\}\mathrm{d}\eta\\
&\quad>0.
\end{aligned}$$

It can be shown by a similar argument that $H_h(\hat{t}) > 0$, $I(\hat{t}) > 0$, $T_r(\hat{t}) > 0$, $T_c(\hat{t}) > 0$, $F(\hat{t}) > 0$, $E_b(\hat{t}) > 0$, and $R_b(\hat{t}) > 0$.

This contradicts the fact that $\hat{t}$ is the supremum because at least one of the state variables should be equal to zero at $\hat{t}$. Therefore $\hat{t} = t_{\max}$. Hence $H_e(t) \geq 0$, $\forall\, t > 0$. Similarly, it can be shown that $H_h(t) \geq 0$, $I(t) \geq 0$, $T_r(t) \geq 0$, $T_c(t) \geq 0$, $F(t) \geq 0$, $E_b(t) \geq 0$, and $R_b(t) \geq 0$ for any time $t > 0$. Hence, every solution of the model system (6.1)-(6.8) will always be positive for all non-negative initial conditions. This completes the proof. □

Invariant regions.

The model system (6.1)-(6.8) is analysed in an apposite biologically feasible region $\mathcal{D}_2$. The model system (6.1)-(6.8) is shown to be dissipative, that is, solutions of the model are uniformly bounded in a subset $\mathcal{D}_2$ of $\mathbb{R}^8_+$. Let $P(t) = H_e(t) + H_h(t)$. Since all the parameters and state variables of model system (6.1)-(6.8) are non-negative for all time $t \geq 0$, then from Equation (6.1),

$$\frac{\mathrm{d}P(t)}{\mathrm{d}t} \leq \Pi_h - \mu_h P(t).$$

Using a standard comparison theorem by Lakshmikantham *et al.* [95], it can be shown that

$$P(t) \leq P(0)e^{-\mu_h t} + \frac{\Pi_h}{\mu_h}(1 - e^{-\mu_h t}).$$

Whenever $P(0) \leq \Pi_h/\mu_h$, solutions of model system (6.1)-(6.8) are increasing monotonically and are bounded above by Π_h/μ_h. Conversely, whenever $P(0) > \Pi_h/\mu_h$, solutions of model system (6.1)-(6.8) are monotone decreasing and bounded below by Π_h/μ_h. In both cases, at limiting equilibrium, $\lim_{t\to\infty} P(t) = \Pi_h/\mu_h$.

From Equation (6.4),

$$\frac{\mathrm{d}T_r}{\mathrm{d}t} \leq \varepsilon_r \Lambda_v + \tau_1 F T_r,$$

that is,

$$\frac{\mathrm{d}T_r}{\mathrm{d}t} - \tau_1 F T_r \leq \varepsilon_r \Lambda_v.$$

Thus,

$$T_r(t) \leq \left(T_r(0) + \int_0^t \varepsilon_r \Lambda_v \exp\left\{-\tau_1 \int_0^\eta F(\theta)\mathrm{d}\theta\right\}\mathrm{d}\eta\right) \exp\left\{\tau_1 \int_0^t F(\theta)\mathrm{d}\theta\right\}.$$

Since the integrands of the above relation are continuous functions on the compact set $[0,t]$, then by the boundedness theorem, they are bounded on the set. The integrands are thus Riemann integrable on $[0,t]$ and the integrals are finite. This implies that

$$T_r(t) \leq (T_r(0) + c_1)c_2 = m_1,$$

where $c_1 = \int_0^t \varepsilon_r \Lambda_v \exp\left\{-\tau_1 \int_0^\eta F(\theta)\mathrm{d}\theta\right\}\mathrm{d}\eta$ and $c_2 = \exp\left\{\tau_1 \int_0^t F(\theta)\mathrm{d}\theta\right\}$.

Similarly, from Equation (6.5),

$$T_c(t) \leq \left(T_c(0) + \int_0^t \varepsilon_c \Omega_v \exp\left\{-\tau_2 \int_0^\eta E_b(\theta)\mathrm{d}\theta\right\}\mathrm{d}\eta\right)\exp\left\{\tau_2 \int_0^t E_b(\theta)\mathrm{d}\theta\right\}.$$

Thus, $T_c(t) \leq (T_c(0) + c_3)c_4 = m_2$, where $c_3 = \int_0^t \varepsilon_c \Omega_v \exp\left\{-\tau_2 \int_0^\eta E_b(\theta)\mathrm{d}\theta\right\}\mathrm{d}\eta$ and $c_4 = \exp\left\{\tau_2 \int_0^t E_b(\theta)\mathrm{d}\theta\right\}$. Hence, the region $\mathcal{D}_1$,

$\mathcal{D}_1 = \Big\{(H_e(t), H_h(t), I(t), T_r(t), T_c(t), F(t), E_b(t), R_b(t)) \in \mathbb{R}_+^8 : P(t) \leq \dfrac{\Pi_h}{\mu_h}, T_r(t) \leq m_1,$ $T_c(t) \leq m_2, I(t) \geq 0, F(t) \geq 0, E_b(t) \geq 0, R_b(t) \geq 0\}$ is positively invariant and attracting for the model system (6.1)-(6.8).

From Equation (6.1), using the fact that $P(t) = H_e(t) + H_h(t) \leq \dfrac{\Pi_h}{\mu_h}$, it follows that

$$\begin{aligned}
\frac{\mathrm{dH}_e}{\mathrm{dt}} &= \Pi_h + \omega H_h - \gamma(1-\varepsilon_v)H_e(t)E_b(t) - \phi\varepsilon_h H_e(t) - \mu_h H_e(t) \\
&\leq \Pi_h + \omega H_h(t) - (\phi\varepsilon_h + \mu_h)H_e(t) \\
&\leq \Pi_h + \omega\left(\frac{\Pi_h}{\mu_h} - H_e(t)\right) - (\phi\varepsilon_h + \mu_h)H_e(t) \\
&= \Pi_h\left(\frac{\mu_h + \omega}{\mu_h}\right) - (\omega + \mu_h + \phi\varepsilon_h)H_e(t) \\
&= (\omega + \mu_h + \phi\varepsilon_h)\left(\frac{\Pi_h(\omega + \mu_h)}{\mu_h(\omega + \mu_h + \phi\varepsilon_h)} - H_e(t)\right) \\
&= (\omega + \mu_h + \phi\varepsilon_h)(H_e^* - H_e(t)),
\end{aligned}$$

where $H_e^* = \dfrac{\Pi_h(\omega + \mu_h)}{\mu_h(\omega + \mu_h + \phi\varepsilon_h)}$.

Hence,

$$H_e(t) \leq H_e^* - (H_e^* - H_e(0))e^{-kt},$$

where $k = \omega + \mu_h + \phi\varepsilon_h$. From the above relation, $H_e(t)$ either approaches H_e^* asymptotically or there exists some finite time after which $H_e(t) \leq H_e^*$.

From Equation (6.2),

$$\begin{aligned}
\frac{\mathrm{d}H_h}{\mathrm{d}t} &= \phi\varepsilon_h H_e - \omega H_h - \mu_h H_h \\
&\leq \phi\varepsilon_h[\frac{\Pi_h}{\mu_h} - H_h] - \bar{c}H_h \\
&= \frac{\phi\varepsilon_h(\Pi_h - \mu_h H_h)}{\mu_h} - \bar{c}H_h \\
&= \left[\left(\frac{\Pi_h\phi\varepsilon_h}{\phi\varepsilon_h\mu_h + \mu_h\bar{c}} - H_h\right)(\phi\varepsilon_h + \bar{c})\right] \\
&= (\bar{c} + \phi\varepsilon_h)(H_h^* - H_h),
\end{aligned}$$

where $H_h^* = \dfrac{\Pi_h\phi\varepsilon_h}{\mu_h(\bar{c} + \phi\varepsilon_h)}$ and $\bar{c} = \omega + \mu_h$.

Hence,

$$H_h(t) \leq H_h^* - (H_h^* - H_h(0))e^{-kt}.$$

This implies that $H_h(t)$ either approaches H_h^* asymptotically or there exists some finite time after which $H_h(t) \leq H_h^*$. Consequently, any solution $H_e(t)$, $H_h(t)$, $I(t)$, $T_r(t)$, $T_c(t)$, $F(t)$, $E_b(t)$, and $R_b(t)$ at $t \geq 0$, of model system (6.1)-(6.8), that commences in the positive orthant $\mathbb{R}_+^8$, either remains confined in, enters, or asymptotically approaches the region $\mathcal{D}_2$, where

$\mathcal{D}_2 = \{(H_e(t), H_h(t), I(t), T_r(t), T_c(t), F(t), E_b(t), R_b(t)) \in \mathcal{D}_1 : H_e \leq H_e^*, H_h \leq H_h^*, I \geq 0, T_r \geq 0, T_c \geq 0, F \geq 0, E_b \geq 0, R_b \geq 0\}$.

Lemma 6.1.2. *The region $\mathcal{D}_2$ is positively invariant and attracting for the model system* (6.1)-(6.8) *with initial conditions in $\mathbb{R}_+^{10}$.*

6.1.2 Existence and stability of equilibria

Local stability of the CFE

The *Chlamydia*-free equilibrium (CFE) of the model system (6.1)-(6.8), which is obtained by setting the right hand side of the model system (6.1)-(6.8) to zero, and then choosing solutions where $E_b = R_b = I = F = 0$, is given by

$$\begin{aligned}
E_0 &= \{H_e^*, H_h^*, I^*, T_r^*, T_c^*, F^* E_b^*, R_b^*\}, \\
&= \left(\frac{\Pi_h(\omega + \mu_h)}{\mu_h(\omega + \mu_h + \phi\varepsilon_h)}, \frac{\Pi_h\phi\varepsilon_h}{\mu_h(\omega + \mu_h + \phi\varepsilon_h)}, 0, \frac{\varepsilon_v\Lambda_v}{\mu_t}, \frac{\varepsilon_c\Omega_v}{\mu_t}, 0, 0, 0\right). \qquad (6.9)
\end{aligned}$$

Using the next generation operator method (as described by van den Driessche and Watmough [157]) on the model system (6.1)-(6.8), the linear stability of the equilibrium E_0 can be established. Using the notations in [157], the matrices $\mathbf{F}$ and $\boldsymbol{V}$, for the transmission (new infection) terms and transition terms of the infected subsystem (formed by the differential equations for compartments $I, E_b,$ and R_b in model equations (6.3), (6.7), and (6.8), respectively), respectively, are given by

$$\boldsymbol{F} = \begin{pmatrix} 0 & \gamma(1-\varepsilon_v)H_e^* & 0 \\ 0 & 0 & 0 \\ 0 & 0 & 0 \end{pmatrix} \tag{6.10}$$

and

$$\boldsymbol{V} = \begin{pmatrix} \kappa & 0 & 0 \\ -\kappa N_E & \alpha\varepsilon_a + \mu_e + \gamma(1-\varepsilon_v)H_e^* & 0 \\ -\kappa N_{\mathrm{R1}} & 0 & \mu_e \end{pmatrix}. \tag{6.11}$$

Thus, the basic reproduction number $\mathcal{R}_0$ of the model system (6.1)-(6.8), given by the spectral radius of the next generation matrix $\boldsymbol{F}\boldsymbol{V}^{-1}$, is

$$\mathcal{R}_0 = \frac{N_E\gamma\left(1-\varepsilon_v\right)H_e^*}{\gamma\left(1-\varepsilon_v\right)H_e^* + (\alpha\varepsilon_a + \mu_e)}. \tag{6.12}$$

The basic reproduction number $\mathcal{R}_0$ is written in such a way that one can track the contribution of the infected and infectious classes (infected epithelial cells and elementary bodies, respectively) to the epidemic. The $\mathcal{R}_0$ expression in (6.12) is simply the product of the infection rate of healthy epithelial cells by EBs ($\gamma(1-\varepsilon_v)H_e^*$), number of infectious *Chlamydia* (EB) released by a bursting infected epithelial cell (N_E), and the expected duration of infectiousness of EBs $\left(\dfrac{1}{\gamma\left(1-\varepsilon_v\right)H_e^* + (\alpha\varepsilon_a + \mu_e)}\right)$.

Implementing *Theorem 2* of van den Driessche and Watmough [157], the following result is established.

Lemma 6.1.3. *The Chlamydia-free equilibrium (CFE) E_0, of the model system* (6.1)-(6.8)*, is locally stable whenever $\mathcal{R}_0 \leq 1$ and unstable if $\mathcal{R}_0 > 1$.*

Global stability of CFE

Theorem 6.1.4. *The CFE of the model system* (6.1)-(6.8)*, given by Equation* (6.9)*, is globally asymptotically stable (GAS) in $\mathcal{D}_2$ whenever $\mathcal{R}_0 \leq 1$ and unstable otherwise.*

Proof. Consider the candidate Lyapunov function

$$\mathbb{V} = N_E I(t) + E_b(t),$$

with Lyapunov derivative (where a dot represents differentiation with respect to t) given by

$$\begin{aligned}
\dot{\mathbb{V}} &= N_E\dot{I} + \dot{E}_b \\
&= N_E(\gamma(1-\varepsilon_v)H_eE_b - \kappa I - \rho IF) + (N_E\kappa I - \gamma(1-\varepsilon_v)H_eE_b - \varepsilon_a\alpha E_b - \mu_e E_b) \\
&= E_b(\gamma(1-\varepsilon_v)H_e(N_E-1)) - N_E\rho IF - \alpha\varepsilon_a E_b - \mu_e E_b \\
&= E_b(\gamma(1-\varepsilon_v)H_e(N_E-1) - \alpha\varepsilon_a - \mu_e) - N_E\rho IF \\
&\leq E_b(\gamma(1-\varepsilon_v)H_e^*(N_E-1) - \alpha\varepsilon_a - \mu_e) - N_E\rho IF \,(\text{since } N_E - 1 > 0 \& H_e \leq H_e^* \text{ in } \mathcal{D}_2) \\
&= E_b(\gamma(1-\varepsilon_v)N_E H_e^* - \gamma(1-\varepsilon_v)H_e^* - \alpha\varepsilon_a - \mu_e) - N_E\rho IF \\
&= E_b\left((\gamma(1-\varepsilon_v)H_e^* + \alpha\varepsilon_a + \mu_e)\left(\frac{\gamma(1-\varepsilon_v)N_E H_e^*}{\gamma(1-\varepsilon_v)H_e^* + \alpha\varepsilon_a + \mu_e} - 1\right)\right) - N_E\rho IF \\
&= E_b(\gamma(1-\varepsilon_v)H_e^* + \alpha\varepsilon_a + \mu_e)(\mathcal{R}_0 - 1) - N_E\rho IF < 0, \quad \text{when } \mathcal{R}_0 \leq 1.
\end{aligned}$$

Since all the model parameters and variables are non-negative, it follows that $\dot{\mathbb{V}} < 0$ for $\mathcal{R}_0 \leq 1$ and $\dot{\mathbb{V}} = 0$ if and only if $E_b = I = 0$. Hence, $\mathbb{V}$ is a Lyapunov function on $\mathcal{D}_2$. Furthermore, $\mathcal{D}_2$ is a compact and absorbing subset of $\mathbb{R}^8_+$, and the largest compact invariant set in $\{(H_e, H_h, T, T_r, T_c, F, E_b, R_b) \in \mathcal{D}_2 : \dot{\mathbb{V}} = 0\}$ is the singleton E_0. Thus, by Lasalle's invariance principle [65], $I \to 0$ and $E_b \to 0$ as $t \to \infty$. Substituting $I = E_b = R_b = 0$ into the model equations (6.1)-(6.8) shows that $H_e \to H_e^*$, $H_h \to H_h^*$, $T_r \to T_r^*$, $T_c \to T_c^*$, and $R_b \to 0$ as $t \to \infty$. Hence, every solution of the model system (6.1)-(6.8), with initial conditions in $\mathcal{D}_2$, approaches the CFE E_0 as $t \to \infty$ (that is, the CFE E_0 is GAS in $\mathcal{D}_2$) whenever $\mathcal{R}_0 \leq 1$.

□

Existence of CPE

In order to obtain the *Chlamydia*-present equilibrium (CPE) of model system (6.1)-(6.8), we set the right hand sides of the model equations (6.1)-(6.8) to zero, and solve for all its state variables. We also express the state variables in terms of the force of infection

$$\lambda^* = \gamma E_b^{**}. \tag{6.13}$$

Thus, the CPE of model system (6.1)-(6.8) is given by

$$E_1 = \{H_e^{**}, H_h^{**}, I^{**}, T_r^{**}, T_c^{**}, F^{**} E_b^{**}, R_b^{**}\}, \tag{6.14}$$

where

$$\begin{aligned}
H_e^{**} &= \frac{\pi_h\,(\omega+\mu_h)}{\lambda^*\,(1-\varepsilon_v)\,(\omega+\mu_h)+\mu_h\,(\phi\varepsilon_h+\omega+\mu_h)},\\
H_h^{**} &= \frac{\pi_h\phi\varepsilon_h}{\lambda^*\,(1-\varepsilon_v)\,(\omega+\mu_h)+\mu_h\,(\phi\varepsilon_h+\omega+\mu_h)},\\
I^{**} &= \frac{\lambda^*(1-\varepsilon_v)H_e^{**}}{\kappa+\rho F^{**}},\\
T_r^{**} &= \frac{\varepsilon_r\Lambda_v}{\mu_t-\tau_1 F^{**}},\ \mu_t > \tau_1 F^{**},\\
T_c^{**} &= \frac{\varepsilon_c\Omega_v}{\mu_t-\tau_2 F^{**}},\ \mu_t > \tau_2 F^{**},\\
F^{**} &= \frac{1}{6}\frac{Z^{2/3}+2C_2Z^{1/3}-12C_3C_1+4C_2^2}{C_1Z^{1/3}},\\
E_b^{**} &= \frac{D_1}{\gamma D_2}\left(\frac{\kappa\mathcal{R}_0}{\kappa+\rho F^{**}}-1\right)\\
R_b^{**} &= \frac{N_{R1}\kappa I^{**}+N_{R2}\rho I^{**}F^{**}}{\mu_e},
\end{aligned} \tag{6.15}$$

where

$Z = 12\sqrt{3}\sqrt{27\,{C_1}^2{C_4}^2+4\,C_1{C_3}^3+4\,{C_2}^3C_4-18\,C_1C_2C_3C_4-{C_2}^2{C_3}^2}C_1+108\,C_4{C_1}^2+8\,{C_2}^3-36\,C_3C_2C_1>0,$

$C_1 = k_6\tau_1\tau_2\rho,$

$C_2 = \rho k_2+\rho k_4+\rho\,\mu_t\tau_1+\rho\,\mu_t\tau_2,$

$C_3 = \rho\,k_6{\mu_t}^2+\rho\,k_1+\rho\,k_3+k_2k_5+k_4k_5,$

$C_4 = k_1k_5+k_3k_5,$

$k_1 = \mu_t\psi_1\varepsilon_r\Lambda_v,\ k_2 = \tau_2\psi_1\varepsilon_r\Lambda_v,\ k_3 = \mu_t\psi_2\varepsilon_c\Omega_v,\ k_4 = \tau_1\psi_2\varepsilon_c\Omega_v,\ k_5 = \kappa\,(N_E-1),$ $k_6 = \alpha\,\varepsilon_a+\mu_e,$

$D_1 = \mu_h(\varepsilon_a\alpha+\mu_e)(\omega+\mu_h+\phi\varepsilon_h)+\gamma(1-\varepsilon_v)(\omega+\mu_h)\Pi_h,$ and

$D_2 = (\varepsilon_a\alpha+\mu_e)(\omega+\mu_h)(1-\varepsilon_v).$

Note that $E_b^{**}>0$ if $\mathcal{R}_0 > 1+\dfrac{\rho F^{**}}{\kappa}$. $D_1>0$, $D_2>0$, $C_1>0$, $C_2>0$, $C_3>0$, and $C_4>0$, since all the model parameters are positive.

Substituting for E_b^{**} in the relation (6.13), we obtain

$$\lambda^* = \frac{D_1}{D_2}\left(\frac{\kappa\mathcal{R}_0}{\kappa + \rho F^{**}} - 1\right). \tag{6.16}$$

From the expression for F^{**} in Equations (6.15) (by direct calculation using the *Maple* software), we see that F^{**} is a strictly positive constant (independent of λ^*), since all the model parameters are positive. Thus, the term $\frac{\rho F^{**}}{\kappa} > 0$ at the CPE. This implies that $1 + \frac{\rho F^{**}}{\kappa} > 1$. Hence, λ^* is biologically relevant, that is, $\lambda^* > 0$, only when $\mathcal{R}_0 > 1 + \frac{\rho F^{**}}{\kappa} > 1$.

Lemma 6.1.5. *The model system* (6.1)-(6.8) *has one positive Chlamydia-present (endemic) equilibrium* E_1 *whenever* $\mathcal{R}_0 > 1$ *and no positive equilibrium otherwise.*

Thus, the above mathematical analyses show that the model system (6.1)-(6.8) has a globally asymptotically stable *Chlamydia*-free equilibrium (CFE) whenever $\mathcal{R}_0 \leq 1$, and a unique *Chlamydia*-present equilibrium (CPE) when $\mathcal{R}_0 > 1$. Simply put, the *C. trachomatis* infection will be cleared if $\mathcal{R}_0 \leq 1$, and would persist otherwise.

6.2 Numerical Simulations

6.2.1 Sensitivity analysis

Sensitivity analysis quantifies how variability (prediction imprecision) in predictors (input parameters) influence the value of outcome variables (responses) [16, 73]. In order to examine the sensitivity of $\mathcal{R}_0$ to variations in some parameters, we use Latin Hypercube Sampling (LHS) and partial rank correlation coefficient (PRCC) with 10000 Monte Carlo simulations per run. LHS is a stratified Monte Carlo sampling technique used for unbiased sampling of predictors in a multi-dimensional parameter space [73]. It is a very efficient sampling design which allows for the variation of predictor values simultaneously, in which each value is used only once in the analysis [16]. In the LHS, each predictor's estimation uncertainty is modelled by treating the predictor as a random variable. Probability density functions are then defined for each predictor, each of the marginal distributions are stratified into N equiprobable serial intervals, and a single value is then randomly chosen from every interval, for each predictor. In the analysis, each value of each predictor, which is obtained from each sampling interval, is used only once but the entire parameter space is efficiently and fairly sampled. Then, the distribution of the outcome variables can be derived by running the model N times with each of the sampled set of parameters [16, 73].

The LHS is useful for executing an uncertainty analysis [16, 73]. Uncertainty analysis is useful for evaluating the prediction imprecision in a response due to the uncertainty in estimating the predictor. Sensitivity analysis extends uncertainty analysis by ranking the predictors in terms of their contribution (order of importance) to the variability of each

of the responses [16, 73]. A sensitivity analysis is performed by the calculation of PRCCs for each predictor (sampled by the LHS scheme) and each model outcome variable [16].

The calculation of PRCCs is useful for classifying the importance of predictor-response correlations [73]. It enables the establishment of the statistical relationship between each predictor and each response(s), other predictors being held constant at their expected value [16]. A PRCC measures the degree of monotonicity between a specific predictor and a response. The sign (positive or negative) of the PRCC of a predictor indicates the qualitative (but not quantitative) affiliation (increase or decrease, respectively) it has with the response [16, 73]. The magnitude of the PRCC shows how important the uncertainty in the estimation of the predictor value is, to the prediction imprecision in the response value [16]. The relative importance of predictors can be determined via a comparison of the values of their PRCCs [16]. One can also access the monotonicity between a predictor and response by examining scatter plots of its PRCCs [16].

The sampling and sensitivity analysis methods used in SaSAT (Sampling and Sensitivity Analysis Tools [73]) were implemented in order to conduct uncertainty and sensitivity analysis on the model system (6.1)-(6.8). In the analysis, we use PRCCs, as described above, to distinguish and measure statistical influence, in particular, the monotonicity of the input variables on the response, which is the basic reproduction number $\mathcal{R}_0$. Figure 6.2 is the tornado plot of the PRCC of all the predictors of our model system as described in Table 6.3. It connotes the importance of the uncertainty of individual predictors, with respect to their contribution to the variability in the basic reproduction number $\mathcal{R}_0$ of chlamydial infections, as described by the model system (6.1)-(6.8). Tornado plots are used for illustrating the results of sensitivity analyses [73]. Input parameters with positive PRCCs are depicted by bar plots to the right, and with positive values on the horizontal axis, while input parameter with negative PRCCs are depicted by bar plots to the left, and with negative values on the horizontal axis.

In order to investigate the existence of any non-monotonicity between the basic reproduction number $\mathcal{R}_0$ and selected predictors/parameters (those with high absolute values of PRCC), we produce scatter plots of their PRCCs and examine them. The plots compare the basic reproduction number $\mathcal{R}_0$ (log 10 scale) against each selected parameter. For this analysis, predictors with fairly significant monotonic relationships with the $\mathcal{R}_0$ alone are displayed.

Figures 6.3 and 6.4 display the monotonic relationship between the indicated parameters and the log scale of the basic reproduction number $\mathcal{R}_0$. Simply put, they illustrate the variations in $\mathcal{R}_0$ against the input variables. Obviously, at $\log(\mathcal{R}_0) = 0$, $\mathcal{R}_0 = 1$. Figures 6.3(a), 6.3(b), and 6.4(c) show the monotonic relationship between Π_h, the rate of replenishment/production of healthy epithelial cells, γ, the effective contact rate between healthy epithelial cells and EB forms, and N_E, the number of EB forms released on lysis of infected cells, respectively, and the basic reproduction number $\mathcal{R}_0$. The figures indicate that a monotonic increase in the specified predictors produces a monotonic increase in

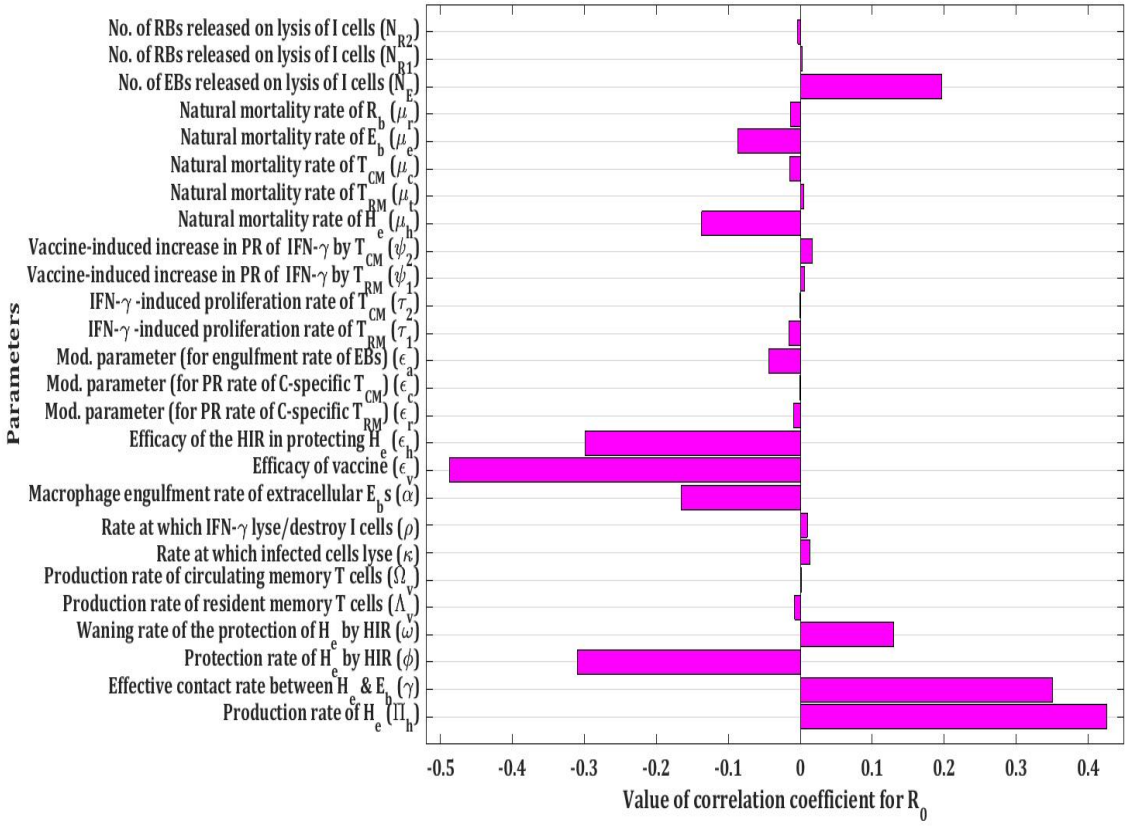

Figure 6.2: Tornado plot of the PRCC of $\mathcal{R}_0$ to the input parameters of model system (6.1)-(6.8), as described in Table 6.3, using $\mathcal{R}_0$ as the output. Mod. = Modification; HIR = Humoral immune response; No.= Number; PR = Production rate; T_{RM} = Tissue-resident memory T cells; T_{CM} = Circulating memory T cells.

the response $\mathcal{R}_0$. It can be seen on Figure 6.3(d) that there exists some monotonic but weak relationship between ω, the waning rate of the protection of epithelial cells by the humoral immune response, and $\mathcal{R}_0 = 1$. The figure indicates that a monotonic increase in ω will produce a slight monotonic increase in $\mathcal{R}_0$.

Figures 6.3(c) and 6.4(a) show the monotonic relationship between ϕ, the rate of protection of healthy epithelial cells by the humoral immune response, α, the macrophage engulfment rate of extracellular EB forms, respectively, and the basic reproduction number $\mathcal{R}_0$. The figures indicate that a monotonic decrease in the specified predictors produces a monotonic decrease in the response $\mathcal{R}_0$. The predictor that shows the most significant correlation to the the basic reproduction number $\mathcal{R}_0$ is ε_v, the efficacy of the *Chlamydia* vaccine. It can be seen that on Figure 6.4(b) that the higher the efficacy of the vaccine, the lower the $\mathcal{R}_0$. In particular, it can be seen that a vaccine of an efficacy of about 90% will facilitate the prevention of the progression of a *Chlamydia* infection, hence, eradicating the infection.

We carried out further numerical investigation (sensitivity analysis) by increasing the rates at which some biological processes occur in order to see how they affect $\mathcal{R}_0$, and

thus the prognosis of the disease. When the highest range of only ϕ, the protection rate of healthy epithelial cells by the humoral immune response, was increased to 35 hr^{-1}, $\mathcal{R}_0$ could not be brought below unity. This suggests that the protection conferred upon epithelial cells by the humoral immune response is not enough to prevent chlamydial infection, even if it is higher than the known biological plausibility. However, when both ϕ and α (the macrophage engulfment rate of EBs) were increased to 20 hr^{-1}, it was seen that $\mathcal{R}_0$ was brought below unity. This would be good for the prognosis of chlamydial infection if those values were biologically plausible, but they are not currently plausible. These results are not graphically displayed here.

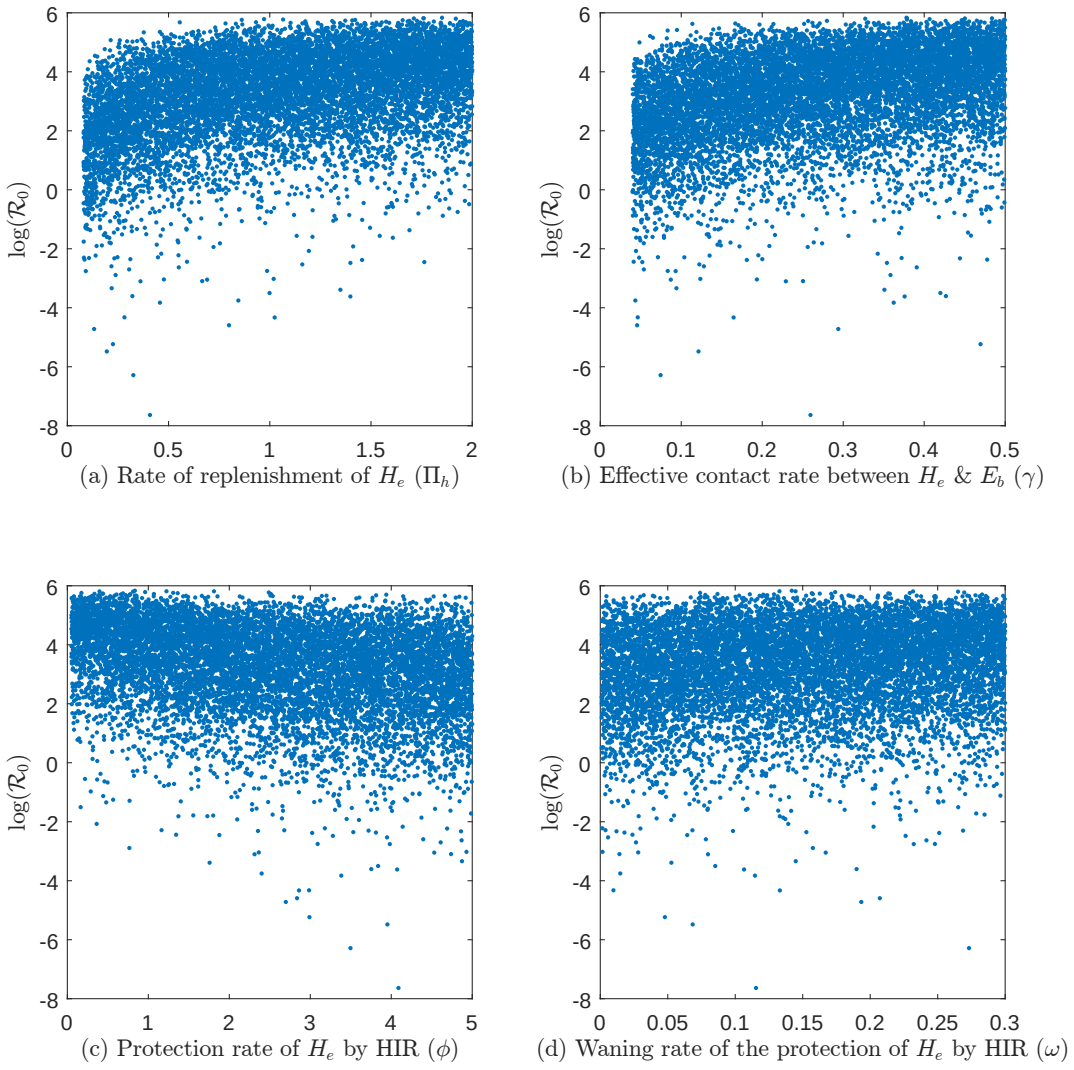

(a) Rate of replenishment of H_e (Π_h)

(b) Effective contact rate between H_e & E_b (γ)

(c) Protection rate of H_e by HIR (ϕ)

(d) Waning rate of the protection of H_e by HIR (ω)

Figure 6.3: Scatter plots that compare the basic reproduction number $\mathcal{R}_0$ against selected parameters. HIR means the humoral immune response.

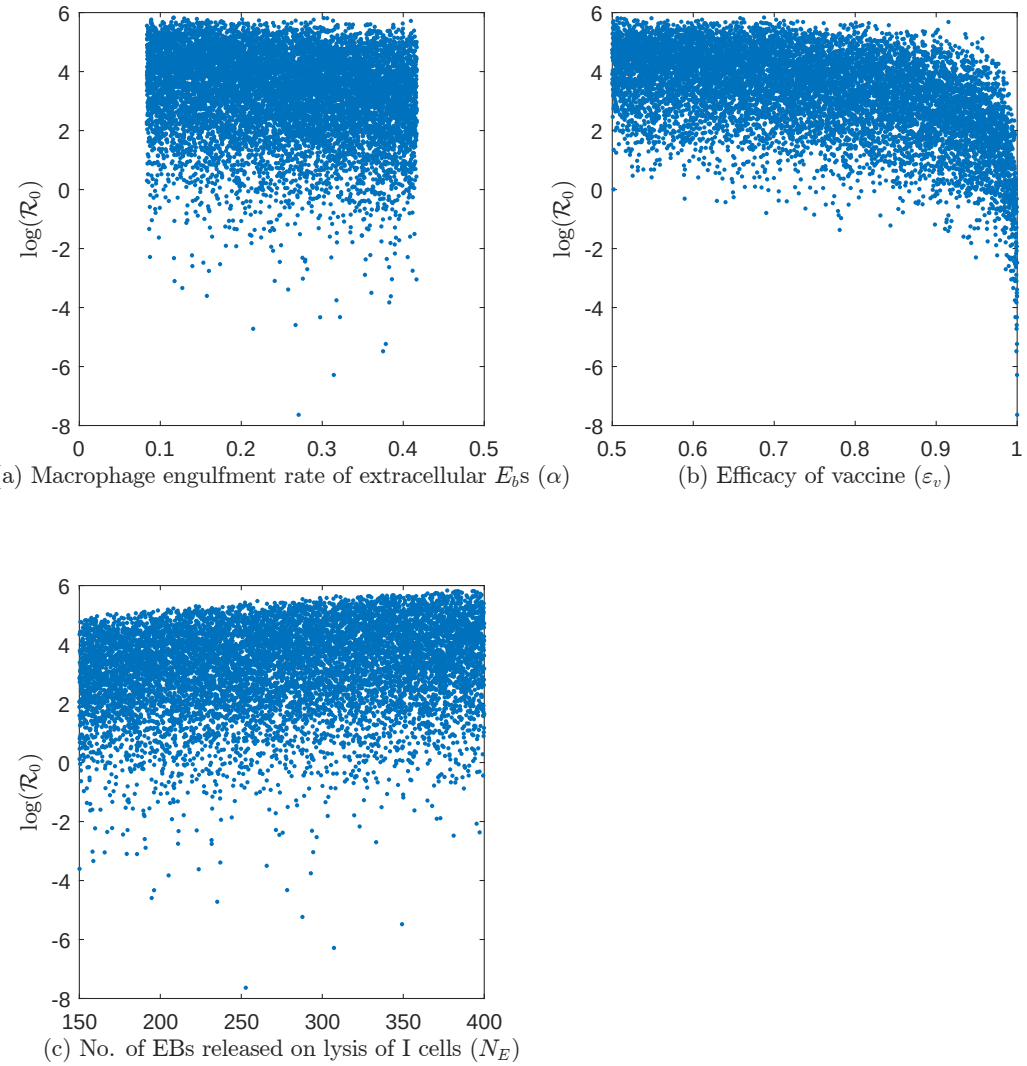

(a) Macrophage engulfment rate of extracellular E_bs (α)

(b) Efficacy of vaccine (ε_v)

(c) No. of EBs released on lysis of I cells (N_E)

Figure 6.4: Scatter plots that compare the basic reproduction number $\mathcal{R}_0$ against selected parameters.

Parameters	Baseline Value	Range	Reference
Π_h	2.1	[1,2.1] hr^{-1}	[142, 169]
γ	0.000083	0.00008333 hr^{-1}	[Assumed]
ϕ	3	[0.05,5] hr^{-1}	[142]
ω	0.1	0.1 hr^{-1}	[142]
Λ_v	0.009	[0.003,0.009] hr^{-1}	[Assumed]
Ω_v	0.002	[0.002083,0.003333] hr^{-1}	[133]
κ	0.020833	0.0138-0.025 hr^{-1}	[169]
ρ	4	[0.05,5] hr^{-1}	[142]
α	0.3	[0.08333,0.41667] hr^{-1}	[169]
ε_v		$(0, 1]$	[Assumed]
ε_h	0.5	$(0, 1]$	[Assumed]
ε_r	1.2	$[1, 2]$	[Assumed]
ε_c	1.2	$[1, 2]$	[Assumed]
ε_a	1.2	$[1, 2]$	[Assumed]
τ_1	0.001	$[0.0005, 1]$	[Assumed]
τ_2	0.001	$[1, 2]$	[Assumed]
ψ_1	0.00005	$[1, 2]$	[Assumed]
ψ_2	0.00005	$[1, 2]$	[Assumed]
μ_h	0.0008333	0.08333 hr^{-1}	[169]
μ_t	0.004	[0.0008333,0.00625] hr^{-1}	[133]
μ_c	0.004	[0.0008333,0.00625] hr^{-1}	[133]
μ_e	0.005	[0.00375,0.015] hr^{-1}	[32]
N_E	200	150-400	[142]
N_{R1}	10	10-50	[Assumed]
N_{R2}	20	10-50	[Assumed]

Table 6.4: Values and ranges of the parameters of the model system (6.1)-(6.8). Assumed values/ranges are reasonably chosen so that they drive a within-host *Chlamydia* infection.

6.2.2 Results

We investigate the *Chlamydia* burden in an *in vivo Chlamydia* infection post-vaccination, with varying vaccine efficacy, by tracking the concentrations of elementary bodies, infected epithelial cells, and protected epithelial cells over 1000 hours post-infection. Using the parameter values in Table 6.4, the model system (6.1)-(6.8) was simulated for varying values of ε_v, $0 \leq \varepsilon_v \leq 1$, the vaccine efficacy, and ε_h, $0 \leq \varepsilon_h \leq 1$, the efficacy of the humoral immune response in protecting healthy epithelial cells. The corresponding concentrations of the EB forms, infected epithelial cells, and of healthy epithelial cells protected from *Chlamydia* infection by the humoral immune response, are all graphically displayed on Figures 6.5, Figures 6.6, and Figures 6.7, respectively.

Numerical results, as shown graphically on both Figures 6.5 and 6.6, of the model system (6.1)-(6.8), show that for some combinations of the vaccine efficacy (ε_v) and the efficacy of the humoral immune response in protecting epithelial cells, (ε_h), the *Chlamydia* infection does not burden the host system in the presence of the *Chlamydia* vaccine. This is characterised by the clearance of the pathogen by the final time of the simulation (that is, concentrations of EB forms and of infected epithelial cells are both zero). As shown on Figure 6.7, for such combinations of ε_v and ε_h, surges in the concentrations of healthy

epithelial cells that are protected by the humoral immune response (H_h), in the presence of the vaccine, also indicate the anti-*Chlamydia* potency of the vaccine.

Based on the numerical results shown on Figure 6.5, an efficacy of 45% is sufficient for an effective *Chlamydia* vaccine. However, an important characteristic of the vaccine is that its presence in the host system should have the ability to (1) boost the natural humoral immune response which protects healthy epithelial cells from infection to at least 90% of its biologically plausible potency; (2) boost the production of resident and circulating memory T cells each by 20%; and (3) increase the rate at which macrophages engulf extracellular *Chlamydia* (EB forms) by 20% (this may mediate antibody-dependent cell-mediated cytotoxicity (ADCC)). An effective *Chlamydia* vaccine may also sufficiently have an efficacy of 65%, but it should have the ability to boost the natural humoral immune response by at least 85% of its biologically plausible potency, other rates being equal.

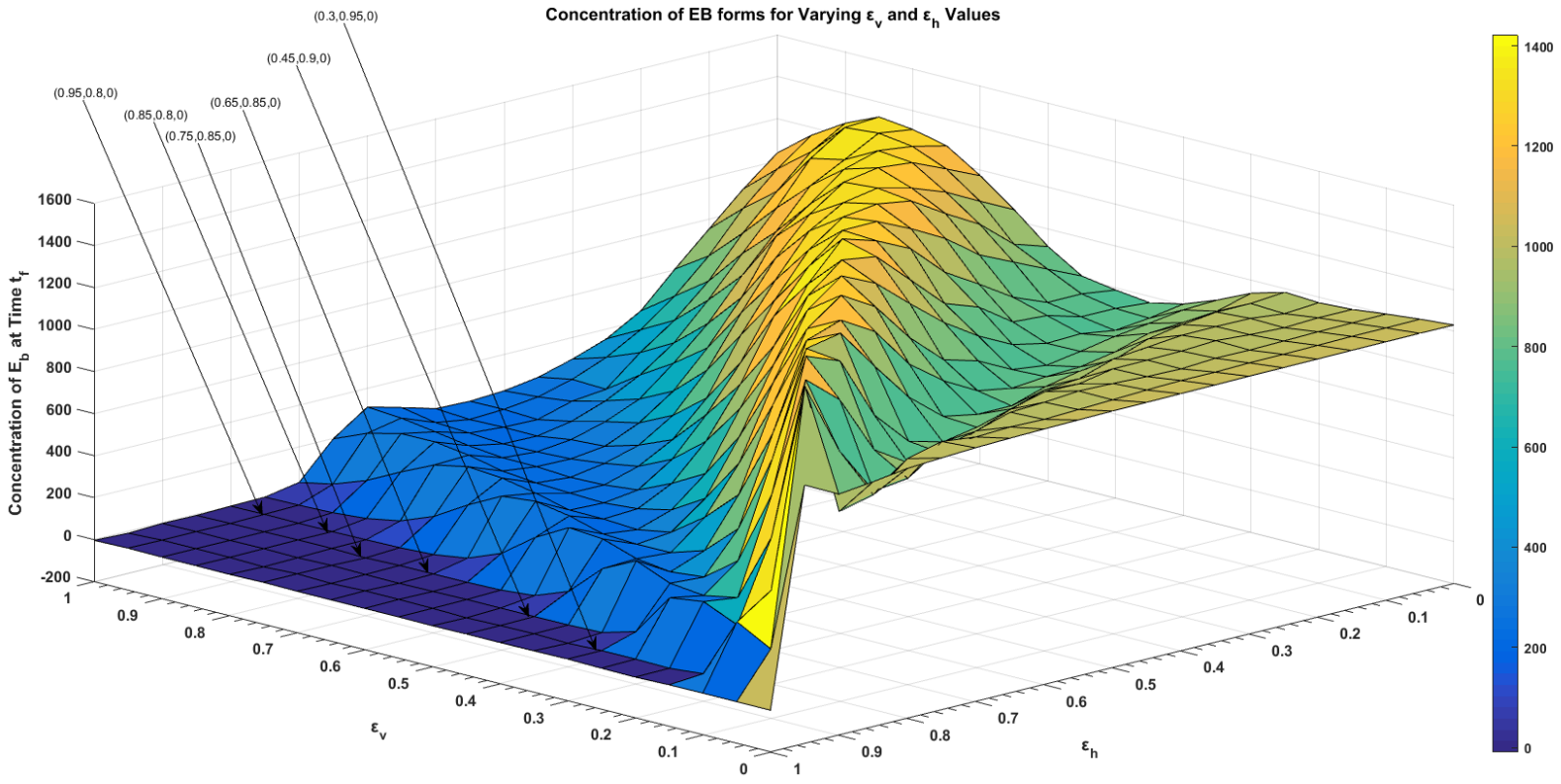

Figure 6.5: Numerical simulation of the *Chlamydia* model system (6.1)-(6.8), showing a 3D representation of the concentration of elementary body forms (*Chlamydia* burden) at the end of the simulation (time $t_f = 1000$ hours post-infection), for varying values of ε_v, the vaccine efficacy, and ε_h, the efficacy of the humoral immune response in protecting healthy epithelial cells.

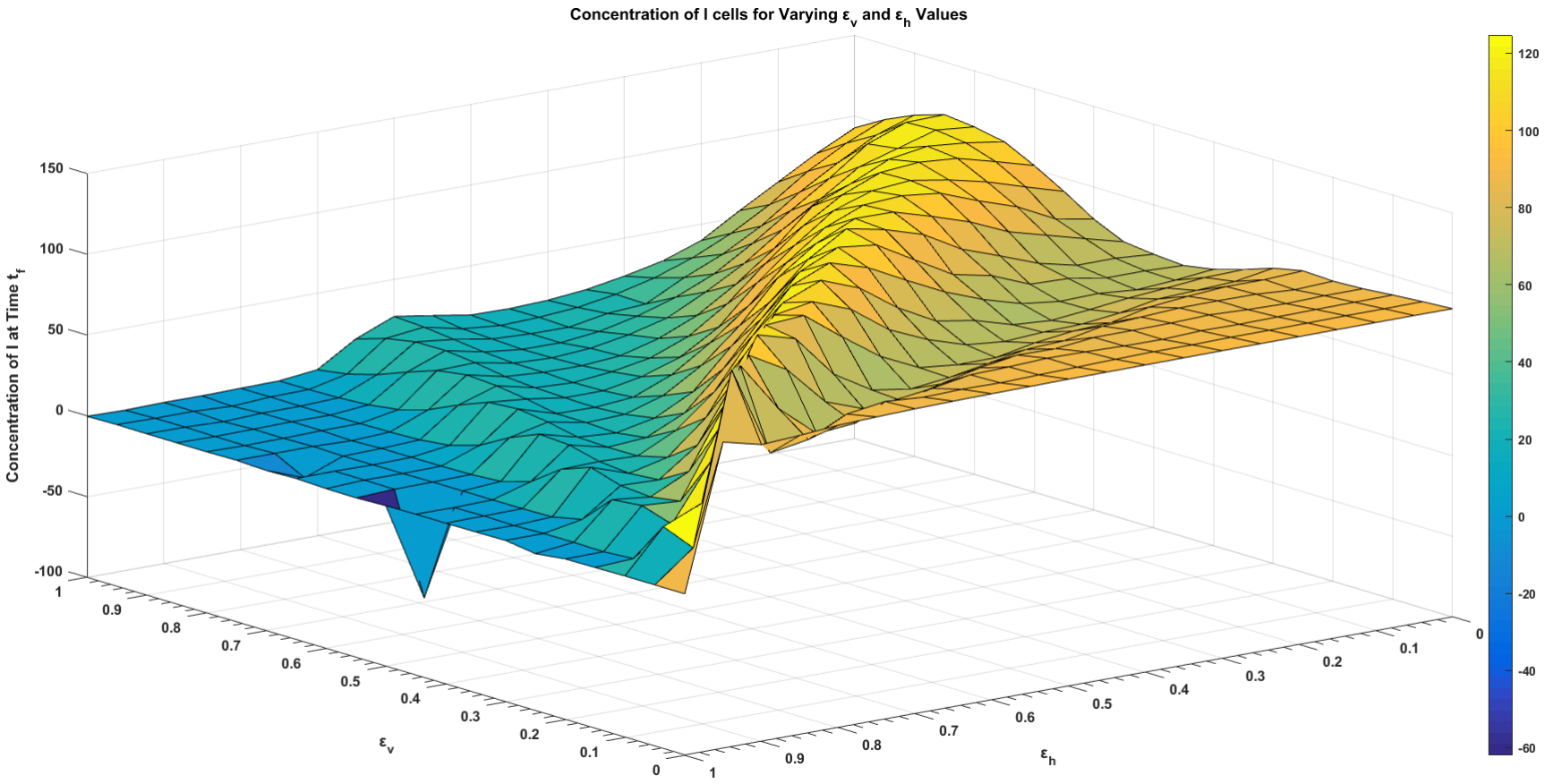

Figure 6.6: Numerical simulation of the *Chlamydia* model system (6.1)-(6.8), showing a 3D representation of the concentration of infected epithelial cells at the end of the simulation (time $t_f = 1000$ hours post-infection), for varying values of ε_v, the vaccine efficacy, and ε_h, the efficacy of the humoral immune response in protecting healthy epithelial cells.

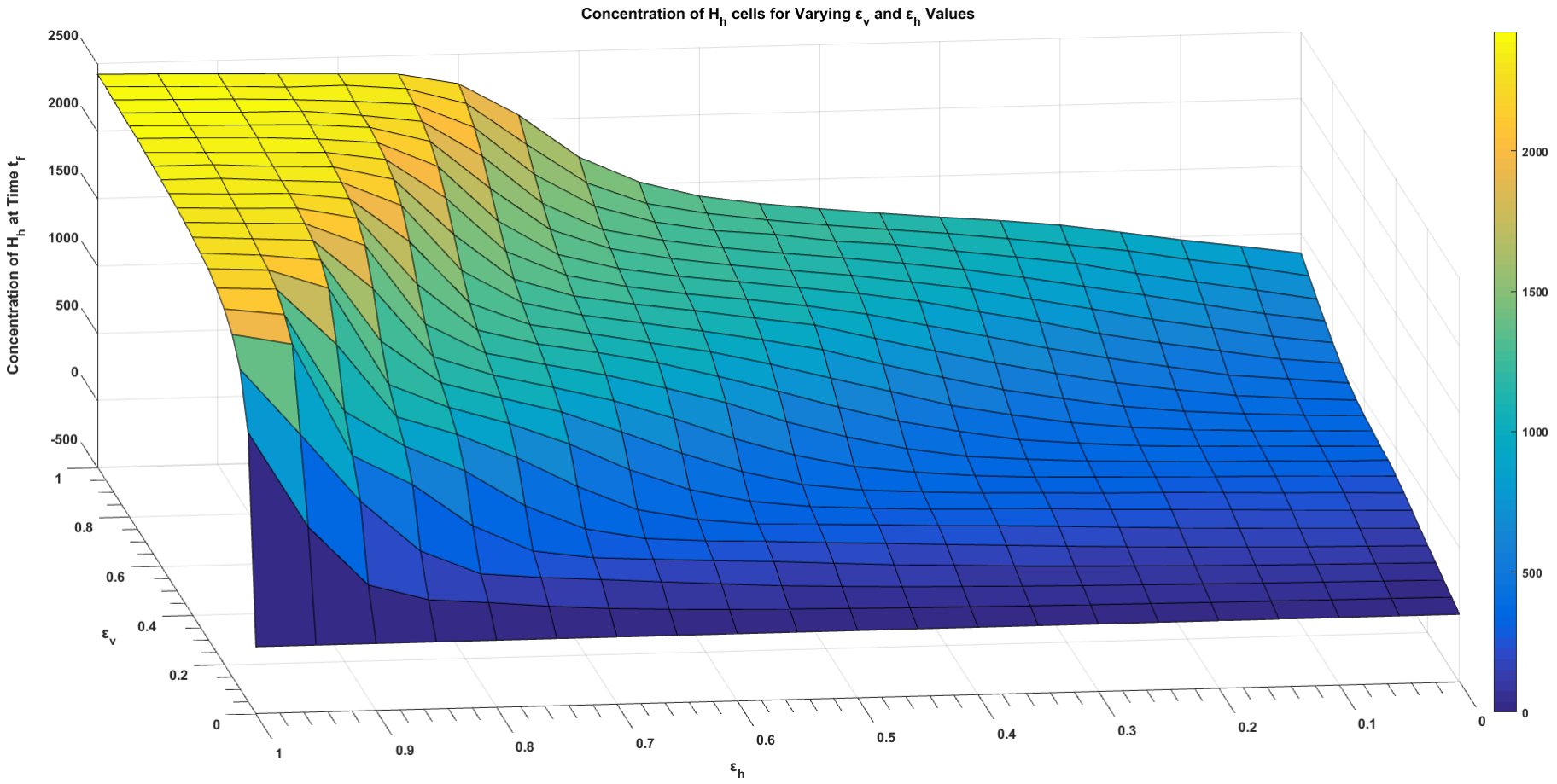

Figure 6.7: Numerical simulation of the *Chlamydia* model system (6.1)-(6.8), showing a 3D representation of the concentration of protected healthy epithelial cells at the end of the simulation (time $t_f = 1000$ hours post-infection), for varying values of ε_v, the vaccine efficacy, and ε_h, the efficacy of the humoral immune response in protecting healthy epithelial cells.

6.2.3 Critical Vaccine Efficacy

High vaccine efficacies are often difficult to achieve in real world experiments. It has been established that all vaccines are partially efficacious, that is, vaccine efficacies are always less than a 100% [146]. Thus, we estimate the critical efficacy of an effective *Chlamydia* vaccine if it does not need to be up to 100%. The biological interpretation of our vaccine efficacy is the reduction of the probability of infection of a healthy epithelial cell per contact with an infectious *Chlamydia* (EB forms). We solve for the expression for the critical vaccine efficacy (ε_v^c), by first making ε_v^c the subject of the relation in Equation 6.12. This gives:

$$\varepsilon_v = 1 - \frac{\mathcal{R}_0(\alpha\varepsilon_a + \mu_e)}{\gamma H_e^*(N_E - \mathcal{R}_0)}, \tag{6.17}$$

where $H_e^* = \dfrac{\Pi_h(\omega + \mu_h)}{\mu_h\,(\omega + \mu_h + \phi\varepsilon_h)}$.

Setting $\mathcal{R}_0$ to 1 in Equation 6.17, we obtain:

$$\varepsilon_v^c = 1 - \frac{\alpha\varepsilon_a + \mu_e}{\gamma H_e^*(N_E - 1)}, \tag{6.18}$$

Lemma 6.2.1. *The basic reproduction number $\mathcal{R}_0 < 1$ whenever $\varepsilon_v > \varepsilon_v^c$.*

Whenever the vaccine efficacy ε_v is greater than the critical vaccine efficacy ε_v^c, *Chlamydia* is cleared from the host system, since $\mathcal{R}_0 < 1$, and Theorem 6.1.4 guarantees the *in vivo* clearance of the pathogen under this setting. Numerical results of Lemma 6.2.1 are shown in Figure 6.8, for three different values of ε_v. For parameter values shown in Table 6.4, the critical vaccine efficacy $\varepsilon_v^c = 0.86$. Figures 6.8a and 6.8b show that for values of $\varepsilon_v < \varepsilon_v^c$, the infection may not be abated, even in the presence of a *Chlamydia* vaccine pre-infection. However, for any value $\varepsilon_v > \varepsilon_v^c$, the infection can be eliminated from the host system. Figure 6.8c also shows the impact of the vaccine efficacy on protected epithelial cells. It indicates that for values of $\varepsilon_v < \varepsilon_v^c$, the ability of the humoral immune response to protect healthy epithelial cells from *Chlamydia* infection may wane, while it would increase for values of $\varepsilon_v > \varepsilon_v^c$.

We note that the numerical value of the critical vaccine efficacy (ε_v^c) depends on other model parameters, such as the efficacy of the humoral immune response in protecting healthy epithelial cells (ε_h) amongst others. Thus considering the implications of Lemma 6.2.1 and Theorem 6.1.4, we assess the impact of the *Chlamydia* vaccine by depicting contour plots of the basic reproduction number $\mathcal{R}_0$ as a function of ε_v, the vaccine efficacy, and ε_h, the efficacy of the humoral immune response in protecting healthy epithelial cells in Figure 6.9. In Figure 6.9, it can be seen that for values of $\mathcal{R}_0 \leq 1$, the use of an imperfect *Chlamydia* vaccine can lead to the elimination of the disease. For example, for relatively low values of $\mathcal{R}_0$, such as $\mathcal{R}_0 = 0.85$, the use of a *Chlamydia* vaccine with

a modest efficacy of 85%, and with a 75% efficacy in the protection of healthy epithelial cells from *Chlamydia* infection, can bring about the elimination of chlamydial infection. A relatively low $\mathcal{R}_0$ value of 0.9 would also yield $\varepsilon_v = 80\%$ and $\varepsilon_h = 80\%$. Note that we have only used values of ε_v and ε_h between the interval $[0.3, 1]$ because we observed that values of the parameters between the interval $[0, 0.3)$ do not necessarily yield relatively low values of $\mathcal{R}_0$, for parameter values in Table 6.4.

We differentiate the basic reproduction number $\mathcal{R}_0$ with respect to ε_v. This gives:

$$\frac{\partial \mathcal{R}_0}{\partial \varepsilon_v} = -\frac{N_E \gamma(\alpha\varepsilon_a + \mu_e) H_e^*}{(\gamma\,(1-\varepsilon_v)\,H_e^* + (\alpha\varepsilon_a + \mu_e))^2} < 0. \tag{6.19}$$

Equation 6.19 shows that $\mathcal{R}_0$ is a decreasing function of ε_v, which implies that a vaccine with a good efficacy will reduce the *in vivo* concentration of *Chlamydia*.

We monitor the effect of efficacy of the humoral response in the protection of healthy epithelial cells from chlamydial infection, by differentiating $\mathcal{R}_0$ with respect to ε_h. This gives:

$$\frac{\partial \mathcal{R}_0}{\partial \varepsilon_h} = -\frac{\mu_h \phi \gamma \Pi_h N_E (1-\varepsilon_v)(\omega + \mu_h)(\alpha\varepsilon_a + \mu_e)}{(\mu_h(\alpha\varepsilon_a + \mu_e)(\omega + \mu_h + \phi\varepsilon_h) + \gamma\Pi_h(1-\varepsilon_v)(\omega + \mu_h))^2} < 0. \tag{6.20}$$

Equation 6.20 shows that $\mathcal{R}_0$ is a decreasing function of ε_h, which implies that if the vaccine brings about more protection of healthy epithelial cells from infection, then the reproduction number $\mathcal{R}_0$ decreases.

We also monitor the effect of the vaccine-induced increase in the engulfment rate of EB forms of *Chlamydia* by antibodies (macrophages) by differentiating $\mathcal{R}_0$ with respect to ε_a. This gives:

$$\frac{\partial \mathcal{R}_0}{\partial \varepsilon_a} = -\frac{N_E \alpha \gamma (1-\varepsilon_v) H_e^*}{(\gamma\,(1-\varepsilon_v)\,H_e^* + (\alpha\varepsilon_a + \mu_e))^2} < 0. \tag{6.21}$$

Equation 6.21 shows that $\mathcal{R}_0$ is a decreasing function of ε_a, which implies that if the vaccine increases the concentration of extracellular *Chlamydia* engulfed by antibodies, then the reproduction number $\mathcal{R}_0$ decreases.

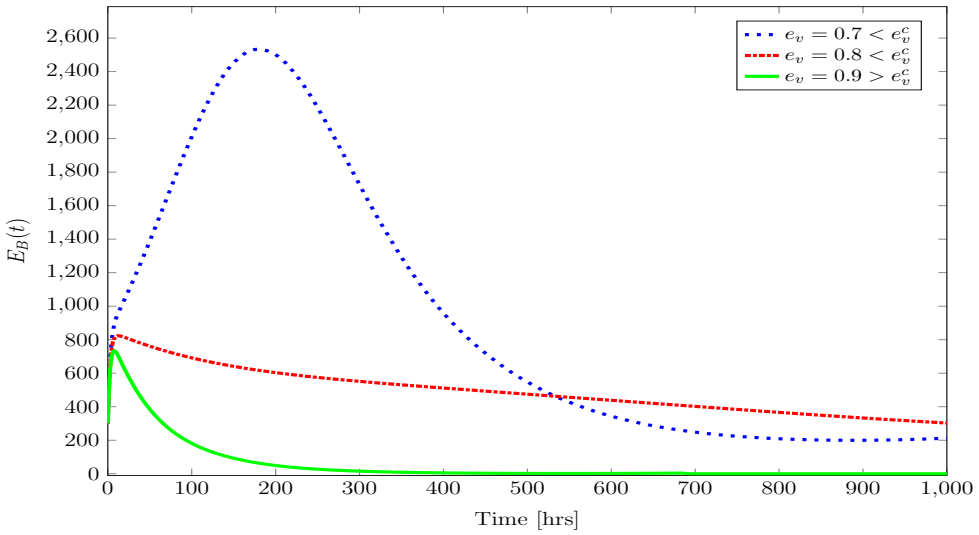

(a) Concentration of elementary bodies, $E_b(t)$

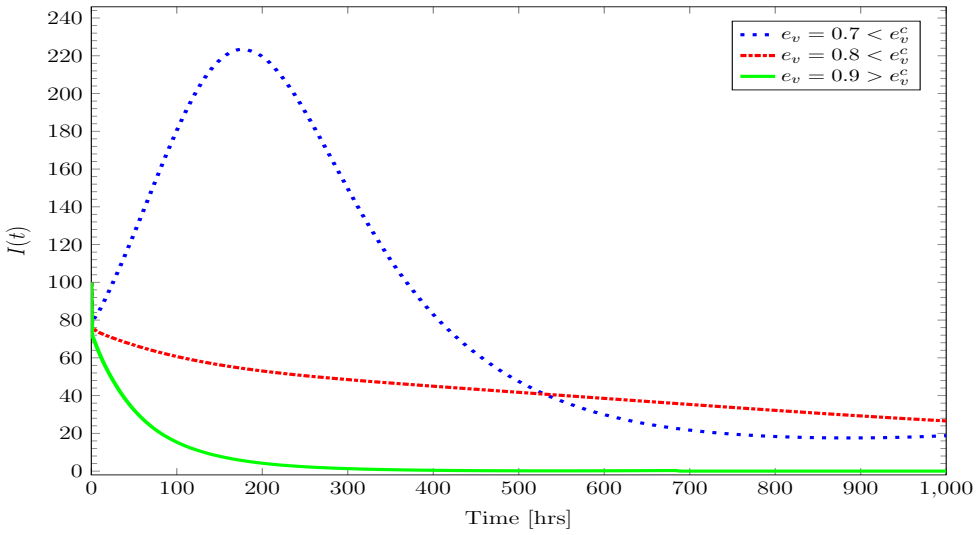

(b) Concentration of infected epithelial cells, $I(t)$

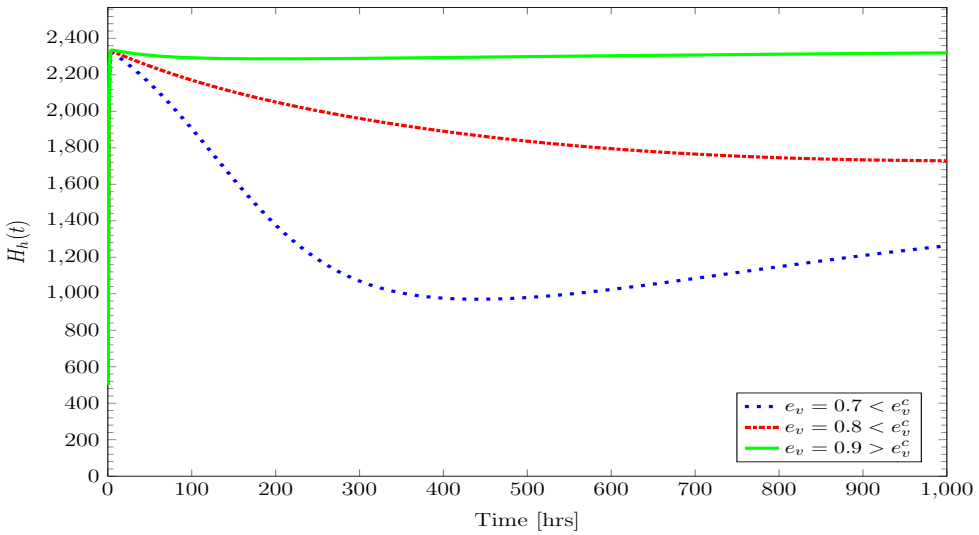

(c) Concentration of protected healthy epithelial cells, $H_h(t)$

Figure 6.8: Numerical simulation of the *Chlamydia* model system (6.1)-(6.8), showing the time course plot of (a) $E_b(t)$, concentration of elementary body forms, (b) $I(t)$, concentration of infected epithelial cells, and (c) $H_h(t)$, concentration of protected healthy epithelial cells, respectively, all over 1000 hours post infection, and for $\varepsilon_v = 0.7 < \varepsilon_v^c$, $\varepsilon_v = 0.8 < \varepsilon_v^c$, and $\varepsilon_v = 0.9 > \varepsilon_v^c$.

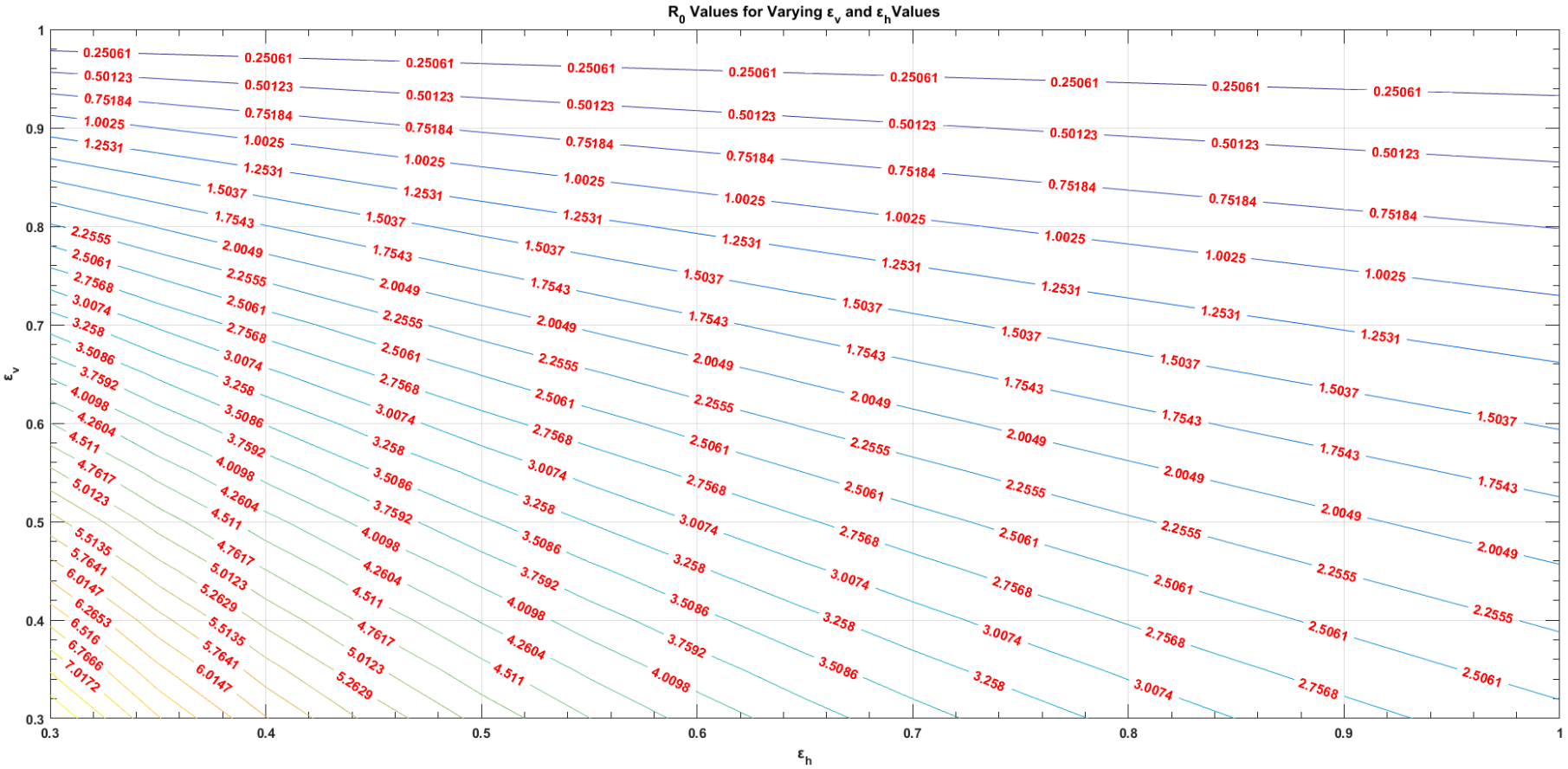

Figure 6.9: Simulation of the *Chlamydia* vaccine model system (6.1)-(6.8), showing contour plots of $\mathcal{R}_0$ as a function of ε_v, the vaccine efficacy, and ε_h, the efficacy of the humoral immune response in protecting healthy epithelial cells. Note that $\varepsilon_v^c = 0.86$.

6.3 Discussion

In this chapter, we have extended the mathematical modelling literature by theoretically assessing the potential role of an imperfect anti-*Chlamydia* vaccine on the within-host dynamics of *C. trachomatis*. In this study, we investigated the impact of a potentially effective mucosal *Chlamydia* vaccine on the within-host dynamics and prognosis of a genital chlamydial infection. We also explored how efficacious a *Chlamydia* vaccine should be if it must (1) elicit protective immunity against chlamydial challenge, and (2) efficiently clear a chlamydial infection upon a re-challenge with *Chlamydia*. The developed model uses a prototype vaccine that induces similar protective immunity like that described by the study of Stary *et al.* [149], which has been discussed in Section 2.4.

In addition to the incorporation of the effects of a potentially efficacious mucosal *Chlamydia* vaccine, our model specifically extends the work by Sharomi and Gumel [142] by (i) adding a new compartment for the dynamics of *Chlamydia*-specific resident memory T cells; (ii) adding a new compartment for the dynamics of *Chlamydia*-specific circulating memory T cells; (iii) allowing for the proliferation of resident memory T cells and circulating memory T cells; (iv) allowing for a vaccine-induced (additional) protective immunity against infection of healthy epithelial cells by *Chlamydia* via antibody blocking; and (v) adding a compartment for the inhibitory action of IFN-γ. We carried out qualitative and stability analysis of the model. The model has a globally asymptotically stable *Chlamydia*-free equilibrium when its associated basic reproduction number $\mathcal{R}_0 \leq 1$. The model also has a unique *Chlamydia*-present equilibrium when the basic reproduction number $\mathcal{R}_0 > 1$.

We quantified how the variability in model parameters affect the value of the basic reproduction number $\mathcal{R}_0$ by carrying out sensitivity analysis of $\mathcal{R}_0$ to input parameters. In particular, we investigated the monotonic relationship between the model's basic reproduction number $\mathcal{R}_0$ and some predictor variables, in particular Π_h, the rate of replenishment/production of healthy epithelial cells, γ, the effective contact rate between healthy epithelial cells and EB forms, and N_E, the number of EB forms released on lysis of infected cells. Simulation results indicate that a monotonic increase in the specified predictors produces a monotonic increase in the response $\mathcal{R}_0$. In addition, an investigation of the monotonic relationship between ϕ, the rate of protection of healthy epithelial cells by the humoral immune response, α, the macrophage engulfment rate of extracellular EB forms, and the basic reproduction number $\mathcal{R}_0$, indicates that a monotonic decrease in the specified predictor variables produces a monotonic decrease in the response $\mathcal{R}_0$. The predictor variable that shows the most significant inverse correlation to the $\mathcal{R}_0$ was ε_v, the efficacy of the *Chlamydia* vaccine. Summarily, the sensitivity analysis results suggest that a *Chlamydia* vaccine of an efficacy of about 90% may facilitate the prevention of the progression of a *Chlamydia* infection, hence, eradicating the infection.

We investigated the *Chlamydia* burden in an *in vivo Chlamydia* infection post-vaccination, for varying values of ε_v, $0 \leq \varepsilon_v \leq 1$, the vaccine efficacy, and ε_h, $0 \leq \varepsilon_h \leq 1$, the efficacy of the humoral immune response in protecting healthy epithelial cells, by tracking the concentrations of elementary bodies, infected epithelial cells, and protected epithelial cells over 1000 hours post-infection. The vaccine was shown to be able to possess sufficiently low efficacies, however, it must also satisfy some other immune-related conditions if it must be effective. We also obtained the mathematical expression for, and the values of, the *critical vaccine efficacy*, using parameter values presented in Table 6.4.

Results of the numerical simulations of the model show that a vaccine with a minimum (critical) efficacy of 86% may be required for the *in vivo* control of *Chlamydia* burden, which is characterised by the concentrations of infectious *Chlamydia* (EB forms) and of infected epithelial cells. We also assessed the impact of the described *Chlamydia* vaccine by depicting contour plots of $\mathcal{R}_0$ as a function of ε_v, the vaccine efficacy, and ε_h, the efficacy of the humoral immune response in protecting healthy epithelial cells. Simulation results indicate that for values of $\mathcal{R}_0 \leq 1$, the use of an imperfect *Chlamydia* vaccine should lead to the clearance of the pathogen.

In conclusion, we found that a *Chlamydia* vaccine that (1) decreases the concentration of newly infected epithelial cells; (2) increases the concentration of extracellular *Chlamydia* engulfed by antibodies; (3) boosts the protection of healthy epithelial cells from infection; may reduce the concentration of *Chlamydia in vivo*, thereby eliminating the chlamydial infection overall. Candidate vaccines that possess similar properties as described by our model results may be efficacious in the *in vivo* control of *Chlamydia trachomatis* genital infection. We however note that results of this model should be viewed in the light of its associated parameters and assumptions.

7 Conclusions

In this chapter we summarise the major contributions of the thesis, and propose areas for future work. This thesis has addressed some crucial biological questions with regards to the within-host dynamics and treatment of chlamydial infections, as outlined in Chapter 1. To recap, the research questions addressed are:

1. Why are there treatment failures in the control of genital chlamydial infection? In particular, could existing treatment regimen be inhibiting intracellular *Chlamydia* growth later than expected, thereby resulting in some of them thriving for repeat infection? In the presence of antimicrobial treatments, what role does the different component of the chlamydial developmental cycle play in the pathogenesis of the disease? How can these treatment regimens be improved?
2. Are treatment failures consequences of sub-optimal treatment regimen? Under what treatment conditions can the effective and efficient clearance of *Chlamydia* be achieved *in vivo*? Do we need more therapeutic agents in the clearance of the infection? How and when should such treatments be initiated in infected individuals?
3. How do we treat chronic chlamydial infections? In particular, how can we prevent, or even reverse, the development of severe sequelae of chlamydial infections in the human population?
4. How would an imperfect *Chlamydia* vaccine impact on the dynamics and prognosis of a genital chlamydial infection *in vivo*? How efficacious should a *Chlamydia* vaccine be if it must facilitate the prevention of the progression of a *Chlamydia* infection?

The thesis has extended the mathematical modelling literature by achieving its aims as outlined in Chapter 1. To recap, the objectives of the thesis were:

1. Construction of new mathematical models of (genital) chlamydial infection in humans or animals that better account for the complexity of the immune response to infection, and importantly, reinfection events caused by chlamydial persistence, than existing models.

2. Enhancement of the above and existing models, such that they are able to describe the effects of existing treatments and of proposed vaccination strategies.
3. Formation of new hypotheses regarding repeated chlamydial infections based on model analysis.
4. Proposition of optimal treatment and vaccination strategies based on the above.

7.1 Model for the timing of the inhibitory effects of antibiotics on *Chlamydia*

In this thesis, a mathematical model that investigates (1) the optimal timing of the inhibitory activity of antibiotic treatments in a typical chlamydial infection, and (2) the effect of this activity on the yield of *Chlamydia* at the end of the chlamydial developmental cycle, was presented. This investigation was done by examining how different timing of the commencement of antibiotic inhibitory activity (in an active antibiotic delivery of an *in vitro* testing), within the CDC and on a single cell level, will impact on the prognosis of a genital chlamydial infection. This antibiotic delivery was assumed to be dependent on the pharmacokinetics of the treatment administered. The prototype antibiotic used was azithromycin, particularly the use of the *in vivo* equivalence of a single 1 g oral dose treatment according to the World Health Organisation (WHO) recommended guidelines. The presented model, which was based on a system of three ordinary differential equations, accounted for the concentrations of intracellular reticulate body (RB) and elementary body (EB) forms of *Chlamydia*, and the intracellular concentration of azithromycin.

The presented model was investigated under five different treatment scenarios: the time at which the (intracellular) inhibitory activity of azithromycin against chlamydial growth commences (1) coincides with EB-RB differentiation; (2) occurs during RB replication; (3) coincides with RB-EB differentiation; (4) occurs during asynchronous RB-EB differentiation and RB replication; and (5) occurs at cell lysis. Under the described treatment scenarios, the concentration of infectious progenies (EB forms of *Chlamydia*) were tracked. Model results indicated that the effectiveness of antibiotics in the clearance of intracellular *Chlamydia* may be a function of the time at which its inhibitory activity commences. In particular, the results of the model suggested that for the effective antibiotic inhibition of *Chlamydia*, the efficient inhibitory activity of the drug should at least commence at the start of the cellular infection. A stronger and faster intracellular penetration of antibiotics may achieve this.

Thus, we hypothesised that the discovery and development of more effective routes of antibiotic administration, through the targeted delivery of antibiotics, may bring about the effective treatment of chlamydial infections. Targeted delivery of drugs is a treatment strategy that aims to selectively deliver antibiotics to the pathogen of interest at the infection site, where they can best exert their therapeutic effect. This strategy, which has been recently explored for chlamydial infections (see [64]), has been proven to be significantly more effective in the suppression of *Chlamydia* more than the use of antibiotics alone.

Our model results have shown that targeted drug delivery, which may facilitate a faster and higher delivery of antibiotics to the intracellular pathogen before its developmental cycle progresses, may be a solution to the effective treatment of chlamydial infections.

We note that it may be worthwhile investigating the impact of including treatments/drugs that boost or strengthen the immune system's response to chlamydial infections. This is because we suspect that if chlamydial infections are treated with effective antibiotics (irrespective of the CDC stage of administration) and in the presence of an enhanced immune response there may not be any EBs released on lysis of infected host cells. It may be interesting to investigate the impact of an enhanced cell-mediated response in particular as it has been reported to be more effective than the humoral immune response. The investigation of the impact of effective chlamydial infection treatments/vaccines on the within-host dynamics of chlamydial infection, that is, that which involves both intracellular and extracellular *Chlamydia* forms is proposed for future work.

7.2 Optimal control models for the treatment of *Chlamydia trachomatis* genital infection

We presented two ordinary differential equation models, using techniques of optimal control theory, for the optimal treatment of a chlamydial infection.

7.2.1 Model for the treatment of genital chlamydial infections

The first optimal control model was used to determine hypothetical optimal treatment strategies that may not only minimise the production of free extracellular *Chlamydia*, but possibly enhance the cell-mediated immune response (that is, cytotoxic immune response) in the clearance of chlamydial infection. The model described the cellular dynamics of the interaction processes between extracellular *Chlamydia*, uninfected epithelial cells and *Chlamydia*-infected epithelial cells. The model also described the role of the humoral and cell-mediated immunity in the *Chlamydia* developmental cycle. We proposed that alongside antibiotic activity, the presence of a proteasome-specific inhibitor such as lactacystin may enhance the capacity of the cell-mediated immune response in the clearance of *Chlamydia* infection. We also hypothesised that treatment failures are perhaps the consequences of sub-optimal treatment regimens. The two therapeutic treatments explored are: (1) drugs that reduce, or possibly eliminate, the production of viable *Chlamydia* (bacteriostatic or bactericidal agents, respectively) and (2) drugs that act as proteasome-specific inhibitor, which may enhance the cell-mediated immune response in the clearance of chlamydial infection prior to the lysis of infected epithelial cells, since *Chlamydia*-infected cells would be able to present their chlamydial peptides to T cells [141].

We presented some qualitative analysis of the model and stability analysis of the *Chlamydia*-free equilibrium. Using optimal control theory, we derived and analysed the conditions for the optimal control/treatment of genital chlamydial infection. Existence and

uniqueness of the optimal controls were proved. We also characterised the controls using Pontryagin's Maximum Principle and the resulting optimality system was solved numerically.

Numerical results of the model indicated that an optimal and effective clearance of a *Chlamydia* infection may be achieved by the administration of a combined chemotherapy of drugs that are bacteriostatic on *Chlamydia* and of drugs that are proteasome-specific inhibiting. The results indicated that the optimal combination therapy is a dynamic one, in that the treatment is adjusted over the course of the treatment intervention whereby one begins with a (maximal) strong dosing scheme, followed by a lessening of treatment over time, either by the reduction of drug dosage or strength. The control problem also indicated that bacteriostatic agents that will increase the chances of the survival of healthy epithelial cells are especially essential for timely reduction of free extracellular *Chlamydia* and the overall clearance of a *Chlamydia* infection.

These suggested treatment strategies, which require that strong doses of the two drugs be administered and maintained within a therapeutic band for days, could mean that patients have to take multiple-doses of the treatment regimen. This is unrealistic because of the issue of patient compliance. However drug delivery systems that can make such treatment regimens a reality can be designed. Such systems can enhance the permeability and spatiotemporal release of chlamydial antibiotics (such as azithromycin, which already has a long half-life) at concentrations higher than the minimum inhibitory concentration (MIC) of *Chlamydia*, may facilitate its bioavailability at very high concentrations for several days. The use of a transdermal patch to constantly deliver desired concentrations of the drug over time may also be able to provide the therapeutically effective drug concentration that suits our model's suggested optimal treatment strategy. We suggest that therapeutic interventions that adhere to these control strategies may be very effective in combating *Chlamydia* infections. Our approach has provided a framework for the design of new protocols for optimal treatment strategies for genital chlamydial infections.

7.2.2 Model for the treatment of chronic chlamydial infection

Using a second optimal control model, we addressed the concern of the development of *Chlamydia* persistence, which causes severe sequelae in chronic chlamydial infections. As the literature suggest, the combination of a tryptophan and antibiotic treatment may facilitate an improved treatment of chronic *Chlamydia* infections characterised by chlamydial persistence. Our model used these two therapeutic strategies for the optimal treatment of chronic genital chlamydial infection. Specifically, the two therapeutic treatments explored are: (1) tryptophan supplement, in the form of 1-MT, which blocks the intracellular formation of persistent *Chlamydia*, while also facilitating the 'recovery' of persistently infected cells by reversing IFN-γ-induced persistence in intracellular *Chlamydia* (thereby increasing the susceptibility of *Chlamydia* to antibiotic treatment), and (2) bacteriostatic agents (which reduces the concentration of infected cells by blocking the intracellular

growth of *Chlamydia*, thereby inducing some chlamydial persistence). The model was used to determine optimal treatment strategies that not only minimise the production of free extracellular *Chlamydia*, but also minimise the production of persistent intracellular *Chlamydia* by blocking the formation of persistent *Chlamydia*, and reversing already established persistence into actively replicating *Chlamydia* forms, for clearance by the immune system and antibiotics. Basic qualitative analyses of the model were also done and existence results for the optimal controls were presented.

The presented optimal control model accounted for: (i) the blockage of IFN-γ-induced persistence by tryptophan supplementation; (ii) the reversal of established chlamydial persistence, either induced by IFN-γ or antibiotics, using tryptophan supplementation; (iii) the effects of the humoral and cell-mediated immune responses; (iv) the antimicrobial effects of an antibiotic therapy; (v) reduction of the production of EBs; and (vi) short duration of treatment with minimal dosage administration.

Numerical results of the model suggested that monotherapy with tryptophan supplement alone, suffices for the clearance of the chronic infection. Model results also suggested that the high immunomodulatory effects of the tryptophan supplement 1-MT is necessary for the treatment of a chronic chlamydial infection. The results also suggested that the optimal therapy is a dynamic one, in that the treatment is adjusted over the duration of the treatment, whereby one administers the maximum dosage for some days and then gradually lessens the treatment either in strength or concentration. As discussed in the previous section, the suggested treatment strategies could imply the use of multiple-dose treatment by patients, which may be impractical due to the common issue of patience compliance. Hence, we suggest that designs of drug delivery systems, which can ensure a controlled release/delivery of drugs over a particular period of time, while also maintaining the drugs' concentrations within a therapeutic band, can make such treatment regimens a reality.

Thus, we suggest that single therapy with a tryptophan supplement, in the presence of a strong immune system, may be the optimal course of action in the clearance of a chronic *Chlamydia* infection, as it aids the clearance of the pathogen itself, limitation of side effects of drugs, and the survival of healthy epithelial cells. Our model results also suggested that even if the immune system is not at its best, the optimal course of action in the clearance of the infection may be a combination therapy with a bacteriostatic agent and tryptophan supplement, as the bacteriostatic agent may clear the actively replicating *Chlamydia* while tryptophan aids with the clearance of persistence.

Importantly, we acknowledge the likely adverse impact of tryptophan on the host immune system. When a tryptophan supplement is taken, indoleamine 2,3-dioxygenase (IDO) 1 is expressed. This leads to tryptophan depletion and the generation of bioactive catabolites known as kynurenines. This process can induce the suppression of the innate and adaptive immunity by some cells of the immune system, thereby promoting tolerogenic responses. The kynurenine pathway of tryptophan catabolism modifies immunological

and neurological responses to inflammation. It promotes neurological comorbidities such as pain, depression, and fatigue [116]. These are undesirable health consequences. As such, the use of tryptophan supplements in the treatment of chronic chlamydial infection should be used with caution and subjected to thorough clinical tests. In addition, direct pharmacology for monotherapy and combination therapy of treatments need to be investigated further. We suggest that therapeutic interventions that adhere to these control strategies may be effective in treating chronic *Chlamydia* infections. The presented model and subsequent analysis has provided a framework for the design of new and improved treatment strategies for chronic chlamydial infection.

7.3 Model for an imperfect mucosal *Chlamydia* vaccine

It has been suggested that the development of a prophylactic *Chlamydia* vaccine is the only feasible solution to the effective population level control of chlamydial infections and its associated complications. We presented a model that uses a prototype mucosal vaccine that induces protective immunity like that described by the study of Stary *et al.* [149]. We have extended the mathematical modelling literature by theoretically assessing the potential role of such an imperfect anti-*Chlamydia* vaccine on the within-host dynamics of *C. trachomatis* and the prognosis for a genital chlamydial infection. We also explored how efficacious a *Chlamydia* vaccine should be if it must (1) elicit protective immunity against chlamydial challenge, and (2) efficiently clear a chlamydial infection upon a re-challenge with *Chlamydia*.

We carried out qualitative and stability analysis of the model. The model has a globally asymptotically stable *Chlamydia*-free equilibrium when its associated basic reproduction number $\mathcal{R}_0 \leq 1$. The model also has a unique *Chlamydia*-present equilibrium when the basic reproduction number $\mathcal{R}_0 > 1$. We also quantified how the variability in model parameters affect the value of the basic reproduction number $\mathcal{R}_0$ by carrying out sensitivity analysis of $\mathcal{R}_0$ to the parameters. We found that the parameter with the most significant (negative) correlation to $\mathcal{R}_0$ was the vaccine efficacy ε_v.

Model results indicated that that a vaccine with a critical efficacy of 86% may be required for the *in vivo* control of *Chlamydia* burden, which is characterised by the concentrations of infectious *Chlamydia* (EB forms) and of infected epithelial cells. Numerical results also show that for values of $\mathcal{R}_0 \leq 1$, the use of an imperfect *Chlamydia* vaccine may lead to the clearance of (intracellular and inter-cellular) *Chlamydia*. Importantly, we suggest that an imperfect *Chlamydia trachomatis* vaccine may proffer protective immunity against *Chlamydia* infection and facilitate immune-mediated clearance of *Chlamydia* if it can potentially recruit memory T cells that will induce (1) a decrease in the concentration of newly infected epithelial cells; (2) an increase in the concentration of extracellular *Chlamydia* engulfed by antibodies; (3) a boost in the protection of healthy epithelial cells from infection via antibody blocking. Candidate vaccines that possess similar properties may be efficacious in the *in vivo* control of *Chlamydia trachomatis* genital infection.

7.4 Limitations of study and potential future directions

We acknowledge that there are several limitations to this study. Some of them are listed below.

(i) Model parameters that describe biological processes may have been overestimated and may not accurately reflect *in vivo* dynamics of *Chlamydia* and the immune response. In particular, the effects of the cell-mediated immune response may have been over-emphasised, thereby resulting in an improved clearance of a chlamydial infection as compared to what happens *in vivo*. We suggest that collaboration with experimental scientists may facilitate the accurate development of more realistic mathematical models of chlamydial dynamics and the treatment of (chronic) chlamydial infection, especially in the estimation of parameters.

(ii) Results of the optimisation of the treatments are subject to change when weight parameters of the objective functionals are varied. Thus we suggest that future developments of these models that investigate numerical results when varying model parameters should be considered.

(iii) For the optimal control models, an investigation into the administration of the treatments/drugs at discrete time intervals may facilitate the investigation of more realistic treatment regimens based on the current treatment guidelines of genital chlamydial infections.

(iv) The presented models have been kept fairly generic and further studies are required for the development of more comprehensive models that accurately describes the complex within-host interaction between *Chlamydia*, host epithelial cells, and the host immune response.

(v) The use of tryptophan supplements can modify immunological and neurological responses to inflammation. Thus, its use in the combination therapy of chronic genital chlamydial infections should be subjected to further theoretical and clinical investigations. In addition, direct pharmacology for monotherapy and combination therapy of treatments need to be investigated further.

(vi) In the case of an infectious disease such as genital *Chlamydia*, it is not unreasonable to anticipate that the values of some (biological) parameters are patient specific. Consequently, there can be significant uncertainty in the determination of (biological) parameter values. Thus, the models presented in Chapters 3-5 could be usefully extended by the carrying out of uncertainty and sensitivity analyses.

A Mathematical Tools

A.1 LaSalle's Invariance Principle

The following definitions and theorems have been adapted from [88] and [1].

Consider the autonomous system

$$\dot{\mathbf{x}} = \mathbf{f}(\mathbf{x}),\ \mathbf{f}(\mathbf{0}) = \mathbf{0}, \tag{A.1}$$

where $\mathbf{x}$ is a vector of variables.

Definition A.1.1. *A set* $\mathbf{M}$ *is*

1. *an invariant set with respect to system* (A.1) *if*

$$\mathbf{x}(\mathbf{0}) \in \mathbf{M} \Rightarrow \mathbf{x}(\mathbf{t}) \in \mathbf{M},\ \forall\, t \in \mathbb{R}. \tag{A.2}$$

2. *a positively invariant set with respect to system* (A.1) *if*

$$\mathbf{x}(\mathbf{0}) \in \mathbf{M} \Rightarrow \mathbf{x}(\mathbf{t}) \in \mathbf{M},\ \forall\, t \geq 0. \tag{A.3}$$

Theorem A.1.1 (La Salle's Theorem)**.** *Let* $\bar{\Omega} \subset \bar{\mathcal{D}} \subset \mathbb{R}^n$ *be a compact positively invariant set with respect to the system dynamics* (A.1)*. Let* $\mathbf{f}(\mathbf{x})$ *be a locally Lipschitz function defined over the domain* $\bar{\mathcal{D}} \subset \mathbb{R}^n$*. Let* $V : \bar{\mathcal{D}} \to \mathbb{R}$*, where* $V(\mathbf{x})$ *is a continuously differentiable function, such that* $\dot{V}(\mathbf{x}) \leq 0$ *(negative semidefinite) in* $\bar{\Omega}$*. Let* $\bar{E}$ *be the set of all points in* $\bar{\Omega}$ *where* $\dot{V}(\mathbf{x}) = 0$*, and* $\mathbf{M}$ *is the largest invariant set in* $\bar{E}$*. Then, every solution starting in* $\bar{\Omega}$ *approaches* $\mathbf{M}$ *as* $t \longrightarrow \infty$*.*

Theorem A.1.2 (La Salle's Invariance Principle)**.** *Let* $\mathbf{f}(\mathbf{x})$ *be a locally Lipschitz function defined over the domain* $\bar{\mathcal{D}} \subset \mathbb{R}^n$ *which contains the origin (*$0 \in \bar{\mathcal{D}}$*). Let* $V : \bar{\mathcal{D}} \to \mathbb{R}$*, where* $V(\mathbf{x})$ *is a continuously differentiable positive definite function, such that* $\dot{V}(\mathbf{x}) \leq 0$ *(negative semidefinite) in* $\bar{\mathcal{D}}$*. Let* $\bar{S} = \left\{\mathbf{x} \in \bar{\mathcal{D}} | \dot{V}(\mathbf{x}) = 0\right\}$*.*

- *If no trajectory (solution) of the system can stay in* $\bar{S}$ *other than the trivial trajectory* $\mathbf{x}(\mathbf{0}) \equiv \mathbf{0}$*, then the origin is asymptotically stable.*

- *Moreover, if $\bar{\Omega} \subset \bar{\mathcal{D}}$ is compact and positively invariant, then it is a subset of the region of attraction.*
- *Furthermore, if $\bar{\mathcal{D}} \subset \mathbb{R}^n$ and $V(\mathbf{x})$ is radially unbounded, that is, $V(\mathbf{x}) \longrightarrow \infty$, as $\|\mathbf{x}\| \to \infty$, then the origin is globally asymptotically stable.*

A.2 Mayer Form of an Optimal Control Problem

Consider an optimal control problem with system equations

$$\dot{x}(t) = f(t, x(t), u_1(t), u_2(t)), \quad t_0 \leq t \leq t_f, \tag{A.4}$$

where the vector $x \in \mathbb{R}^n$ denotes the state system, $(u_1^*, u_2^*) \in \Gamma$, where Γ, the set of admissible controls is defined as

$$\Gamma = \{(u_1, u_2) | u_1 \text{ and } u_2 \text{ are Lebesgue measurable}, a \leq u_1 \leq b,\ a \leq u_2 \leq b, t \in [t_0, t_f]\}, \tag{A.5}$$

and $x(t_0) = x_0$ are the initial conditions. Let the objective functional of the system be

$$J(u_1, u_2) = \int_{t_0}^{t_f} G(t, x(t), u_1(t), u_2(t))\mathrm{d}t + \phi(x(t_f)), \tag{A.6}$$

where $\phi(x(t_f))$, called the payoff term, is a goal with respect to the final state $x(t_f)$.

The optimal control problem defined above is in the Bolza (functional) form. Every problem in this form can be converted into an equivalent problem in Mayer form [23, 25, 124].

The Bolza form can be reformulated into the Mayer form by the introduction of an auxiliary state variable $x_a(t)$, which is defined by the differential equation (DE)

$$\dot{x_a}(t) = G(t, x(t), u_1(t), u_2(t)), \tag{A.7}$$

with initial condition $x_a(t_0) = 0$. This initial value problem can then be inserted into the the DE in Equation (A.4) alongside $x(t)$.

The equivalent optimal control formulation, the Mayer form, is then obtained as:

$$\begin{aligned} \text{minimise}: \quad & J(u_1, u_2) = x_a(t_f) + \phi(x(t_f)), \\ \text{subject to}: \quad & \dot{x}(t) = f(t, x(t), u_1(t), u_2(t)); \quad x(t_0) = x_0 \\ & \dot{x_a}(t) = G(t, x(t), u_1(t), u_2(t)); \quad x_a(t_0) = 0 \\ & t_0 \leq t \leq t_f. \end{aligned} \tag{A.8}$$

A.3 Pontryagin's Maximum Principle

Consider the optimal control problem (A.4)-(A.6). The Pontryagin's Maximum Principle (PMP) converts the problem of finding controls that minimise the objective functional subject to the differential equation and initial condition, to that of the point-wise minimisation of a Hamiltonian with respect to the controls [100, Page 14]. Using Theorems 1.2 and 1.3 of Lenhart and Workman [100, Page 13], including the remarks that follow, the implementation of the PMP is summarised as follows. To use the PMP, we need to form a set of necessary conditions that an optimal control pair $(u_1^*(t), u_2^*(t))$ for the system (A.4)-(A.6) must satisfy.

1. Introduce adjoint variable $\lambda(t)$, like a Lagrange multiplier.
2. Generate the necessary conditions by forming the Hamiltonian H,

$$\begin{aligned} H(t, x(t), u_1(t), u_2(t), \lambda(t)) &= G(t, x(t), u_1(t), u_2(t)) + \lambda(t) f(t, x(t), u_1(t), u_2(t)), \\ &\equiv \text{integrand} + \text{adjoint} * \text{RHS of DE}. \end{aligned} \tag{A.9}$$

3. Minimise the Hamiltonian with respect to (u_1, u_2) at (u_1^*, u_2^*) (over all *admissible* controls, that is, all controls that adhere to the bounds on u_1 and u_2) to obtain the *optimality condition*

$$\begin{aligned} \frac{\partial \mathrm{H}}{\partial \mathrm{u_1}} &= G_{u_1}(t, x^*(t), u_1^*(t), u_2^*(t)) + \lambda(t) f_{u_1}(t, x^*(t), u_1^*(t), u_2^*(t)) = 0 \\ \frac{\partial \mathrm{H}}{\partial \mathrm{u_2}} &= G_{u_2}(t, x^*(t), u_1^*(t), u_2^*(t)) + \lambda(t) f_{u_2}(t, x^*(t), u_1^*(t), u_2^*(t)) = 0 \end{aligned} \tag{A.10}$$

4. Write the adjoint differential equation and the transversality boundary conditions. The *adjoint equation* is

$$\dot{\lambda}(t) = -\frac{\partial \mathrm{H}(t, x^*(t), u_1^*(t), u_2^*(t))}{\partial \mathrm{x}}, \tag{A.11}$$

with boundary condition (*transversality condition*)

$$\lambda(t_f) = \dot{\phi}(x^*(t_f). \tag{A.12}$$

There are now four unknowns, viz $u_1^*(t)$, $u_2^*(t)$, $x^*(t)$, and $\lambda(t)$.

5. Solve the optimality Equations (A.10) for $u_1^*(t)$ and $u_2^*(t)$ in terms of $x^*(t)$, and $\lambda(t)$. This will eliminate $u_1^*(t)$ and $u_2^*(t)$. Due to the bounds on u_1 and u_2 (see Equation (A.5) and Sections 8.1 and 12.1 of [100]), the optimal controls $u_1^*(t)$ and $u_2^*(t)$ will have the following expression:

$$u_1^* = \begin{cases} a & \text{if} \quad \dfrac{\partial \mathrm{H}}{\partial \mathrm{u}_1} \geq 0 \\ a \leq u_1^* \leq b & \text{if} \quad \dfrac{\partial \mathrm{H}}{\partial \mathrm{u}_1} = 0 \\ b & \text{if} \quad \dfrac{\partial \mathrm{H}}{\partial \mathrm{u}_1} \leq 0 \end{cases}, \tag{A.13}$$

$$u_2^* = \begin{cases} a & \text{if} \quad \dfrac{\partial \mathrm{H}}{\partial \mathrm{u}_2} \geq 0 \\ a \leq u_2^* \leq b & \text{if} \quad \dfrac{\partial \mathrm{H}}{\partial \mathrm{u}_2} = 0 \\ b & \text{if} \quad \dfrac{\partial \mathrm{H}}{\partial \mathrm{u}_2} \leq 0 \end{cases}. \tag{A.14}$$

6. Substitute for the expressions of the *characterisation of the optimal control*, which is obtained from Equations (A.13) and (A.14), in the two differential Equations (A.4) and (A.11). These, together with the two boundary conditions form the *optimality system*. Solve the optimality system.
7. Finally, after finding the optimal state and adjoint, solve for the optimal control.

A.4 Next Generation Method (NGM): Necessary Assumptions

Below are the assumptions that the functions described in Equations (4.10) and (4.11) (and consequently those described in Equations (4.14), and (4.15), for the basic *Chlamydia* model system (4.1)-(4.3)) satisfy, according to Driessche and Watmough [157].

(A1) *If $x \geq 0$, then $\mathcal{F}_i$, $\mathcal{V}_i^+$, $\mathcal{V}_i^- \geq 0$ for $i = 1, \ldots, n$.*
Since each function represents a directed transfer of individuals/species, they are all non-negative.

(A2) *If $x_i = 0$, then $\mathcal{V}_i^- = 0$. In particular, if $x \in \mathbf{X}_s$, then $\mathcal{V}_i^- = 0$ for $i = 1, \ldots, m$.*
If the compartment is empty, then there can be no transfer of individuals out of the compartment by death, infection, nor any other means.

(A3) *$\mathcal{F}_i = 0$ if $i > m$.*
This is true because of the simple fact that the incidence of infection for uninfected compartments is zero.

(A4) *If $x \in \mathbf{X}_s$, then $\mathcal{F}_i(x) = 0$ and $\mathcal{V}_i^+ = 0$ for $i = 1, \ldots, m$.*
To ensure that the disease free subspace is invariant, we assume that if the population is free of disease then the population will remain free of disease. That is, there is no (density independent) immigration of infectives.

(A5) *If $\mathcal{F}$ is set to zero, then all eigenvalues of $Df(x_0)$ have negative real parts, where x_0 is the disease free equilibrium.*
This condition is based on the derivatives of f near a disease-free-equilibrium (DFE). Here, a DFE of (4.11) *is defined to be a (locally asymptotically) stable equilibrium solution of the disease free model* (4.11)*, that is,* (4.11) *restricted to $\mathbf{X}_s$. Note that we need not assume that the model has a unique DFE. Consider a population near the DFE x_0. If the population remains near the DFE (that is, if the introduction of a few infective individuals does not result in an epidemic) then the population will return to the DFE according to the linearized system*

$$\dot{x} = Df(x_0)(x - x_0), \tag{A.15}$$

where $Df(x_0)$ is the derivative $\partial f_i / \partial x_j$ evaluated at the DFE, x_0 (that is, the Jacobian matrix). Here, and in what follows, some derivatives are one sided, since x_0 is on the domain boundary. We restrict our attention to systems in which the DFE is stable in the absence of new infection. Hence the above condition is valid.

B Appendix

B.1 Investigating the Effects of Varying Weight Parameters(Chapter 4 Model)

In this section, we investigate and discuss the effects of different weight parameter combination on the qualitative results of the optimal control problem (this include the time series of interacting species, the optimal controls, and the corresponding values of the objective functional). In these investigations, both treatment controls are used.

In Figure B.1, higher weightings of A_1 were tested. These do not result in any improvement in the prognosis of the infection as Figures B.1 (a)-(c) reflect. Moreover, for higher A_1 values, treatment u_2 (proteasome-specific inhibitor) is required to be given for a fairly longer time, while its effect on treatment u_1 (bacteriostatic agent) is imperceptible. The values of the objective functional also increased significantly for increasing values of A_1, which do not lead to the minimisation of the systemic costs of the treatments as required. These results suggest that heavier penalisation of the systemic cost of minimising the concentration of infected cells would require longer administration of the proteasome-specific inhibiting treatment, which acts intracellularly (within infected cell before lysis), despite the fact that it does not affect clinical outcomes.

In Figure B.2, higher weightings of A_2 were tested, which allowed for imperceptibly shorter, and slightly higher treatment doses of treatments u_1 and u_2, respectively, for increasing values of A_2. However, these do not result in any improvement in the prognosis of the infection as Figures B.2 (a)-(c) reflect. Nevertheless, the values of the objective functional increased for increasing values of A_2, which do not lead to the minimisation of the systemic costs of the treatments as required. These results suggest that heavier penalisation of the systemic cost of using treatment u_1, that is increased toxicity of the bacteriostatic treatement (antibiotics), does not really affect clinical outcomes, but the relative doses of the treatments as a function of drug toxicity.

In Figure B.3, higher weightings of A_3 were tested, which allowed for slightly higher treatment doses of treatments u_2 only, for increasing values of A_3. It's effect on treatment u_1 is imperceptible. However, these do not result in any improvement in the prognosis

of the infection as Figures B.3 (a)-(c) reflect. Nevertheless, the values of the objective functional insignificantly increased for increasing values of A_3, which do not lead to the minimisation of the systemic costs of the treatments as required. These results suggest that heavier penalisation of the systemic cost of using treatment u_2, that is increased toxicity of the proteasome-specific inhibiting treatment, does not really affect clinical outcomes, but the relative doses of the treatments as a function of drug toxicity.

In Figure B.4, higher weightings of A_4 were tested. The optimal control solution predicts that for heavier penalisation of the systemic cost of minimising the concentration of *Chlamydia* at the end of the treatment, the bacteriostatic treatment should be given at the maximum tolerable dose by the end of the treatment. It's effect on treatment u_2 is imperceptible. Nevertheless, all these do not result in any improvement in the prognosis of the infection as Figures B.4 (a)-(c) reflect. Furthermore, the values of the objective functional increased slightly for increasing values of A_4, which do not lead to the minimisation of the systemic costs of the treatments as required.

In Figure B.5, higher weightings of A_5 were tested, which allowed for imperceptibly longer doses of both treatments u_1 and u_2, for increasing values of A_5. These do not result in improved clinical outcomes of the infection as Figures B.5 (a)-(c) reflect. Nevertheless, the values of the objective functional slightly increased for increasing values of A_5, which do not lead to the minimisation of the systemic costs of the treatments as required.

Table B.1 below gives a summary of variation in the weight parameters (A_1, A_2, A_3, A_4, and A_5) on the values of the state variables (C_{end}, E_{end}, and I_{end}), objective functional (J_{end}), and the controls ($u_{1_{end}}$ and $u_{2_{end}}$), at the end of the treatment.

A_1	A_2	A_3	A_4	A_5	C_{end}	E_{end}	I_{end}	J_{end}	$u_{1_{end}}$	$u_{2_{end}}$
5	50	50	1	5	0.2877	163.3260	0.0421	126.8092	0.3145	0.0046
50	50	50	1	5	0.2439	163.3358	0.0348	341.5589	0.2742	0.0048
100	50	50	1	5	0.2114	163.3428	0.0296	577.1924	0.2454	0.0050
200	50	50	1	5	0.1613	163.3525	0.0219	1047.9274	0.1982	0.0051
300	50	50	1	5	0.1358	163.3560	0.0183	1518.6548	0.1780	0.0053
5	100	50	1	5	0.5682	163.2724	0.0829	219.1615	0.3113	0.0088
5	200	50	1	5	1.1705	163.1533	0.1724	402.1073	0.3245	0.0182
5	300	50	1	5	1.6938	163.0559	0.2467	584.0970	0.3110	0.0266
5	50	100	1	5	0.2890	163.3256	0.0423	127.0333	0.3160	0.0024
5	50	200	1	5	0.2896	163.3254	0.0424	127.2120	0.3167	0.0011
5	50	300	1	5	0.2899	163.3254	0.0425	127.3423	0.3170	0.0008
5	50	50	5	5	0.1067	163.3584	0.0172	127.7434	0.4624	0.0056
5	50	50	10	5	0.0602	163.3680	0.0100	128.3081	0.5047	0.0057
5	50	50	50	5	0.0189	163.3422	0.0177	129.1780	1.0000	0.0007
5	50	50	1	10	0.2018	163.3434	0.0289	127.1726	0.2782	0.0040
5	50	50	1	20	0.1240	163.3587	0.0174	127.6703	0.2403	0.0035
5	50	50	1	50	0.0585	163.3691	0.0081	128.4144	0.2118	0.0031
5	50	50	1	100	0.0311	163.3743	0.0043	129.0537	0.2001	0.0032

Table B.1: Summary of variations in the weight parameters and their corresponding effects.

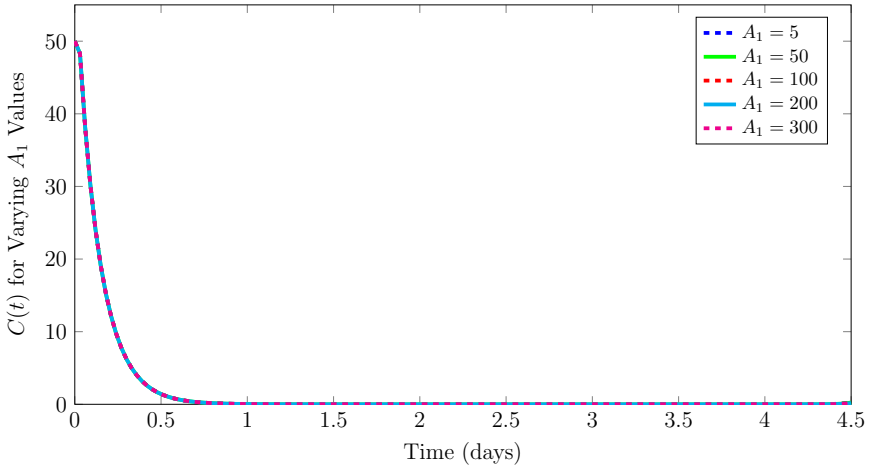
$C(t)$ for Varying A_1 Values
Time (days)
$A_1 = 5$
$A_1 = 50$
$A_1 = 100$
$A_1 = 200$
$A_1 = 300$

(a)

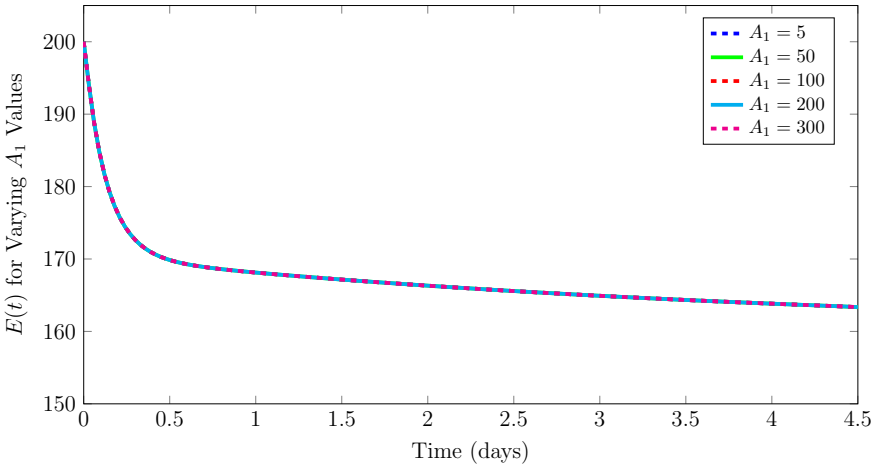
$E(t)$ for Varying A_1 Values
Time (days)
$A_1 = 5$
$A_1 = 50$
$A_1 = 100$
$A_1 = 200$
$A_1 = 300$

(b)

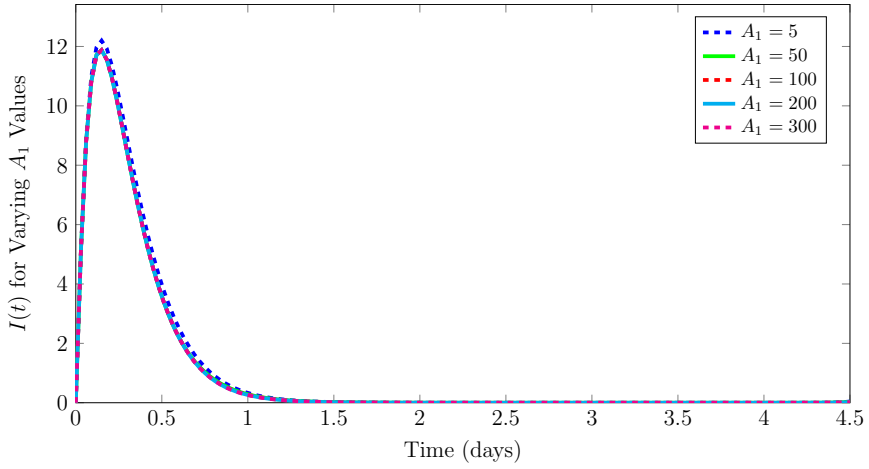
$I(t)$ for Varying A_1 Values
Time (days)
$A_1 = 5$
$A_1 = 50$
$A_1 = 100$
$A_1 = 200$
$A_1 = 300$

(c)

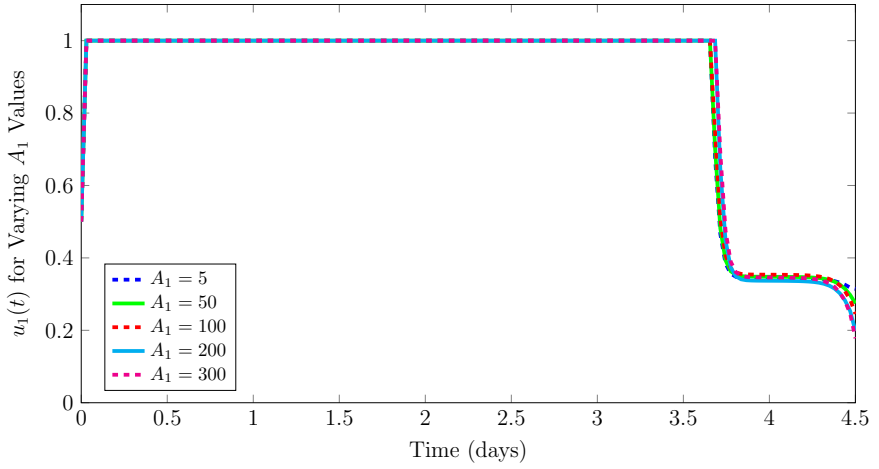
$u_1(t)$ for Varying A_1 Values
Time (days)
$A_1 = 5$
$A_1 = 50$
$A_1 = 100$
$A_1 = 200$
$A_1 = 300$

(d)

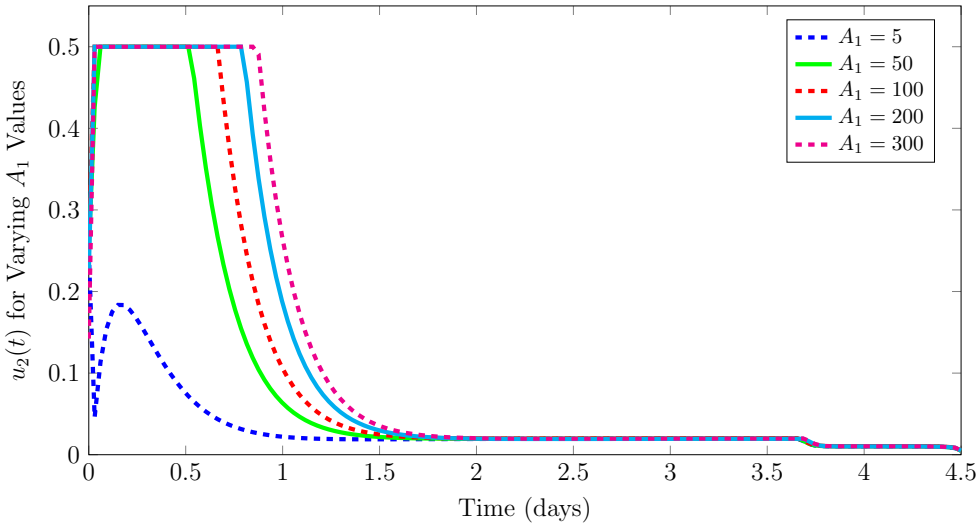

(e)

Figure B.1: Time series of *Chlamydia* model (4.4)-(4.6) showing the effect of variation in the value of the weight parameter A_1 ($A_1 \in [5, 50, 100, 200, 300]$, with objective functional values $(126.8092, 341.5590, 577.1926, 1047.9277, 1518.6331)$, respectively) on the concentrations of interacting species (a) $C(t)$, free extracellular chlamydial particles, (b) $E(t)$, healthy epithelial cells, and (c) $I(t)$, *Chlamydia*-infected epithelial cells, and on the optimal evolution for both controls (d) u_1 (optimal bacteriostatic treatment), and (e) u_2 (optimal proteasome-specific inhibitor). Other weight parameters are fixed ($(A_2, A_3, A_4, A_5) = (50, 50, 1, 5)$).

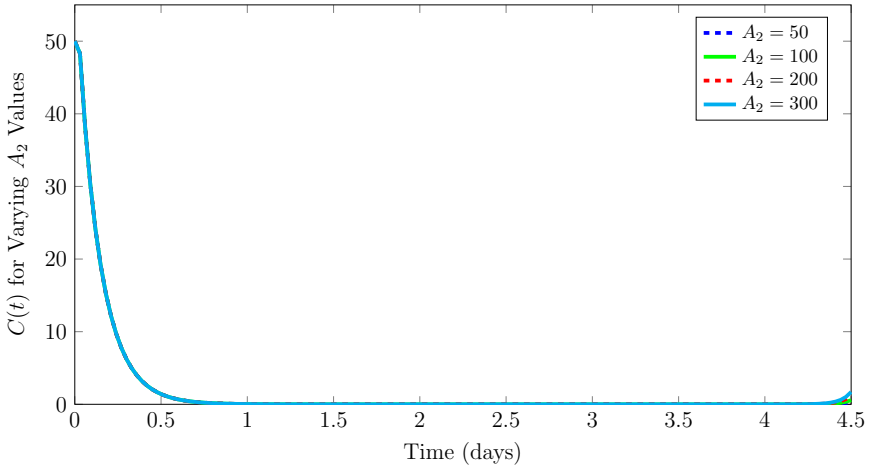
$C(t)$ for Varying A_2 Values
Time (days)
$A_2 = 50$
$A_2 = 100$
$A_2 = 200$
$A_2 = 300$

(a)

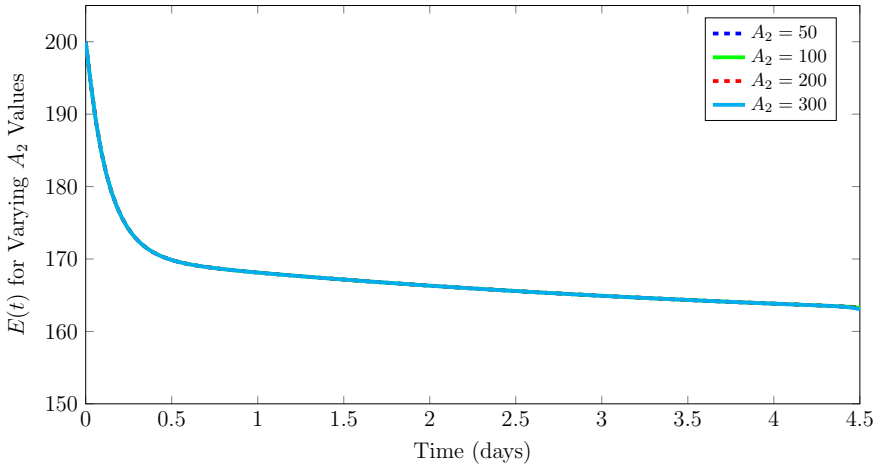
$E(t)$ for Varying A_2 Values
Time (days)
$A_2 = 50$
$A_2 = 100$
$A_2 = 200$
$A_2 = 300$

(b)

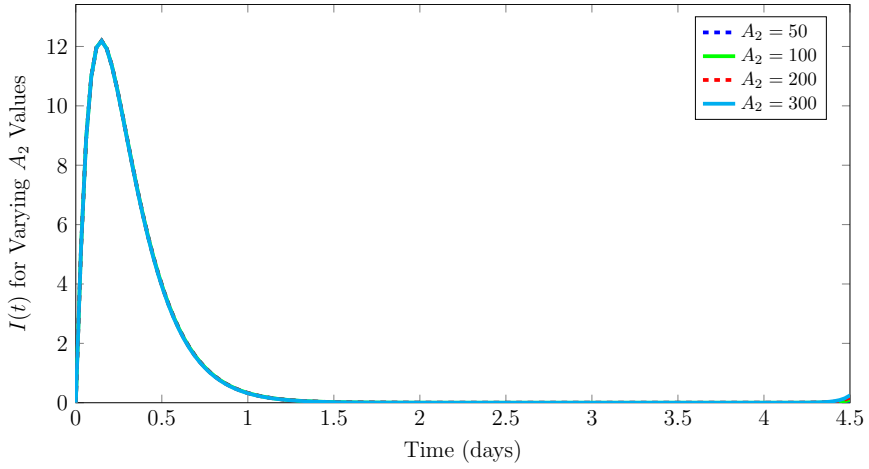
$I(t)$ for Varying A_2 Values
Time (days)
$A_2 = 50$
$A_2 = 100$
$A_2 = 200$
$A_2 = 300$

(c)

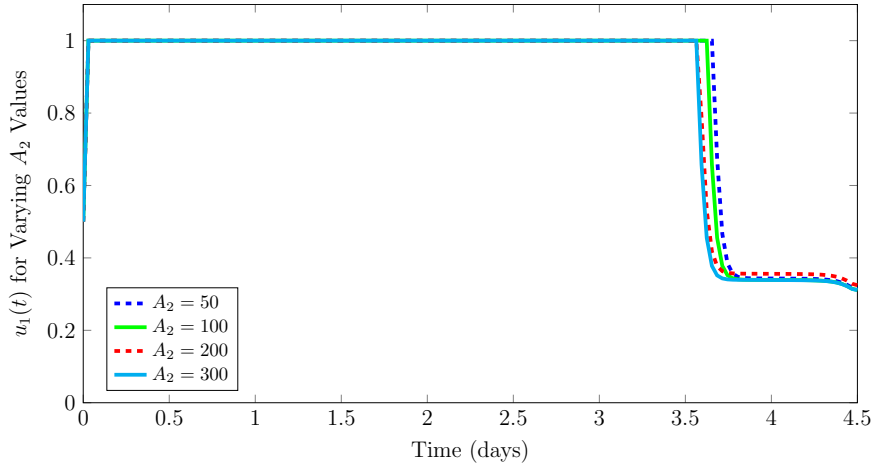
$u_1(t)$ for Varying A_2 Values
Time (days)
$A_2 = 50$
$A_2 = 100$
$A_2 = 200$
$A_2 = 300$

(d)

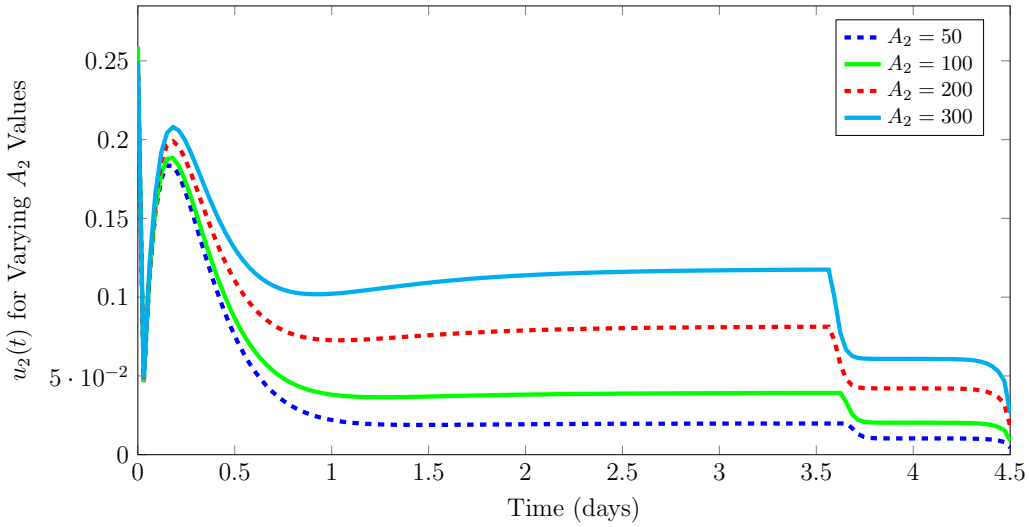

(e)

Figure B.2: Time series of *Chlamydia* model (4.4)-(4.6) showing the effect of variation in the value of the weight parameter A_2 ($A_2 \in [50, 100, 200, 300]$, with objective functional values $(126.8092, 219.1615, 402.1073, 584.0970)$, respectively) on the concentrations of interacting species (a) $C(t)$, free extracellular chlamydial particles, (b) $E(t)$, healthy epithelial cells, and (c) $I(t)$, *Chlamydia*-infected epithelial cells, and on the optimal evolution for both controls (d) u_1 (optimal bacteriostatic treatment), and (e) u_2 (optimal proteasome-specific inhibitor). Other weight parameters are fixed ($(A_1, A_3, A_4, A_5) = (5, 50, 1, 5)$).

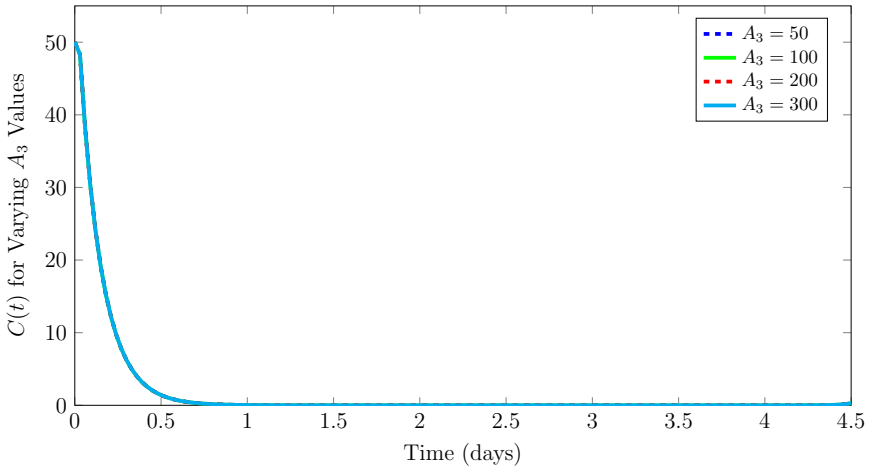
$C(t)$ for Varying A_3 Values
Time (days)
$A_3 = 50$
$A_3 = 100$
$A_3 = 200$
$A_3 = 300$

(a)

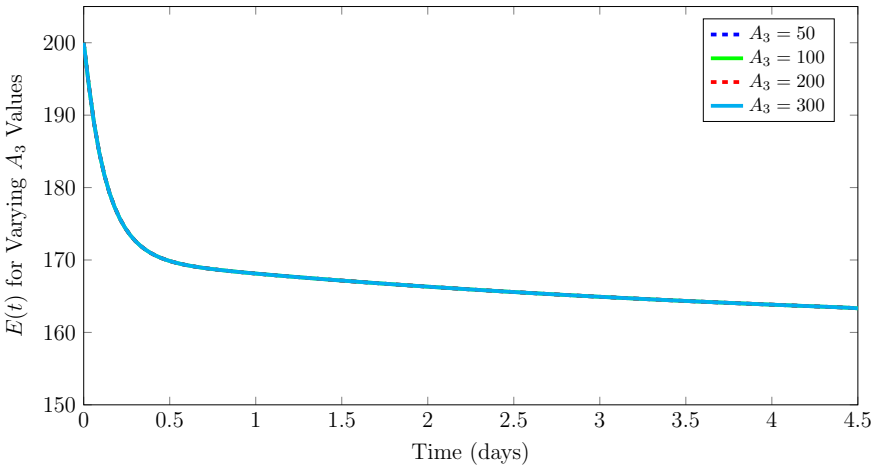
$E(t)$ for Varying A_3 Values
Time (days)
$A_3 = 50$
$A_3 = 100$
$A_3 = 200$
$A_3 = 300$

(b)

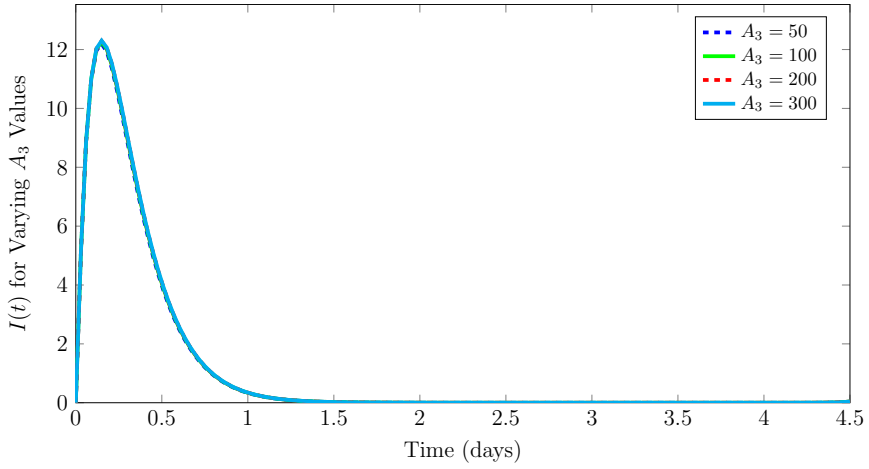
$I(t)$ for Varying A_3 Values
Time (days)
$A_3 = 50$
$A_3 = 100$
$A_3 = 200$
$A_3 = 300$

(c)

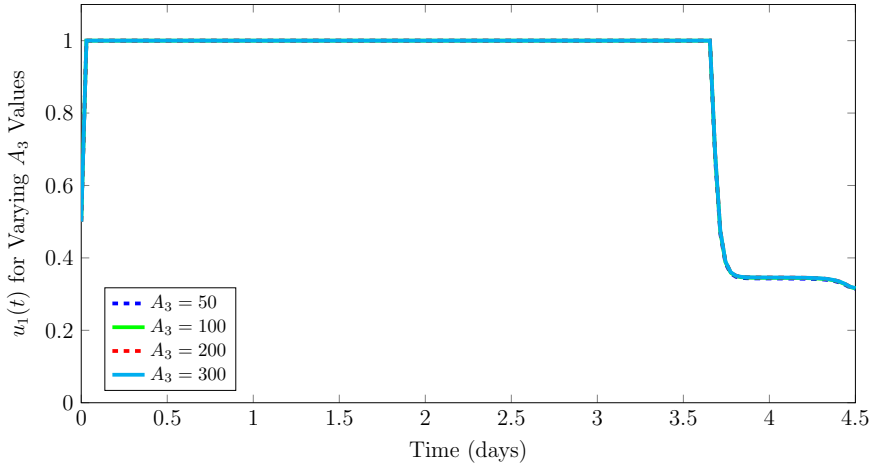
$u_1(t)$ for Varying A_3 Values
Time (days)
$A_3 = 50$
$A_3 = 100$
$A_3 = 200$
$A_3 = 300$

(d)

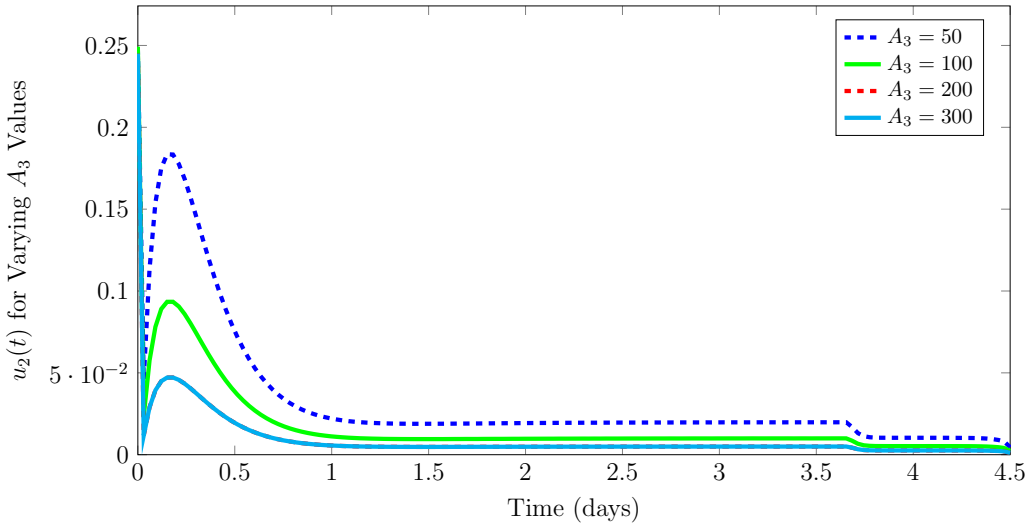

(e)

Figure B.3: Time series of *Chlamydia* model (4.4)-(4.6) showing the effect of variation in the value of the weight parameter A_3 ($A_3 \in [50, 100, 200, 300]$, with objective functional values $(126.8092, 127.0333, 127.2120, 127.3423)$, respectively) on the concentrations of interacting species (a) $C(t)$, free extracellular chlamydial particles, (b) $E(t)$, healthy epithelial cells, and (c) $I(t)$, *Chlamydia*-infected epithelial cells, and on the optimal evolution for both controls (d) u_1 (optimal bacteriostatic treatment), and (e) u_2 (optimal proteasome-specific inhibitor). Other weight parameters are fixed ($(A_1, A_2, A_4, A_5) = (5, 50, 1, 5)$).

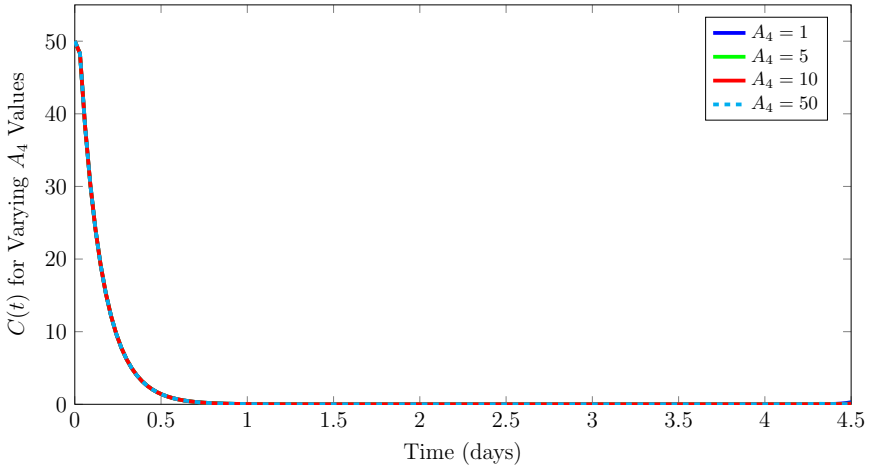
$C(t)$ for Varying A_4 Values
Time (days)
$A_4 = 1$
$A_4 = 5$
$A_4 = 10$
$A_4 = 50$

(a)

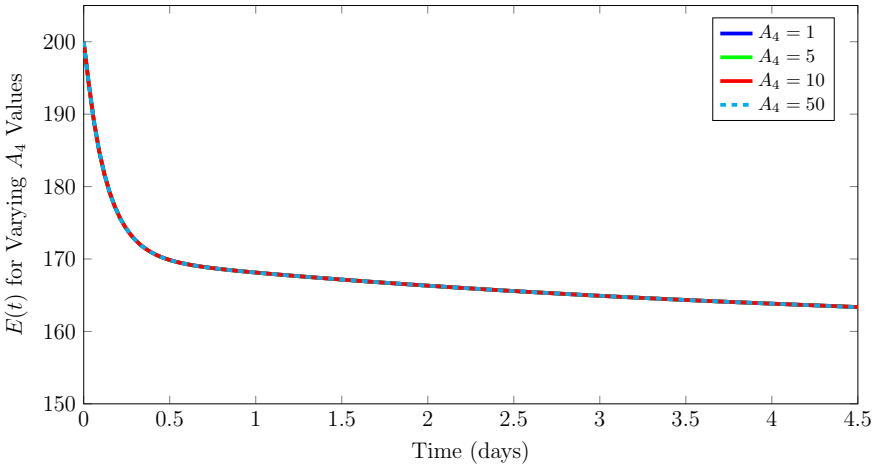
$E(t)$ for Varying A_4 Values
Time (days)
$A_4 = 1$
$A_4 = 5$
$A_4 = 10$
$A_4 = 50$

(b)

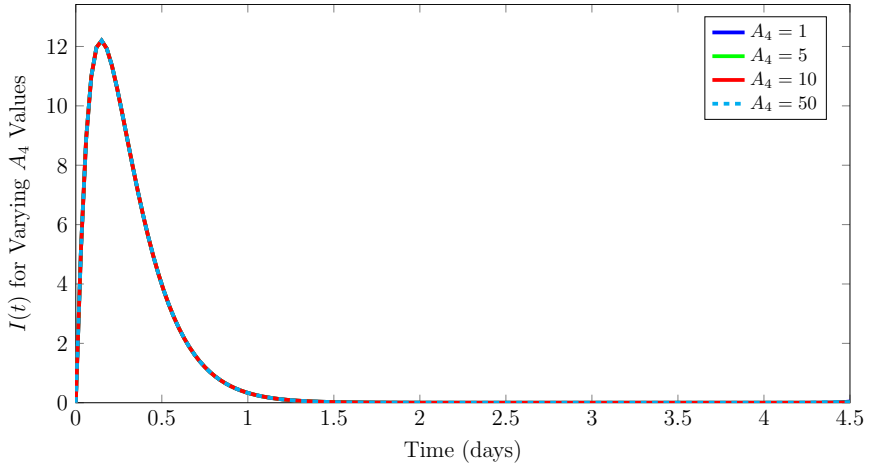
$I(t)$ for Varying A_4 Values
Time (days)
$A_4 = 1$
$A_4 = 5$
$A_4 = 10$
$A_4 = 50$

(c)

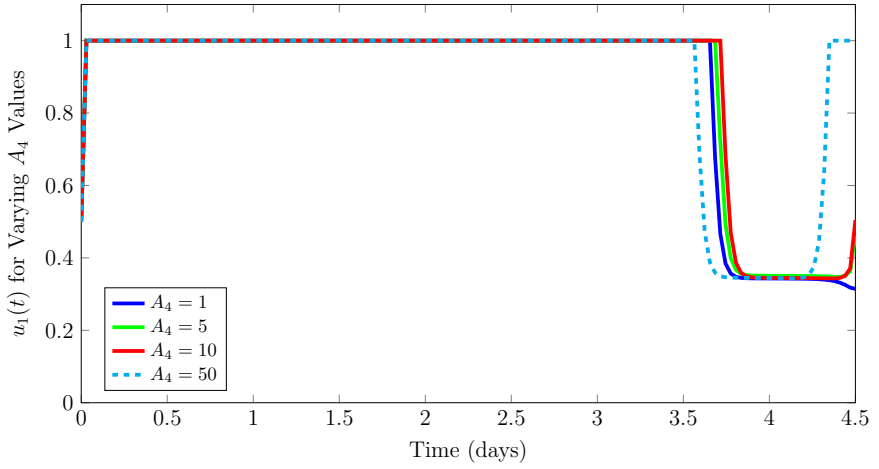
$u_1(t)$ for Varying A_4 Values
Time (days)
$A_4 = 1$
$A_4 = 5$
$A_4 = 10$
$A_4 = 50$

(d)

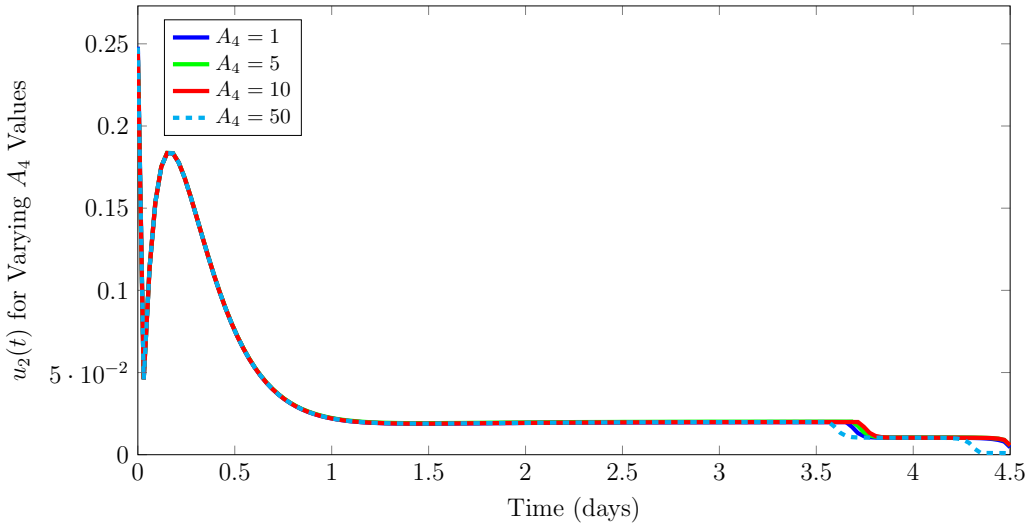

(e)

Figure B.4: Time series of *Chlamydia* model (4.4)-(4.6) showing the effect of variation in the value of the weight parameter A_4 ($A_4 \in [1, 5, 10, 20, 50, 100]$, with objective functional values $(126.8092, 127.7434, 128.3081, 142.8141, 129.1780, 145.6416)$, respectively) on the concentrations of interacting species (a) $C(t)$, free extracellular chlamydial particles, (b) $E(t)$, healthy epithelial cells, and (c) $I(t)$, *Chlamydia*-infected epithelial cells, and on the optimal evolution for both controls (d) u_1 (optimal bacteriostatic treatment), and (e) u_2 (optimal proteasome-specific inhibitor). Other weight parameters are fixed ($(A_1, A_2, A_3, A_5) = (5, 50, 50, 5)$).

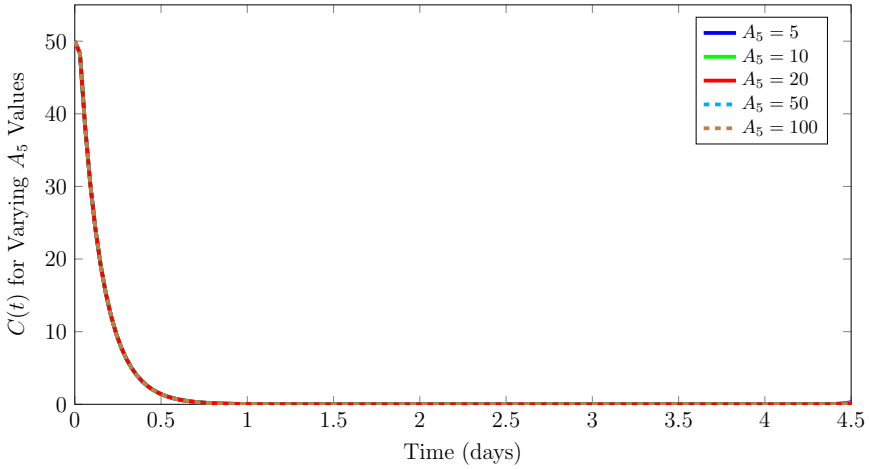
$C(t)$ for Varying A_5 Values
Time (days)
$A_5 = 5$
$A_5 = 10$
$A_5 = 20$
$A_5 = 50$
$A_5 = 100$

(a)

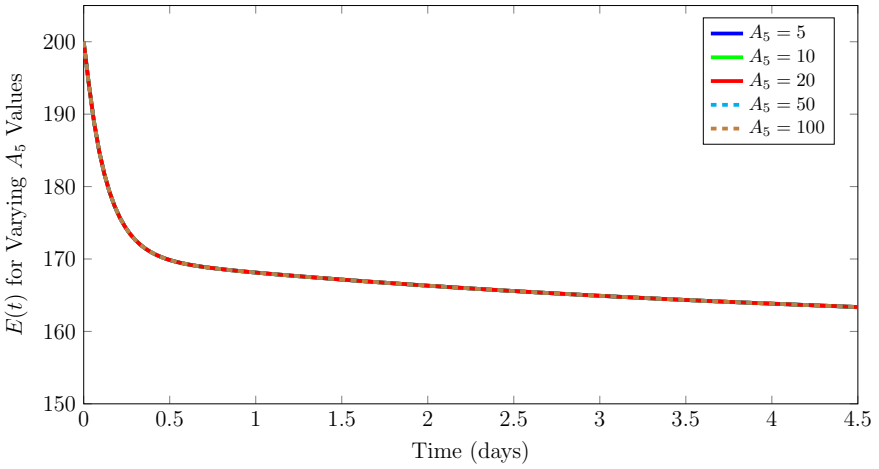
$E(t)$ for Varying A_5 Values
Time (days)
$A_5 = 5$
$A_5 = 10$
$A_5 = 20$
$A_5 = 50$
$A_5 = 100$

(b)

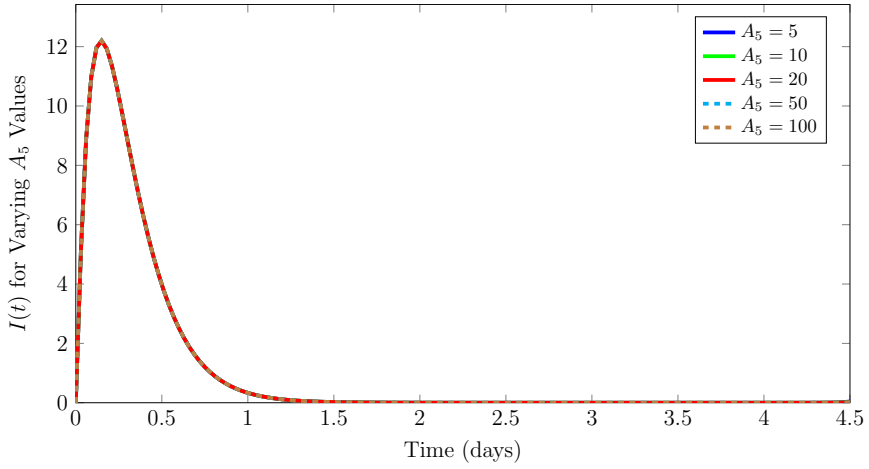
$I(t)$ for Varying A_5 Values
Time (days)
$A_5 = 5$
$A_5 = 10$
$A_5 = 20$
$A_5 = 50$
$A_5 = 100$

(c)

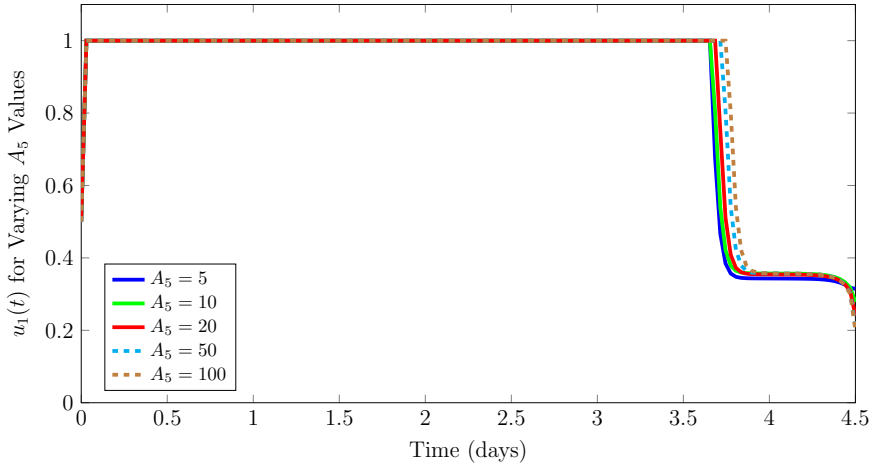
$u_1(t)$ for Varying A_5 Values
Time (days)
$A_5 = 5$
$A_5 = 10$
$A_5 = 20$
$A_5 = 50$
$A_5 = 100$

(d)

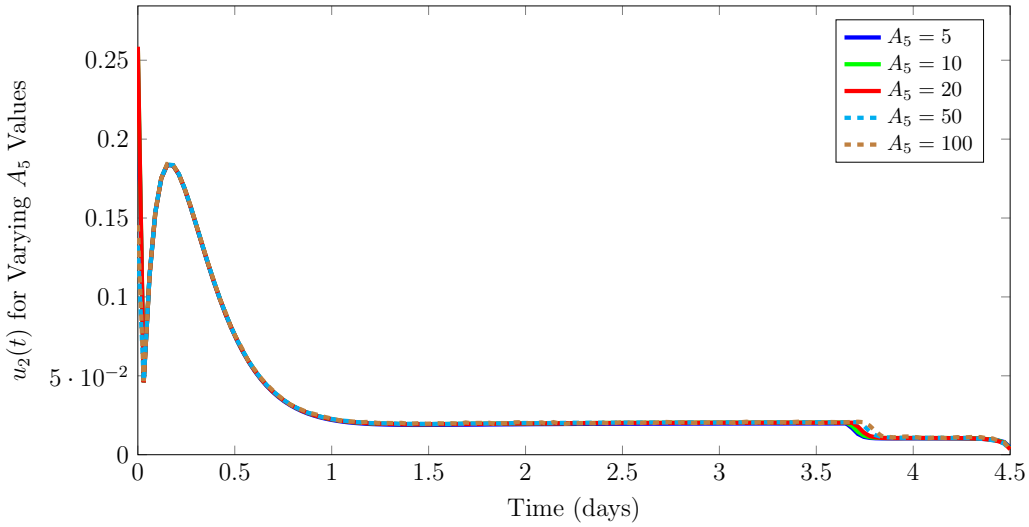

(e)

Figure B.5: Time series of *Chlamydia* model (4.4)-(4.6) showing the effect of variation in the value of the weight parameter A_5 ($A_5 \in [5, 10, 20, 50, 100]$, with objective functional values $(126.8092, 127.1726, 127.6703, 128.4144, 129.0537)$, respectively) on the concentrations of interacting species (a) $C(t)$, free extracellular chlamydial particles, (b) $E(t)$, healthy epithelial cells, and (c) $I(t)$, *Chlamydia*-infected epithelial cells, and on the optimal evolution for both controls (d) u_1 (optimal bacteriostatic treatment), and (e) u_2 (optimal proteasome-specific inhibitor). Other weight parameters are fixed ($(A_1, A_2, A_3, A_4) = (5, 50, 50, 1)$).

B.2 Investigating the Effects of Varying Final Treatment Time (Chapter 4 Model)

In this section, we investigate and discuss the effects of different final time of treatment on the qualitative results of the optimal control problem (this include the time series of interacting species, the optimal controls, and the corresponding values of the objective functional). In these investigations, both treatment controls are used.

In Figure B.6, different values of T_f were tested, which allowed for longer treatment doses of both treatments u_1 (bacteriostatic treatment), and u_2 (proteasome-specific inhibitor), for increasing values of T_f. However, these do not result in any improvement in the prognosis of the infection as Figures B.6 (a)-(c) reflect. Nevertheless, the values of the objective functional increased quite significantly for increasing values of T_f, which do not lead to the minimisation of the systemic costs of the treatments as required. These results suggest that increasing the duration of treatment will not necessarily yield better clinical outcomes.

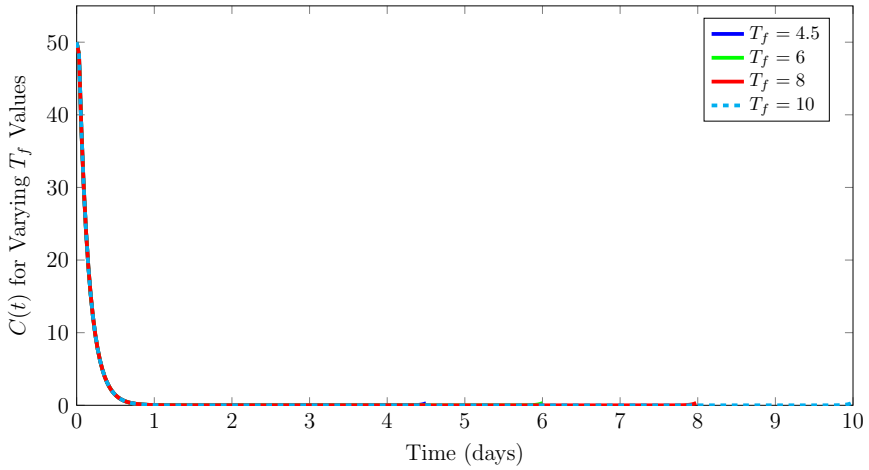
$C(t)$ for Varying T_f Values
Time (days)
$T_f = 4.5$
$T_f = 6$
$T_f = 8$
$T_f = 10$

(a)

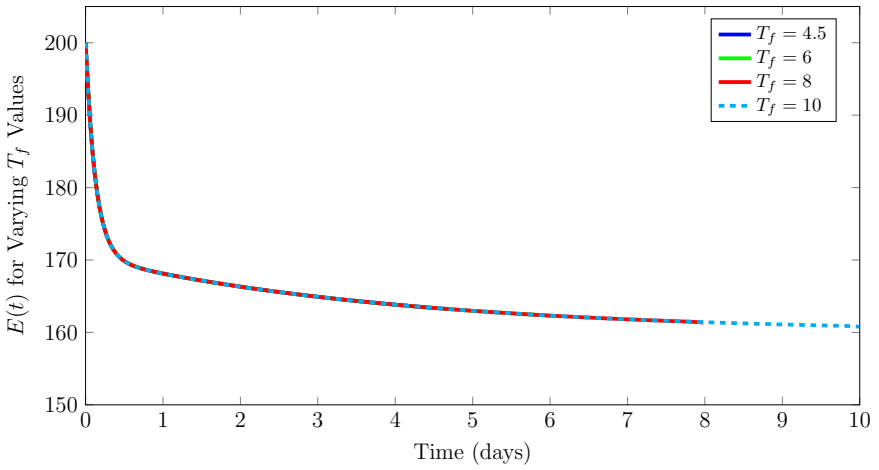
$E(t)$ for Varying T_f Values
Time (days)
$T_f = 4.5$
$T_f = 6$
$T_f = 8$
$T_f = 10$

(b)

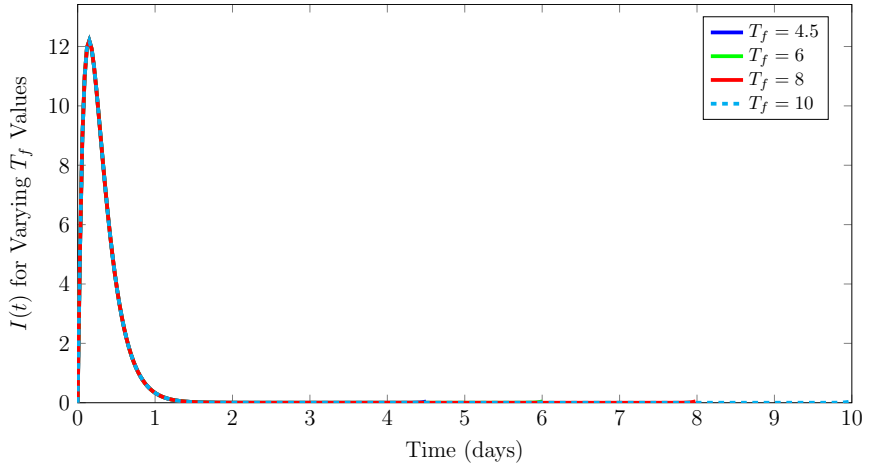
$I(t)$ for Varying T_f Values
Time (days)
$T_f = 4.5$
$T_f = 6$
$T_f = 8$
$T_f = 10$

(c)

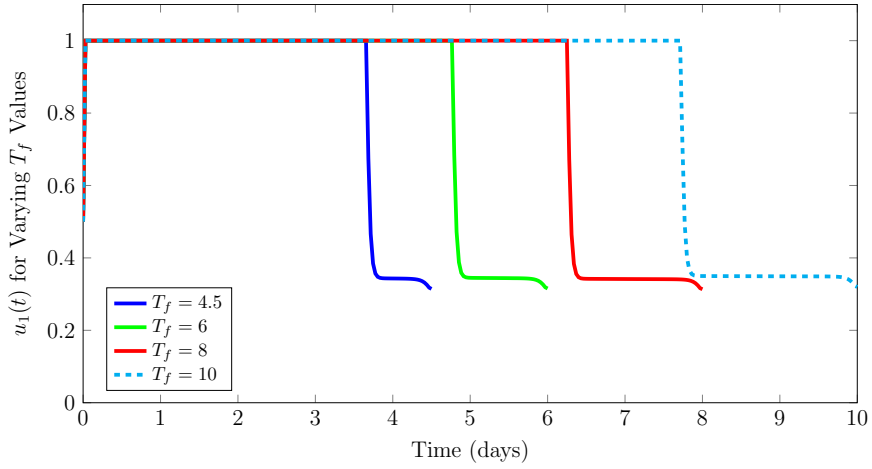
$u_1(t)$ for Varying T_f Values
Time (days)
$T_f = 4.5$
$T_f = 6$
$T_f = 8$
$T_f = 10$

(d)

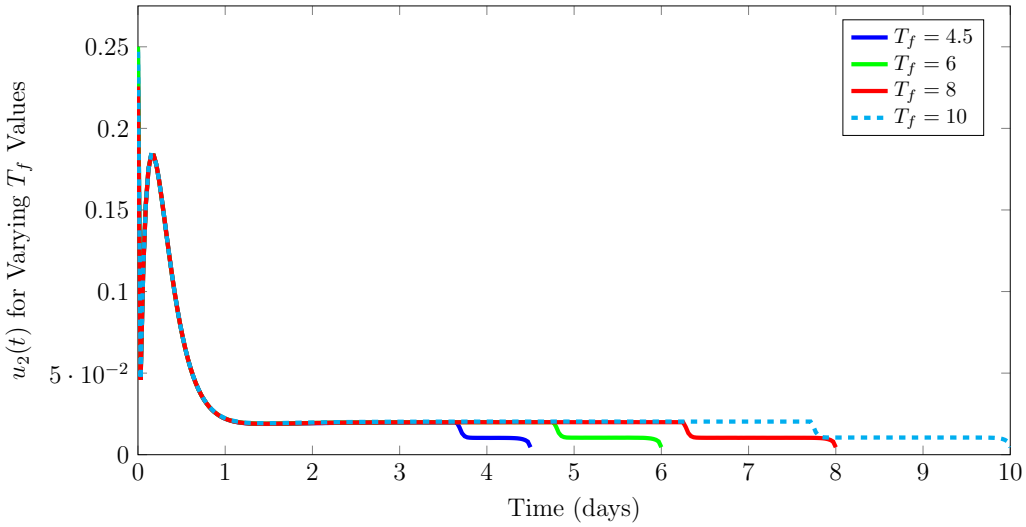

(e)

Figure B.6: Time series of *Chlamydia* model (4.4)-(4.6) showing the effect of variation in the value of the final time of treatment, T_f ($T_f \in [4.5, 8, 12, 15, 20]$, with objective functional values $(126.8092, 193.9386, 275.4131, 331.2908, 429.2486)$, respectively) on the concentrations of interacting species (a) $C(t)$, free extracellular chlamydial particles, (b) $E(t)$, healthy epithelial cells, and (c) $I(t)$, *Chlamydia*-infected epithelial cells, and on the optimal evolution for both controls (d) u_1 (optimal bacteriostatic treatment), and (e) u_2 (optimal proteasome-specific inhibitor). Other model parameters are fixed.

B.3 Investigating the Effects of Varying Weight Parameters(Chapter 5 Model)

In this section, we investigate and discuss the effects of different weight parameter combinations on the qualitative results of the optimal control problem (this include the time series of interacting species, the optimal controls, and the corresponding values of the objective functional). In these investigations, both treatment controls are used.

In Figure B.7, higher weightings of A_1 were tested. These result in poorer prognosis of the infection as Figures B.7 (a)-(d) reflect. Moreover, for higher A_1 values, treatment u_1 (tryptophan supplement) is required to be given for a slightly longer time. On the other hand, for higher values of A_1, treatment u_2 (bacteriostatic agent) is required to be given at significantly higher concentrations for longer time. Furthermore, the values of the objective functional also increased significantly for increasing values of A_1, which do not lead to the minimisation of the systemic costs of the treatments as required. These results suggest that heavier penalisation of the systemic cost of minimising the concentration of infected cells would require the administration of higher doses of the bacteriostatic treatment for long periods of time, despite the fact that it does not affect clinical outcomes positively.

In Figure B.8, higher weightings of A_2 were tested, which allowed for significantly longer and high doses of treatment u_1 (tryptophan supplement), but shorter and lesser doses of treatment u_2 (bacteriostatic agent), for increasing values of A_2. However, these do not result in any improvement in the prognosis of the infection as Figures B.8 (a)-(d) reflect. Nevertheless, the values of the objective functional increased for increasing values of A_2, which do not lead to the minimisation of the systemic costs of the treatments as required. These results suggest that heavier penalisation of the systemic cost of minimising the concentration of persistently infected cells would require the administration of high and longer doses of the tryptophan supplement treatment for longer periods of time, but shorter and lower doses of the bacteriostatic treatment, despite the fact that these do not affect clinical outcomes.

In Figure B.9, higher weightings of A_3 were tested, which allowed for slightly shorter doses of treatment u_1 (tryptophan supplement), but higher doses of treatment u_2 (bacteriostatic agent), for increasing values of A_3. However, these do not result in any improvement in the prognosis of the infection as Figures B.9 (a)-(d) reflect. Nevertheless, the values of the objective functional increased for increasing values of A_3, which do not lead to the minimisation of the systemic costs of the treatments as required. These results suggest that heavier penalisation of the systemic cost of using treatment u_1, that is, increased toxicity of the tryptophan supplement treatment, does not affect clinical outcomes, but the relative doses of the treatments as a function of drug toxicity.

In Figure B.10, higher weightings of A_4 were tested, which allowed for slightly longer doses of treatment u_1 (tryptophan supplement), but significantly shorter doses of treatment u_2 (bacteriostatic agent), for increasing values of A_4. However, these do not result in any improvement in the prognosis of the infection as Figures B.10 (a)-(d) reflect. Nevertheless, the values of the objective functional imperceptibly increased for increasing values of A_4, which do not necessarily lead to the minimisation of the systemic costs of the treatments as required. These results suggest that heavier penalisation of the systemic cost of using treatment u_2, that is, increased toxicity of the bacteriostatic treatment, does not affect clinical outcomes, but the relative doses of the treatments as a function of drug toxicity.

In Figure B.11, higher weightings of A_5 were tested, which allowed for imperceptibly shorter doses of treatment u_1 (tryptophan supplement), but slightly higher doses of treatment u_2 (bacteriostatic agent), for increasing values of A_5. However, these do not result in any improvement in the prognosis of the infection as Figures B.11 (a)-(d) reflect. Nevertheless, the values of the objective functional imperceptibly increased for increasing values of A_5, which do not necessarily lead to the minimisation of the systemic costs of the treatments as required. These results suggest that heavier penalisation of the minimisation of the concentration of *Chlamydia* at the end of the treatment would require the administration of slightly higher doses of the bacteriostatic treatment. However, these do not affect clinical outcomes.

In Figure B.12, higher weightings of A_6 were tested, which allowed for significantly longer and higher doses of treatment u_1 (tryptophan supplement), but significantly lower and shorter doses of treatment u_2 (bacteriostatic agent), for increasing values of A_6. However, these do not result in any improvement in the prognosis of the infection as Figures B.12 (a)-(d) reflect. Moreover, the values of the objective functional increased for increasing values of A_6, which do not necessarily lead to the minimisation of the systemic costs of the treatments as required. These results suggest that heavier penalisation of the minimisation of the concentration of persistently infected cells at the end of the treatment would require the administration of significantly higher and longer doses of the tryptophan supplement treatment, but significantly lower and shorter doses of the bacteriostatic treatment. These however do not affect clinical outcomes.

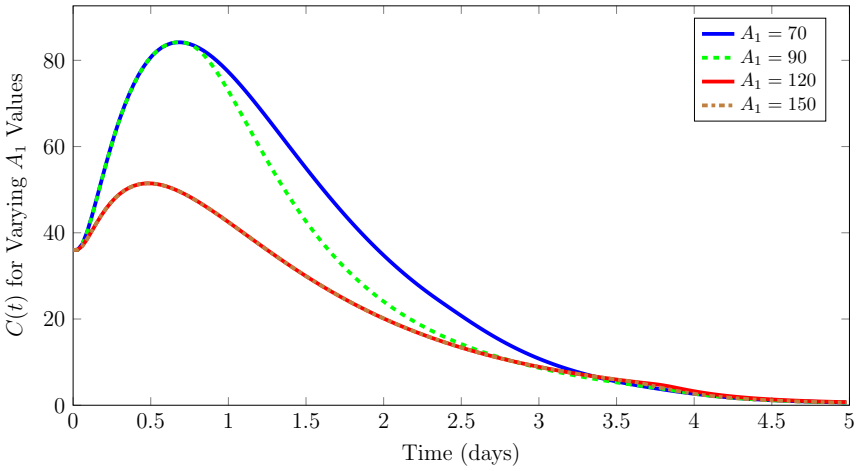
$C(t)$ for Varying A_1 Values
Time (days)
$A_1 = 70$
$A_1 = 90$
$A_1 = 120$
$A_1 = 150$

(a)

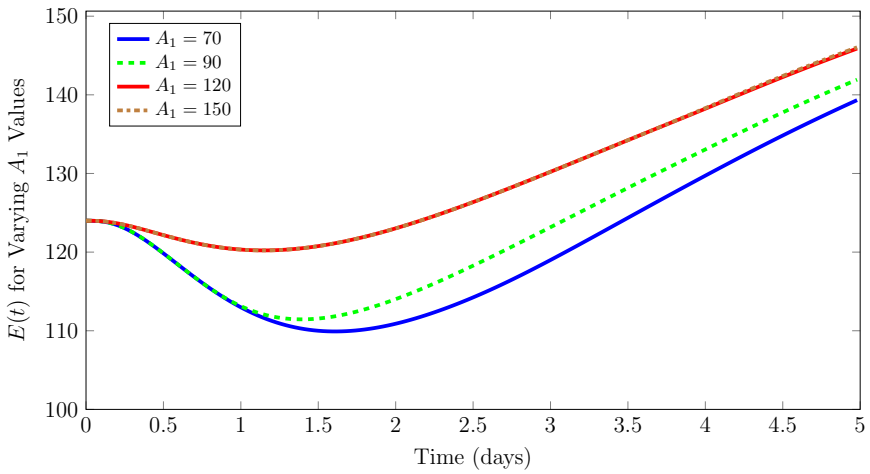
$E(t)$ for Varying A_1 Values
Time (days)
$A_1 = 70$
$A_1 = 90$
$A_1 = 120$
$A_1 = 150$

(b)

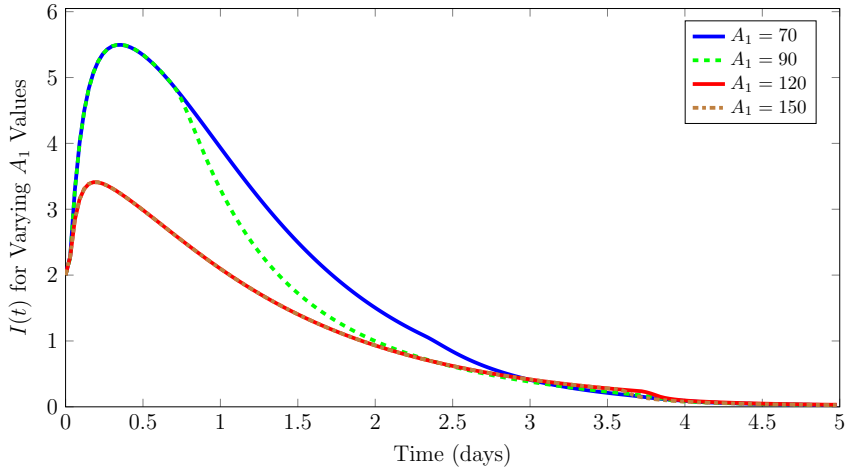
$I(t)$ for Varying A_1 Values
Time (days)
$A_1 = 70$
$A_1 = 90$
$A_1 = 120$
$A_1 = 150$

(c)

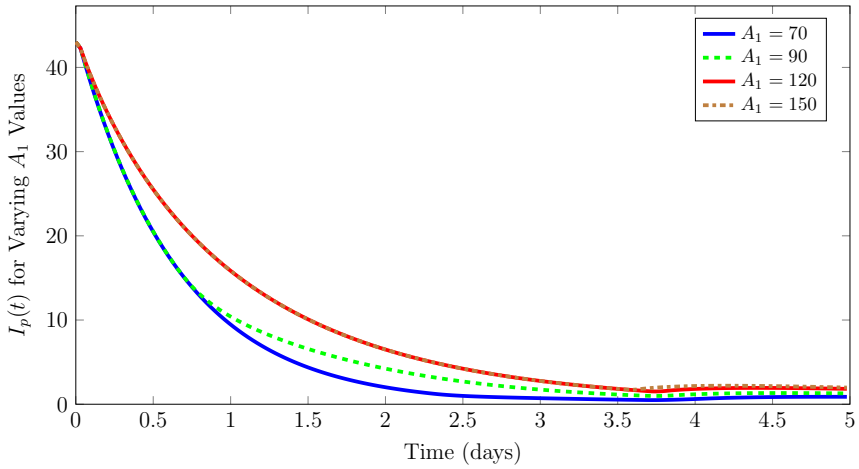
$I_p(t)$ for Varying A_1 Values
Time (days)
$A_1 = 70$
$A_1 = 90$
$A_1 = 120$
$A_1 = 150$

(d)

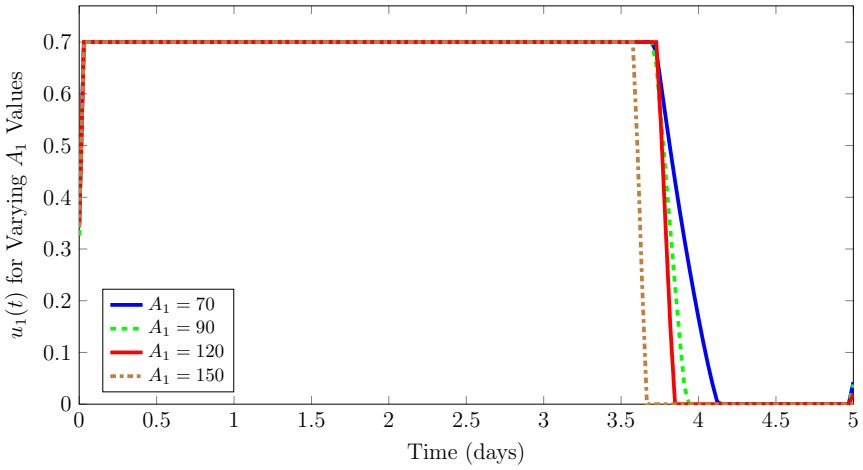

(e)

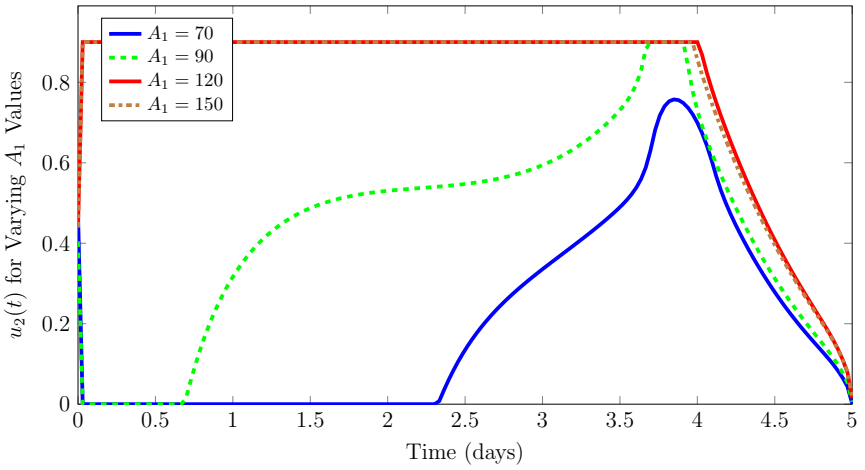

(f)

Figure B.7: Time series of *Chlamydia* model (4.4)-(4.6) showing the effect of variation in the value of the weight parameter A_1 ($A_1 \in [70, 90, 120, 150]$, with objective functional values $(1433.5856, 1596.4009, 1753.3537, 1909.4035)$, respectively) on the concentrations of interacting species (a) $C(t)$, free extracellular chlamydial particles, (b) $E(t)$, healthy epithelial cells, (c) $I(t)$, *Chlamydia*-infected epithelial cells, and (c) $I_p(t)$, persistently infected epithelial cells, and on the optimal evolution for both controls (d) u_1 (tryptophan supplementation treatment), and (e) u_2 (bacteriostatic agents). Other weight parameters are fixed ($(A_2, A_3, A_4, A_5, A_6) = (20, 90, 20, 1, 5)$).

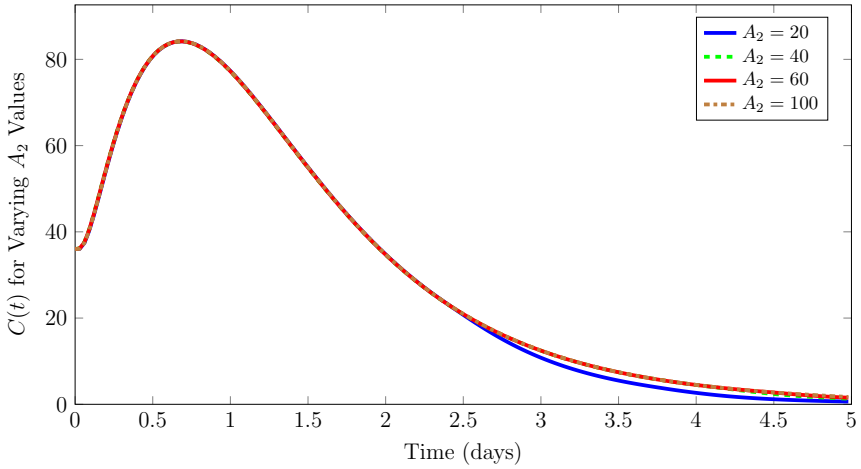
$C(t)$ for Varying A_2 Values
Time (days)
$A_2 = 20$
$A_2 = 40$
$A_2 = 60$
$A_2 = 100$

(a)

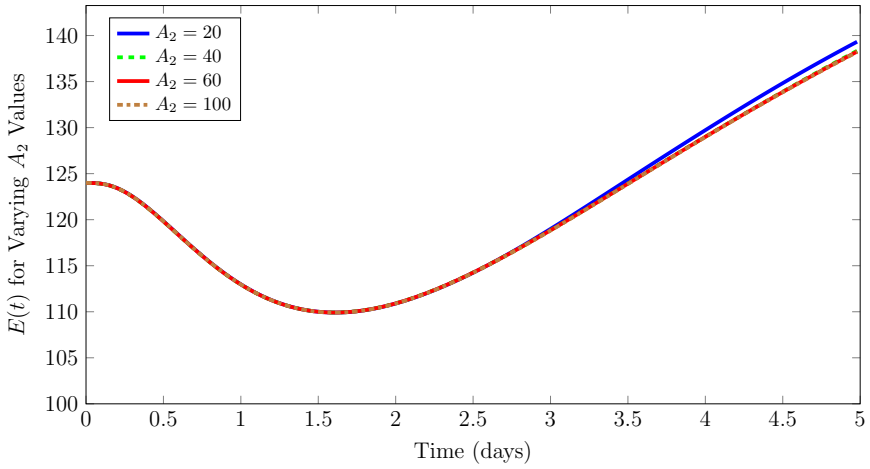
$E(t)$ for Varying A_2 Values
Time (days)
$A_2 = 20$
$A_2 = 40$
$A_2 = 60$
$A_2 = 100$

(b)

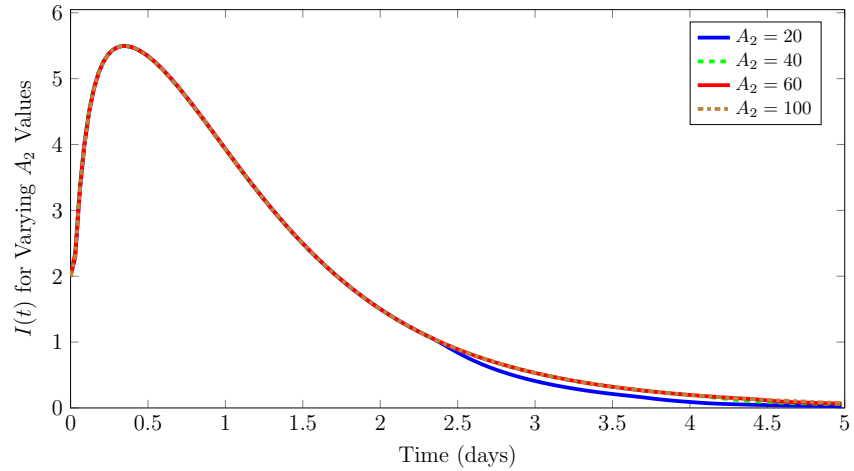
$I(t)$ for Varying A_2 Values
Time (days)
$A_2 = 20$
$A_2 = 40$
$A_2 = 60$
$A_2 = 100$

(c)

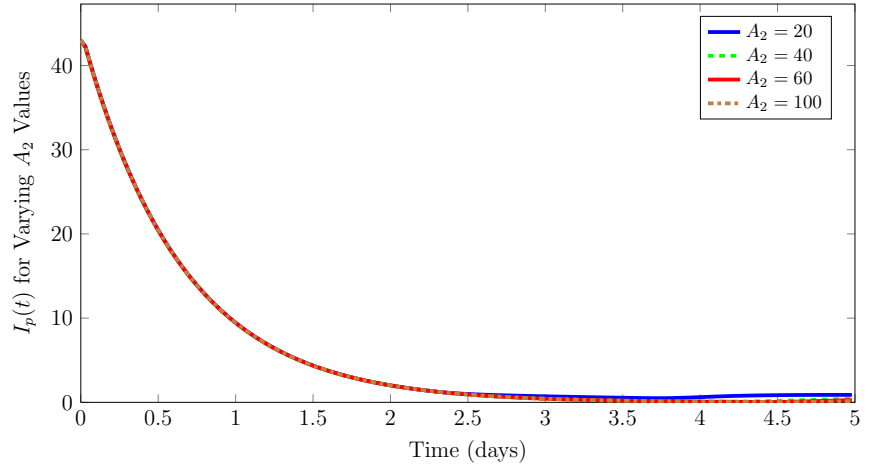
$I_p(t)$ for Varying A_2 Values
Time (days)
$A_2 = 20$
$A_2 = 40$
$A_2 = 60$
$A_2 = 100$

(d)

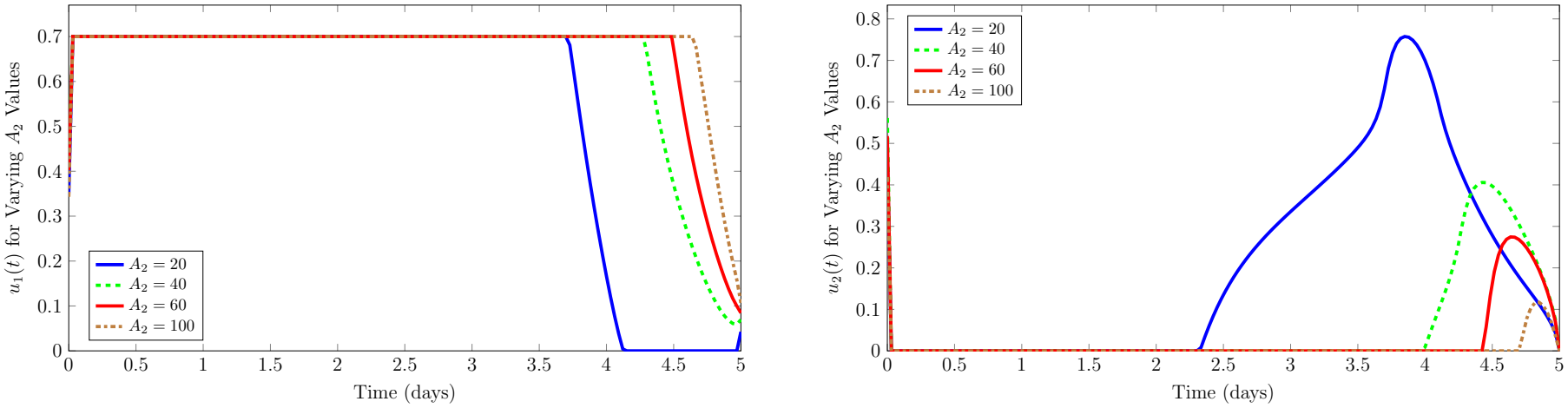

(e) (f)

Figure B.8: Time series of *Chlamydia* model (4.4)-(4.6) showing the effect of variation in the value of the weight parameter A_2 ($A_2 \in [20, 40, 60, 100]$, with objective functional values $(1433.5856, 2011.3671, 2587.1339, 3741.7231)$, respectively) on the concentrations of interacting species (a) $C(t)$, free extracellular chlamydial particles, (b) $E(t)$, healthy epithelial cells, (c) $I(t)$, *Chlamydia*-infected epithelial cells, and (c) $I_p(t)$, persistently infected epithelial cells, and on the optimal evolution for both controls (d) u_1 (tryptophan supplementation treatment), and (e) u_2 (bacteriostatic agents). Other weight parameters are fixed ($(A_1, A_3, A_4, A_5, A_6) = (70, 90, 20, 1, 5)$).

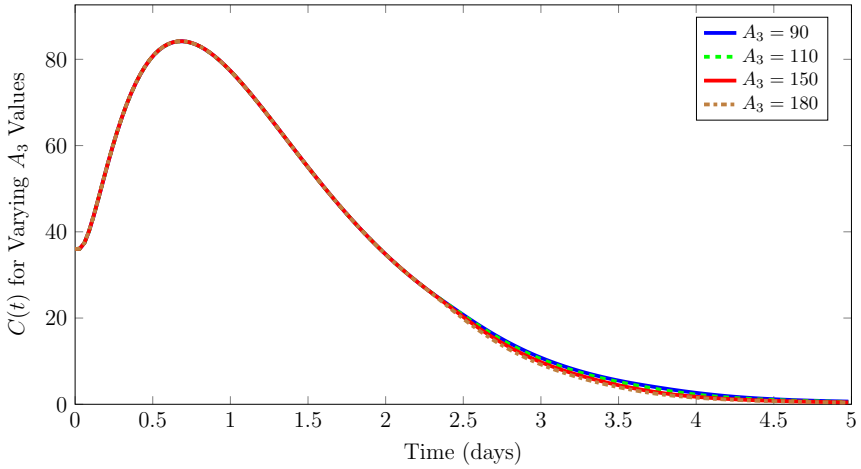
$C(t)$ for Varying A_3 Values
Time (days)
$A_3 = 90$
$A_3 = 110$
$A_3 = 150$
$A_3 = 180$

(a)

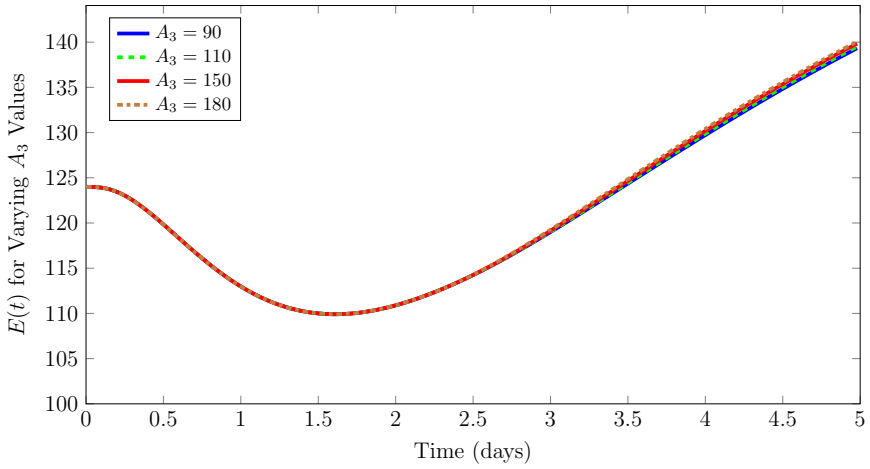
$E(t)$ for Varying A_3 Values
Time (days)
$A_3 = 90$
$A_3 = 110$
$A_3 = 150$
$A_3 = 180$

(b)

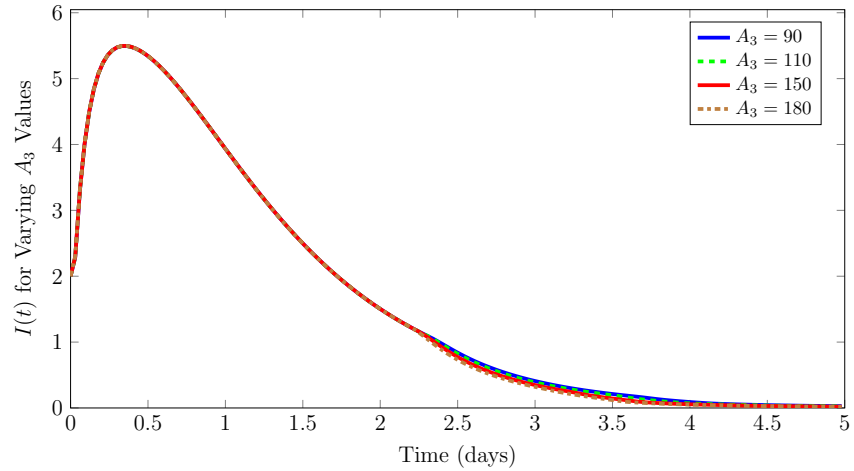
$I(t)$ for Varying A_3 Values
Time (days)
$A_3 = 90$
$A_3 = 110$
$A_3 = 150$
$A_3 = 180$

(c)

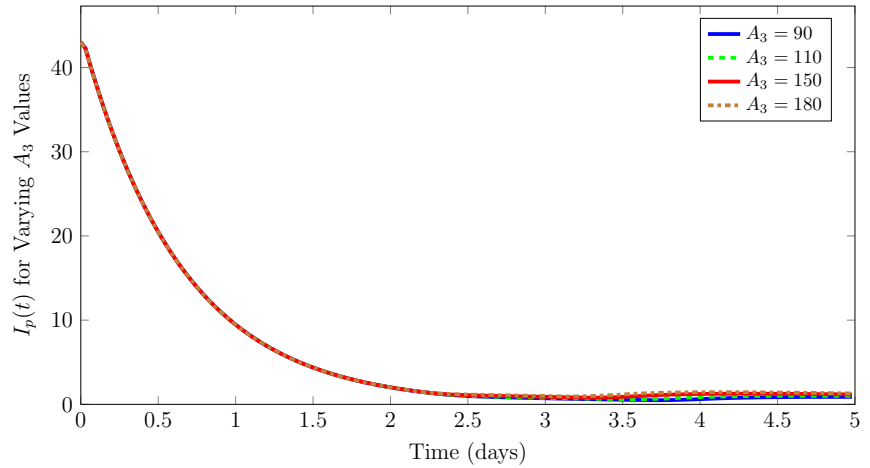
$I_p(t)$ for Varying A_3 Values
Time (days)
$A_3 = 90$
$A_3 = 110$
$A_3 = 150$
$A_3 = 180$

(d)

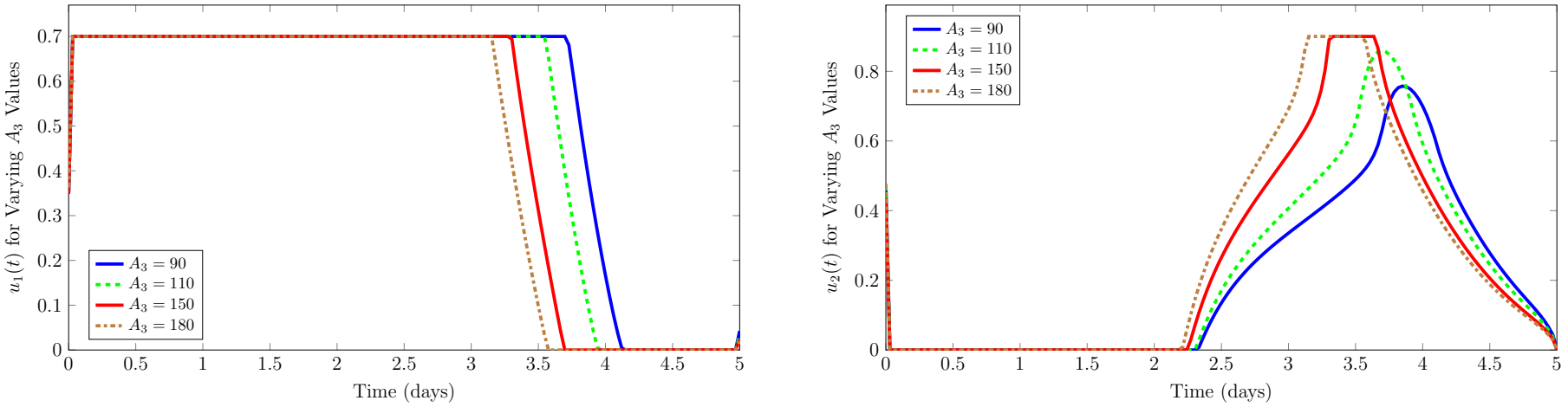

Figure B.9: Time series of *Chlamydia* model (4.4)-(4.6) showing the effect of variation in the value of the weight parameter A_3 ($A_3 \in [90, 110, 150, 180]$, with objective functional values $(1433.5856, 1451.0910, 1484.5167, 1507.5932)$, respectively) on the concentrations of interacting species (a) $C(t)$, free extracellular chlamydial particles, (b) $E(t)$, healthy epithelial cells, (c) $I(t)$, *Chlamydia*-infected epithelial cells, and (c) $I_p(t)$, persistently infected epithelial cells, and on the optimal evolution for both controls (d) u_1 (tryptophan supplementation treatment), and (e) u_2 (bacteriostatic agents). Other weight parameters are fixed ($(A_1, A_2, A_4, A_5, A_6) = (70, 20, 20, 1, 5)$).

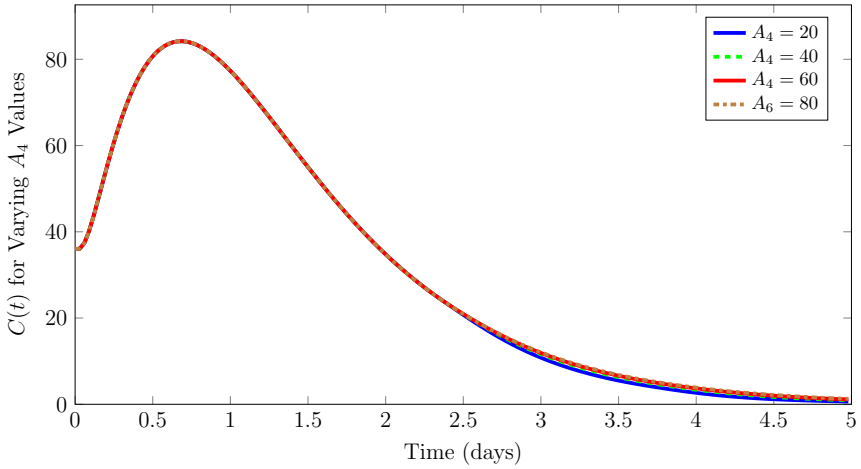
$C(t)$ for Varying A_4 Values
Time (days)
$A_4 = 20$
$A_4 = 40$
$A_4 = 60$
$A_6 = 80$

(a)

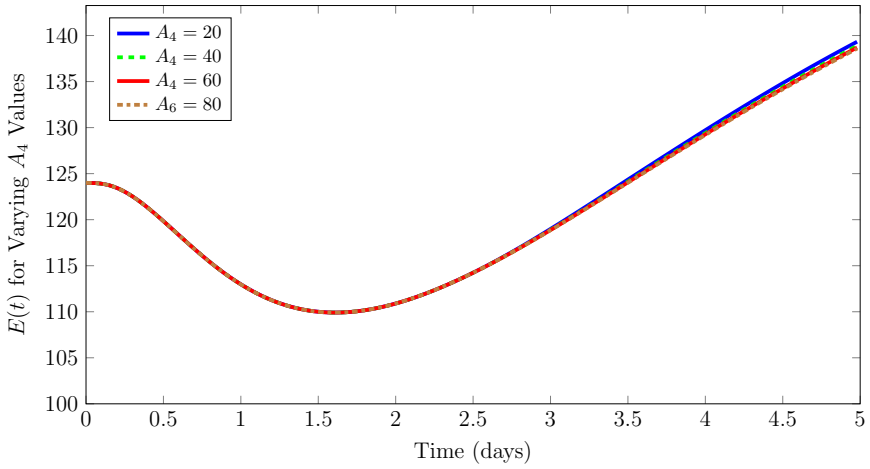
$E(t)$ for Varying A_4 Values
Time (days)
$A_4 = 20$
$A_4 = 40$
$A_4 = 60$
$A_6 = 80$

(b)

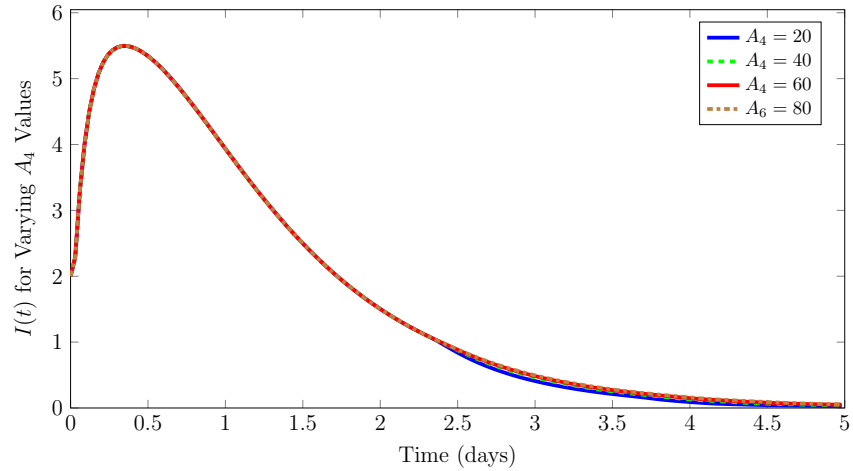
$I(t)$ for Varying A_4 Values
Time (days)
$A_4 = 20$
$A_4 = 40$
$A_4 = 60$
$A_6 = 80$

(c)

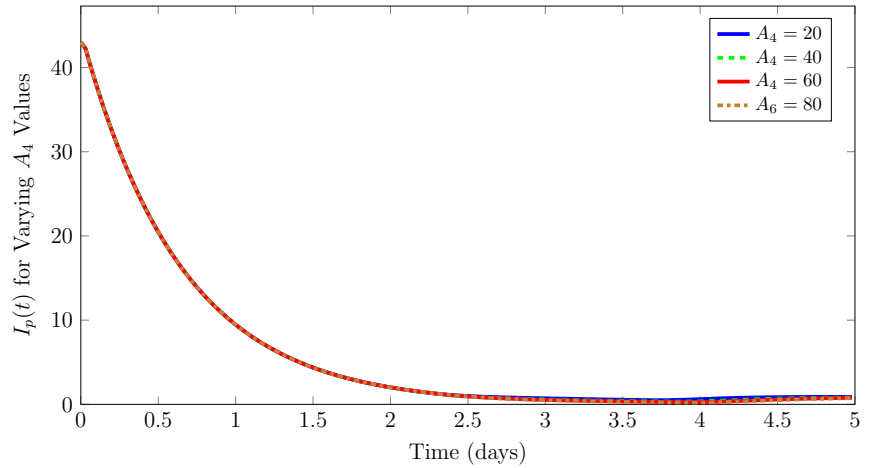
$I_p(t)$ for Varying A_4 Values
Time (days)
$A_4 = 20$
$A_4 = 40$
$A_4 = 60$
$A_6 = 80$

(d)

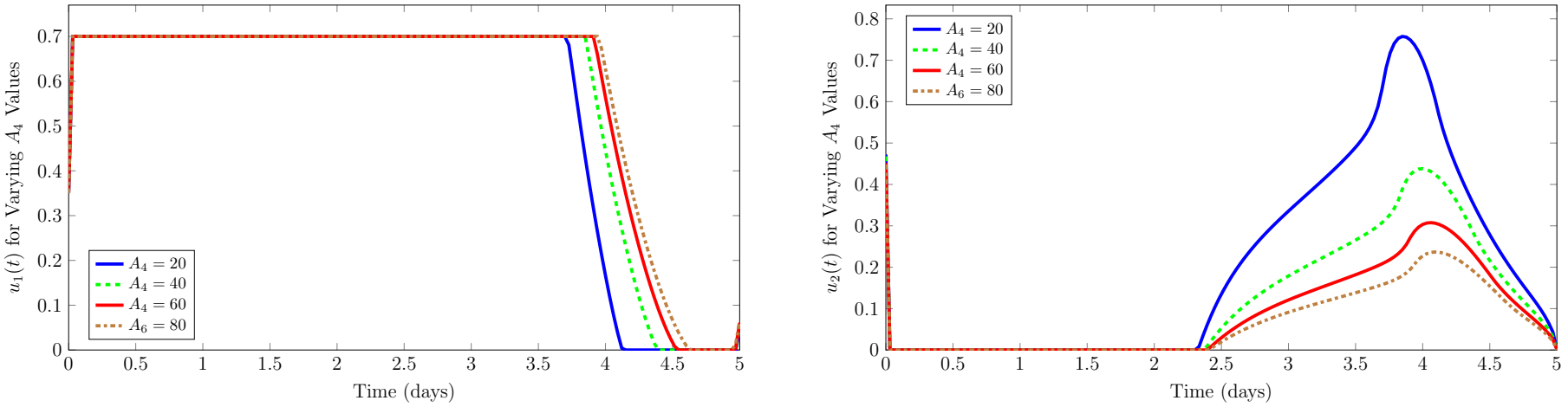

(e) (f)

Figure B.10: Time series of *Chlamydia* model (4.4)-(4.6) showing the effect of variation in the value of the weight parameter A_4 ($A_4 \in [20, 40, 60, 80]$, with objective functional values $(1433.5856, 1436.2320, 1437.7002, 1438.4729)$, respectively) on the concentrations of interacting species (a) $C(t)$, free extracellular chlamydial particles, (b) $E(t)$, healthy epithelial cells, (c) $I(t)$, *Chlamydia*-infected epithelial cells, and (c) $I_p(t)$, persistently infected epithelial cells, and on the optimal evolution for both controls (d) u_1 (tryptophan supplementation treatment), and (e) u_2 (bacteriostatic agents). Other weight parameters are fixed ($(A_1, A_2, A_3, A_5, A_6) = (70, 20, 90, 1, 5)$).

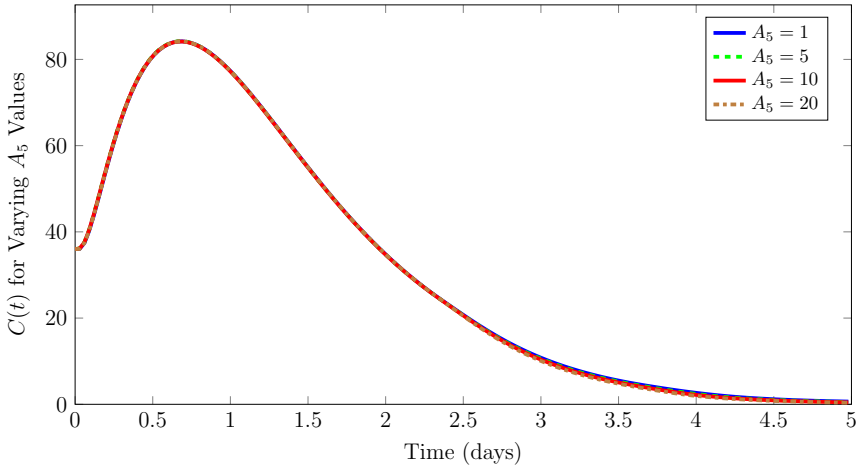
$C(t)$ for Varying A_5 Values
Time (days)
$A_5 = 1$
$A_5 = 5$
$A_5 = 10$
$A_5 = 20$

(a)

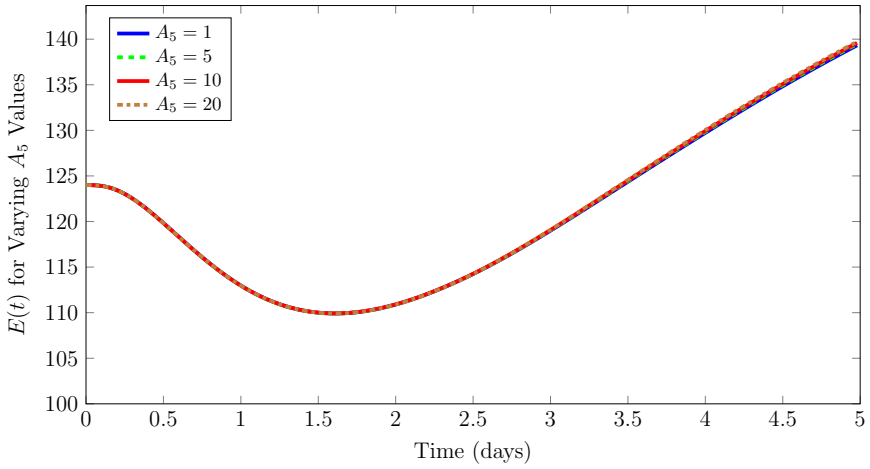
$E(t)$ for Varying A_5 Values
Time (days)
$A_5 = 1$
$A_5 = 5$
$A_5 = 10$
$A_5 = 20$

(b)

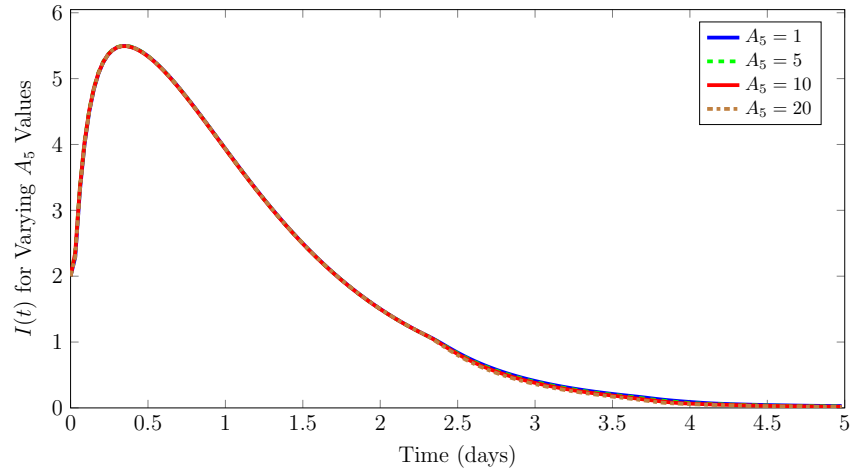
$I(t)$ for Varying A_5 Values
Time (days)
$A_5 = 1$
$A_5 = 5$
$A_5 = 10$
$A_5 = 20$

(c)

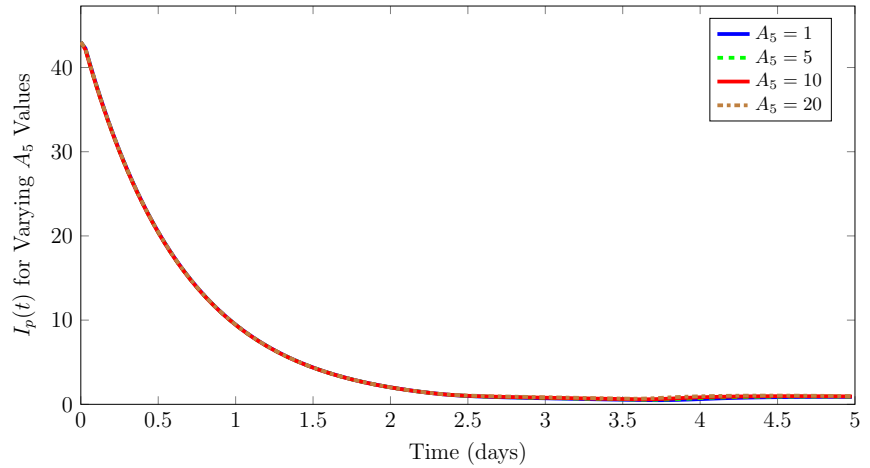
$I_p(t)$ for Varying A_5 Values
Time (days)
$A_5 = 1$
$A_5 = 5$
$A_5 = 10$
$A_5 = 20$

(d)

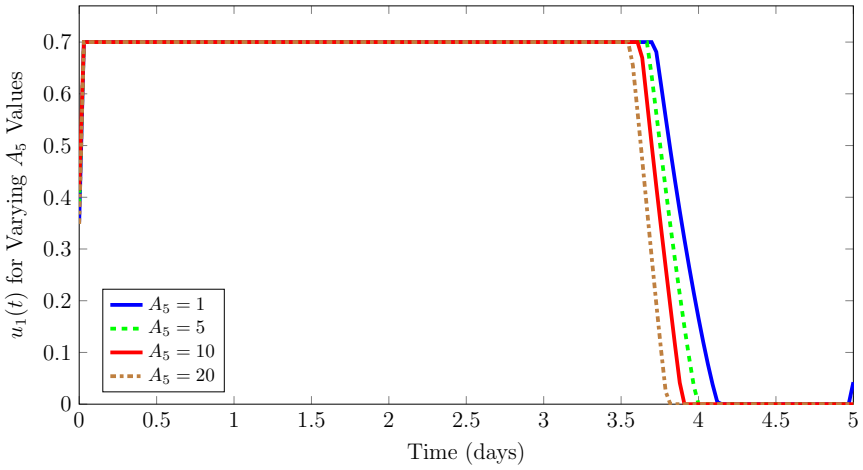

(e)

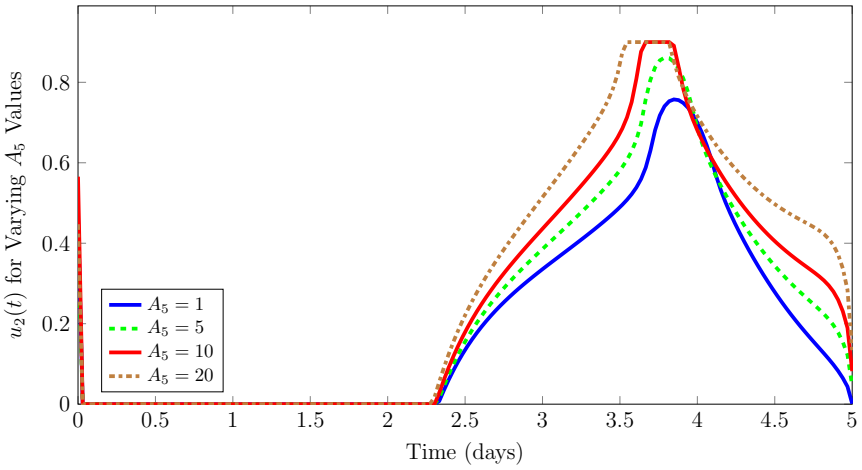

(f)

Figure B.11: Time series of *Chlamydia* model (4.4)-(4.6) showing the effect of variation in the value of the weight parameter A_5 ($A_5 \in [1, 5, 10, 20]$, with objective functional values $(1433.5856, 1432.1733, 1431.6031, 1435.1588)$, respectively) on the concentrations of interacting species (a) $C(t)$, free extracellular chlamydial particles, (b) $E(t)$, healthy epithelial cells, (c) $I(t)$, *Chlamydia*-infected epithelial cells, and (c) $I_p(t)$, persistently infected epithelial cells, and on the optimal evolution for both controls (d) u_1 (tryptophan supplementation treatment), and (e) u_2 (bacteriostatic agents). Other weight parameters are fixed ($(A_1, A_2, A_3, A_4, A_6) = (70, 20, 90, 20, 5)$).

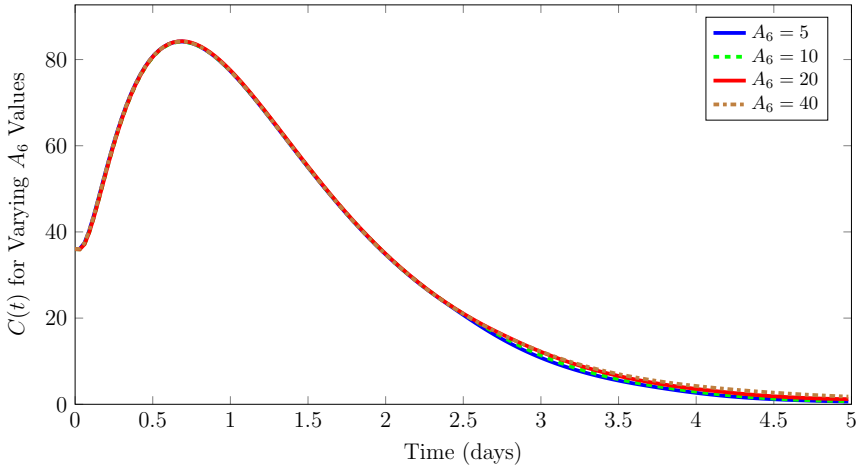
$C(t)$ for Varying A_6 Values
Time (days)
$A_6 = 5$
$A_6 = 10$
$A_6 = 20$
$A_6 = 40$

(a)

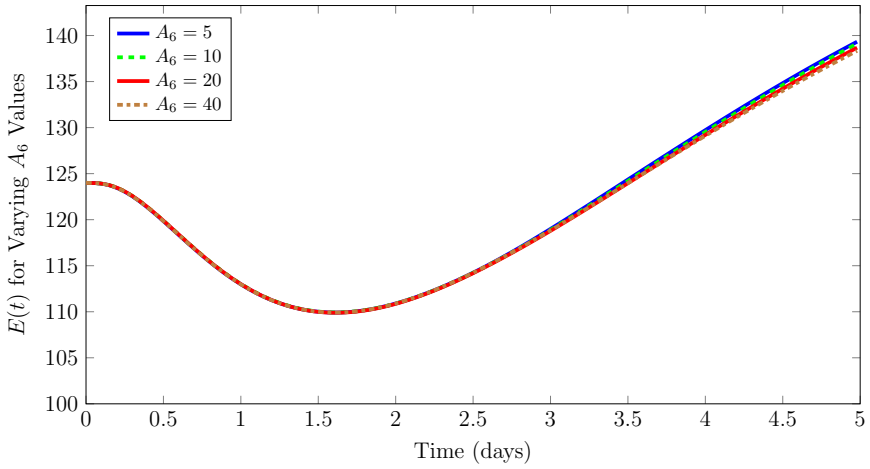
$E(t)$ for Varying A_6 Values
Time (days)
$A_6 = 5$
$A_6 = 10$
$A_6 = 20$
$A_6 = 40$

(b)

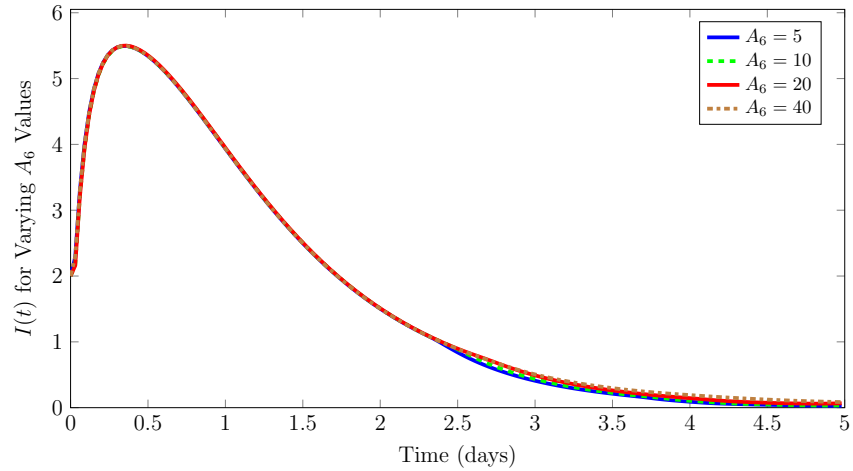
$I(t)$ for Varying A_6 Values
Time (days)
$A_6 = 5$
$A_6 = 10$
$A_6 = 20$
$A_6 = 40$

(c)

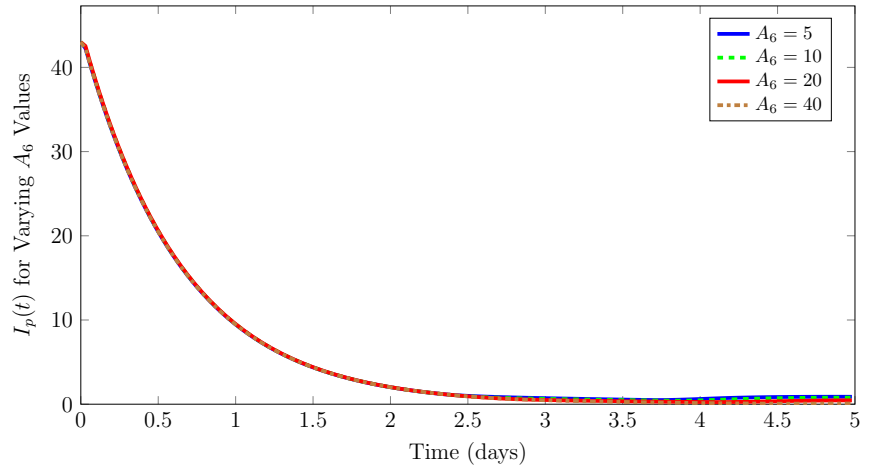
$I_p(t)$ for Varying A_6 Values
Time (days)
$A_6 = 5$
$A_6 = 10$
$A_6 = 20$
$A_6 = 40$

(d)

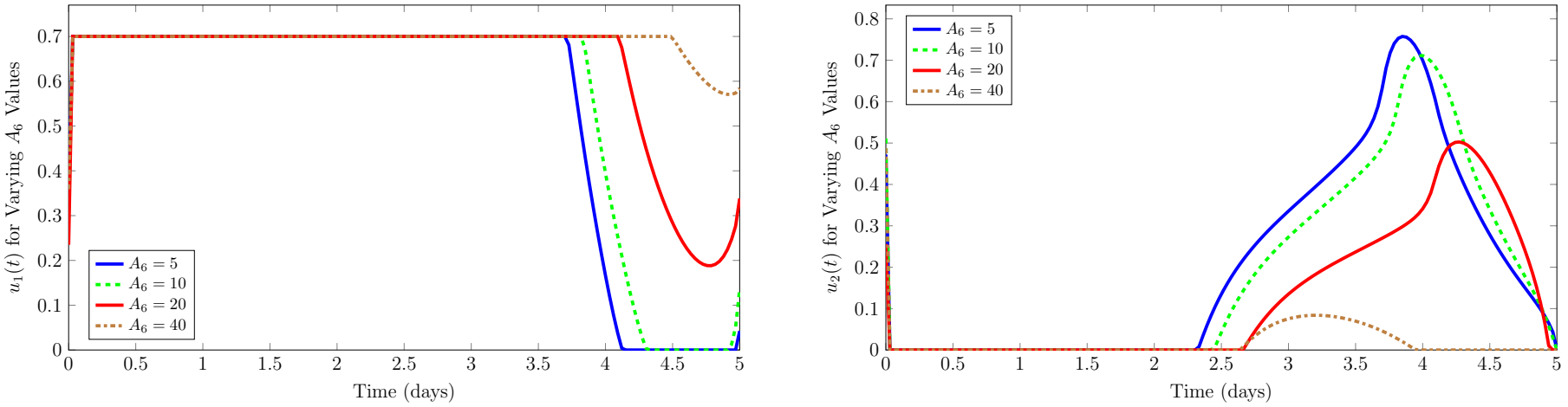

Figure B.12: Time series of *Chlamydia* model (4.4)-(4.6) showing the effect of variation in the value of the weight parameter A_6 ($A_6 \in [5, 10, 20, 40]$, with objective functional values $(1433.5856, 1437.0098, 1443.3248, 1448.4589)$, respectively) on the concentrations of interacting species (a) $C(t)$, free extracellular chlamydial particles, (b) $E(t)$, healthy epithelial cells, (c) $I(t)$, *Chlamydia*-infected epithelial cells, and (c) $I_p(t)$, persistently infected epithelial cells, and on the optimal evolution for both controls (d) u_1 (tryptophan supplementation treatment), and (e) u_2 (bacteriostatic agents). Other weight parameters are fixed ($(A_1, A_2, A_3, A_4, A_5) = (70, 20, 90, 20, 1)$).

B.4 Investigating the Effects of Varying Treatment Duration (Chapter 5 Model)

In this section, we investigate and discuss the effects of different final time of treatment on the qualitative results of the optimal control problem (this include the time series of interacting species, the optimal controls, and the corresponding values of the objective functional). In these investigations, both treatment controls are used.

In Figure B.13, different values of T_f were tested, which allowed for slightly longer treatment doses of treatment u_1 (tryptophan supplement treatment), and significantly longer and higher doses of treatment u_2 (bacteriostatic treatment), for increasing values of T_f. However, these do not result in any improvement in the prognosis of the infection as Figures B.13 (a)-(d) reflect. Nevertheless, the values of the objective functional increased quite significantly for increasing values of T_f, which do not lead to the minimisation of the systemic costs of the treatments as required. These results suggest that increasing the duration of treatment will not necessarily yield better clinical outcomes.

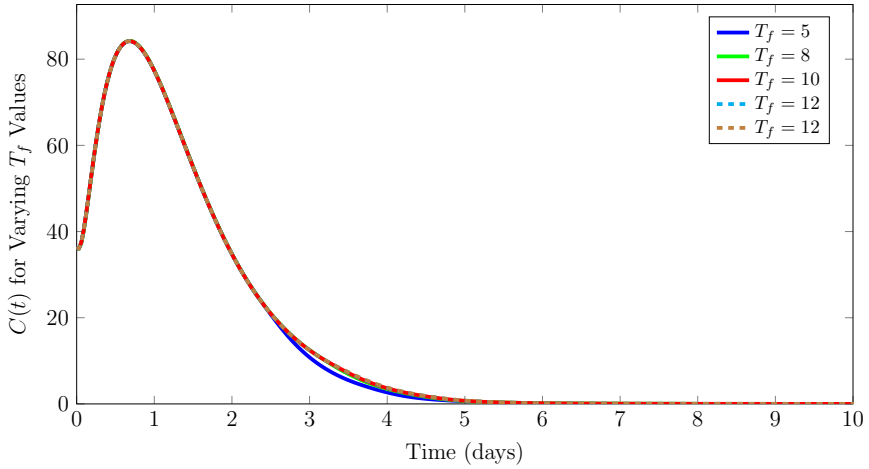
$C(t)$ for Varying T_f Values
Time (days)
$T_f = 5$
$T_f = 8$
$T_f = 10$
$T_f = 12$
$T_f = 12$

(a)

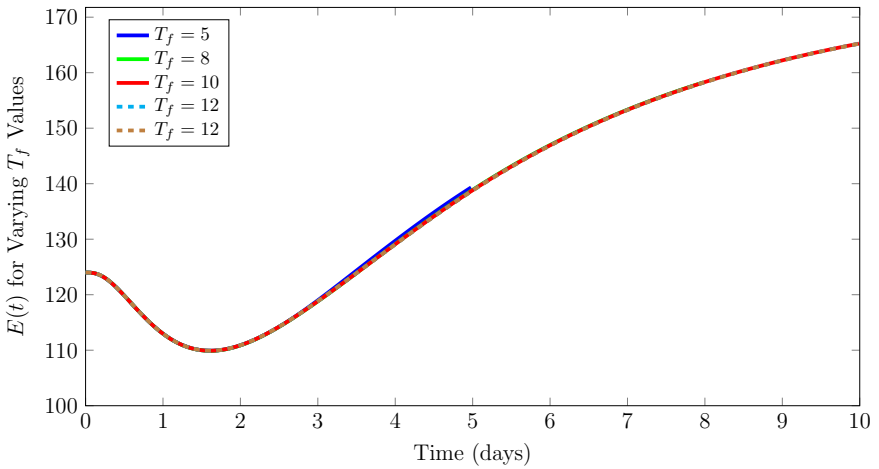
$E(t)$ for Varying T_f Values
Time (days)
$T_f = 5$
$T_f = 8$
$T_f = 10$
$T_f = 12$
$T_f = 12$

(b)

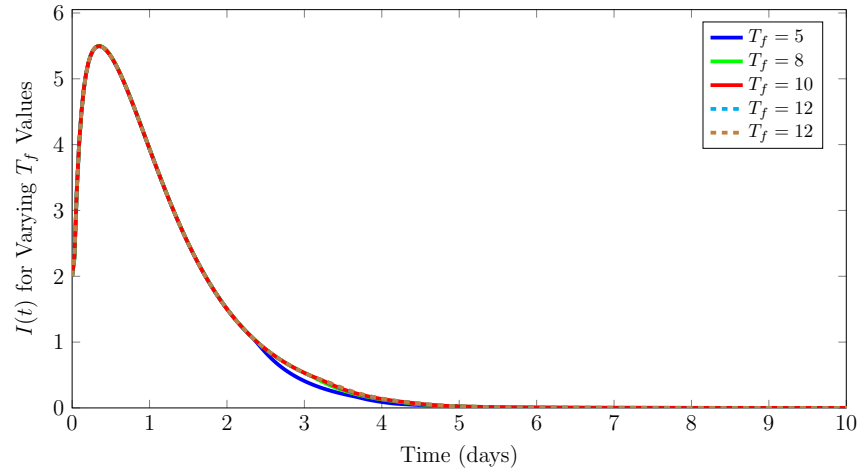
$I(t)$ for Varying T_f Values
Time (days)
$T_f = 5$
$T_f = 8$
$T_f = 10$
$T_f = 12$
$T_f = 12$

(c)

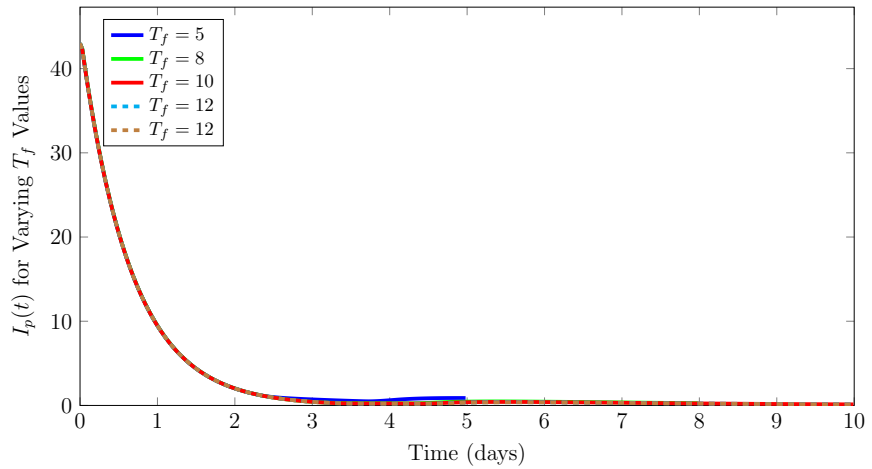
$I_p(t)$ for Varying T_f Values
Time (days)
$T_f = 5$
$T_f = 8$
$T_f = 10$
$T_f = 12$
$T_f = 12$

(d)

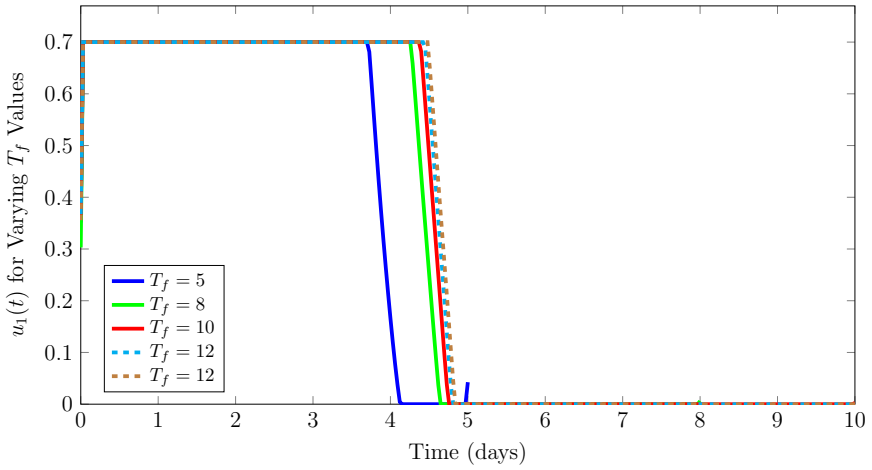

(e)

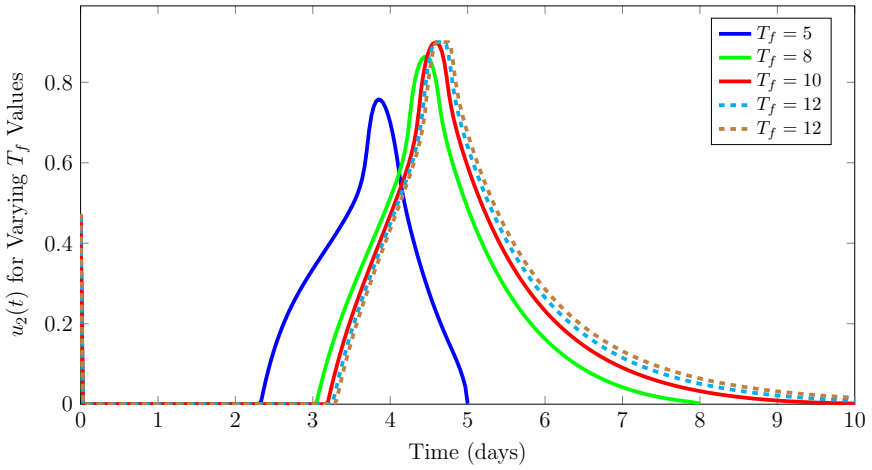

(f)

Figure B.13: Time series of *Chlamydia* model (5.1)-(5.4) showing the effect of variation in the value of the final time of treatment, T_f ($T_f \in [5, 8, 10, 12, 15]$, with objective functional values $(1433.5856, 1470.7691, 1476.2584, 1479.9195, 1482.7511)$, respectively) on the concentrations of interacting species (a) $C(t)$, free extracellular chlamydial particles, (b) $E(t)$, healthy epithelial cells, and (c) $I(t)$, *Chlamydia*-infected epithelial cells, (d) $I_p(t)$, persistently infected epithelial cells, and on the optimal evolution for both controls (d) u_1 (tryptophan supplement treatment), and (e) u_2 (bacteriostatic treatment). Other model parameters are fixed.

Bibliography

[1] Lecture 2: 4. LaSalles Invariance Principle . Available at: http://www.cds.caltech.edu/archive/help/uploads/wiki/files/237/Lecture2_notes_CDS270.pdf. Accessed June 6, 2018.

[2] Malaria and malaria vaccine candidates. Technical Report, The College of Physicians of Philadelphia, 2017. Accessed January 23, 2018. Available at https://www.historyofvaccines.org/content/articles/malaria-and-malaria-vaccine-candidates#Source15.

[3] Agacfidan, A., Moncada, J., and Schachter, J. In vitro activity of azithromycin (cp-62,993) against *Chlamydia trachomatis* and *Chlamydia pneumoniae*. *Antimicrob. Agents Chemother. 37(9)* (1993), 1746–1748.

[4] Agrawal, T., Vats, V., Salhan, S., and Mittal, A. The mucosal immune response to *Chlamydia trachomatis* infection of the reproductive tract in women. *Journal of Reproductive Immunology 83*, 1 (2009), 173–178.

[5] Agusto, F. Optimal chemoprophylaxis and treatment control strategies of a tuberculosis transmission model. *World journal of modelling and simulation 5*, 3 (2009), 163–173.

[6] AIDS*info*. The HIV Life Cycle. Technical Report, U.S. Department of Health and Human Services (HHS), 2017. Accessed January 23, 2018. Available at https://aidsinfo.nih.gov/understanding-hiv-aids/fact-sheets/19/73/the-hiv-life-cycle.

[7] Aniţa, S., Arnăutu, V., and Capasso, V. *An introduction to optimal control problems in life sciences and economics: from mathematical models to numerical simulation with MATLAB®*. Springer Science & Business Media, 2011.

[8] Averette, H. Autoradiographic analysis of cell proliferation kinetics in human genital tissues. *Obstetrics and gynecology (New York. 1953) (0029-7844) 31*, 4 (1968), 580.

[9] Bagher-Oskouei, M., Mallet, D. G., Amirshahi, A., and Pettet, G. J. Mathematical modelling of the interaction of *Chlamydia Trachomatis* with the immune system. In *Proceedings of the World Congress on Engineering and Computer Science* (San Francisco, USA, October 20-22 2010), no. II. (International Conference on Computational Biology) WCECS.

[10] Bastidas, R. J., Elwell, C. A., Engel, J. N., and Valdivia, R. H. Chlamydial intracellular survival strategies. *Cold Spring Harb. Perspect. Med.* (2013). doi: 10.1101/cshperspect.a010256.

[11] Batteiger, B. E., Tu, W., Ofner, S., Van Der Pol, B., Stothard, D. R., Orr, D. P., Katz, B. P., and Fortenberry, J. D. Repeated *Chlamydia trachomatis* genital infections in adolescent women. *The Journal of Infectious Diseases 201*, 1 (2010), 42–51.

[12] Batteiger, B. E., Xu, F. J., Johnson, R. E., and Rekart, M. L. Protective immunity to *Chlamydia trachomatis* genital infection: Evidence from human studies. *The Journal of Infectious Diseases 201* (2010), S178–S189.

[13] Beck, A. *Introduction to Nonlinear Optimization: Theory, Algorithms, and Applications with MATLAB.* SIAM, 2014. Available at: url-http://www.siam.org/books/mo19/.

[14] Becker, J., and Wittmann, C. Bio-based production of chemicals, materials and fuels - corynebacterium glutamicum as versatile cell factory. *Current Opinion in Biotechnology 23*, 4 (2012), 631 – 640. Nanobiotechnology Systems biology.

[15] Bhengraj, A. R., Vardhan, H., Srivastava, P., Salhan, S., and Mittal, A. Decreased susceptibility to azithromycin and doxycycline in clinical isolates of *Chlamydia trachomatis* obtained from recurrently infected female patients in India. *Chemotherapy 56*, 5 (2010), 371–377.

[16] Blower, S. M., and Dowlatabadi, H. Sensitivity and uncertainty analysis of complex models of disease transmission: An HIV model, as an example. *International Statistical Review / Revue Internationale de Statistique 62*, 2 (1994), 229–243.

[17] Brunham, R. C. Immunology. a *Chlamydia* vaccine on the horizon. *Science 348*, 6241 (2015), 1322.

[18] Brunham, R. C., and Rey-Ladino, J. Immunology of *Chlamydia* infection: Implications for a *Chlamydia trachomatis* vaccine. *Nature Reviews: Immunology 5* (2005), 149–161. doi:10.1038/nri1551.

[19] Burns, J. A., Cliff, E. M., and Doughty, S. E. Sensitivity analysis and parameter estimation for a model of *Chlamydia trachomatis* infection. *Journal of Inverse & Ill-Posed Problems 15*, 3 (2007), 243 – 256.

[20] Cady, S. G., and Sono, M. 1-methyl-dl-tryptophan, β-(3-benzofuranyl)-dl-alanine (the oxygen analog of tryptophan), and β-[3-benzo(b)thienyl]-dl-alanine (the sulfur analog of tryptophan) are competitive inhibitors for indoleamine 2,3-dioxygenase. *Archives of Biochemistry and Biophysics 291*, 2 (1991), 326 – 333.

[21] Cameron, I. L. {CHAPTER} 3 - cell proliferation and renewal in the mammalian body*. In *Cellular and Molecular Renewal in the Mammalian Body*, I. L. CAMERON and J. D. THRASHER, Eds. Academic Press, 1971, pp. 45 – 85.

[22] CDC. Centers for Disease Control and Prevention: Sexually Transmitted Disease Surveillance 2013. Technical Report, CDC, 2014. Available at: `http://www.cdc.gov/std/stats13/surv2013-print.pdf` [Accessed January 22, 2014].

[23] Chachuat, B. Nonlinear and dynamic optimization: from theory to practice. Tech. rep., Laboratoire d'Automatique, Ecolé Polytechnique Flédlérale de Lausanne, 2007. Available at: https://infoscience.epfl.ch/record/111939/files/Chachuat_07(IC32).pdf.

[24] Chachuat, B. Optimal control. Available at: http://la.epfl.ch/files/content/sites/la/files/shared/import/migration/IC_32/oc-3_solution.pdf, 2009. Accessed December 21, 2016.

[25] Chachuat, B. Optimal control lecture 17-18: Problem formulation. Available at: https://lawww.epfl.ch/webdav/site/la/shared/import/migration/IC_32/Slides17-18.pdf, 2009. Accessed May 31, 2018.

[26] Chemicals, S. Indoximod (NLG-8189). Available at: http://www.selleckchem.com/products/indoximod-nlg-8189.html. Accessed October 12, 2017.

[27] Christian, J. G., Heymann, J., Paschen, S. A., Vier, J., Schauenburg, L., Rupp, J., Meyer, T. F., Häcker, G., and Heuer, D. Targeting of a chlamydial protease impedes intracellular bacterial growth. *PLOS Pathogens 7*, 9 (09 2011), 1–11.

[28] Coddington, E. *An Introduction to Ordinary Differential Equations*. Prentice-Hall Inc., 1961.

[29] Coddington, E., and Levinson, N. *Theory of Ordinary Differential Equations*. Mc-Graw Hill Co., Inc., 1955.

[30] Conrad, T. A., Yang, Z., Ojcius, D., and Zhong, G. A path forward for the chlamydial virulence factor CPAF. *Microbes and infection 15*, 14 (2013), 1026–1032.

[31] Conrado, R. J., Varner, J. D., and DeLisa, M. P. Engineering the spatial organization of metabolic enzymes: mimicking nature's synergy. *Current Opinion in Biotechnology 19*, 5 (2008), 492 – 499. Tissue, cell and pathway engineering.

[32] Craig, A. P., Rank, R. G., Bowlin, A. K., Wand, H., and Wilson, D. P. Target cell limitation constrains chlamydial load in persistent infections: results from mathematical modelling applied to mouse genital tract infection data. *Pathogens and Disease 0* (2014), 1–8.

[33] Croicu, A.-M. Short- and long-term optimal control of a mathematical model for hiv infection of $cd4^+t$ cells. *Bulletin of Mathematical Biology* (2015), 1–37.

[34] D., T.-R., and B.J., T. The rôle of *Chlamydia trachomatis* in genital-tract and associated diseases. *Journal of Clinical Pathology 33*, 3 (1980), 205–233.

[35] Darville, T., and Hiltke, T. J. Pathogenesis of genital tract disease due to *Chlamydia trachomatis*. *Journal of infectious diseases 201*, Supplement 2 (2010), S114–S125.

[36] de Pillis, L., Gu, W., Fister, K., Head, T., Maples, K., Murugan, A., Neal, T., and Yoshida, K. Chemotherapy for tumors: An analysis of the dynamics and a study of quadratic and linear optimal controls. *Mathematical Biosciences 209*, 1 (2007), 292 – 315.

[37] DE PILLIS, L. G., FISTER, K. R., GU, W., HEAD, T., MAPLES, K., NEAL, T., MURUGAN, A., and KOZAI, K. Optimal Control of Mixed Immunotherapy And Chemotherapy of Tumors. *Journal of Biological Systems 16*, 01

(2008), 51–80.

[38] Dean, D., Suchland, R. J., and Stamm, W. E. Evidence for long-term cervical persistence of *Chlamydia trachomatis* by *Omp1* genotyping. *Journal of Infectious Diseases 182* (2000), 909–916.

[39] Deuflhard, P., and Bornemann, F. *Scientific computing with ordinary differential equations, Texts in applied mathematics*, vol. 42. Springer, Berlin, 2002.

[40] Diekmann, O., Heesterbeek, J. A. P., and Metz, J. A. J. On the definition and the computation of the basic reproduction ratio Ro in models for infectious diseases in heterogeneous populations. *Journal of Mathematical Biology 28* (1990), 365–382.

[41] Diekmann, O., Heesterbeek, J. A. P., and Roberts, M. G. The construction of next-generation matrices for compartmental epidemic models. *Journal of the Royal Society Interface 7* (2010), 873–885.

[42] Dixon, R. E., Hwang, S. J., Hennig, G. W., Ramsey, K. H., Schripsema, J. H., Sanders, K. M., and Ward, S. M. Chlamydia infection causes loss of pacemaker cells and inhibits oocyte transport in the mouse oviduct. *Biology of Reproduction 80* (2009), 665–673. DOI 10.1095/biolreprod.108.073833.

[43] Dreses-Werringloe, U., Padubrin, I., Zeidler, H., , and Köhler, L. Effects of azithromycin and rifampin on *Chlamydia trachomatis* infection in vitro. *Antimicrob. Agents Chemother. 45(11)* (2001).

[44] Dukers-Muijrers, N. H. T. M., Morré, S. A., Speksnijder, A., van der Sande, M. A. B., and Hoebe, C. J. P. A. *Chlamydia trachomatis* test-of-cure cannot be based on a single highly sensitive laboratory test taken at least 3 weeks after treatment. *PLoS ONE 7*, 3 (2012), e34108.

[45] Eko, F. O., He, Q., Brown, T., McMillan, L., Ifere, G. O., Ananaba, G. A., Lyn, D., Lubitz, W., Kellar, K. L., Black, C. M., and Igietseme, J. U. A novel recombinant multisubunit vaccine against *Chlamydia*. *The Journal of Immunology 173*, 5 (2004), 3375–3382.

[46] Eko, F. O., Lubitz, W., McMillan, L., Ramey, K., Moore, T. T., Ananaba, G. A., Lyn, D., Black, C. M., and Igietseme, J. U. Recombinant *Vibrio cholerae* ghosts as a delivery vehicle for vaccinating against *Chlamydia trachomatis*. *Vaccine 21*, 15 (2003), 1694–1703.

[47] Eko, F. O., Mania-Pramanik, J., Pais, R., Pan, Q., Okenu, D. M., Johnson, A., Ibegbu, C., He, C., He, Q., Russell, R., Black, C. M., and Igietseme, J. U. *Vibrio cholerae* ghosts (VCG) exert immunomodulatory effect on dendritic cells for enhanced antigen presentation and induction of protective immunity. *BMC Immunology 15*, 1 (2014), 1.

[48] Ekong, E. E., Okenu, D. N., Mania-Pramanik, J., He, Q., Igietseme, J. U., Ananaba, G. A., Lyn, D., Black, C., and Eko, F. O. A *Vibrio cholerae* ghost-based subunit vaccine induces cross-protective chlamydial immunity that is enhanced by CTA2B, the nontoxic derivative of cholera toxin. *FEMS Immunology and Medical Microbiology 55*, 2 (2009), 280–291.

[49] EMA. First malaria vaccine receives positive scientific opinion from ema: Mosquirix to be used for vaccination of young children, together with established antimalarial interventions. Technical Report, The European Medicines Agency (EMA), 2015. Available at `http://www.ema.europa.eu/docs/en_GB/document_library/Press_release/2015/07/WC500190447.pdf`.

[50] Fahey, J. V., Humphrey, S. L., Stern, J. E., and Wira, C. R. Secretory component production by polarized epithelial cells from the human female reproductive tract. *Immunological Investigations 27*, 3 (1998), 167–180.

[51] Fahey, J. V., Schaefer, T. M., Channon, J. Y., and Wira, C. R. Secretion of cytokines and chemokines by polarized human epithelial cells from the female reproductive tract. *Human reproduction (Oxford, England) 20*, 6 (2005), 1439–1446.

[52] Fields, K. A., and Hackstadt, T. Evidence for the secretion of *Chlamydia trachomatis* copn by a type iii secretion mechanism. *Molecular Microbiology 38*, 5 (2000), 1048–1060.

[53] Fisher, D. J., Fernandez, R. E., Adams, N. E., and Maurelli, A. T. Uptake of biotin by *Chlamydia* spp. through the use of a bacterial transporter (bioy) and a host-cell transporter (smvt). *PLoS ONE 7(9)* (2012). 46052. doi:10.1371/journal.pone.0046052.

[54] Fister, K., Lenhart, S., and McNally, J. Optimizing chemotherapy in an HIV model. *Electronic Journal of Differential Equations 1998* (1998), 1–12.

[55] Fleming, W., and Rishel, R. *Deterministic and Stochastic Optimal Control*. Springer New York, New York, NY, 1975, ch. Existence and Continuity Properties of Optimal Controls, pp. 60–79.

[56] Foulds, G., Shepard, R. M., and Johnson, R. B. The pharmacokinetics of azithromycin in human serum and tissues. *Journal of Antimicrobial Chemotherapy 25* (1990), 73–82. Suppl. A.

[57] Garnett, G. P., and Anderson, R. M. Sexually transmitted diseases and sexual behavior: Insights from mathematical models. *Journal of Infectious Diseases 174*, Supplement 2 (1996), S150–S161.

[58] Gaynor, M., and Mankin, A. S. Macrolide antibiotics: binding site, mechanism of action, resistance. *Current topics in medicinal chemistry 3*, 9 (2003), 949–960.

[59] Geisler, W., Uniyal, A., Lee, J., Lensing, S., Johnson, S., Perry, R., Kadrnka, C., and Kerndt, P. Azithromycin versus doxycycline for urogenital *Chlamydia trachomatis* infection. *New England Journal of Medicine 373*, 26 (2015), 2512–2521.

[60] Golden, M. R., Whittington, W. L., Handsfield, H. H., Hughes, J. P., Stamm, W. E., Hogben, M., Clark, A., Malinski, C., Helmers, J. R., Thomas, K. K., and Holmes, K. K. Effect of expedited treatment of sex partners on recurrent or persistent gonorrhea or chlamydial infection. *New England Journal of Medicine 352*, 7 (2005), 676–685.

[61] Gottlieb, S., Martin, D., Xu, F., Byrne, G., and Brunham, R. Summary: The natural history and immunobiology of *Chlamydia trachomatis* genital infection

and implications for *Chlamydia* control. *The Journal of Infectious Diseases 201(S2)* (2010), S190–S204.

[62] GSK. Gsk's malaria candidate vaccine, mosquirix^{TM} (rts,s), receives positive opinion from european regulators for the prevention of malaria in young children in sub-saharan africa. Technical Report, GSK Press Release, 2015. Accessed January 23, 2018. Available at `https://us.gsk.com/en-us/media/press-releases/2015/gsk-s-malaria-candidate-vaccine-mosquirixtm-rtss-receives-positive-opinion-from-european-regulators-for-the-prevention-of-malaria-in-young-children-in-sub-saharan-africa/`.

[63] Hafner, L. M., Wilson, D. P., and Timms, P. Development status and future prospects for a vaccine against *Chlamydia trachomatis* infection. *Vaccine 32*, 14 (2014), 1563 – 1571.

[64] Hai, J., Serradji, N., Mouton, L., Redeker, V., Cornu, D., El Hage Chahine, J.-M., Verbeke, P., and Hmadi, M. Targeted Delivery of Amoxicillin to *C. trachomatis* by the Transferrin Iron Acquisition Pathway. *PLOS ONE 11*, 2 (02 2016), 1–18.

[65] Hale, J. K. Ordinary differential equations. *Pure and Applied Mathematics XXI, Wiley-Interscience [John Wiley and Sons], New York* (1969).

[66] Hammerschlag, M. R. The intracellular life of *Chlamydiae*. In *Seminars in Pediatric Infectious Diseases* (2002), vol. 13, Elsevier, pp. 239–248.

[67] Handsfield, H. H. M. Questioning azithromycin for chlamydial infection. *Sexually Transmitted Diseases 38*, 11 (2011), 1028–1029.

[68] He, Q., Martinez-Sobrido, L., Eko, F. O., Palese, P., Garcia-Sastre, A., Lyn, D., Okenu, D., Bandea, C., Ananaba, G. A., Black, C. M., and Igietseme, J. U. Live-attenuated influenza viruses as delivery vectors for *Chlamydia* vaccines. *Immunology 122*, 1 (2007), 28–37.

[69] Heffernan, J., Smith, R., and Wahl, L. Perspectives on the basic reproductive ratio. *Journal of The Royal Society Interface 2*, 4 (2005), 281–293.

[70] Hethcote, H. W. The mathematics of infectious diseases. *Society for Industrial and Applied Mathematics (SIAM) 42* (2000), 599–653.

[71] Heuer, D., Brinkmann, V., Meyer, T. F., and Szczepek, A. J. Expression and translocation of chlamydial protease during acute and persistent infection of the epithelial HEp-2 cells with *Chlamydophila (Chlamydia) pneumoniae*. *Cellular Microbiology 5*, 5 (2003), 315–322.

[72] Hoare, A., Bavoil, P., Wilson, D., and Timms, P. Spatial constraints within the chlamydial host cell inclusion predict interrupted development and persistence. *BMC Microbiology 8*, 5 (2008).

[73] Hoare, A., Regan, D. G., and Wilson, D. P. Sampling and sensitivity analyses tools (SaSAT) for computational modelling. *Theoretical Biology and Medical Modelling 5*, 1 (2008), 4–4.

[74] Hocking, J. S., Vodstrcil, L. A., Huston, W. M., Timms, P., Chen, M. Y., Worthington, K., McIver, R., Tabrizi, S. N., and on behalf of the Australian Chlamydia Treatment Study (ACTS) investigators. A cohort

study of *Chlamydia trachomatis* treatment failure in women: A study protocol. *BMC Infectious Diseases 13*, 1 (2013), 379–379.

[75] Hogan, R. J., Mathews, S. A., Mukhopadhyay, S., Summersgill, J. T., and Timms, P. Chlamydial persistence: beyond the biphasic paradigm. *Infection and Immunity 72*, 4 (2004), 1843–1855.

[76] Horner, P. The case for further treatment studies of uncomplicated genital *Chlamydia trachomatis* infection. *Sexually Transmitted Infections 82*, 4 (2006), 340–343.

[77] Horner, P. J. Azithromycin antimicrobial resistance and genital *Chlamydia trachomatis* infection: duration of therapy may be the key to improving efficacy. *Sexually Transmitted Infections 88*, 3 (2012), 154–156.

[78] Huang, Z., Feng, Y., Chen, D., Wu, X., Huang, S., Wang, X., Xiao, X., Li, W., Huang, N., Gu, L., Zhong, G., and Chai, J. Structural basis for activation and inhibition of the secreted *Chlamydia* protease CPAF. *Cell Host & Microbe 4*, 6 (2008), 529 – 542.

[79] Hybiske, K., and Stephens, R. S. Mechanisms of host cell exit by the intracellular bacterium *Chlamydia*. *Proceedings of the National Academy of Sciences 104*, 27 (2007), 11430–11435.

[80] Ibana, J. A., Belland, R. J., Zea, A. H., Schust, D. J., Nagamatsu, T., AbdelRahman, Y. M., Tate, D. J., Beatty, W. L., Aiyar, A. A., and Quayle, A. J. Inhibition of indoleamine 2,3-dioxygenase activity by levo-1-methyl tryptophan blocks gamma interferon-induced chlamydia trachomatis persistence in human epithelial cells. *Infection and Immunity 79*, 11 (2011), 4425–4437.

[81] Igietseme, J. U., Eko, F. O., and Black, C. M. *Chlamydia* vaccines: recent developments and the role of adjuvants in future formulations. *Expert Review of Vaccines 10*, 11 (2011), 1585–1596.

[82] Igietseme, J. U., He, Q., Joseph, K., Eko, F. O., Lyn, D., Ananaba, G., Campbell, A., Bandea, C., and Black, C. M. Role of T Lymphocytes in the pathogenesis of *Chlamydia* Disease. *The Journal of Infectious Diseases 200*, 6 (2009), 926–934.

[83] Joshi, H. R. Optimal control of an HIV immunology model. *Optimal Control Applications and Methods 23*, 4 (2002), 199–213.

[84] Kari, L., Whitmire, W. M., Olivares-Zavaleta, N., Goheen, M. M., Taylor, L. D., Carlson, J. H., Sturdevant, G. L., Lu, C., Bakios, L. E., Randall, L. B., Parnell, M. J., Zhong, G., and Caldwell, H. D. A live-attenuated chlamydial vaccine protects against trachoma in nonhuman primates. *The Journal of Experimental Medicine 208*, 11 (2011), 2217–2223.

[85] Karrakchou, J., Rachik, M., and Gourari, S. Optimal control and infectiology: Application to an HIV/AIDS model. *Applied Mathematics and Computation 177*, 2 (2006), 807 – 818.

[86] Karunakaran, K. P., Yu, H., Foster, L. J., and Brunham, R. C. Development of a *Chlamydia trachomatis* T cell vaccine. *Human Vaccines 6*, 8 (2010), 676–680.

[87] Kaushic, C., Murdin, A. D., Underdown, B. J., and Wira, C. R. *Chlamydia trachomatis* infection in the female reproductive tract of the rat: Influence of progesterone on infectivity and immune response. *Infection and Immunity 66(3)* (1998), 893–898.

[88] Khalil, H. K. Nonlinear Systems and Control Lecture # 10. The Invariance Principle. Available at: `https://www.egr.msu.edu/~khalil/NonlinearSystems/Sample/Lect_10.pdf`. Accessed June 6, 2018.

[89] Kirschner, D., Lenhart, S., and Serbin, S. Optimal control of the chemotherapy of HIV. *Journal of mathematical biology 35*, 7 (1997), 775–792.

[90] Kohanski, M. A., Dwyer, D. J., and Collins, J. J. How antibiotics kill bacteria: from targets to networks. *Nat. Rev. Microbiol. 8*, 6 (2010), 423–435.

[91] Kong, F., and Hocking, J. Treatment challenges for urogenital and anorectal *Chlamydia trachomatis*. *BMC Infectious Diseases 15*, 1 (2015), 293.

[92] Kong, F. Y. S., Tabrizi, S. N., Law, M., Vodstrcil, L. A., Chen, M., Fairley, C. K., Guy, R., Bradshaw, C., and Hocking, J. S. Azithromycin Versus Doxycycline for the Treatment of Genital *Chlamydia* Infection: A Meta-analysis of Randomized Controlled Trials. *Clinical Infectious Diseases 59*, 2 (2014), 193–205.

[93] Koo, D. *Elements of Optimization: With Applications in Economics and Business*. Springer Science & Business Media, 2013.

[94] La Salle, J. *The Stability of Dynamical Systems*. Society for Industrial and Applied Mathematics, 1976.

[95] Lakshmikantham, V., Leela, S., and Martynyuk, A. A. *Stability analysis of nonlinear systems*. Springer, 1989.

[96] Lampe, M. F., Wilson, C. B., Bevan, M. J., and Starnbach, M. N. Gamma interferon production by cytotoxic T lymphocytes is required for resolution of *Chlamydia trachomatis* infection. *Infection and Immunity 66*, 11 (1998), 5457–5461.

[97] Larson, N., and Ghandehari, H. Polymeric conjugates for drug delivery. *Chemistry of Materials 24*, 5 (2012), 840–853. PMID: 22707853.

[98] Le Negrate, G., Krieg, A., Faustin, B., Loeffler, M., Godzik, A., Krajewski, S., and Reed, J. C. *Chla*dub1 of *Chlamydia trachomatis* suppresses nf-κb activation and inhibits iκbα ubiquitination and degradation. *Cellular Microbiology 10*, 9 (2008), 1879–1892.

[99] Lea, A. P., and Lamb, H. M. Azithromycin: A pharmacoeconomic review of its use as a single-dose regimen in the treatment of uncomplicated urogenital *Chlamydia trachomatis* infections in women. *Pharmacoeconomics 12(5)* (1997), 596–611.

[100] Lenhart, S., and Workman, J. T. *Optimal control applied to biological models*. CRC Press, London, UK, 2007.

[101] Li, J., Blakeley, D., and Smith?, R. J. The Failure of R_0. *Computational and Mathematical Methods in Medicine 2011*, 527610 (2011).

[102] Liechty, W. B., Kryscio, D. R., Slaughter, B. V., and Peppas, N. A. Polymers for drug delivery systems. *Annual Review of Chemical and Biomolecular Engineering 1*, 1 (2010), 149–173. PMID: 22432577.

[103] Llano-Sotelo, B., Dunkle, J., Klepacki, D., Zhang, W., Fernandes, P., Cate, J. H. D., and Mankin, A. S. Binding and action of cem-101, a new fluoroketolide antibiotic that inhibits protein synthesis. *Antimicrobial Agents and Chemotherapy 54*, 12 (2010), 4961–4970.

[104] L.M., H., and P., T. Development of a vaccine for *Chlamydia trachomatis*: challenges and current progress. *Vaccine: Development and Therapy 2015* (2015), 45–58.

[105] Loomis, W. P., and Starnbach, M. N. T cell responses to *Chlamydia trachomatis*. *Current Opinion in Microbiology 5*, 1 (2002), 87–91.

[106] Malhotra, M., Sood, S., Mukherjee, A., Muralidhar, S., Bala, M., et al. Genital *Chlamydia trachomatis*: an update. *Indian Journal of Medical Research 138*, 3 (2013), 303.

[107] Mallet, D. G., Bagher-Oskouei, M., Farr, A. C., Simpson, D. P., and Sutton, K.-J. A mathematical model of chlamydial infection incorporating movement of chlamydial particles. *Bull. Math. Biol. 75* (2013), 2257–2270. DOI 10.1007/s11538-013-9891-9.

[108] Mallet, D. G., Heymer, K., and Wilson, D. P. A novel cellular automata-partial differential equation model for understanding chlamydial infection and ascension of the female genital tract. *PAMM Proc. Appl. Math. Mech. 7* (2007), 2120001–2120002. DOI 10.1002/pamm.200700031.

[109] Mallet, D. G., Heymer, K.-J., Rank, R. G., and Wilson, D. P. Chlamydial infection and spatial ascension of the female genital tract: a novel hybrid cellular automata and continuum mathematical model. *FEMS Immunol. Med. Microbiol. 57* (2009), 173–182.

[110] Marks, E., and Lycke, N. Immunity Against *Chlamydia trachomatis*. In *Immunity Against Mucosal Pathogens*. Springer, 2008, pp. 433–458.

[111] Martin, D. H., Mroczkowski, T. F., Dalu, Z., McCarty, J., Jones, R. B., Hopkins, S. J., and Johnson, R. B. A controlled trial of a single dose of azithromycin for the treatment of chlamydial urethritis and cervicitis. *The New England Journal of Medicine 327(13)* (1992), 921–925.

[112] Mascellino, M. T., Boccia, P., and Oliva, A. Immunopathogenesis in *Chlamydia trachomatis* infected women. *ISRN Obstetrics and Gynecology 2011* (2011).

[113] Masopust, D., Choo, D., Vezys, V., Wherry, E. J., Duraiswamy, J., Akondy, R., Wang, J., Casey, K. A., Barber, D. L., Kawamura, K. S., Fraser, K. A., Webby, R. J., Brinkmann, V., Butcher, E. C., Newell, K. A., and Ahmed, R. Dynamic T cell migration program provides resident memory within intestinal epithelium. *The Journal of Experimental Medicine 207*, 3 (2010), 553–564.

[114] MathWorks. fmincon. Available at: `https://au.mathworks.com/help/optim/ug/fmincon.html`. Accessed January 20, 2017.

[115] Mcasey, M., Mou, L., and Han, W. Convergence of the forward-backward sweep method in optimal control. *Comput. Optim. Appl. 53*, 1 (2012), 207–226.

[116] Mellor, A. L., Lemos, H., and Huang, L. Indoleamine 2,3-dioxygenase and tolerance: Where are we now? *Frontiers in Immunology 8* (2017), 1360.

[117] Munday, P. E., Thomas, B. J., Gilroy, C. B., Gilchrist, C., and Taylor-Robinson, D. Infrequent detection of *Chlamydia trachomatis* in a longitudinal study of women with treated cervical infection. *Genitourinary Medicine 71*, 1 (1995), 24–26.

[118] MVI. Vaccine development. Technical Report, Malaria Vaccine Initiative, 2018. Accessed January 23, 2018. Available at `http://www.malariavaccine.org/malaria-and-vaccines/vaccine-development`.

[119] Neu, H. C. Clinical microbiology of azithromycin. *The American Journal of Medicine 91(3)* (1991), 12S–18S. Suppl. 3A.

[120] Niger, A. M., and Gumel, A. B. Immune response and imperfect vaccine in malaria dynamics. *Mathematical Population Studies 18*, 2 (2011), 55–86.

[121] Osteen, K. G., Hill, G. A., Hargove, J. T., and Gorstein, F. Development of a method to isolate and culture highly purified populations of stromal and epithelial cells from human endometrial biopsy specimens. *Fertility and Sterility 52*, 6 (1989), 965–972.

[122] Parnham, M. J., Haber, V. E., Giamarellos-Bourboulis, E. J., Perletti, G., Verleden, G. M., and Vos, R. Azithromycin: Mechanisms of action and their relevance for clinical applications. *Pharmacology & Therapeutics 143*, 2 (2014), 225 – 245.

[123] Peuchant, O., Duvert, J. P., Clerc, M., Raherison, S., Bébéar, C., Bebear, C. M., and De Barbeyrac, B. Effects of antibiotics on *Chlamydia trachomatis* viability as determined by real-time quantitative pcr. *Journal of medical microbiology 60*, 4 (2011), 508–514.

[124] Pietz, J. A. Pseudospectral Collocation Methods for the Direct Transcription of Optimal Control Problems. Master thesis, Rice University, Houston, Texas, April 2003. Available at `http://www.caam.rice.edu/tech_reports/2003/TR03-10.pdf`. Assessed May 31, 2018.

[125] Pontryagin, L. S., Boltyanskiy, V. G., Gamkrelidze, R. V., and Mishchenko, E. F. *The Mathematical Theory of Optimal Processes*. Wiley, New Jersey, 1962.

[126] Quinn, T. C., and Gaydos, C. A. Treatment for *Chlamydia* infection - doxycycline versus azithromycin. *New England Journal of Medicine 373*, 26 (2015), 2573–2575. PMID: 26699174.

[127] Rank, R., and Whittum-Hudson, J. Protective immunity to chlamydial genital infection: evidence from animal studies. *The Journal of Infectious Diseases 201(S2)* (2010), S168–S177.

[128] Rank, R. G., and Yeruva, L. Hidden in plain sight: chlamydial gastrointestinal infection and its relevance to persistence in human genital infection. *Infection and Immunity 82*, 4 (2014), 1362–1371.

[129] Raulston, J. E. Pharmacokinetics of azithromycin and erythromycin in human endometrial epithelial cells and in cells infected with *Chlamydia trachomatis*. *Journal of Antimicrobial Chemotherapy 34*, 5 (1994), 765–776.

[130] Rekart, M. L., and Brunham, R. C. Epidemiology of chlamydial infection: are we losing ground? *Sex Transm. Infect. 84* (2008), 87–91.

[131] Reveneau, N., Crane, D. D., Fischer, E., and Caldwell, H. D. Bactericidal activity of first-choice antibiotics against gamma interferon-induced persistent infection of human epithelial cells by chlamydia trachomatis. *Antimicrobial Agents and Chemotherapy 49*, 5 (2005), 1787–1793.

[132] Rey-Ladino, J., Ross, A. G., and Cripps, A. W. Immunity, immunopathology, and human vaccine development against sexually transmitted *Chlamydia trachomatis*. *Human Vaccines & Immunotherapeutics 10*, 9 (2014), 2664–2673.

[133] Ribeiro, R. M., Mohri, H., Ho, D. D., and Perelson, A. S. In vivo dynamics of T cell activation, proliferation, and death in HIV-1 infection: why are $CD4^+$ but not $CD8^+$ T cells depleted? *Proceedings of the National Academy of Sciences 99*, 24 (2002), 15572–15577.

[134] Sbarbati, R., de Boer, M., Marzilli, M., Scarlattini, M., Rossi, G., and van Mourik, J. Immunologic detection of endothelial cells in human whole blood. *Blood 77*, 4 (1991), 764–769.

[135] Schachter, J. *Chlamydia trachomatis* Infections. In *Opportunistic Intracellular Bacteria and Immunity*. Kluwer Academic Press, 1999, pp. 213–231.

[136] Schmidt, S. K., Siepmann, S., Kuhlmann, K., Meyer, H. E., Metzger, S., Pudelko, S., Leineweber, M., and Däubener, W. Influence of tryptophan contained in 1-methyl-tryptophan on antimicrobial and immunoregulatory functions of indoleamine 2, 3-dioxygenase. *PloS one 7*, 9 (2012), e44797.

[137] Schroder, K., Hertzog, P. J., Ravasi, T., and Hume, D. A. Interferon-γ: an overview of signals, mechanisms and functions. *Journal of Leukocyte Biology 75*, 2 (2004), 163–189.

[138] Schwebke, J. R., Rompalo, A., Taylor, S., Seña, A. C., Martin, D. H., Lopez, L. M., Lensing, S., and Lee, J. Y. Re-evaluating the treatment of nongonococcal urethritis: Emphasizing emerging pathogens-a randomized clinical trial. *Clinical Infectious Diseases 52*, 2 (2011), 163–170.

[139] Scieux, C., Bianchi, A., Chappey, B., Vassias, I., and Pérol, Y. In-vitro activity of azithromycin against *Chlamydia trachomatis*. *Journal of Antimicrobial Chemotherapy 25* (1990). Suppl. A, 7-10.

[140] Shambayati, B. *Cytopathology*. Oxford University Press, Oxford, UK, 2011. Page 26.

[141] Sharma, J., Dong, F., Pirbhai, M., and Zhong, G. Inhibition of proteolytic activity of a chlamydial proteasome/protease-like activity factor by antibodies from humans infected with chlamydia trachomatis. *Infection and immunity 73*, 7 (2005), 4414–4419.

[142] Sharomi, O., and Gumel, A. B. Mathematical study of in-host dynamics of *Chlamydia trachomatis*. *IMA Journal of Applied Mathematics 77*, 2 (2012), 109–139.

[143] Sharomi, O., and Malik, T. Optimal control in epidemiology. *Annals of Operations Research* (2015), 1–17.

[144] Shaw, E. I., Dooley, C. A., Fischer, E. R., Scidmore, M. A., Fields, K. A., and Hackstadt, T. Three temporal classes of gene expression during the *Chlamydia trachomatis* developmental cycle. *Molecular Microbiology 37*, 4 (2000), 913–925.

[145] Singla, M. Role of tryptophan supplementation in the treatment of *Chlamydia*. *Medical Hypotheses 68*, 2 (2007), 278 – 280.

[146] Smith, P. Regulatory and public health challenges for vaccines inducing modest efficacy. Global Vaccine and Immunization Forum Washington DC. London School of Hygiene & Tropical Medicine. Available at: `http://www.who.int/immunization/research/forums_and_initiatives/01_Smith_GVIRF_Regulatory_Public_Health_Challenges.pdf?ua=1`, March 4 2014. Accessed October 31, 2017.

[147] Stadnyk, A. Cytokine production by epithelial cells. *The FASEB Journal 8*, 13 (1994), 1041–1047.

[148] Stamm, W. E. Azithromycin in the treatment of uncomplicated genital chlamydial infections. *The American Journal of Medicine 91(3)* (1991), 19S–22S. Suppl. 3A.

[149] Stary, G., Olive, A., Radovic-Moreno, A., Gondek, D., Alvarez, D., Basto, P., Perro, M., Vrbanac, V., Tager, A., Shi, J., Yethon, J., Farokhzad, O., Langer, R., Starnbach, M., and von Andrian, U. A mucosal vaccine against *Chlamydia trachomatis* generates two waves of protective memory T cells. *Science 348*, 6241 (2015), aaa8205–aaa8205.

[150] Steingrimsson, O., Olafsson, J. H., Thorarinsson, H., Ryan, R. W., Johnson, R. B., and Tilton, R. C. Azithromycin in the treatment of sexually transmitted disease. *Journal of Antimicrobial Chemotherapy 25* (1990), 109–114. Suppl. A.

[151] Talwar, G. P., and Srivastava, L. M. *Textbook of Biochemistry and Human Biology*, 3 ed. Prentice-Hall of India Learning Private Limited, Delhi, India, 2002.

[152] Tang, L., Chen, J., Zhou, Z., Yu, P., Yang, Z., and Zhong, G. *Chlamydia*-secreted protease CPAF degrades host antimicrobial peptides. *Microbes and Infection 17*, 6 (2015), 402 – 408.

[153] Taylor, B. D., Darville, T., Tan, C., Bavoil, P. M., Ness, R. B., and Haggerty, C. L. The role of *Chlamydia trachomatis* polymorphic membrane proteins in inflammation and sequelae among women with pelvic inflammatory disease. *Infectious Diseases in Obstetrics and Gynecology 2011* (2011), 989762.

[154] Tchuenche, J. M., Khamis, S. A., Agusto, F. B., and Mpeshe, S. C. Optimal control and sensitivity analysis of an influenza model with treatment and vaccination. *Acta Biotheoretica 59*, 1 (2010), 1–28.

[155] Tram, N. D. T., and Ee, P. L. R. Macromolecular conjugate and biological carrier approaches for the targeted delivery of antibiotics. *Antibiotics 6*, 3 (2017).

[156] Trudnowski, R. J., and Rico, R. C. Specific gravity of blood and plasma at 4 and 37°c. *Clinical Chemistry 20*, 5 (1974), 615–616.

[157] van den Driessche, P., and Watmough, J. Reproduction numbers and subthreshold endemic equilibria for compartmental models of disease transmission. *Mathematical Biosciences 180* (2002), 29–48.

[158] Vicent, M. J., Dieudonné, L., Carbajo, R. J., and Pineda-Lucena, A. Polymer conjugates as therapeutics: future trends, challenges and opportunities. *Expert Opinion on Drug Delivery 5*, 5 (2008), 593–614. PMID: 18491984.

[159] Vickers, D. M., and Osgood, N. D. The arrested immunity hypothesis in an immunoepidemiological model of *Chlamydia trachomatis*. *Theoretical Population Biology 93* (2014), 52–62.

[160] Vickers, D. M., Zhang, Q., and Osgood, N. Immunobiological outcomes of repeated chlamydial infection from two models of within-host population dynamics. *PLoS ONE 4*, 9 (2009), e6886.

[161] White, H. D., Prabhala, R. H., Humphrey, S. L., Crassi, K. M., Richardson, J. M., and Wira, C. R. A method for the dispersal and characterization of leukocytes from the human female reproductive tract. *American Journal of Reproductive Immunology 44* (2000), 96–103.

[162] WHO. World Health Organisation: Global incidence and prevalence of selected curable sexually transmitted infections 2008. Technical Report, WHO, 2012. Available at: `http://www.who.int/hiv/pub/sti/who_hiv_aids_2001.02.pdf` [Accessed January 22, 2014].

[163] WHO. World Health Organisation. Immunization, Vaccines, and Biologicals. Technical Report, Geneva: World Health Organisation, 2013. Available at: `http://who.int/immunization/topics/en/index.html`.

[164] WHO. World Health Organisation: Report on global sexually transmitted infection surveillance 2013. Technical Report, Geneva: World Health Organisation, 2014. Available at: `http://apps.who.int/iris/bitstream/10665/112922/1/9789241507400_eng.pdf` [Accessed January 22, 2014].

[165] WHO. Tables of malaria vaccine projects globally : The rainbow tables 2015. Technical Report, World Health Organization, 2015. Available at `http://www.who.int/immunization/research/development/Rainbow_tables/en/`, Accessed February 19, 2016.

[166] WHO. Malaria vaccine: WHO position paper - January 2016. Technical Report, World Health Organization, 2016.

[167] Wilson, D., Bavoil, P., McElwain, D., and Timms, P. Type III secretion, contact-dependent model for the intracellular development of *Chlamydia*. *Bulletin of Mathematical Biology 68(1)* (2006), 161–178.

[168] Wilson, D., McElwain, D., and Timms, P. A mathematical model for the investigation of the Th1 immune response to *Chlamydia trachomatis*. *Mathematical Biosciences 182(1)* (2003), 27–44.

[169] Wilson, D. P. Mathematical modelling of *Chlamydia*. *ANZIAM 45* (2004), C201–C214.

[170] Wilson, D. P., Mathews, S., Wan, C., Pettitt, A. N., and McElwain, D. L. S. Use of a quantitative gene expression assay based on micro-array techniques and a mathematical model for the investigation of chlamydial generation time. *Bulletin of Mathematical Biology 66(3)* (2004), 523.

[171] Wilson, D. P., and McElwain, D. L. S. A model of neutralization of *Chlamydia trachomatis* based on antibody and host cell aggregation on the elementary body surface. *Journal of Theoretical Biology 226*, 3 (2004), 321–330.

[172] Wira, C. R., Ghosh, M., Smith, J. M., Shen, L., Connor, R. I., Sundstrom, P., Frechette, G. M., Hill, E. T., and Fahey, J. V. Epithelial cell secretions from the human female reproductive tract inhibit sexually transmitted pathogens and *Candida albicans* but not *Lactobacillus*. *Mucosal Immunology 4*, 3 (2011), 335–342.

[173] Wira, C. R., Grant-Tschudy, K. S., and Crane-Godreau, M. A. Epithelial cells in the female reproductive tract: a central role as sentinels of immune protection. *American Journal of Reproductive Immunology 53*, 2 (2005), 65–76.

[174] Wiser, A. *Chlamydia Trachomatis*. Available at: `http://www.austincc.edu/microbio/2704w/ct.htm`. Accessed September 12, 2015.

[175] Yang, C., Starr, T., Song, L., Carlson, J. H., Sturdevant, G. L., Beare, P. A., Whitmire, W. M., and Caldwell, H. D. Chlamydial lytic exit from host cells is plasmid regulated. *mBio 6*, 6 (2015), e0164815.

[176] Yang, X., and Brunham, R. C. T lymphocyte immunity in host defence against *Chlamydia trachomatis* and its implication for vaccine development. *Canadian Journal of Infectious Diseases 9*, 2 (1998), 99–109.

[177] Yang, Z., Tang, L., Zhou, Z., and Zhong, G. Neutralizing antichlamydial activity of complement by *Chlamydia*-secreted protease CPAF. *Microbes and Infection 18*, 11 (2016), 669 – 674.

[178] Yasser M. AbdelRahman, R. J. B. The chlamydial developmental cycle. *FEMS Microbiology Reviews 29* (2005), 949–959. doi:10.1016/j.femsre.2005.03.002.

[179] Yeruva, L., Melnyk, S., Spencer, N., Bowlin, A., and Rank, R. G. Differential susceptibilities to azithromycin treatment of chlamydial infection in the gastrointestinal tract and cervix. *Antimicrobial Agents and Chemotherapy 57*, 12 (2013), 6290–6294.

[180] Zhang, Q., Huang, Y., Gong, S., Yang, Z., Sun, X., Schenken, R., and Zhong, G. *In Vivo* and *Ex Vivo* Imaging Reveals a Long-Lasting Chlamydial Infection in the Mouse Gastrointestinal Tract following Genital Tract Inoculation. *Infection and Immunity 83*, 9 (2015), 3568–3577.